U.PORTO
FEUP FACULDADE DE ENGENHARIA
UNIVERSIDADE DO PORTO

DEPARTMENT OF MECHANICAL ENGINEERING AND INDUSTRIAL MANAGEMENT

MECHANICAL PERFORMANCE OF BIODEGRADABLE, LOW TOXICITY ESTER BASED INDUSTRIAL GEAR OILS

NUNO FILIPE RIBEIRO CARDOSO

2007

NUNO FILIPE RIBEIRO CARDOSO

MECHANICAL PERFORMANCE OF BIODEGRADABLE, LOW TOXICITY ESTER BASED INDUSTRIAL GEAR OILS

A DISSERTATION SUBMITTED TO THE FACULTY OF ENGINEERING
FOR THE DEGREE OF *MASTER OF SCIENCE IN INDUSTRIAL MAINTENANCE*

Supervisor: Prof. Jorge H. O. Seabra
Co-supervisor: Dr. Luís M. M. L. Magalhães

DEPARTMENT OF MECHANICAL ENGINEERING AND INDUSTRIAL MANAGEMENT
FACULTY OF ENGINEERING
UNIVERSITY OF PORTO

2007

ABSTRACT

Environmental awareness leads to a growing interest in biodegradable non-toxic lubricants. However, the key aspect for any industrial application is technical performance and technical advantages proved in dedicated tests. Environmental compatibility is usually viewed in respect to biodegradability and toxicity. While the first issue is reached by using a suitable bio-degradable base fluid, low toxicity requires an additivation that is environmentally friendly, too. However, lubricant performance (friction, wear, lifetime, load bearing, efficiency etc.) has a major impact on its overall environmental compatibility. Premature wear, high energy needs are as well harmful to the environment.

Three new gear oil formulations based on highly or fully saturated esters were formulated (two of them biodegradable and with low toxicity containing an environmentally friendly additivation and derived from renewable resources), and a reference paraffinic mineral oil, containing an additive package for extra protection against micropitting, was selected for comparison.

The new environmentally friendly oils specially suited for industrial gear applications were formulated in order to have the following characteristics in comparison to non biodegradable products: biodegradability, low-toxicity additivation, CLP gear oil performance (DIN 51517), competitive price/performance ratio, similar or better gear wear performance, better gear scuffing load carrying capacity, similar or better gear micropitting performance and lower gear power loss.

The chemical, physical and environmental properties of the new lubricants were measured and compared with those of paraffinic mineral gear oil, used as reference.

The tribological performance of these gear oils combined with different gear materials was evaluated in terms of wear (Four-Ball wear test), scuffing load carrying capacity (FZG gear scuffing test), gear micropitting (FZG gear micropitting test) and gear power loss (FZG gear power loss test).

Comparisons were made between reference mineral gear oil and the ester lubricants in the following aspects:

- Physical properties (viscosity, viscosity index, density);
- Efficiency in a gearbox (power loss in FZG tests with several operating conditions);
- Protection against typical gear failures (scuffing, micropitting and excessive wear in FZG tests).

The following aspects related with the interactions between the tribo-reactive materials (MoST coating and High Pressure Nitrided Steel) and the ester lubricants (including the two biodegradable and non-toxic ones) were studied in detail:

- Characterization of the micro/nano mechanisms of damage due to those interactions, using SEM and other techniques of surface analysis;
- Quantification of the protection against the typical gear failures promoted by these combinations, when compared with normal solutions on FZG tests;
- Modellization and measurement of energetic efficiency of those combinations on FZG tests.

SUMÀRIO

A consciência ambiental tem conduzido a um interesse crescente em lubrificantes biodegradáveis e não tóxicos. No entanto, os aspectos fundamental para qualquer aplicação industrial são o desempenho e as vantagens técnicas comprovadas através de testes específicos. A compatibilidade ambiental normalmente é vista no que diz respeito à biodegradabilidade e à toxicidade. Enquanto a primeira é alcançada usando um fluído base biodegradável adequado, a baixa toxicidade requer também uma aditivação que seja amiga do ambiente. Porém, o desempenho do lubrificante (atrito, desgaste, vida útil, capacidade de carga, eficiência etc.) tem um impacto significativo na sua compatibilidade ambiental global. Um desgaste prematuro e/ou elevadas necessidades de energia são também prejudiciais para o ambiente.

Foram seleccionadas três novas formulações de óleos de engrenagens baseados em esteres altamente ou totalmente saturados (dois deles biodegradáveis, com baixa toxicidade, contendo uma aditivação amiga do ambiente e obtidos a partir de fontes renováveis) e um óleo mineral de referência de base parafinica, com um pacote de aditivos para protecção extra contra a fadiga de contacto.

O novos óleos biodegradáveis desenvolvidos para aplicações de engrenagens industriais foram seleccionados de forma a que possuíssem as seguintes características em comparação com os produtos não biodegradáveis: bidodegradabilidade, aditivação de baixa toxicidade, desempenho em engrenagens de acordo com as especificações CLP (DIN 51517), relação de preço/desempenho competitiva, desempenho semelhante ou melhor em termos de desgaste e de dissipação de potência, melhor desempenho em termos de gripagem.

A propriedades químicas, físicas e ambientais dos novos lubrificantes foram medidas e comparadas com as do óleo mineral para engrenagens, usado como referência.

O desempenho de tribologico destes lubrificantes combinado com engrenagens de diferentes materiais foi avaliado em termos resistência ao desgaste (Teste de desgaste de Quatro-esferas), à gripagem (Ensaio FZG de gripagem), à fadiga de contacto (Ensaio FZG de fadiga de contacto em engrenagens) e em termos de potência dissipada (Ensaio FZG de perda de potência).

Foram efectuadas comparações entre um óleo mineral de referência para engrenagens e os óleos biodegradáveis e não-tóxicos nos seguintes aspectos:

- Propriedades físicas (viscosidade, índice de viscosidade e densidade);
- A sua eficiência numa caixa de engrenagens (potência dissipada em ensaios FZG com diversas condições de funcionamento);
- Protecção contra as avarias típicas de engrenagens (gripagem, pitting e desgaste excessivo em ensaios FZG);

Os seguintes aspecto relacionados com as interacções entre os materiais tribo-reactivos (Revestimento MoST, aço nitrurado a alta pressão) e o lubrificante biodegradável e não tóxico foram estudados em detalhe:

- Caracterização dos micro/nano mecanismos de dano devidos a estas interacções, utilizando SEM e outras técnicas de análise superficial;
- Quantificação da protecção contra avarias típicas em engrenagens, promovida por estas combinações, quando comparada com soluções normais em ensaios FZG;
- Modelização e medição da eficiência energética de tais combinações em ensaios FZG.

SOMMAIRE

La conscience environnemental a conduit à un intérêt croissant dans les lubrifiants biodégradables et aucun toxique. Cependant, l'aspectes fondamentales pour toute les application industrielles son la performance et les avantages techniques prouvés dans les épreuves spécifiques. La compatibilité environnemental est vue habituellement dans ce qui dit respect a la biodegradabilité et a la toxicité. Pendant que la première question est atteinte avec un fluide base biodégradable convenable, la basse toxicité exige une additivation qui est écologiquement amical, aussi. Cependant, la performance du lubrifiante (frottement, usure, duration, capacité de charge, efficience etc.) a un impact majeur sur sa compatibilité avec l'environnement totale. Le usure prématurе, les hauts besoins d'énergie sont bien comme malfaisant à l'environnement.

Trois nouvelles formulations des huiles pour engrenages basé sur esters hautement ou totalement saturé ont été formulés (deux d'eux biodégradable et avec toxicité basse qui contient des additifs écologiquement amical et ont dérivé de ressources renouvelables), et un huile minérale de référence, contenant un paquet des additif pour protection supplémentaire contre la fatigue du contact ont été sélectionnés pour comparaison.

Les nouvelles huiles biodégradables, développées pour applications des engrenages industrielles ont été sélectionnées pour avoir les caractéristiques suivantes par rapport à produits non biodégradables: biodégradabilité, additivation de basse toxicité, performanece avec engrenages en accord avec les spécifications CLP (DIN 51517), rapport de pris/performance compétitif, performance semblable ou meilleure quant à l'usure et le dissipation de puissance, mieux performance meilleure quant au grippage.

Les propriétés chimiques, physiques et environnementales des nouveaux lubrifiants ont été mesurés et comparées avec ce de l'huile minérale pour engrenages, utilisé comme référence.

La performance de tribologique de ces lubrifiants combiné avec des engrenages de différents matériels a été évaluée quant à la résistance à l'usure (Essai d'usure de Quatre-balles), à grippage (Essai FZG de grippage), à la fatigue de contact (Essai FZG de fadigue de contact) et quant à puissance dissipé (Essai FZG de perte du puissance).

Ont été effectuées des comparaisons entre une huile minérale de référence pour engrenages et les huiles biodégradables et não-tóxicos dans les suivants aspects : :

- Propriétés physiques (viscosité, indice de viscosité et densité);
- Son efficacité dans une boîte des engrenages (puissance dissipé à des essais FZG avec de diverses conditions de fonctionnement) ;
- Protection contre les pannes typiques des engrenages (grippage, fadigue de contact et usure excessive à des essais FZG) ;

Les suivants aspects rapportés avec les interactions entre les matériels des tribo-reactive (Revêtement MoST, acier nitruré à haute pression) et le lubrifiant biodégradable et non toxique ont été étudiés en détail :

- Caractérisation du micro/nano mécanismes de dommages dus à ces interactions, utilisant SEM et autres techniques d'analyse superficielle ;
- Quantification de la protection contre des pannes typiques dans des engrenages, promue par ces combinaisons, quand comparée avec des solutions normales à des essais FZG
- Modélisation et mesure de l'efficacité énergétique de telles combinaisons à des essais FZG.

KEYWORDS

Biodegradable lubricants

Low toxicity additivation

Esters

Gear scuffing

Gear micropitting

Gear efficiency / power losse

Wear

Friction coeficient

PALAVRAS CHAVE

Lubrificantes biodegradáveis

Aditivação de baixa toxicidade

Esteres

Gripagem de engrenagens

Fadiga de contacto em engrenagens

Perdas de potência / Eficiência em egrenagens

Desgaste

Coeficiente de atrito

MOTS-CLÉS

Lubrifiants biodégradables

Additivation de basse toxicité

Esters

Grippage des engrenages

Fadigue de contact dans les engrenages

Perte de puissance / Efficience dans les engrenages

Usure

Coefficient de frottement

ACKNOWLEDGMENTS

I would like to express my gratitude to my supervisor Prof. Jorge Seabra, for his excellent guidance and support throughout the course of this study. I also express my appreciation to my co-supervisor Prof. Luís Magalhães for his guidance and for his careful review of this dissertation.

I wish to thank my colleagues and staff of CETRIB-INEGI, Beatriz Graça, Armando Campos, Jorge Castro, Ramiro Martins and José Brandão for their co-operation and support during this research work.

I also wish to thank to FEUP and to CETRIB – INEGI (Tribology and Industrial Maintenance Unit of the Institute of Mechanical Engineering and Industrial Management) for have made available the human, the materials and the financial resources essential for the execution of this work.

I would like to express my gratitude to the European Union for the financial support given to this work through the Projects: "EREBIO – Emission reduction from engines and transmissions substituting harmful additives in biolubricants by triboreactive materials" (Proposal nº. GRD2-2001-50119, Contract Nº G3RD-CT-2002-00796-EREBIO) and "BIOMON – Towards long-life biolubricants using advanced design and monitoring tools" (Proposal nº 508208, Contract nº COOP-CT-2004-508208).

My sincere gratitude to the folloing persons, companies and instituitions, for their support during this work:

- Mrs. Amaya Iguarta, from *Fundation TEKNIKER*, in Eibar, Spain,
- Mr. Álvaro Brito, from *A. BRITO, Indústria Portuguesa de Engrenagens, Lda*, in Porto, Portugal;
- Mr. Rolf Luther, from FUCHS PETROLUB AG, in Mannheim, Germany;
- Mr. Harold Bock, from ROWE MINERALÖLWERK GMBH, in Bubenheim, Germany.

Finally, I am indebted to my family and friends for their encouragement and support.

To my parents,

NOMENCLATURE

Symbol	Designation	Units
A_{base}	Base support area	m^2
A_h	Horizontal surface area of case	m^2
A_i	Immersed area	m^2
A_{rad}	Radiation surface area of case	m^2
A_v	Vertical surface area of case	m^2
C	Lubricant constant (see Table 3.8)	N/s.°K
$CPUC$	Ferrometry index for the concentration of wear particles	/
D	Bearing mean diameter	m
DL	Ferrometry index for the amount of large particles	/
DS	Ferrometry index for the amount of small particles	/
E^*	Equivalent Young Modulus	Pa
F_a	Axial force	N
F_{bt}	Tooth normal force, transverse section	N
F_r	Radial force	N
F_R	Froud number	/
$ISUC$	Ferrometry index for the severity of wear large particles	/
K_f	Lubricant thermal conductivity	W/(m.°K)
K_{FZG}	FZG load stage	/
L	Thermal parameter	/
L_{ca}	Characteristic horizontal length	m
L_t	Total roughness measurement length	mm
M_{r1}	Peak material ratio	%
M_{r2}	Valley material ratio	%
N	Input rotating speed	rpm
P_0	Contact pressure	Pa
P_{fr}	Gear friction losses	W
P_{in}	Input power	W
P_{M0}	Bearing load dependent losses	W
P_{M1}	Bearing no load dependent losses	W
P_{sl}	Seal losses	W
P_{spl}	Gear churning losses	W
PLP	Ferrometry index for the percentage of large particles	/
Q_{cn}	Heat removal by conduction	W
Q_{rad}	Heat removal by radiation	W
Q_{ncn}	Heat removal by natural convection	W
R_a	Roughness average (DIN 4768, ISO 4287)	µm
Re	Reynolds number	

R_k	Core roughness depth (DIN 4776)	µm
R_{max}	Maximum peak-to-valley height (DIN 4768)	µm
R_{pk}	Reduced peak height (DIN 4776)	µm
R_{vk}	Reduced valley depth (DIN 4776)	µm
R_q	RMS roughness average (DIN 4768, ISO 4287)	µm
R_X	Equivalent radius	m
$R_{Z\text{-}D}$	Mean peak-to-valley height (DIN 4768)	µm
T	Distance from contact point to pitch point of contact line	m
T_0	Oil bath temperature	°C
T_a	Ambient temperature	°K
T_{CR}	Critical lubricant temperature	°C
T_w	Wall temperature	°K
T_{wheel}	Wheel torque	N.m
U_1	Pinion surface speed	m/s
U_2	Wheel surface speed	m/s
VI	Lubricant Viscosity Index	/
V_{oil}	Oil volume	m^3
V_S	Sliding rate	m/s
X_L	Lubricant factor	/

a	Constant from the viscosity equation (see Table 1.1)	cSt
a_1	Constant from the piezoviscosity equation (see Table 1.1)	bar
a_2	Constant from the piezoviscosity equation (see Table 1.1)	bar/°C
b	Face width	mm
b_1	Constant from the piezoviscosity equation (see Table 1.1)	/
b_2	Constant from the piezoviscosity equation (see Table 1.1)	1/°C
c	Constant from equation (5.15)	/
c_1	Constant from equation (5.16)	/
d	Dilution factor	/
d_P	Pitch diameter	m
d_i	Shaft diameter	m
$f_{0,1}$	Coefficients for bearings losses	/
f_{cn}	Conduction factor	/
g_a	Length of recess path	m
g_f	Length of approach path	m
h_0	Lubricant film thickness	µm
h_{0T}	Corrected lubricant film thickness	µm
h_{ca}	Height of case	m
h_h	Natural convection coefficient, horizontal surface	$W/(m^2.K)$
h_v	Natural convection coefficient, vertical surface	$W/(m^2.K)$
m	Constant from the viscosity equation (see Table 1.1)	/

n	Constant from the viscosity equation (see Table 1.1)	/
p_b	Base pitch	m
z_1	Pinion teeth number	/
z_2	Wheel teeth number	/
α	Piezoviscosity coefficient (see Table 1.1)	Pa-1
α_{rad}	Radiation heat transfer coefficient	/
α_v	Thermal expansion (see Table 1.1)	g/(cm^3.°C)
β	Thermoviscosity (see Table 1.1)	cSt/°C
ε	Case surface emissivity	/
η	Dynamic viscosity	mPa.s
Λ	Specific lubricant film thickness (see 4.5.4)	/
λ_c	Cutt-off filter	mm
μ	Friction coefficient	/
μ_m	Average friction coefficient	/
ν	Kinematic viscosity (see Table 1.1)	mm^2/s
$\nu_{\Sigma c}$	Sum velocity at pitch point	m/s
ρ	Specific weight (see Table 1.1)	kg/m^3
ρ_c	Equivalent curvature radius at pitch point	mm
σ	Equivalent roughness	µm
Φ_T	Thermal correction factor	/

TABLE OF CONTENTS

ABSTRACT I

SUMÀRIO II

SOMMAIRE III

ACKNOWLEDGMENTS VII

NOMENCLATURE XI

TABLE OF CONTENTS XV

LIST OF FIGURES XIX

LIST OF TABLES XXVII

INTRODUCTION 1

1 GEAR OILS, GEAR MATERIALS AND GEAR TESTING 3

1.1 Gear oils 3

1.1.1 Chemical properties 3

1.1.2 Physical properties 3

1.1.3 Biodegradability and toxicity properties 4

1.2 Gear materials and surface coatings 6

1.2.1 Carburizing steel - DIN 20 MnCr 5 6

1.2.2 Nitriding steel – DIN 34 CrNiMo 6 7

1.2.3 Mechanical Properties of the tested gear materials 8

1.2.4 Disulfide Molybdenium – Titanium composite surface coating 9

1.3 Gear testing procedures 9

1.3.1 FZG test rig 9

1.3.2 FZG test gears 10

1.4 Post-testing analysis 11

1.4.1 Mass loss 11

1.4.2 Analytical ferrography and ferrometric wear indexes 11

1.4.3 Visual inspection 11

1.4.4 SEM 12

1.4.5 Surface roughness and topography 12

2 FOUR-BALL WEAR TESTS 13

2.1 Standard Test Method for Wear Preventive Characteristic of Lubricating Oils 13

2.2 Four-Ball wear test results 14

2.3 Discussion on Four-Ball test results 15

2.4 Four-Ball wear test conclusions 17

3 GEAR SCUFFING TESTS 19
3.1 Gear scuffing 19
3.2 Gear material and surface roughness 21
3.3 Gear scuffing test procedure 21
3.4 Gear scuffing results 22
3.5 Discussion on gear scuffing tests 24
3.5.1 FZG A20/16.6/90 gear scuffing test 24
3.5.2 FZG A10/16.6/90 gear scuffing test 27
3.5.3 Critical lubricant temperature T_{CR} - Scuffing analysis for gear lubricants 29
3.6 Conclusions on gear scuffing tests 31

4 GEAR MICROPITTING TESTS 33
4.1 Gear micropitting 33
4.2 Test gears 35
4.3 Gear micropitting test procedure 38
4.4 Gear micropitting results 39
4.4.1 Mass loss 39
4.4.2 Ferrometry 40
4.4.3 Analytical Ferrography 42
4.4.4 Visual inspection 45
4.4.5 Surface roughness 48
4.4.6 Surface topography 50
4.4.7 SEM analysis of the teeth flanks of the nitrided steel gears 55
4.5 Discussion on gear micropitting tests 58
4.5.1 Mass loss 58
4.5.2 Ferrometry 59
4.5.3 Analytical Ferrography 61
4.5.4 Lubricant film thickness 62
4.5.5 Micropitting area 63
4.5.6 SEM and surface topography 64
4.5.7 Gear Micropitting Failure Criteria 65
4.6 Conclusions on gear micropitting tests 67

5 GEAR POWER LOSS TESTS 69
5.1 Power loss inside a gearbox 69
5.2 Test gears 70
5.3 Gear power loss test procedure 71
5.4 Results 73
5.4.1 Carburized gears 73
5.4.1.1 Operating temperature 73
5.4.1.2 Mass loss 77

5.4.1.3 Oil analysis after test 78
5.4.1.3.1 Ferrometry 78
5.4.1.3.2 Analytical ferrography 79
5.4.1.3.3 After test kinematic viscosity 83
5.4.1.4 Visual inspection 83
5.4.1.5 Surface roughness 85
5.4.2 High pressure nitrided gears 89
5.4.2.1 Operating temperature 89
5.4.2.2 Mass loss 93
5.4.2.3 Oil analysis after test 93
5.4.2.3.1 Ferrometry 93
5.4.2.3.2 Analytical ferrography 94
5.4.2.4 Visual inspection 95
5.4.2.5 Surface roughness 97
5.5 Power loss model 99
5.5.1 Load dependent power losses 101
5.5.1.1 Gear friction losses 101
5.5.1.2 Bearing friction losses 101
5.5.2 No load power losses 101
5.5.2.1 Gear churning losses 101
5.5.2.2 Bearings churning losses 101
5.5.2.3 Seals power losses 102
5.5.3 Heat removal from the test box 102
5.5.3.1 Convection 102
5.5.3.2 Radiation 102
5.5.3.3 Conduction 103
5.5.4 FZG test gearbox simulation 103
5.5.4.1 Structure of the thermal balance model for the FZG test gearbox 103
5.5.4.2 Calculation of the friction coefficient 103
5.5.4.2.1 Carburized gears 104
5.5.4.2.2 High pressure nitrided gears 107
5.5.4.3 Updated friction coefficients 109
5.5.4.3.1 Carburized gears 109
5.5.4.3.2 High pressure nitrided gears 114
5.5.4.4 Friction coefficient comparison 118
5.5.4.4.1 Carburized gears 118
5.5.4.4.2 High pressure nitrided gears 123
5.6 Conclusions on FZG gear power loss tests 127

6 DISCUSSION AND CONCLUSIONS 129
6.1 Discussion 129
6.1.1 Four ball wear tests 129
6.1.2 FZG gear scuffing tests 129

6.1.3 FZG gear micropitting tests 129
6.1.4 FZG gear power loss tests 130
6.2 Conclusions 130
6.3 Future works: 131

REFERENCES 133

APPENDIX A – FOUR BALL TESTS DATA SHEETS 137

APPENDIX B – GEAR SCUFFING TESTS DATA SHEETS 145
FZG gear scuffing test of M1 gear oil using A20 gear 147
FZG gear scuffing test of M1 gear oil using A10 gear 149
FZG gear scuffing test of E1 gear oil using A20 gear 151
FZG gear scuffing test of E1 gear oil using A10 gear 153
FZG gear scuffing test of E2 gear oil using A20 gear 155
FZG gear scuffing test of E2 gear oil using A10 gear 157

APPENDIX C – GEAR MICROPITTING TESTS DATA SHEETS 159
FZG gear micropitting test of carburized gear lubricated by M1 gear oil (C-M1) 161
FZG gear micropitting test of carburized gear lubricated by E1 gear oil (C-E1) 166
FZG gear micropitting test of carburized gear lubricated by E2 gear oil (C-E2) 171
FZG gear micropitting test of carburized gear lubricated by E3 gear oil (C-E3) 176
FZG gear micropitting test of nitrided gear lubricated by M1 gear oil (N-M1) 181
FZG gear micropitting test of nitrided gear lubricated by E1 gear oil (N-E1) 187
FZG gear micropitting test of nitrided gear lubricated by E2 gear oil (N-E2) 193
FZG gear micropitting test of coated gear lubricated by M1 gear oil (Mo-M1) 199
FZG gear micropitting test of coated gear lubricated by E1 gear oil (Mo-E1) 204
FZG gear micropitting test of coated gear lubricated by E2 gear oil (Mo-E2) 209
Pinion tooth flank of a carburized gear after grinding and heat treatment 214
Pinion tooth flank of a nitrided gear after grinding and heat treatment 216

APPENDIX D – FZG GEAR POWER LOSS TESTS DATA SHEETS 219
FZG gear power loss test of carburized gear lubricated by M1 gear oil 221
FZG gear power loss test of carburized gear lubricated by E1 gear oil 223
FZG gear power loss test of carburized gear lubricated by E2 gear oil 225
FZG gear power loss test of carburized gear lubricated by E3 gear oil 227
FZG gear power loss test of nitrided gear lubricated by M1 gear oil 229
FZG gear power loss test of nitrided gear lubricated by E2 gear oil 231

LIST OF FIGURES

Figure 1.1 – Variation of lubricant viscosity with temperature (ASTM D341). 4

Figure 1.2 – Variation of lubricant density with temperature [6]. 4

Figure 1.3 - High pressure nitriding process parameters. 8

Figure 1.4 – Variation of the hardness with depth within the nitriding layer. 8

Figure 1.5- Picture and schematic view of the FZG Gear Test Rig. 10

Figure 1.6 - FZG type A (left) and type C (right) gears. 11

Figure 2.1 - Four-Ball Test Machine. 13

Figure 2.2 – Schematic view of the Four-Ball arrangement. 14

Figure 2.3 - Relation between Viscosity at 75°C and Wear Scar Diameters [μm].....16

Figure 2.4 - Average ISUC index vs. average wear scar diameter for the tested lubricants. 16

Figure 2.5 – Wear scar surface of each lubricant: (a) M1, (b) E1 and (c) E2.....17

Figure 3.1 - Evolution of the surface roughness of the teeth flanks during a standard FZG A20/8.3/90 scuffing test [19]. 20

Figure 3.2 - Evolution of the scuffing marks on the pinion teeth flanks during the standard test (FZG A20/8.3/90), from load stage K9 to load K11[19]. 20

Figure 3.3 – Scuffing load stage reached by each lubricant (in tests A20/16.6/90 and A10/16.6/90). 23

Figure 3.4 – Oil bath temperature at the end of the scuffing stage. 23

Figure 3.5 – Pinion mass loss.....23

Figure 3.6 - Oil bath temperature at the end of each load stage on A20/16.6/90 FZG gear scuffing tests. 25

Figure 3.7 - Roughness measurement location (a- radial direction; b- axial direction). 25

Figure 3.8 – Photography of tooth flanks after scuffing test FZG A20/16.6/90. 26

Figure 3.9 - Oil bath temperature at the end of each load stage on A10/16.6/90 FZG gear scuffing test. 27

Figure 3.10 – Photography of tooth flanks after scuffing test FZG A10/16.6/90.....28

Figure 3.11 – FZG type A gear geometry and reference points along mesh line[23]. 30

Figure 3.12 – $\mu P_{0B} V_s T_B$ as a function of oil bath temperature for point *B* of meshing line (pinion tip – wheel root). 30

Figure 4.1 - Rolling and sliding directions. a) Beginning of engagement. b) End of engagement [28].....35

Figure 4.2 – R_{ZD} calculated from the roughness measurements made in axial and radial directions on the teeth flanks of each tested gear after grinding and heat treatment.....37

Figure 4.3 – R_a calculated from the roughness measurements made in axial and radial directions on the teeth flanks of each tested gear after grinding and heat treatment.....37

Figure 4.4 – R_{PK} calculated from the roughness measurements made in axial and radial directions on the teeth flanks of each tested gear after grinding and heat treatment.....37

Figure 4.5 – Mass loss results. 40

Figure 4.6 - Evolution of the *CPUC* index during the gear micropitting tests. 41

Figure 4.7 – Evolution of the *ISUC* index during the gear micropitting tests. 41

Figure 4.8 – Example of a large size wear particle found in the lubricant sample collected after load stage K3 of the C-M1 micropitting test (magnification 1000x). 44

Figure 4.9 - Example of small wear particles found in the lubricant sample collected after load stage K6 of the C-M1 micropitting test (magnification 1000x). 45

Figure 4.10 - Friction polymer detected in N-E2 micropitting test after load stage K8 (magnification 1000x).....45

Figure 4.11 - Roughness measurements location (a- radial direction; b- axial direction). ..48

Figure 4.12 – Pinion roughness profiles measured after load stage K8 along the axial direction and below pitch line.....49

Figure 4.13 – Pinion roughness profiles measured after load stage K9 along the axial direction and below pinion pitch line. 50

Figure 4.14 - Topography measurements location. 51

Figure 4.15 – Topography measurements in the carburized gears. 52

Figure 4.16 - Topography measurements in the high pressure nitrided gears.....53

Figure 4.17 - Topography measurements in the coated gears. 53

Figure 4.18 - Cumulative mass loss for the three lubricants during gear micropitting tests. 59

Figure 4.19 - Cumulative *CPUC* ferrometric index during micropitting test (d=0.1). 60

Figure 4.20 - Cumulative *CPUC* vs. cumulative mass loss during gear micropitting tests....60

Figure 4.21 - Lubricant film thickness along the gear meshing line. 63

Figure 4.22 - Evolution of the micropitted area during gear micropitting tests. 64

Figure 4.23 – Percentage of area of micropitts with a depth greater than 5 μm presented in Table 4.18 having into account each gear material. 65

Figure 4.24 - Failure criteria according to FVA [14], after load stage K8.....66

Figure 4.25 - Failure criteria according to FVA [14], after load stage K9.....66

Figure 5.1 – Test box of the FZG gear test rig (opened).....70

Figure 5.2 - Oil sump temperature during tests with carburized gears (vertical – temperature in ºC, horizontal – time in hours, gear wheel speed and torque indicated).....74

Figure 5.3 - Stabilized oil bath temperature *vs.* input speed and input torque measured during the tests with the carburized gears. 75

Figure 5.4 - Stabilized oil sump temperature vs. input power. 76

Figure 5.5 - Stabilized oil sump temperature *vs.* wheel torque. 76

Figure 5.6 - Stabilized oil sump temperature *vs.* wheel speed. 77

Figure 5.7 - Gear mass loss measurements expressed in g per 10^6 cycles (carburized gears).....77

Figure 5.8 - Evolution of *DL* and *DS* wear particles indexes during the power loss tests with carburized gears. 79

Figure 5.9 - Evolution of *CPUC* and *ISUC* wear particles indexes during the gear power loss tests with the carburized gears. 79

Figure 5.10 - Example of small size wear particles and some brilliant contact fatigue particles of larger size present in the M1 gear oil sample collected after load stage k7 (Magnification = 200x, *d*=0.1). 80

Figure 5.11 - Friction polymers detected in the E1 ester oil sample collected after load stage k7 (Magnification 1000X; *d*=0.1).....80

Figure 5.12 - Small wear particles involved by friction polymers (E1 lubricant after load stage 9; Magnification 1000X; *d*=0.01). 82

Figure 5.13 - Friction polymers detected in the E2 ester oil sample collected after load stage k7 (Magnification 1000X; *d*=0.1).....82

Figure 5.14 - Non-metallic compounds found in the M1 mineral oil sample after load stage K9 (Magnification 1000X; *d*=0.1). 82

Figure 5.15 - Flank of a carburized gear pinion tooth after manufacturing, showing grinding marks. 84

Figure 5.16 - Flank of a carburized gear pinion tooth after test using the reference mineral oil. 84

Figure 5.17 - Flank of a carburized gear pinion tooth after test using the E1 lubricant (scuffing marks are observed above the pitch line. 84

Figure 5.18 - Flank of a carburized gear pinion tooth after test using the E2 lubricant.....85

Figure 5.19 - Flank of a carburized gear pinion tooth after test using the E3 lubricant.....85

Figure 5.20 - Roughness profiles measured in axial direction above pitch line (carburized gears). 86

Figure 5.21 - Roughness profiles measured in axial direction below pitch line (carburized gears). 86

Figure 5.22 - Roughness profiles measured in radial direction above pitch line (carburized gears). 88

Figure 5.23 - Roughness profiles measured in radial direction below pitch line (carburized gears). 88

Figure 5.24 - Oil sump temperature during tests with nitrided gears (vertical – temperature in ºC, horizontal – time in hours, gear wheel speed and torque indicated).....90

Figure 5.25 - Stabilized oil bath temperature *vs.* input speed and input torque measured during the tests with the carburized and nitrided gears. 91

Figure 5.26 - Stabilized oil sump temperature vs. input power (nitrided gears). 91

Figure 5.27 - Stabilized oil sump temperature *vs.* wheel torque (nitrided gears).....92

Figure 5.28 - Stabilized oil sump temperature *vs.* wheel speed (nitrided gears).....92

Figure 5.29 - Gear mass loss measurements expressed in g per 10^6 cycles (nitrided gears).....93

Figure 5.30 - Evolution of *DL* and *DS* wear particles indexes during the power loss tests of nitrided gears. 93

Figure 5.31 - Evolution of *CPUC* and *ISUC* wear particles indexes during the gear power loss tests of nitrided gears. 94

Figure 5.32 - Flank of a nitrided gear pinion tooth after manufacturing, showing grinding marks. 95

Figure 5.33 - Flank of a nitrided gear pinion tooth after test using the reference mineral oil. 96

Figure 5.34 - Flank of a nitrided gear pinion tooth after test using the E2 ester oil. 96

Figure 5.35 - Flank of a nitrided gear wheel tooth after test using the reference mineral oil M1. 96

Figure 5.36 - Roughness profiles measured in axial direction above pitch line (nitrided gears).....97

Figure 5.37 - Roughness profiles measured in axial direction below pitch line (nitrided gears).....97

Figure 5.38 - Roughness profiles measured in radial direction above pitch line (nitrided gears).....98

Figure 5.39 - Roughness profiles measured in radial direction below pitch line (nitrided gears).....98

Figure 5.40 – Forms of power loss and heat evacuation of the FZG test box. 100

Figure 5.41 - Program structure for friction coefficient parameters optimization. 104

Figure 5.42 – Stabilization temperature for reference mineral oil: experimental vs. numerical values (carburized gears, X_L=1). 105

Figure 5.43 - Stabilization temperature for ester oil E1: experimental vs. numerical values (carburized gears, X_L=1)..... 105

Figure 5.44 – Stabilization temperature for ester oil E2: experimental vs. numerical values (carburized gears, X_L=1)..... 106

Figure 5.45 – Stabilization temperature for ester oil E3: experimental vs. numerical values (carburized gears, X_L=1)..... 106

Figure 5.46 – Stabilization temperature for reference mineral oil: experimental vs. numerical values (nitrided gears, X_L=1). 107

Figure 5.47 – Stabilization temperature for ester oil E2: experimental vs. numerical values (nitrided gears, X_L=1). 108

Figure 5.48 - Experimental vs. numerical stabilization temperature of the reference mineral oil, for each load stage and operating speed (carburized gears).... 110

Figure 5.49 - Experimental vs. numerical stabilization temperature of the E1 ester oil, for each load stage and operating speed (carburized gears)..... 110

Figure 5.50 - Experimental vs. numerical stabilization temperature of the E2 ester oil, for each load stage and operating speed (carburized gears)..... 111

Figure 5.51 - Experimental vs. numerical stabilization temperature of the E3 ester oil, for each load stage and operating speed (carburized gears)..... 111

Figure 5.52 - Numerical stabilization temperature for each load stage for the four lubricants (Carburized gears; Troom=25ºC)..... 112

Figure 5.53 - Updated vs. Standard friction coefficient for reference mineral oil (carburized gears). 112

Figure 5.54 - Updated vs. Standard friction coefficient for the E1 ester oil (carburized gears)..... 113

Figure 5.55 - Updated vs. Standard friction coefficient for the E2 ester oil (carburized gears)..... 113

Figure 5.56 - Updated vs. Standard friction coefficient for the E3 ester oil (carburized gears)..... 114

Figure 5.57 - Experimental vs. numerical stabilization temperature of the reference mineral oil, for each load stage and operating speed (nitrided gears). 115

Figure 5.58 - Experimental vs. numerical stabilization temperature of the E2 ester oil, for each load stage and operating speed (nitrided gears)..... 115

Figure 5.59 - Numerical stabilization temperature for each load stage for the lubricants M1 and E2 (carburized gears and nitrided gears; Troom=25ºC)..... 116

Figure 5.60 - Updated vs. Standard friction coefficient for reference mineral oil (nitrided gears). 117

Figure 5.61 - Updated vs. Standard friction coefficient for the E2 ester oil (nitrided gears)..... 117

Figure 5.62 - Friction coefficient at stabilization temperatures with carburized gears. .. 118

Figure 5.63 - Friction coefficient reduction at stabilization temperatures provided by the ester oils in comparison to the reference mineral oil with carburized gears at stabilization temperatures. 119

Figure 5.64 - Power losses distribution as function of load at 2000 rpm for reference mineral oil (M1) with carburized gears and at stabilization temperatures... 120

Figure 5.65 - Power losses distribution as function of load at 2000 rpm for Ester E1 with carburized gears and at stabilization temperatures..... 120

Figure 5.66 - Power losses distribution as function of load at 2000 rpm for Ester E2 with carburized gears and at stabilization temperatures..... 121

Figure 5.67 - Power losses distribution as function of load at 2000 rpm for Ester E3 with carburized gears and at stabilization temperatures..... 121

Figure 5.68 - Power losses as function of load at 2000 rpm and with carburized gears at stabilization temperatures. 122

Figure 5.69 – Global efficiency vs FZG Load stage (with carburized gears at stabilization temperatures)..... 122

Figure 5.70 - Friction coefficient at stabilization temperatures of nitrided and of carburized gears. 123

Figure 5.71 - Friction coefficient reduction at stabilization temperatures provided by the E2 ester oil with both materials and by the mineral oil with the nitrided steel in comparison to the mineral oil with the nitrided and the carburized gears (at stabilization temperatures)..... 124

Figure 5.72 - Power losses distribution as function of load at 2000 rpm for reference mineral oil (M1) with nitrided gears (at stabilization temperatures). 125

Figure 5.73 - Power losses distribution as function of load at 2000 rpm for Ester E2 with nitrided gears (at stabilization temperatures). 125

Figure 5.74 - Power losses as a function of load at 2000 rpm and with nitrided of the carburized gears at stabilization temperatures. 126

Figure 5.75 – Global efficiency vs FZG Load stage (of the nitrided and the carburized gears at stabilization temperatures)..... 126

LIST OF TABLES

Table 1.1 – Lubricant properties. 5

Table 1.2 – Nominal chemical composition (weight %) of the 20 MnCr 5 carburizing steel. 6

Table 1.3 – Physical properties (average values) at ambient temperature of the 20 MnCr 5 carburizing steel..... 6

Table 1.4 - Average thermal expansion coefficient between 20 ºC and X ºC [in 10 exp(-6) m/(m.K)]. 6

Table 1.5 - Heat treatment steps for the 20 MnCr 5 carburizing steel. 6

Table 1.6 - Nominal chemical composition (weight %) of the 34 CrNiMo 6 steel. 7

Table 1.7 - Physical properties (average values) at ambient temperature of the 34 CrNiMo 6 steel..... 7

Table 1.8 – High pressure nitriding process parameters. 7

Table 1.9 – Mechanical properties of 20 MnCr 5 and 34 CrNiMo 6 materials. 8

Table 1.10 - Geometry of the FZG test gears: Types A20, A10, C14, $C14^{R}$. 10

Table 2.1 – Four-Ball wear test results. 15

Table 2.2 - Ferrography analysis for the tested lubricants. 15

Table 3.1- Factors influencing gear scuffing [19]. 21

Table 3.2 – Average value of roughness parameters for FZG type A gears used in the scuffing tests. 21

Table 3.3 – Operating conditions during the performed scuffing tests. 22

Table 3.4 – A20/16.6/90 gear scuffing test results with lubricants M, E1 and E2. 25

Table 3.5 - Surface roughness measurements on tooth surface before and after the FZG A20/16.6/90 scuffing test- axial direction. 26

Table 3.6 – A10/16.6/90 gear scuffing test results with lubricants M, E1 and E2. 27

Table 3.7 - Surface roughness measurements on tooth surface before and after the FZG A10/16.6/90 scuffing test- axial direction. 29

Table 3.8 – Critical temperature for each industrial gear lubricant tested. 30

Table 4.1 - Factors influencing micropitting, range of influence and suggested remedies [24, 26]. 33

Table 4.2 - Approximate FZG load stage values for conversion of test results in the micro-pitting test [27]. 34

Table 4.3 - Pitting and micropitting conditions. 35

Table 4.4 - Gear quality grade and average surface roughness (pinion and wheel).....36

Table 4.5 - Specific film thickness for standard and performed tests.....36

Table 4.6 – Micropitting tests codification. Test references, materials and lubricants combinations.....38

Table 4.7 - Operating conditions of gear micropitting tests (* at pitch point).....39

Table 4.8 - Ferrograms obtained after each load stage of micropitting tests with carburized gears. (Magnification = 100 x; *d*=0.1).....42

Table 4.9 - Ferrograms obtained after each load stage of micropitting tests with nitrided gears. (Magnification = 100 x; *d*=0.1).....43

Table 4.10 - Ferrograms obtained after each load stage of micropitting tests with coated gears. (Magnification = 100 x; *d*=0.1).....44

Table 4.11 - Visual inspection: Carburized steel.....46

Table 4.12 - Visual inspection: High pressure nitrided steel.....47

Table 4.13 - Visual inspection: Carburized steel with a MoST coating.....47

Table 4.14 - R_{ZD} and R_{VK} roughness parameters calculated from the measurements made after load stage k8 along the axial direction, below pinion pitch line (values in μm).....49

Table 4.15 - R_{ZD} and R_{VK} roughness parameters calculated from the measurements made after each load stage k9 along the axial direction, below pinion pitch line (values in μm).....50

Table 4.16 – Representative unfiltered roughness profiles selected from the topography measurements after load stage K9 (vertical axis units: μm; horizontal axis units: mm).....54

Table 4.17 – Roughness parameter corresponding to the profiles presented in Table 4.16 (values in μm).....55

Table 4.18 – Micropitts deeper than 5 μm.....56

Table 4.19 - SEM micrographs and topography measurements (H. P. Nitrided gears).....57

Table 4.20 - SEM micrographs of cut teeth (H. P. Nitrided gears).....58

Table 4.21 - Analytical ferrography after load stage 9 (d=0.1; magnification: 100X).....61

Table 4.22 - Viscosity and piezoviscosity coefficient of the four lubricants at operating temperature.....63

Table 5.1 - Gear quality grade and average surface roughness (pinion and wheel).....70

Table 5.2 - Specific film thickness between gear teeth: standard *vs* used gears.....71

Table 5.3 - Operating conditions used in the power loss gear tests (FZG test rig – type C gears).....72

Table 5.4 – Gear power loss tests codification. Material and lubricant combinations and test references.....72

Table 5.5 - Ferrogram pictures of the lubricant samples collected during the tests with the carburized gears (Magnification = 100x).....81

Table 5.6 – Lubricant viscosity before and after test (with carburized gears). 83

Table 5.7 – Average roughness parameters measured in axial direction [μm]. 86

Table 5.8 – Average roughness parameters measured in radial direction [μm]. 88

Table 5.9 - Ferrogram pictures of the lubricant samples collected during the tests of the high pressure nitrided gears (Magnification = 100x). 94

Table 5.10 – Average roughness parameters measured in axial direction [μm]. 98

Table 5.11 - Average roughness parameters measured above pitch line in radial direction [μm].....98

Table 5.12 – Values of c_1 of each lubricant (obtained from the tests with carburized gears)..... 109

Table 5.13 – Values of c_1 of each lubricant (obtained from the tests of the nitrided gears)..... 114

INTRODUCTION

High performance lubricants are reaching their technologic limits especially in mixed and boundary lubrication conditions, having high cost. These fluids are mineral based or synthetic hydrocarbons with a large additive package (up to 20%). In these classic additivated lubricants, the chemical reactions of the additives with metallic surfaces guarante reactive layers, which support the load and promote anti-wear protection and friction reduction. At the same time, a growing environmental awareness is leading to an increasing interest in biodegradable low toxicity lubricants [1]. Environmental compatibility is usually viewed in respect to biodegradability and toxicity. While the first issue is reached by using a suitable biodegradable base fluid, low toxicity requires an additivation that is environmentally friendly [2], too.

In the new approach, the fluid continues promoting the hydrodynamic lubrication, the heat transfer and the wear particles removal from the contact. The anti-wear properties required to the fluid will be obtained through a low toxicity additivation and may be reduced. On the other hand, biodegradable and non-toxic properties will be demanded. Lubricant performance (friction, wear, lifetime, load bearing capacity, efficiency etc.) has also a major impact on its overall environmental compatibility and should not be neglected, since premature wear and high energy needs are as well harmful to the environment.

The low-toxicity biodegradable lubricants (base oil and additives) could be combined with tribo-reactive materials (surface coatings in the industrial base materials) to improve the protection against wear, scuffing and contact fatigue.

Coatings and surface treatments are used with success in several industrial applications to decrease the wear and/or the friction. This work intends that these surface treatments partially replace the highly toxic additives (extreme pressure (EP) and anti-wear additives). The additional cost of the surface treatments must be compensated with an increase of the product's life time, quality, efficiency and resulting in environmental benefits.

The tribo-reactive materials or surface coatings with low friction coefficient MoS_2 based were used in gears to be tested together with the biodegradable and low-toxicity lubricants. High Pressure Nitrided Steel was used due its potential self-lubricant properties. The proposed coating is constituted by MoS_2 and Titanium (designated as MoST) and was deposited on carburized gears made of a carburizing steel (DIN 20MnCr5).

The main objective of this work is to show that biodegradable and low-toxicity lubricant formulations (base lubricant and additives) derived from renewable resources can be successfully used in mechanical transmissions, since the materials are adapted to the tribologic properties of these lubricants. The assessment of th mechanical performance of these environemental friendly oil formulations, measured in terms of gear wear, scuffing, micropitting and power loss, will be used as criteria for the suitability of such lubricants for gear transmissions. These results will be of great importance, since the actual limit of 7% to the harmful constituents of eco-labelled lubricants is very high and an ecologically acceptable lubricant in the long term will be free of pernicious constituents.

This dissertation is divided into six chapters. Chapter 1 presents the gear oils, the FZG test rig and the test gears. The following four chapters (2 to 5) present a literature review and the experimental analysis that was carried out in order to evaluate the tribologic performance of gear oils in terms of wear, scuffing load capacity, gear micropitting and gear power loss (each chapter corresponds to one specific test). The last chapter presents the final conclusions.

Chapter 1 presents the four industrial gear oils under study, the main test rig, and the gear geometry and gear materials used in the several gear tests. It also describes the ferrometric wear indexes used to analyse the lubricant samples collected during the gear tests.

Chapter 2 presents Four-Ball Wear Tests that were made to determine the relative wear preventive properties of several mineral and ester biodegradable lubricants. The results obtained through the wear scar diameter measurements and ferrography analysis was used to establish the behaviour of the tested lubricants.

Chapter 3 presents a literature review on gear scuffing, the experimental methodology carried out to determine the scuffing load carrying capacity of the mineral and ester biodegradable lubricants. The analysis of lubricant behaviour in extreme conditions (high pressure, temperature and rotations) was used to estimate their performance in real applications. Finally, the Critical Temperature Scuffing Criterion was used to determine the Critical Temperature characteristic of each lubricant.

Chapter 4 presents a literature review on gear micropitting and the experimental methodology that was followed to evaluate gear micropitting performance of each material/lubricant combination. The micropitting evaluation during the tests is performed using accurate mass loss measurements, Ferrometric oil analysis, inspection of active teeth flanks, surface roughness, topography measurements and SEM analysis.

Chapter 5 presents a literature review about power losses inside a gearbox and describes the FZG power losses tests performed in order to compare the energetic performance of the four industrial gear oils. An energetic model of the FZG test gearbox was used and updated, integrating the mechanisms of power dissipation and heat evacuation, and allowing the determination of oil operating temperature in steady state conditions. The protection against wear provided by each lubricant is also compared.

Chapter 6 presents a general overview of the conclusions corresponding to each specific test and presents the final conclusions.

CHAPTER 1

1 GEAR OILS, GEAR MATERIALS AND GEAR TESTING

1.1 Gear oils

Four industrial gear lubricants were tested and compared: a reference ISO VG 150 mineral oil, containing an additive package to improve micropitting resistance, and three ISO VG 100 ester lubricants, two of them biodegradable with a low toxicity additivation based on harvestable materials. The four oils were formulated as CLP gear oils according to DIN 51517. The main properties of the lubricants used are shown in Table 1.1.

1.1.1 Chemical properties

The reference gear lubricant is based on a paraffinic mineral oil with significant residual sulphur content. It contains an ashless antiwear additive package based on phosphorous and sulphur chemistry and metal-organic corrosion preventives.

In contrast, the other three fluids use an ester base (fully saturated in the case of the E1 and E3 fluids and highly saturated in the case of the E2 lubricant). The absence of unsaturated bonds in these base fluids leads to excellent thermal and oxidative stability. To combine the desired low toxicity with superior gear performance, environmentally compatible, highly efficient additives were added and metal-organic compounds had been completely avoided.

The additive content of the mineral oil is considerably higher than the one of the ester oils, mainly in what concerns the sulphur compounds [3, 4].

E3 fluid is formulated with special, synergistically acting 'PD' additives (Plastic Deformation Technology) which create a smoothing effect in gear sets, in machine elements under load. The additives are based on special mild sulfur components, selected surface-active phosphorus components, special zincdialkyldithiophosphates and liquid, mineral oil-soluble molybdenum components.

1.1.2 Physical properties

The four gear oils have significantly different physical properties. They have almost identical viscosities at 100°C but the ester gear oils have much lower viscosity at lower temperatures, (ester products show higher viscosity index). This beneficial property leads to a wider range of operational temperature when ester oil replaces mineral oil.

Thermal expansion and density of the ester gear oils are higher than those of the mineral oil.

The pressure-viscosity parameter is always larger for the mineral oils than for the ester oils and must be accounted in terms of EHD film thickness [5].

Figure 1.1 and Figure 1.1 show, respectively, the variation of the Kinematic viscosity (ν) and density (ρ) with temperature for all lubricants. Between 60 ºC and 100 ºC the kinematic viscosities (ν) of the all lubricants are very similar. The density of the sster oils are significantly higher than the one of the mineral oil at all temperatures.

1.1.3 Biodegradability and toxicity properties

Standardized and internationally recognized test methods are available for determining the biodegradability (OECD 301B) and environmental toxicity (OECD 201, OECD 202) of lubricants and their components. The mineral oil doesn't match the minimum requirements of 60% biodegradability in 28 days. The ester based oils E1 and E2 show >60% biodegradability according to OECD 301 F (min. 60% are required) in 28 days and pass both toxicity tests. The values ofr lubricant E3 are not available yet.

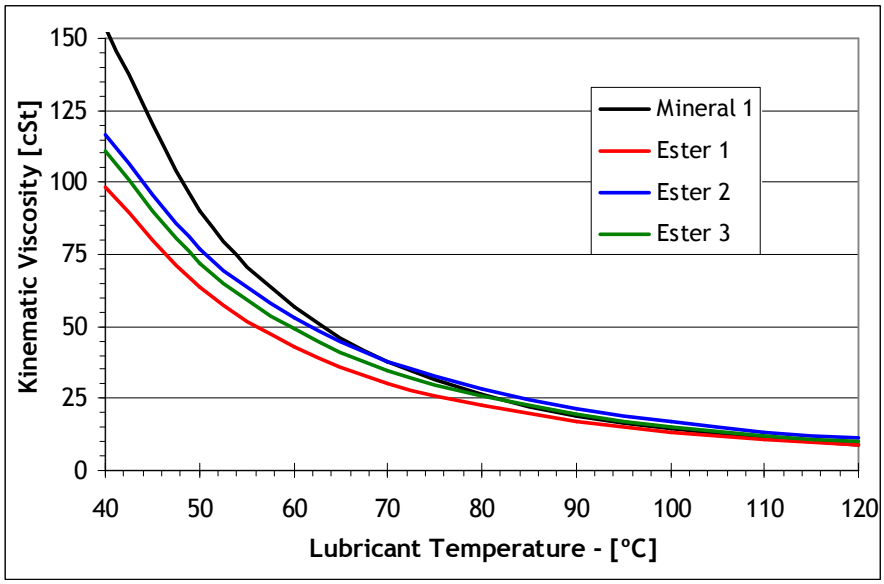


Figure 1.1 – Variation of lubricant viscosity with temperature (ASTM D341).

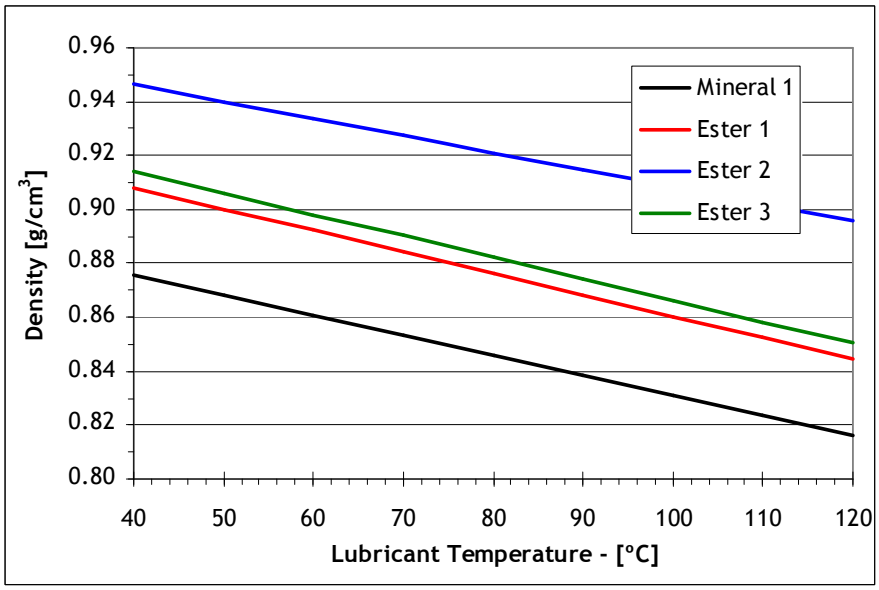


Figure 1.2 – Variation of lubricant density with temperature [6].

Table 1.1 – Lubricant properties.

Parameter	*Method*	*Desig*	*Units*	*Lubricating Oils*			
Lubricant maker				EXXON MOBIL	FUCHS PETROLUB	ROWE	FUCHS PETROLUB
Country				USA	Germany	Germany	Germany
Oil type		/	/	Industrial gear oil			
Base oil	DIN 51451	/	/	Paraffinic mineral oil	Fully saturated ester	Highly saturated ester	Fully saturated ester
Lubricant reference				**M1** (Mineral 1)	**E1** (Ester 1)	**E2** (Ester 2)	**E3** (Ester 3)
Chemical Content							
Zinc	ASTM D 4927	**Zn**	ppm	-	-	-	na
Calcium	ASTM D-4927	**Ca**	ppm	40	-	-	na
Phosphor	ASTM D-4927	**P**	ppm	175	146	300	na
Sulphur	ASTM D-4927	**S**	ppm	15040	180	5500	na
Physical properties							
Density @ 15ºC	DIN 51757	ρ_{15}	g/cm^3	0.894	0.928	0.962	0.934
Kinematic Viscosity @ 40 ºC	DIN 51562	ν_{40}	cSt	153.6	98.4	116.6	110.9
Kinematic Viscosity @ 100 ºC	DIN 51562	ν_{100}	cSt	14.4	13.3	16.9	15.2
Viscosity Index	DIN ISO 2909	***VI***	/	96	152	162	156
Pour point	DIN ISO 3106		ºC	-27	-42	<-30	na
Viscosity and density equations							
Viscosity [7]		**n**	/	3.5268	3.1635	2.8947	3.0404
$LogLog(\nu + a) = m - n.Log(T)$	ASTM D341	**m**	/	9.1413	8.1917	7.5397	7.8988
		a	cSt	0.7	0.7	0.7	0.7
Thermoviscosity [7]		β_{40}	cSt/ºC	0.0570	0.0468	0.0443	0.0461
$\beta = \frac{m}{T} \times \frac{(\nu + a) * Ln(\nu + a)}{\nu}$		β_{100}	cSt/ºC	0.0269	0.0236	0.0232	0.0236
Piezoviscosity [8]		a_1	bar	367		477	
		a_2	bar/ºC	2.96		6.18	
$\alpha(p,T) = \frac{1}{a_1 + a_2 * T + (b_1 + b_2 * T) * p}$		b_1	/	9.98×10^{-3}		3.93×10^{-3}	
		b_2	1/ºC	2.07×10^{-4}		-4.01×10^{-4}	
Thermal expansion [7] $\rho = \rho_{ref}\left[1 - \alpha_v \cdot (T - T_{ref})\right]$		α_v	g/cm^3 ºC	8.26×10^{-4}	8.58×10^{-4}	6.56×10^{-4}	8.53×10^{-4}
Wear properties							
KVA weld load	DIN 51350-2	/	N	2200	2200	-	na
KVA wear scar (1h/300N)	DIN 51350-3	/	mm	0.32	0.35	-	na
Brugger	DIN 51347-2	/	N/mm^2	68	37	-	na
FZG rating	DIN 513540	K_{FZG}	/	>12	?	>12	na
Biodegradability and toxicity properties							
Ready biodegradability	OECD, 301 F		%	<60	≥60	≥60	na
Aquatic toxicity with *Daphnia*	OECD, 202	EL_{50}	mg/l	>1000	>100	>100	na
Aquatic toxicity with *Algae*	OECD, 201	EL_{50}	[mg/l]	>100	>100	>100	na

1.2 Gear materials and surface coatings

The gears used in this work were manufactured using two different materials: carburizing steel and high pressure nitriding steel. Carburized steel gears, coated with molybdenum disulfide - titanium (MoS_2/Ti) composite coating, were also used.

1.2.1 Carburizing steel - DIN 20 MnCr 5

Gears and other highly stressed mechanical components are often made of carburizing steel. In this case the gears were manufactured using DIN 20 MnCr 5 steel. Gears were carburized, quenched in oil and annealed before the final grinding operation as described in Table 1.5.

The nominal chemical composition (weight %) of the 20 MnCr 5 carburizing steel is presented in Table 1.2 and its physical properties are given in Table 1.3 and Table 1.4. The average thermal expansion coefficient for this material is presented in Table 1.4 for several temperature ranges.

The heat treatment generate a carburized depth of **0.8 mm** and a surface hardness **58 – 62 HRC**. The surfaces had a very high hardness, typically around 60 HRC, while the core kept a very high strength and a considerably high elongation. This is a common solution for gear manufacturing.The main applications of the 20 MnCr 5 carburizing steel are highly stressed parts, such as gears, crankshafts, bushings …

Table 1.2 – Nominal chemical composition (weight %) of the 20 MnCr 5 carburizing steel.

C	*Si*	*Mn*	*Cr*	*Mo*	*Ni*	*V*	*W*	*Others*
0.20	0.20	1.25	1.15	-	-	-	-	-

Table 1.3 – Physical properties (average values) at ambient temperature of the 20 MnCr 5 carburizing steel.

Parameter	*Units*	*Value*
Modulus of elasticity	[10 exp(3) N/mm^2]	210
Density	[g/cm^3]	7.85
Thermal conductivity	[W/m.K]	42.0
Specific electric resistivity	[Ohm mm^2/m]	0.16
Specific heat capacity	[J/g.K]	0.46

Table 1.4 - Average thermal expansion coefficient between 20 ºC and X ºC [in 10 exp(-6) m/(m.K)].

Temperature range	*100 ºC*	*200 ºC*	*300 ºC*	*400 ºC*	*500 ºC*
Average thermal expansion coefficient	11.1	12.1	-	-	-

Table 1.5 - Heat treatment steps for the 20 MnCr 5 carburizing steel.

Heat treatment step	Temperature	Time period
Pre-heating	100 ºC;	
Austenitization	900 ºC;	
Carburizing temperature	900 – 950 ºC	05:00 h
Diffusion during cooling	from carburising temperature to 860 ºC	02:30 h
Stabilisation before quenching	860 ºC	00:30 h
Quenching in oil:	60ºC;	
Tempering temperature	220ºC	01:00 h

1.2.2 Nitriding steel – DIN 34 CrNiMo 6

The main applications of the 34 CrNiMo 6 steel are permanently stressed machine elements, engine and vehicle parts, where high strength and toughness are required. This steel can be nitrided at temperatures below 550 ºC.

Gears are often manufactured in nitriding steel. In this case the gears were manufactured in DIN 34 CrNiMo 6 steel and submitted to high pressure nitriding. The nominal chemical composition (weight %) of the 34 CrNiMo 6 nitriding steel is presented in Table 1.6 and its physical properties are given in Table 1.7.

The gears were machined and grinded to their final dimensions before the high pressure nitriding heat treatment. The high pressure nitriding process parameters for the heat treatment of the 34 CrNiMo 6 steel are given in Table 1.8 and shown in Figure 1.3.

A laboratory specimen was analyzed to study the thickness of the nitriding layer. The results are shown in Figure 1.4. The thickness of the nitriding layer is **0.3 mm** and the surface hardness is **32 HRC**.

Table 1.6 - Nominal chemical composition (weight %) of the 34 CrNiMo 6 steel.

C	*Si*	*Mn*	*Cr*	*Mo*	*Ni*	*V*	*W*	*Others*
0.34	0.20	0.65	1.50	0.23	1.50	-	-	-

Table 1.7 - Physical properties (average values) at ambient temperature of the 34 CrNiMo 6 steel.

Parameter	*Units*	*Value*
Modulus of elasticity	[10 exp(3) N/mm^2]	210
Density	[g/cm^3]	7.85
Thermal conductivity	[W/m.K]	**37.7**
Specific electric resistivity	[Ohm mm^2/m]	no data
Specific heat capacity	[J/g.K]	0.46

Table 1.8 – High pressure nitriding process parameters.

Process Parameters	*Gas pressure*	*Duration – stage 1*	*Duration – stage 2*	*Temperature*
NH_3	6 bar	1 hour	1 hour	520 ºC
N_2	2 bar	0,5 hour	20 hour	

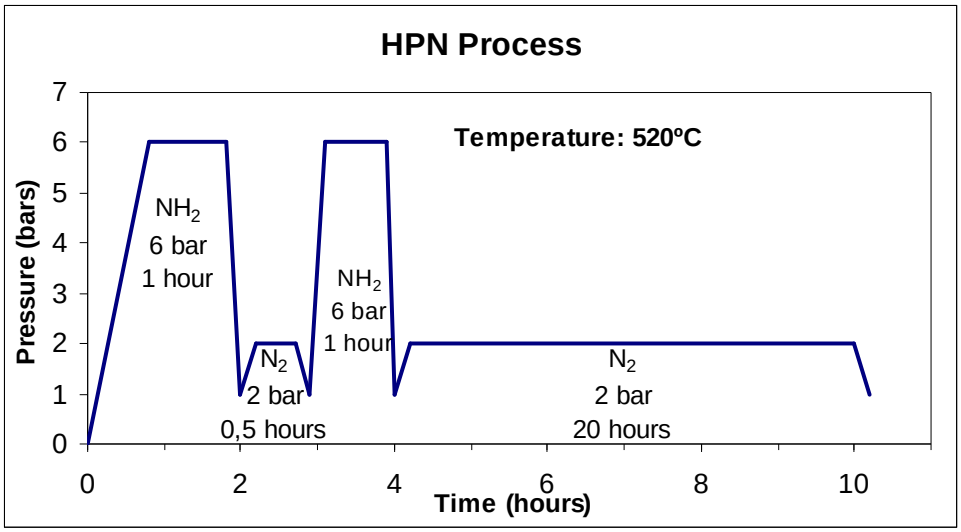


Figure 1.3 - High pressure nitriding process parameters.

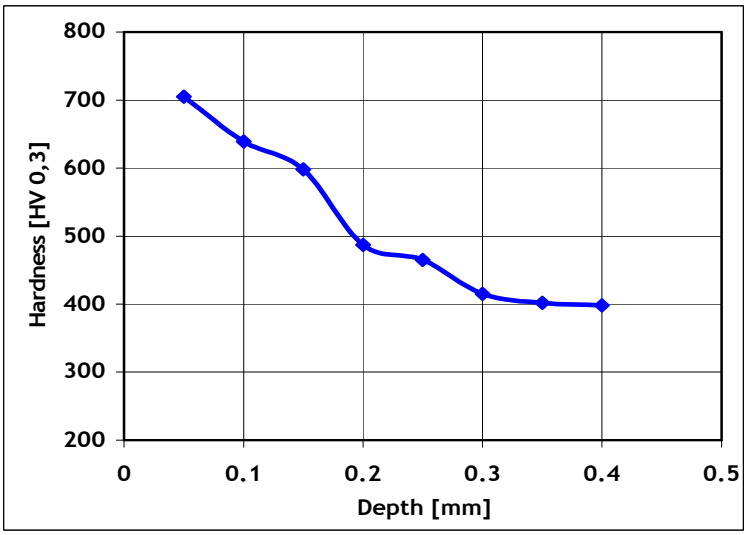


Figure 1.4 - Variation of the hardness with depth within the nitriding layer.

1.2.3 Mechanical Properties of the tested gear materials

Table 1.9 compares the mechanical properties of the gear materials used.

Table 1.9 - Mechanical properties of 20 MnCr 5 and 34 CrNiMo 6 materials.

Properties	*Unit*	*20 MnCr 5 Carburizing steel*	*34 CrNiMo 6 Nitriding steel*
Modulus of elasticity	10^3 N/mm^2	210	210
Density	g/cm^3	7.85	7.85
Poisson's ratio	/	0.3	0.3
Surface hardness	HRC	58 - 62	32
Tensile strength	N/mm^2	1300	na
Yield strength 0.2%	N/mm^2	550	na
Elongation	%	8	na

1.2.4 Disulfide Molybdenium – Titanium composite surface coating

In the last decades surface coating technology was important to achieve increased performance, allowing lower friction coefficients, higher protection against surface failures and higher load capacity. It is very important, in applications with frequent start-stop operations , preventing surface failures, mainly scuffing,.

Multi-layer composite surface coatings made of MoS_2/Titanium [9-11] exhibit good mechanical and tribological properties in several industrial applications. The MoS_2/Titanium composite coatings were deposited by DC Magnetron Sputtering using a standard CFUBMSIP Teer Coatings PVD system with four targets (one Ti and three MoS_2 targets). The coating procedure started with an ion cleaning, followed by a 70nm Ti layer, a 200nm MoS_2/Ti multilayer, a 900 nm MoS_2/Ti (non multilayer) and a last step of 50 nm layer of MoS_2 for coloration [11].

This coating presented a very high Plastic Hardness ($HP=1200\ kg/mm^2$) and a friction coefficient as low as 0.04 (on Pin-on-disc tests) [9, 10]. The coating thickness was *1.2 μm*, almost not affecting the substrate initial roughness [9]. The MoS_2/Ti coating also presented excellent adhesion to steel substrates tested in twin-disc tests at high contact pressure, high slide-to-roll ratio and low specific film thickness [9].

This surface coating promoted a huge increase of the scuffing load carrying capacity in FZG type C gears, 2 load stages at 1500 rpm and 5 load stages at 3000 rpm, representing an increase of 40% and 77% of transmitted power, respectively [9]. The MoS_2/Ti coating improved the efficiency of a transfer gearbox in about 0.5% at the low speed/high torque operating conditions [9].

This coating was applied to carburized steel (DIN 20 MnCr 5) gears.

1.3 Gear testing procedures

1.3.1 FZG test rig

The FZG test rig [12] is a well known back-to-back spur gear test rig with “power circulation”, shown in Figure 1.5. The test pinion (1) and the test wheel (2) are connected by two shafts to the driving gears (3). The front shaft is divided in two parts separated by the load clutch (4). One half of the load clutch can be fixed to the foundation by a locking pin (5) while the other part can be twisted using a load lever and weights (6). After bolting the clutch together the load can be removed and the shaft unlocked. Now a static torque is applied to the system. It that can be measured by the torque measuring clutch (7). The maximum speed of the AC-motor is 3000 rpm. The test gears can be dip lubricated or jet lubricated. When dip lubrication is used, the oil may be heated using the electrical heaters mounted in the test gearbox. The heater and cooling coil allows the settling of a constant oil temperature measured by the temperature sensor (8).

Several types of gear tests [12] may be performed on the FZG gear test rig:

- Gear scuffing tests;
- Gear pitting tests;
- Gear micropitting tests;
- Gear power loss tests.

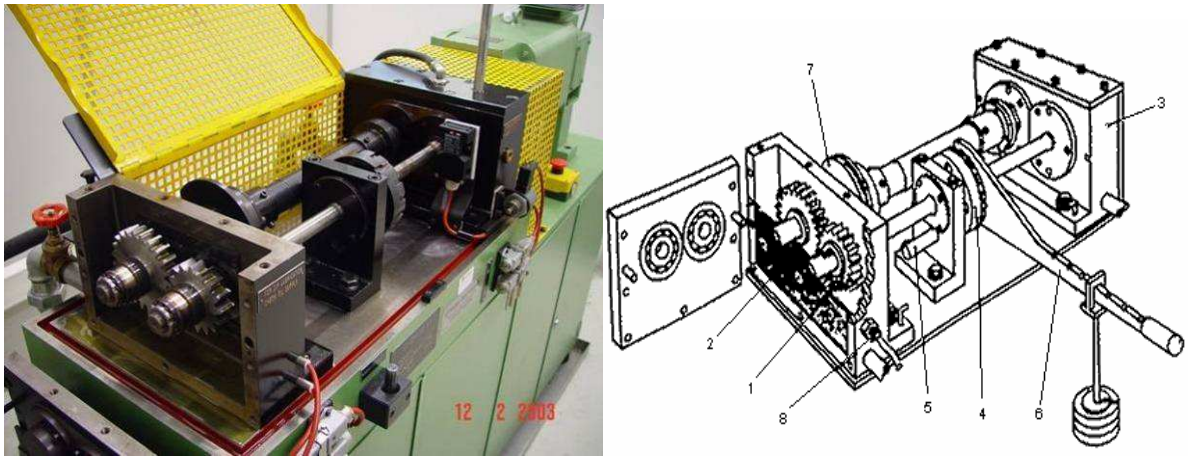


Figure 1.5- Picture and schematic view of the FZG Gear Test Rig.

1.3.2 FZG test gears

Three different types of test gears might be used in the FZG test rig:

- Type A20 for standard gear scuffing tests [12, 13].
- Type A10 for severe gear scuffing tests.
- Type C14 for gear pitting tests [12, 14] and gear power loss tests.
- Type $C14^R$ with increased surface roughness for gear micropitting tests [12, 14, 15].

The different types of FZG test gears are presented in Table 1.10.

The FZG gears used in this work are not of the same gear accuracy grade as proposed in the standards [12-15]. Having lower quality and yielding higher surface roughness, they operate with lower specific film thickness. Another significant difference is the grinding direction on FZG type A gears. According to the standard, it should be Maag criss-cross grinding (15° method) and the available gears are grinded at 0°.

Figure 1.6 shows the geometry of the teeth flanks in FZG type A and type C gears.

Table 1.10 - Geometry of the FZG test gears: Types A20, A10, C14, $C14^R$.

Gear type		*A20*		*A10*		*C14/C14^R*	
		Pinion	Wheel	Pinion	Wheel	Pinion	Wheel
Number of teeth		16	24	16	24	16	24
Module	[mm]	4.5		4.5		4.5	
Centre distance	[mm]	91.5		91.5		91.5	
Pressure angle	[°]	20		20		20	
Face width	[mm]	20		10	20	14	
Addendum modification		+0.853	-0.500	+0.853	-0.500	+0.182	+0.171
Addendum diameter	[mm]	88.68	112.50	88.68	112.50	82.64	118.54
Flank roughness[1]	[μm]	0.35±0.1	0.30±0.1	0.35±0.1	0.30±0.1	0.30±0.1	
Flank roughness ^{R}	[μm]					0.5±0.01	

[1] - **Standard gears are quality grade DIN 5 and have a very good surface roughness of the teeth flanks.**

^{R} - **Increased surface roughness of the teeth flanks for $C14^R$ gears for micropitting tests.**

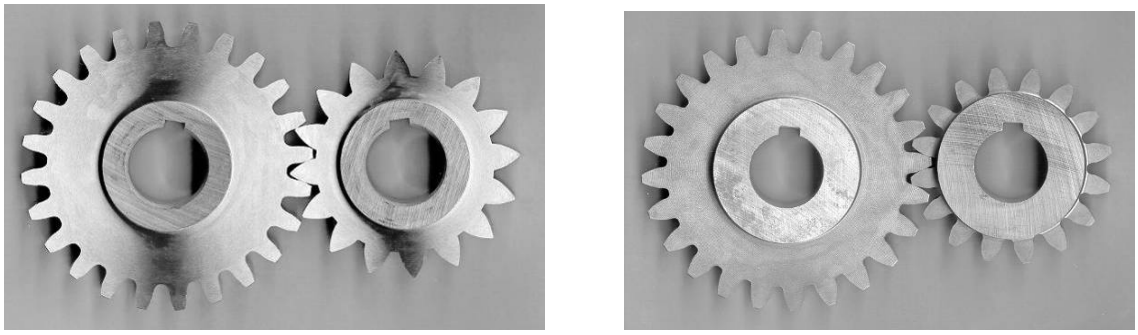


Figure 1.6 - FZG type A (left) and type C (right) gears.

1.4 Post-testing analysis

1.4.1 Mass loss

Gears were weighed with a significant accuracy (0,001 g) at beginning and after each test in order to determine the mass loss during the tests.

1.4.2 Analytical ferrography and ferrometric wear indexes

The characteristics of the wear particles present in the lubricant samples collected during the several gear tests were analysed by analytical ferrography. The Ferrometry indexes *DL* and *DS* were measured and the Ferrometry indexes *CPUC*, *PLP* and *ISUC* were determined.

DL is the ferrometry index for the amount of large particles (size greater than 5 μm),

DS is the ferrometry index for the amount of small particles (size smaller than 5 μm),

PLP is the ferrometry index for the percentage of large particles,

CPUC is the ferrometry index for the concentration of wear particles,

ISUC is the ferrometry index for the severity of wear particles.

The ferrometric indexes *CPUC*, *PLP* and *ISUC* are defined by the following expressions:

$$PLP = \frac{D_L - D_S}{D_L + D_S}(\%) \quad (1.1), \qquad CPUC = \frac{D_L + D_S}{d} \quad (1.2) \qquad \text{and} \qquad ISUC = \frac{D_L^2 - D_S^2}{d^2} \quad (1.3)$$

where *d* is the dilution factor.

1.4.3 Visual inspection

During teeth inspection after each test (and after each load stage in the case of the micropittnig tests), after dismounting and cleaning, teeth surface were photographed with a high resolution camera.

1.4.4 **SEM**

After micropitting tests, the teeth flanks of the nitrided gears were examined by scanning electron microscopy (SEM)[1] using a High resolution (Schottky) Environmental Scanning Electron Microscope with X-Ray Microanalysis and Backscattered Electron Diffraction Pattern Analysis.

1.4.5 Surface roughness and topography

Surface roughness of the teeth flanks was measured in the radial and axial directions, in both cases below and above pitch line. Roughness measurements were performed using a Hommelwerk T4000 device, covering a total measurement length of $\mathbf{L_t=4.8\ mm}$ and a cut-off filter $\boldsymbol{\lambda_c=0.8\ mm}$, and they were digitally filtered [16].

During the micropitting tests, topography measurements were performed on the same device used to measure the surface roughness. Each measurement is composed by 200 roughness profiles measured in axial direction using a total measurement length L_t=12 mm.

[1] The SEM observations were performed at CEMUP – Centro de Materiais da Universidade do Porto, Porto, Portugal (financing contracts ref. REEQ/1062/CTM/2005 and REDE/1512/RME/2005 of 'FCT - Fundação para a Ciência e Tecnologia'). The author want to thank Dr. Carlos Sá from CEMUP for the support concerning SEM analysis.

CHAPTER 2

2 FOUR-BALL WEAR TESTS

2.1 Standard Test Method for Wear Preventive Characteristic of Lubricating Oils

The test method used includes the procedures for a preliminary evaluation of the anti-wear properties of lubricating oils in sliding contact by means of the Four-Ball Wear Test Machine (see Figure 2.1), in accordance with ASTM Standards[2] D4172 - Test Method for Wear Preventive Characteristics of Lubricating Fluids, Four-Ball Method [17], and with ANSI Standard[3] B3.12 - Specification for Metal Balls.

The test uses four steel balls, 12.7 mm diameter each, three of them are clamped together and immersed into the lubricant to be evaluated and the fourth ball, called upper ball, is pressed by 392 N [40 kgf] into the cavity formed by the three clamped balls, originating a three-point contact, as shown in Figure 2.2.



Figure 2.1 - Four-Ball Test Machine.

[2] *For referenced ASTM standards, visit the ASTM website, www.astm.org, or contact ASTM Customer Service at service@astm.org. For Annual Book of ASTM Standards volume information, refer to the standard's Document Summary page on the ASTM website.*

[3] *Available from American National Standards Institute (ANSI), 25 W. 43rd St. 4th Floor, New York, NY 10036.*

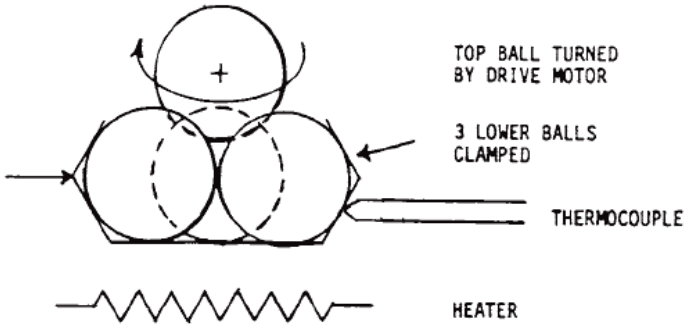


Figure 2.2 – Schematic view of the Four-Ball arrangement.

The temperature during the test is maintained at 75±2°C, the top ball rotating at 1200 rpm during 60 min. Wear scars are generated in the 3 lower balls and a wear track appears in the upper ball.

The wear scars on the three lower balls are measured (±0.01mm accuracy) in two directions: one measurement is made along a radial line from the centre of the holder and a second measurement along a line making 90º with the first measurement. The wear scar diameter is the average value from two measurements. The width of the wear track is also measured on the upper ball.

In order to have reliable data, two tests were performed for each lubricant. The precision of this test method is determined by the Repeatability: the difference between two test results (the smallest one and the largest one) should not exceed 120 μm for lubricating oils.

Additionally, oil lubricant samples were collected after each test and were analyzed by Analytical and Direct Reading Ferrography.

The procedure to collect the lubricant sample at the end of each test was:

1. Drain all the test lubricant (about 8 ml) to a sample bottle;

2. Leaving the three-ball clamped and using an appropriated solvent (petrol benzene) wash the three balls and drain again to the sample bottle;

3. Remove the three balls carefully and flush the oil cup with a solvent jet, draining simultaneously to the sampling bottle.

2.2 Four-Ball wear test results

Table 2.1 presents the wear scar diameters (lower balls) and the wear track (upper ball) measurements made in all tests (E4 lubricant was not tested). The wear scar diameters shown for each lubricant are the average value of the measurements made on the three balls in two directions on each test (Test 1 and Test 2). Ferrography oil analysis results are shown in Table 2.2. More detailed information is presented in Appendix A – Four Ball tests data sheets".

Table 2.1 – Four-Ball wear test results.

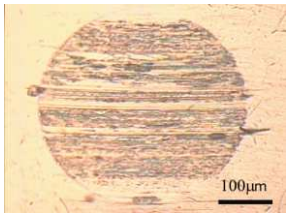
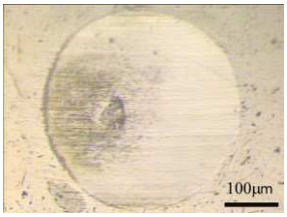
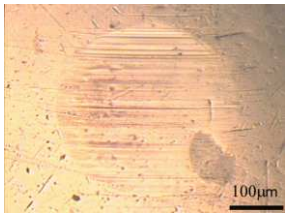
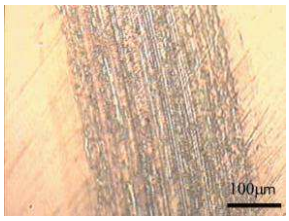
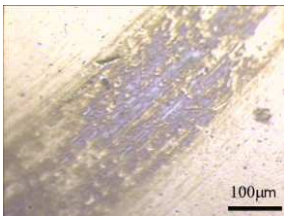
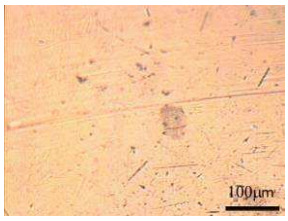
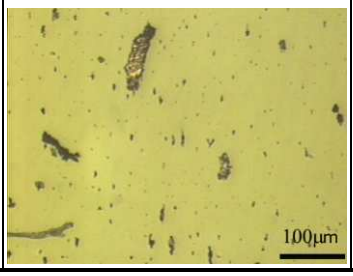
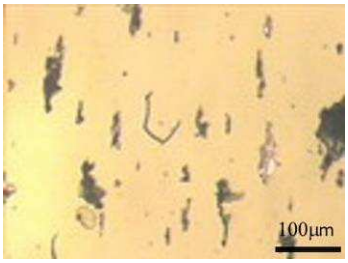
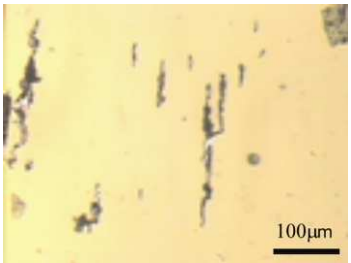
Lubricant		M1	E1	E2
Lower Ball Wear Scar				
Average Wear Scar Diameter	Test1	376 μm	404 μm	364 μm
	Test2	396 μm	392 μm	342 μm
Max. Diff. (<120μm)		30 μm	18 μm	36 μm
Average		**386 μm**	**398 μm**	**353 μm**
Upper Tall Wear Track				
Wear Track Width	Test1	324 μm	360 μm	276 μm
	Test2	420 μm	396 μm	252 μm
Average		**372 μm**	**378 μm**	**264 μm**

Table 2.2 - Ferrography analysis for the tested lubricants.

Lub.	Mineral 1			Ester 1			Ester 2		
Test	1	2	Average	1	2	Average	1	2	Average
DL	4.9	3.5	**4.2**	6.6	1.3	**4.0**	3.7	2.3	**3.0**
DS	2.7	2.4	**2.6**	1.6	0.8	**1.2**	1.65	0.6	**2.7**
PLP	28.9%	18.6%	**23.8%**	61.0%	23.8%	**42.4%**	15.6%	58.6%	**37.1%**
CPUC	7.6	5.9	**6.8**	8.2	2.1	**5.2**	6.4	2.9	**4.7**
ISUC	16.7	6.49	**11.6**	41.1	1.1	**21.0**	6.4	4.9	**5.7**
Ferrograms									

2.3 Discussion on Four-Ball test results

The wear scars diameters produced during the Four-Ball Machine wear test are directly related to the anti-wear properties of fluid lubricants in sliding contacts, as well as the wear volume generated and measured by Ferrography. The presence of anti-wear additives and the lubricant film thickness are two important factors to evaluate the wear conditions during the tests.

Figure 2.3 shows the relation between lubricant viscosity at the operating temperature and the average wear scar diameter for the tested lubricants. The Ester 2 has higher viscosity at the operating temperature (32.7 cSt at 75°C) than lubricants M1 and E1 (31.5 and 28.0 cSt at 75°C respectively) and generated a smaller wear scar diameter (353 μm) and wear track (264 μm) than the M1 and E2 lubricant (386 μm and 372 μm for mineral oil and 398μm and 378μm for Ester E2). Since the three gear oils contain anti-wear and extreme pressure additives, the lubricant viscosity and piezoviscosity affect the film thickness and, consequently, the wear scar diameter, although the differences are small.

The average values of ***DL***, ***DS***, ***CPUC*** and ***ISUC***, presented in Table 2.2, indicate that ester oil E2 generated slightly less wear than the other two gear oils. In Figure 2.4 the average ISUC index is plotted against the average wear scar diameter and a good agreement is obtained.

Figure 2.5 shows wear scars corresponding to the three oils tested. Although their sizes were similar, their surfaces were significantly different. It is clear that the one corresponding to lubricant E2 is the smoothest one and the wear scar surfaces corresponding to the reference mineral oil and ester E1 suffered a more severe wear process than that of the ester oil E2, presenting higher surface roughness and higher surface oxidation.

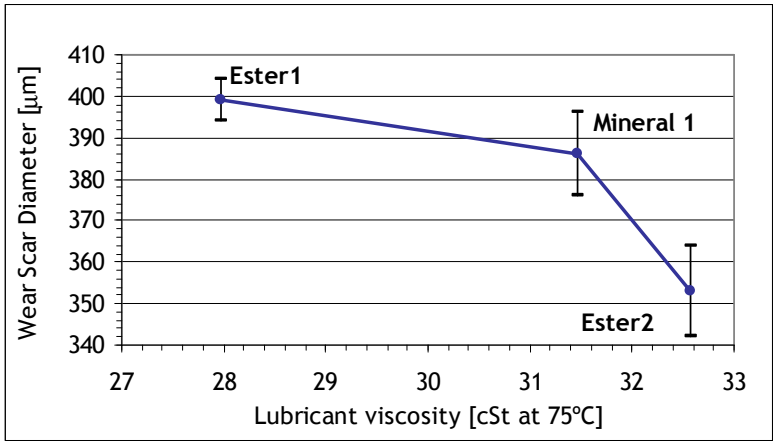


Figure 2.3 - Relation between Viscosity at 75°C and Wear Scar Diameters [μm].

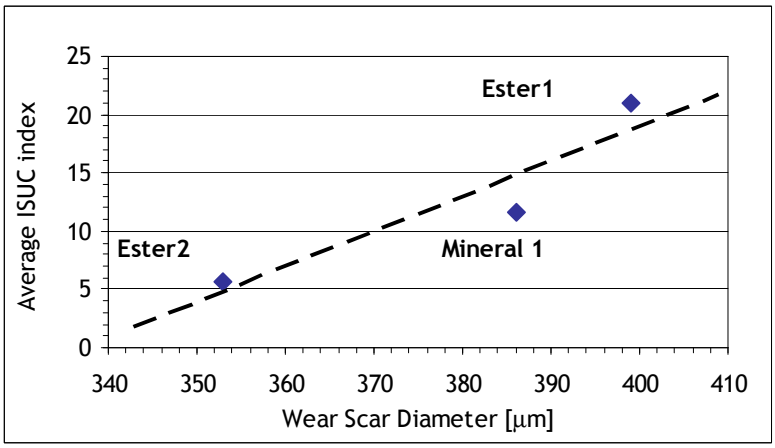


Figure 2.4 - Average ISUC index vs. average wear scar diameter for the tested lubricants.

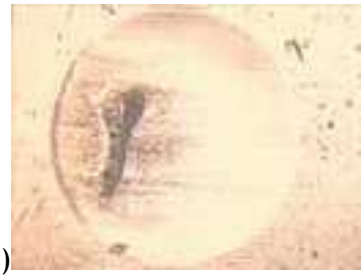
a)  b)  c) 

Figure 2.5 – Wear scar surface of each lubricant: (a) M1, (b) E1 and (c) E2.

2.4 Four-Ball wear test conclusions

Although not absolutely conclusive, the Four-Ball wear test results indicate that:

- ✓ The best results concerning to wear preventive properties were achieved by E2 biodegradable lubricant.
- ✓ The Lubricants M1 and E1 displayed similar behaviour in wear protection, slightly below gear oil E2.
- ✓ The average wear scar diameter and the ISUC index (severity of wear particles index) show a very good correlation.
- ✓ Beside the anti-wear additives, lubricant film thickness (related to lubricant viscosity and piezoviscosity) may have some influence on contact wear.

CHAPTER 3

3 GEAR SCUFFING TESTS

FZG gear scuffing tests were performed to assess the scuffing load carrying capacity of three of the four gear oils under analysis. The reference mineral lubricant M1 and the biodegradable esters E1 and E2 were tested.

FZG gear scuffing tests give quantitative and qualitative information about the influence of several parameters on gear scuffing, such as temperature, load, speed, sliding, specific film thickness, lubricant additives, surface roughness and surface material.

3.1 Gear scuffing

Scuffing is an instantaneous failure. Gear flanks are welded together under pressure and temperature [18], causing the overall destruction of the gear teeth surfaces and significant modification of the teeth flank geometry due to severe destructive wear. The surfaces protection is promoted by the lubricant and it can be provided by hydrodynamic lubrication through thick oil films, physically adsorbed layers of dipoles from the base fluid, the additives or chemical reaction layers from the additives [18]. In the case of the FZG gears, scuffing is a broader concept, integrating also severe modification of the teeth surface roughness without significant modification of the teeth flanks geometry [19].

Figure 3.1 shows the surface evolution of the teeth flanks of a FZG type A gear during a standard FZG A20/8.3/90 test [19]. After running-in (see Figure 3.1) it is still possible to identify the grinding marks on teeth surfaces. The teeth surfaces of the pinion and of the wheel are very similar. The surface roughness is of very good quality after the running-in period, as shown.

Later on, during the scuffing test, the first scuffing marks appear on the teeth flanks of the pinion, as shown on Figure 3.1. Similar marks are visible on the wheel. These are the first signs that the scuffing failure will occur quite soon. The surface roughness profile of the pinion tooth flank shows a scuffing mark, oriented from tooth tip to tooth root, the direction of sliding between the gear teeth, indicating that severe adhesion phenomena has occurred, with material removal.

The DIN 51354 standard [20] considers that scuffing occurs when the sum of all scuffing marks on the flanks of all pinion teeth is greater than the width of one tooth flank (20 mm on the A20 FZG type A gear).

Figure 3.2 shows the evolution of the scuffing marks on the pinion teeth flanks during the standard test (FZG A20/8.3/90), from load stage K9 to load stage K11. The scuffing marks spread from tooth tip to tooth root, never going beyond the primitive line, and from left to right, until the entire tooth flank fails.

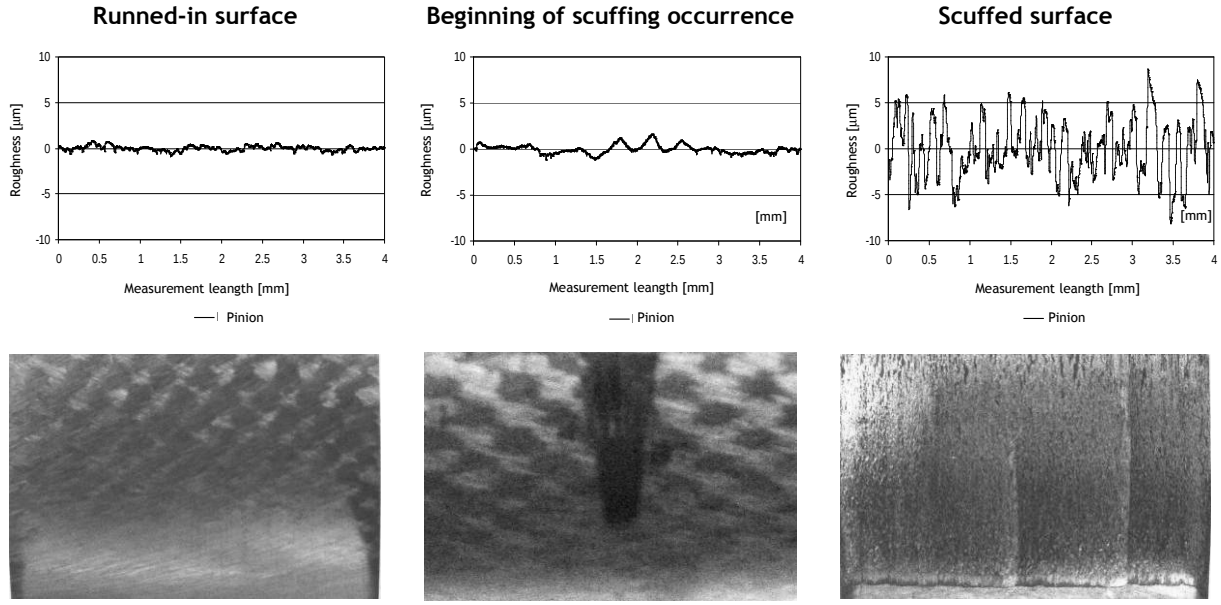


Figure 3.1 - Evolution of the surface roughness of the teeth flanks during a standard FZG A20/8.3/90 scuffing test [19].

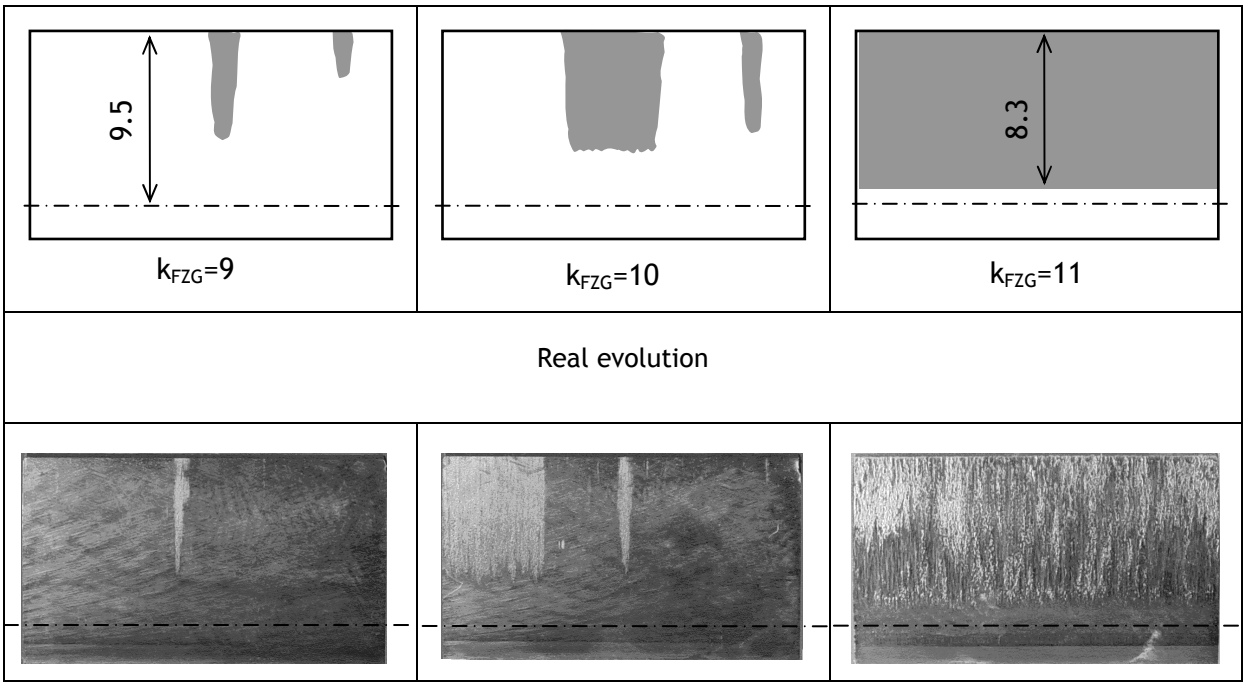


Figure 3.2 - Evolution of the scuffing marks on the pinion teeth flanks during the standard test (FZG A20/8.3/90), from load stage K9 to load K11[19].

Scuffing marks spread over the entire width of the tooth flank at the end of the test, and the corresponding surface roughness (see Figure 3.1) exhibits a very strong increase of the roughness peaks.

Gear scuffing is influenced by the operating conditions such as temperature, load, speed, sliding, specific film thickness, lubricant additives and surface material as well. Table 3.1 shows the factors that are reported to interfere in gear scuffing and their influence of the scuffing load.

Table 3.1- Factors influencing gear scuffing [19].

Increasing Factor	Scuffing Load
lubricant viscosity	↗
lubricant additive chemistry	↗
oil sump temperature	↘
speed	↘
coefficient of friction	↘
gear surface roughness	↘

3.2 Gear material and surface roughness

The gears used in the scuffing tests were made of in DIN 20 MnCr 5 carburizing steel. The surface roughness of the teeth flanks measured in the radial and axial directions (see Figure 3.7) are shown in Table 3.2.

Table 3.2 – Average value of roughness parameters for FZG type A gears used in the scuffing tests.

Gear Type	R_{max}	$R_{Z\text{-}D}$	R_a	R_{pk}	R_k	R_{vk}
A20 axial	1,5	1,0	0,2	0,2	0,5	0,4
A10 axial	1,2	0,7	0,1	0,2	0,4	0,3
A10 radial	8,2	6,2	1,1	1,3	3,7	1,8

3.3 Gear scuffing test procedure

In the standard FZG gear scuffing test (FZG A20/8.3/90, DIN 51354) 20 mm wide type A gears are used, allowing very high sliding rates at the end of the meshing line. The operating speed (wheel) is 1500 rpm, under dip lubrication. Table 3.3 shows the wheel torque corresponding to each load stage in the standard FZG gear scuffing test. The torque is applied progressively from load stage K1 to load stage K12, until scuffing occurs, and each load stage lasts 15 minutes.

Gear running-in takes place during the first 4 load stages, as indicated in Table 3.3. This running-in period is very important, since it avoids premature scuffing failure of the FZG gear. In these first 4 load stages the initial oil bath temperature is not imposed, typically equal to the ambient temperature. After load stage K4 the initial oil bath temperature is set to 90 ± 2 °C. During each load stage the oil temperature increases from the initial value to a final temperature that is mainly dependent on the applied torque and lubricant properties.

Usually, industrial gear oils have a very high scuffing load carrying capacity and they all pass load stage K12 in the standard A20/8.3/90 test. In order to differentiate more clearly the scuffing protection provided by the lubricants under analysis, more severe versions of the standard test were used: A20/16.6/90 test, performed at a pitch speed of 16.6 m/s and using 20 mm wide gears and A10/16.6/90 test, performed at the same pitch speed but using 10 mm wide gears. In the first case the input power is twice that of the standard test and in the second case, beside the higher input power, the hertzian contact pressure between gear teeth is 41.4% higher.

The roughness of the teeth flanks and the mass of the pinion were measured before and after the tests in order to assess the evolution of the surface roughness and to evaluate the pinion mass loss. The temperature of the oil bath is monitored continuously during the tests.

Table 3.3 – Operating conditions during the performed scuffing tests.

Wheel speed	*Stage time*	*Cycles/ stage*	*FZG stage*		*Wheel torque*	*FZG test A20 / 16.6 / 90 Max. Hertz pressure*	*FZG test A10 / 16.6 / 90 Max. Hertz pressure*	*Initial temperature*
rpm	*min*	*-*		K_{FZG}	*N.m*	*GPa*	*GPa*	*ºC*
3000	15	67 500	Running-in	1	5.0	0.15	0.22	free
				2	20.6	0.31	0.44	
				3	53.0	0.50	0.71	
				4	91.2	0.66	0.93	
			Scuffing stages	5	141.2	0.82	1.16	90
				6	203.0	0.99	1.39	
				7	275.1	1.15	1.62	
				8	359.0	1.31	1.85	
				9	453.0	1.47	2.08	
				10	558.9	1.64	2.31	
				11	675.2	1.80	2.54	
				12	801.8	1.96	2.77	

3.4 Gear scuffing results

Figure 3.3 shows the scuffing load stage reached by each lubricant in tests A20/16.6/90 and A10/16.6/90. The ester oils reached scuffing in load stage K12 using 20 mm wide gears (test A20/16.6/90), one load stage more than the mineral oil. The three lubricants reached scuffing in load stage K11 using 10 mm wide gears (test A10/16.6/90). These gear scuffing results are very similar, knowing that the precision of these tests is $\pm$ 1 load stage.

Figure 3.4 shows the maximum oil bath temperature reached by each lubricant during the corresponding scuffing load stage, in tests A20/16.6/90 and A10/16.6/90. The results measured for ester oil E2 were very interesting since it always generated lower temperature than the other two gear oils in both tests, while lubricant E1 displayed the highest temperature. Although reference mineral oil and Ester 2 had the same maximum oil bath temperature in test A20/16.6/90 ($\approx$156 ºC) and the ester E1 had a higher temperature, it must be taken into consideration that the esters reached scuffing in load stage K12 and mineral oil in load stage K11, meaning that the temperature performance of ester oils is better.

Once the film breaks down and scuffing occurs the wear amount of the teeth flanks can be very high. Figure 3.5 shows the pinion mass loss at the end of tests A20/16.6/90 and A10/16.6/90 for each lubricant. However, these pinion mass loss results after scuffing are not significant of the performance of a lubricant.

Taking into account the high severity of the tests performed, the gear scuffing results obtained for the three lubricants are outstanding, confirming the high quality of the biodegradable gear oils, based on highly or fully saturated esters containing low toxicity additivation.

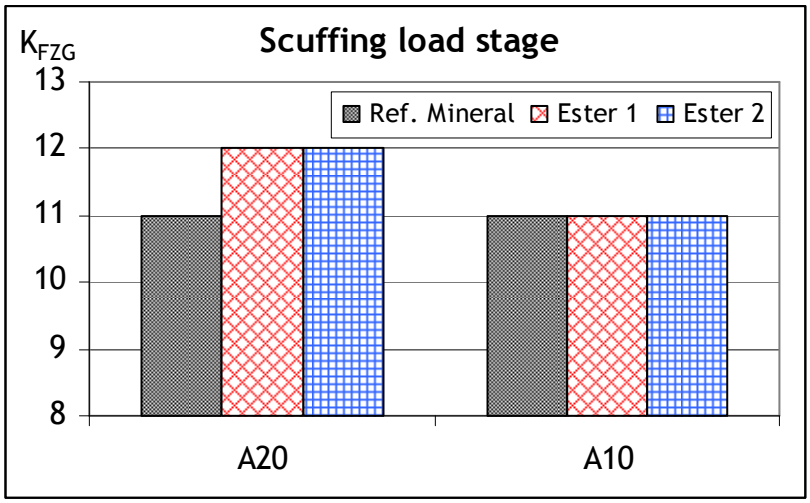


Figure 3.3 - Scuffing load stage reached by each lubricant (in tests A20/16.6/90 and A10/16.6/90).

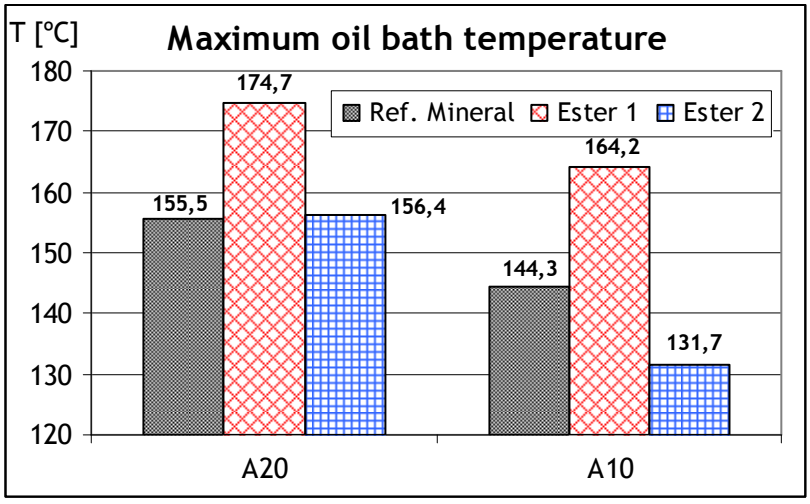


Figure 3.4 - Oil bath temperature at the end of the scuffing stage.

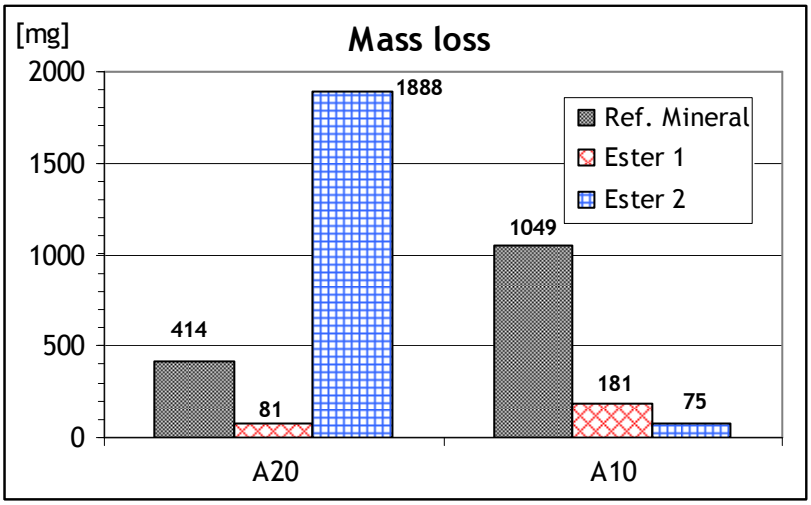


Figure 3.5 - Pinion mass loss.

3.5 Discussion on gear scuffing tests

3.5.1 FZG A20/16.6/90 gear scuffing test

Table 3.4 displays the results obtained for the three lubricants (M1, E1 and E2) in FZG A20/16.6/90 gear scuffing tests. Mineral gear oil reached scuffing in load stage K11. However, the scuffed width was only slightly above the minimum limit (one teeth width = 20 mm). The next load stage (K_{FZG} = 12) was performed and a very severe scuffing failure was obtained with a very significant mass loss of 414 mg. This result suggests that the real scuffing load stage of the mineral oil is between 11 and 12, but the accuracy of this test (± 1 load stage) didn't allow a more accurate evaluation. The gear lubricated by E2 oil suffered a very destructive scuffing failure with high mass loss (1888 mg) while the gear lubricated with E1 oil had a low mass loss.

E1 ester based oil reached a very high temperature at the end of the scuffing load stage. Probably, this is related to the fact that it generates a small film thickness, because it has a similar viscosity to the mineral oil but it has a significantly lower piezoviscosity.

Figure 3.6 shows the oil bath temperatures at the end of each load stage, being interesting to notice that at the end of load stage K11 the oil bath temperature of the three lubricants was almost the same. Scuffing occurred during load stage K12 and several different behaviours were noticed: the temperatures of oils M1 and E1 increased while the temperature of oil E2 remained constant. This particular behaviour of gear oil E2, showing maximum oil bath temperatures almost constant at very high load (from load stages K10 to K12) is related to the base oils combination used and the type of low-toxicity additives used in its formulations.

The surface roughness of the pinion teeth flanks was measured before the test ("*Initial*") and after scuffing ("*Final*") in axial and radial directions (see Figure 3.7). The mean values of the roughness parameters are presented on Appendix B – gear scuffing tests data sheets.

Figure 3.8 shows some significant snapshots taken from the pinions teeth flanks of the tested gears. These pictures show that the teeth flanks of the pinion lubricated with oils M1 and E2 suffered a very severe scuffing failure, showing deep scuffing marks. The pinion lubricated with the ester E1 only presented light and superficial scuffing marks.

The values of the most relevant roughness parameters are reported in Table 3.5. Roughness measurements were made on damaged and undamaged zones of the teeth flanks after scuffing. The analysis of those measurements showed that all roughness parameters suffered a very significant increase (2 to 6 times more) after scuffing, as indicated before in Figure 3.2. The comparison of R_{max} and $R_{Z\text{-}D}$ roughness parameters, between initial values (as manufactured after grinding) and final scuffed values, clearly shows the degradation suffered by the tooth flanks after scuffing. The roughness peaks of teeth flanks were worn out at the undamaged zones, as indicated by the decrease of the R_{pk} parameter, and the surfaces became smoother, as reported before on Figure 3.2.

Table 3.4 - A20/16.6/90 gear scuffing test results with lubricants M, E1 and E2.

Lubricant		Ref. mineral	Ester 1	Ester 2
k_{FZG}		11*	12	12
Mass Loss	[mg]	414*	81	1 888
Maximum Oil Temperature	[°C]	155,5	174,7	156,4
Contact pressure at the scuffing load stage	[GPa]	1,80	1,96	1,96
Oil viscosity at scuffing	[cSt]	4,50	4,16	6,12

(*because the scuffing failure on load stage K11 was not very severe, load stage K12 was performed).

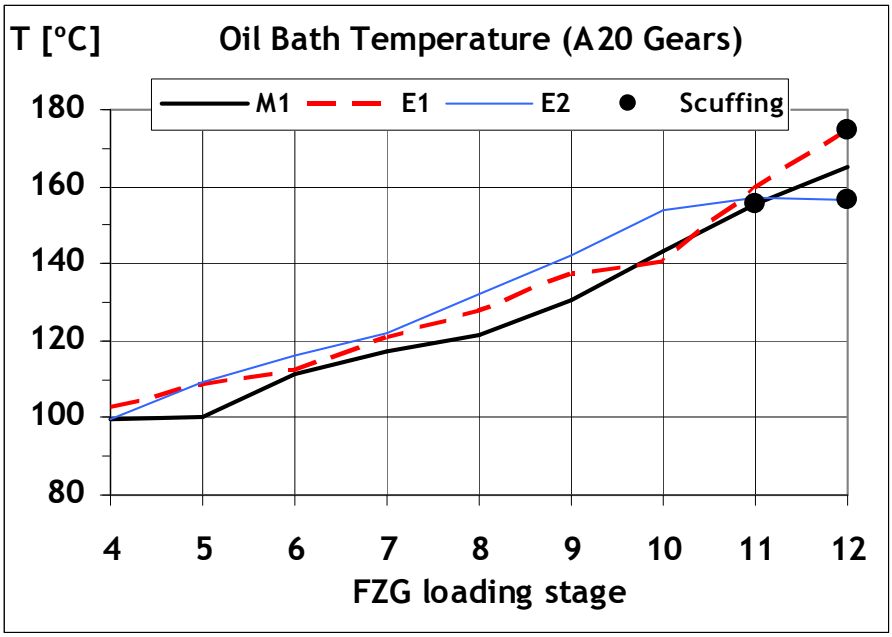


Figure 3.6 - Oil bath temperature at the end of each load stage on A20/16.6/90 FZG gear scuffing tests.

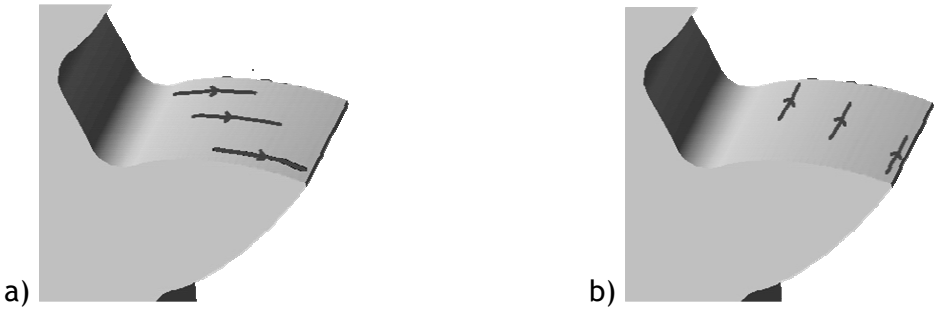


Figure 3.7 - Roughness measurement location (a- radial direction; b- axial direction).

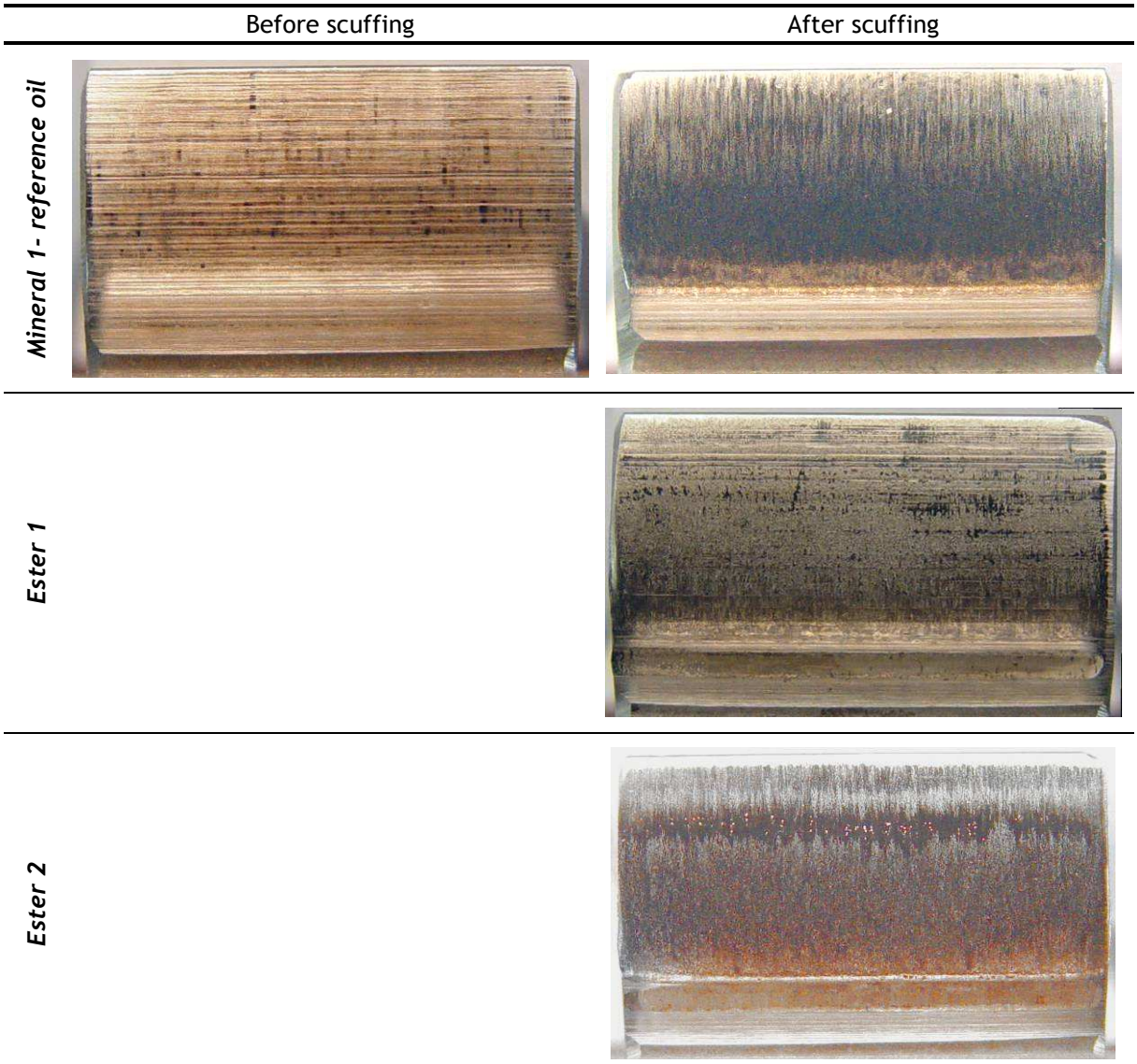


Figure 3.8 – Photography of tooth flanks after scuffing test FZG A20/16.6/90.

Table 3.5 - Surface roughness measurements on tooth surface before and after the FZG A20/16.6/90 scuffing test- axial direction.

Lubricant	*Roughness parameter*	*Pinion Surface Roughness [μm]*					
		R_{max}	$R_{z\text{-}D}$	R_a	R_{pk}	R_k	R_{vk}
Reference mineral	Initial	1,5	0,9	0,1	0,3	0,4	0,4
	Final undamaged	1,5	1,1	0,2	0,1	0,4	0,5
	Final + scuffing	3,2	2,6	0,4	0,3	1,2	0,7
Ester 1	Initial	1,2	0,8	0,1	0,2	0,4	0,3
	Final + scuffing	8,3	6,3	0,9	0,4	2,0	2,6
Ester 2	Initial	1,2	0,8	0,1	0,2	0,4	0,3
	Final + scuffing	8,3	6,3	0,9	0,4	2,0	2,6

3.5.2 FZG A10/16.6/90 gear scuffing test

The FZG gear scuffing test A10/16.6/90 test is more severe than the previous one because the contact pressure between gear teeth is 40 % higher. Table 3.6 shows the results obtained using the three lubricants (M1, E1 and E2) in those tests [21, 22].

All the lubricants reached scuffing on load K11, corresponding to a maximum hertzian pressure of 2.54 GPa. The gear lubricated by the mineral oil suffered a very severe surface failure generating a very high mass loss of the pinion (1049 mg). The gear lubricated by the ester based gear oils suffered less severe failures, generating significantly lower mass losses, 181 mg and 75 mg, respectively.

As in the case of the previous test, lubricant E2 presented the lowest oil bath temperature at the end of the scuffing load stage 132 ºC, against 144 ºC and 164 ºC for oils M1 and E1, respectively.

Figure 3.9 shows the oil bath temperature at the end of each load stage for the three tested lubricants, all showing a similar behaviour until load stage K9. However, in this more severe test, a clear distinction between the three oils is observed, in terms of oil temperature after load stage K9, with lubricant E2 always generating significantly lower temperatures.

Table 3.6 - A10/16.6/90 gear scuffing test results with lubricants M, E1 and E2.

Lubricant		Ref. mineral	Ester 1	Ester 2
k_{FZG}		11	11	11
Mass Loss	[mg]	1049	181	75
Maximum Oil Temperature	[ºC]	144,3	164,2	131,7
Contact pressure at the scuffing load stage	[GPa]	2,54	2,54	2,54
Oil viscosity at scuffing	[cSt]	5,41	4,76	9,03

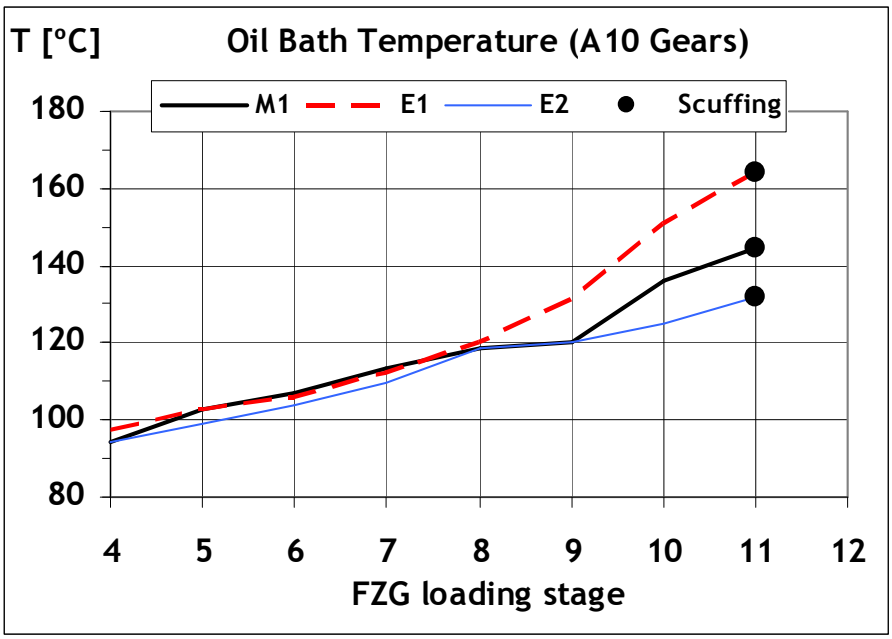


Figure 3.9 - Oil bath temperature at the end of each load stage on A10/16.6/90 FZG gear scuffing test.

The degradation of the tooth flanks started between load stages K7 and K8 with oil E1 (see *FZG gear scuffing test of E1 gear oil using A10 gear* in Appendix B), perhaps explaining the drop in temperature observed at the end of load stage K8, while with M1 and E2 oils it only started on load stage K10. Such differences were probably related to the different chemical compositions and additive packages of the three lubricants.

Figure 3.10 displays snapshots of the pinion tooth flanks. The pinion lubricated by the reference mineral gear oil showed very pronounced and very deep scuffing marks and, although some teeth did not reach scuffing, all of them displayed scuffing scratches in the radial direction. The teeth flanks of the pinion lubricated with the esters are very smooth after scuffing not showing the typical scuffing scratches. Very significant wear is observed at the teeth root in all pinions.

Figure 3.10 also shows the contact zone and the scuffing failure at the teeth flanks of the wheels. In the three tests using reference mineral and ester oils, the wheels suffered a very significant mass loss and a very pronounced modification of the tooth profile.

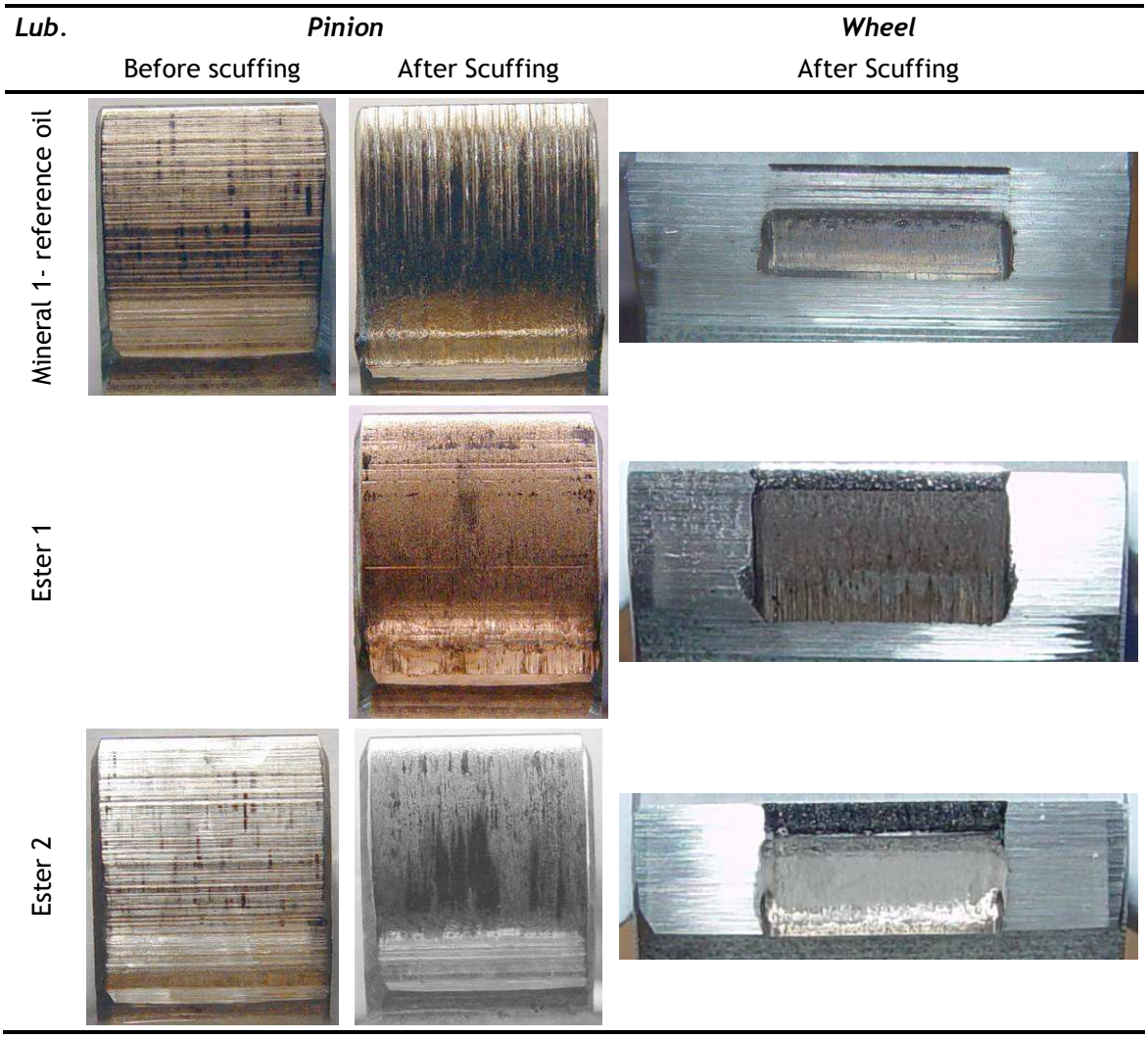


Figure 3.10 – Photography of tooth flanks after scuffing test FZG A10/16.6/90.

All the lubricants had a similar behaviour until load stage K9 (1.85 GPa). After FZG load stage K9, the wheel teeth flanks started to show edge effects due to the different width of pinion and wheel and significant wear marks were observed. That effect generated very severe wear on the wheel after load stage K11, as presented on Figure 3.10. The very large temperature difference between lubricants after load stage K10 may be related to the different behaviour of lubricants in the presence of the edge effects.

Table 3.7 shows the surface roughness parameters measured at the tooth flanks in the axial direction for the three tested gear oils. The comparison of R_{max} and $R_{z\text{-}D}$ roughness parameters, between initial values (as manufactured after grinding) and final scuffed values, clearly shows the degradation suffered by the tooth flanks after scuffing. The roughness parameters of the gear lubricated by the mineral oil ($R_{z\text{-}D}$ = 32.8 μm) indicate a very severe surface failure in agreement with the very high pinion mass loss measured in this case, while the much lower roughness values measured for the ester oils ($R_{z\text{-}D}$ = 7.5 μm for E1 and $R_{z\text{-}D}$ = 4.7 μm for E2) are compatible with their pinion mass loss.

Table 3.7 - Surface roughness measurements on tooth surface before and after the FZG A10/16.6/90 scuffing test- axial direction.

Lubricant	*Roughness parameter*	*Pinion Surface Roughness [μm]*					
		R_{max}	$R_{Z\text{-}D}$	R_a	R_{pk}	R_k	R_{vk}
Reference mineral	Initial	1,3	0,9	0,1	0,2	0,4	0,3
	Final undamaged	1,2	0,7	0,1	0,1	0,3	0,2
	Final + scuffing	32,8	28,0	6,1	12,6	13,8	4,0
Ester 1	Initial	1,0	0,7	0,1	0,2	0,4	0,2
	Final + scuffing	7,5	5,9	0,8	0,8	2,1	2,1
Ester 2	Initial	1,2	0,9	0,1	0,3	0,4	0,3
	Final undamaged	1,4	0,9	0,1	0,1	0,4	0,3
	Final + scuffing	4,7	3,6	0,6	0,6	1,9	1,0

3.5.3 Critical lubricant temperature T_{CR} - Scuffing analysis for gear lubricants

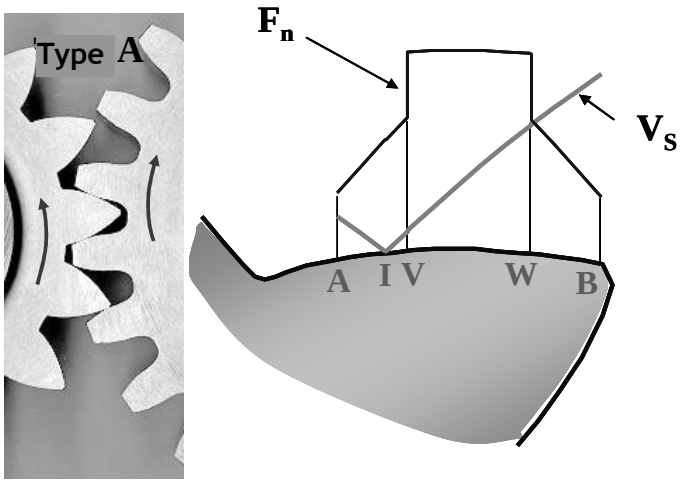
Castro proposed a new scuffing criterion for FZG gears [23]. This criterion is based on a concept named "*Critical lubricant temperature (T_{CR})*" that is the maximum temperature at which a scuffing failure can happen, whatever the load and the speed. The criterion can be stated as:

$$T_{CR} - T_0 \leq \frac{\mu_m . P_O . V_S . T}{C} \tag{3.1}$$

Where T_O is the oil bath temperature and C is a constant dependent of oil type and gear material. P_0 is the contact pressure, V_s is the sliding speed, μ_m is the average friction coefficient, T is the distance from the contact point considered the pitch point (point I) on the meshing line (see Figure 3.11).

Plotting the right part of the inequality against the oil bath temperature, as presented in Figure 3.12, the critical temperature might be assessed graphically by the intersection of the trend line with the horizontal axis.

The critical temperature for each lubricant is displayed in Table 3.8 and, as expected, the mineral lubricant has the lowest critical temperature, fallowed by ester lubricant E1 and the E2 ester fluid has the highest critical temperature [21, 22].



Point	Observations
A	Begin of meshing line.
I	Pitch point.
V	Transition 2-1 meshing teeth pairs.
W	Transition 1-2 meshing teeth pairs.
B	End of meshing line.

Figure 3.11 - FZG type A gear geometry and reference points along mesh line[23].

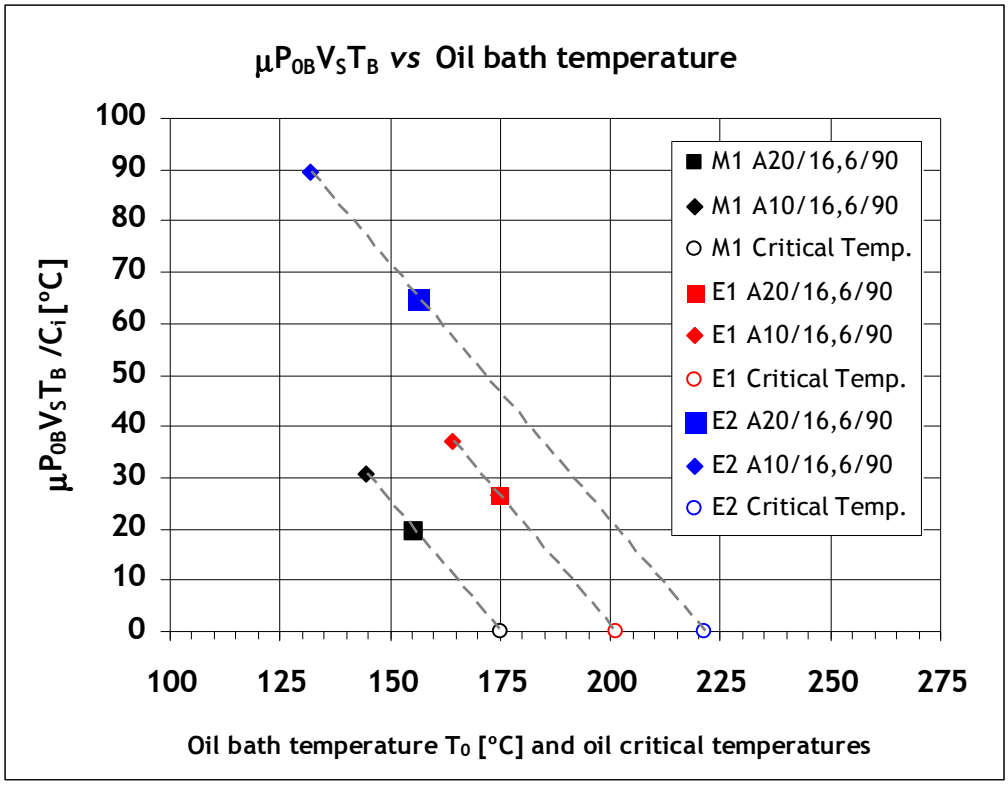


Figure 3.12 - $\mu P_{0B} V_s T_B$ as a function of oil bath temperature for point *B* of meshing line (pinion tip - wheel root).

Table 3.8 - Critical temperature for each industrial gear lubricant tested.

Lubricant	T_{CR} [°C]	C [N/s.°K]
M1	175	8.43×10^5
E1	201	7.07×10^5
E2	221	2.82×10^5

3.6 Conclusions on gear scuffing tests

The results of the gear scuffing test results indicate that the ester based biodegradable and low-toxicity gear oils E1 and E2 presented several advantages compared to the reference mineral oil in terms of gear scuffing load carrying capacity:

- ✓ Higher FZG scuffing load stage in test FZG A20/16.6/90;
- ✓ The same FZG scuffing load stage in test FZG in test FZG A10/16.6/90;
- ✓ Critical oil bath temperature 26ºC and 46ºC higher with lubricants E1 and E2 respectively;
- ✓ Lubricant E2 generated the lowest oil bath temperatures in both gear scuffing tests;
- ✓ Lubricant E1 generated the lowest mass loss after scuffing in both tests;
- ✓ The teeth flanks of the pinion lubricated with the esters are very smooth after scuffing (in test FZG A10/16.6/90 where the three lubricant have same FZG scuffing load stage) not showing the typical scuffing scratches while pinion lubricated by the reference mineral gear oil showed very pronounced and very deep scuffing marks.

Globally, the ester based biodegradable gear oils, E1 and E2, showed a very good anti-wear and anti-scuffing performance, above that of the mineral oil in several aspects.

CHAPTER 4

4 GEAR MICROPITTING TESTS

Micropitting gear tests were performed on the FZG machine (see Figure 1.5) using type C gears (see Table 1.10 and Figure 1.6), in order to compare the micropitting resistance of several combinations of lubricants and gear materials.

Four industrial gear oils were tested (reference mineral oil M1 and the biodegradable and non-toxic esters E1, E2 and E3). The gears were produced using case hardened steel, High Pressure Nitrided steel and case hardened steel with a MoST coating.

Results include photographs of the teeth flanks, mass of pinions and wheels, ferrometry and analytical ferrography, surface roughness measurements, surface topography measurements and SEM analysis.

4.1 Gear micropitting

Micropitting is a contact fatigue wear phenomenon that is observed in combined rolling and sliding contacts operating under elastohydrodynamic lubrication (EHL) or mixed EHL/Boundary lubrication conditions. Micropitting can be regarded as fatigue failure with a net of cracks close to the surface which typically starts during the first 10^5 to 10^6 stress cycles. Cracks propagate at a shallow angle to the surface forming micro-pits with characteristic depth in the range of 5-10μm. The micro-pits coalesce to produce a continuous fractured surface with a dull mate appearance. In case the surface cracks propagate deeper into the material, pitting and spalling can be initiated [24, 25].

Micropitting is known to be influenced by operating conditions such as temperature, load, speed, sliding, specific film thickness, lubricant additives and surface material as well. Table 4.1 shows the factors that are reported to influence micropitting, their range of influence and suggestions for preventing it [24, 26].

Table 4.1 - Factors influencing micropitting, range of influence and suggested remedies [24, 26].

Influencing Factor	*Range of influence*	*Suggested Remedy*
gear surface roughness	1→3 (from 6 μm to 3 μm)	reduce to 0.3 μm
material, heat treatment	1→2.8	retained austenite
lubricant viscosity	1→2	use highest practical viscosity
lubricant additive chemistry	1→2 (equal viscosity of base oil)	use properly selected additives
coefficient of friction	1→1.7	reduce the coefficient of friction
speed	1→1.3	run at high speed
oil temperature	1→1.3 (ΔT = 20 °K)	reduce oil temperature

FVA [27] presents Table 4.2 where the influence of roughness is represented. It allows the conversion of test results obtained with FVA test procedure for different surface roughness (the standard roughness is R_a = 0.5μm). For example, an ISO VG 32 lubricant tested using 0.7 R_a surface roughness gears will fail two load stages earlier.

Not considering lubricant chemistry, the key factors to produce micropitting are mixed film lubrication and combined rolling and sliding. Using a thicker EHL film and smoother surfaces, micropitting can be eluded.

In the case of gears with parallel axis, pure rolling exists only at the pitch point. Above and below this point there is a combination of rolling and sliding and the sliding speed increases when the contact point moves away from the pitch line.

Figure 4.1 presents two teeth at the beginning and at the end of engagement, showing the directions of the rolling (R) and sliding speeds (S).

Table 4.2 - Approximate FZG load stage values for conversion of test results in the micro-pitting test [27].

Surface roughness	*Lubricant: ISO VG*				
R_a [μm]	*32*	*46*	*100*	*220*	*460*
0.3	+2…+3	+2	+1	+0.5…+1	+0.5
0.7	-2…-2	-2	-1	-0.5…-1	-0.5

Micropitting may occur almost anywhere on the gear tooth. However, the contact condition where sliding and rolling directions are opposite is considered to be the most critical. This contact condition always occurs below pitch diameter both for the driving and the driven gears. Micropitting is also often found at addendum due to high sliding and at local high spots in the surface topography associated with high stresses.

The progression of micropitting may eventually result in pitting or spalling. There are also reported cases of micropitting progress up to a point and then stop, sometimes described as a form of running-in or stress relief. Although it may appear innocuous, such loss of metal from the gear surface causes loss of gear accuracy, increased vibration, noise and other related problems. The metal particles released into the oil may be too small to be picked up by filters, but large enough to damage tooth and bearing surfaces.

To distinguish micropitting from pitting in terms of service conditions and mechanisms that lead to those phenomena is not very easy. The complex nature of gear contact makes it difficult to separate individual failure modes.

In order to establish the requirements of a micropitting test, some aspects of pitting and micro-pitting conditions have to be established. This will help to choose a test procedure and to interpret the results. Table 4.3 shows the different conditions of the two types of failure [25].

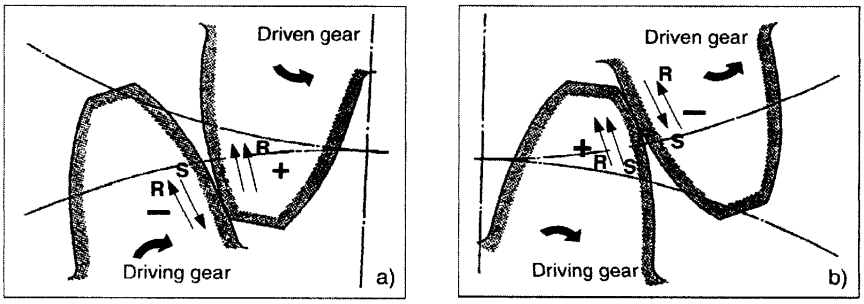


Figure 4.1 - Rolling and sliding directions. a) Beginning of engagement. b) End of engagement [28]

Table 4.3 - Pitting and micropitting conditions.

	Pitting	*Micropitting*
Depth	Zone of highest subsurface stress; may also appear in surface craters	Typically in the range of 5-10 μm or material surface
Size	Visible to the human eye	Invisible to the human eye; grey shaded
Lubrication regime	Elastohydrodynamic – full film	Mixed lubrication
Main cause	Contact pressure	Roughness
Other causes	Hardness; speed; temperature	
Lubricant influence	Little	High
Consequences	spalling; 3 body wear; loosing of tooth resistance	Loosing of geometric accuracy; noise; vibration; may develop pitting
Ways of avoiding	Use lubricants of higher viscosity which don't easily fill surface micro-craters	Increase film thickness; use oils with S-P additives

4.2 Test gears

The gears available to perform the micropitting tests have a "current" quality grade, lower than the "fine" quality grade proposed in the standards [27, 29]. The tested gears have a lower manufacturing geometric accuracy and higher surface roughness, generating a lower specific film thickness. Therefore, lubricants cannot be classified in GF-Classes proposed by FVA. However, the main objective of the tests is to compare the lubricants rather than to classify them in those classes. As the lubricants were tested on similar gears, the results are comparable and reliable.

Table 4.4 shows the gear quality and the average roughness of teeth flanks, as well as gear quality and the average roughness of type C gear specified on FVA micropitting test procedure [14] (see Table 1.10 and Figure 1.6).

Table 4.5 shows specific film thickness, corresponding to the surface roughness at the beginning of the test and torques applied during the running-in FZG load stage (K3 – T_1=28.8 Nm). The differences shown refer to the corresponding specific film thickness with standard gears.

At the beginning of load stage K6 (after running-in), the operating conditions are slightly more favourable. Nevertheless, if standard gears were used the specific film thickness values would be significantly higher. Specific film thickness is different for the four gear oils because they have different piezoviscosity coefficients (see Table 1.1 and Table 4.22). Only points below the pitch line are presented, since micropitting usually appears there.

Table 4.4 - Gear quality grade and average surface roughness (pinion and wheel).

Material and heat treatment	*Gear reference*	*Gear quality grade (ISO 1328)*	*Average roughness R_a of tooth flanks [μm]*	
			Axial direction	*Radial direction*
Standard gear	ZF®	5	/	0,5
20 MnCr 5 case hardened	C-M1	9	0,18	0,96
	C-E1	9	0,14	1,14
	C-E2	9	0,13	1,11
	C-E3	9	0,18	1,29
34 CrNiMo 6 high pressure nitriding	N-M1	9	0,14	1,12
	N-E1	9	0,18	1,13
	N-E2	9	0,18	1,05
20MnCr5 + case hardened + MoS_2/Ti coating	Mo-M1	9	0,25	1,17
	Mo-E1	9	0,69	1,20
	Mo-E2	9	0,27	1,16

Table 4.5 - Specific film thickness for standard and performed tests.

Lubricant	*Gear*	R_a	R_q	ν @90ºC	T_1	pc [a]	Λ [b]		
		[μm]	*[μm]*	*[cSt]*	*[Nm]*	*[Mpa]*	*A*	*I*	*dif (%)*
Reference oil Mineral 1	Standard	0,50	0,99	19,34	28,8	514	0,205	0,342	/
	C-M1	0,96	1,69	19,34	28,8	514	0,120	0,200	-41
	N-M1	1,12	1,98	19,34	28,8	514	0,102	0,171	-50
	Mo-M1	1,17	2,10	19,34	28,8	514	0,097	0,161	-53
Ester 1	Standard	0,50	0,99	18,57	28,8	514	0,145	0,237	/
	C-E1	1,14	2,03	18,57	28,8	514	0,070	0,115	-51
	N-E1	1,13	1,97	18,57	28,8	514	0,073	0,119	-50
	Mo-E1	1,20	2,12	18,57	28,8	514	0,068	0,111	-53
Ester 2	Standard	0,50	0,99	21,63	28,8	514	0,160	0,270	/
	C-E2	1,11	1,96	21,63	28,8	514	0,081	0,136	-49
	N-E2	1,05	1,85	21,63	28,8	514	0,086	0,145	-46
	Mo-E2	1,16	2,05	21,63	28,8	514	0,077	0,130	-52
Ester 3	Standard	0,50	0,99	20,24	28,8	514	0,158	0,256	/
	C-E3	1,29	2,33	20,24	28,8	514	0,067	0,112	-58

a) Contact at pitch point (I).

b) Λ – specific film thickness evaluated in: A – beginning of engagement; I – pitch point.

Figure 4.2, Figure 4.3 and Figure 4.4 show the range of the roughness parameters $R_{Z\text{-}D}$, R_a and R_{PK} respectively, calculated from the measurements made on the teeth flanks of each tested gear, after grinding and heat treatment. The roughness values presented correspond to 3 measurements made on 3 different teeth of the pinion and wheel (totalizing 18 measurements in each direction, axial and radial – see Figure 3.7). This figure clearly shows that the surface roughness of the gears used in these tests is similar. Surface roughness in the radial direction is considerably larger than in the axial direction due to the grinding direction (axial).

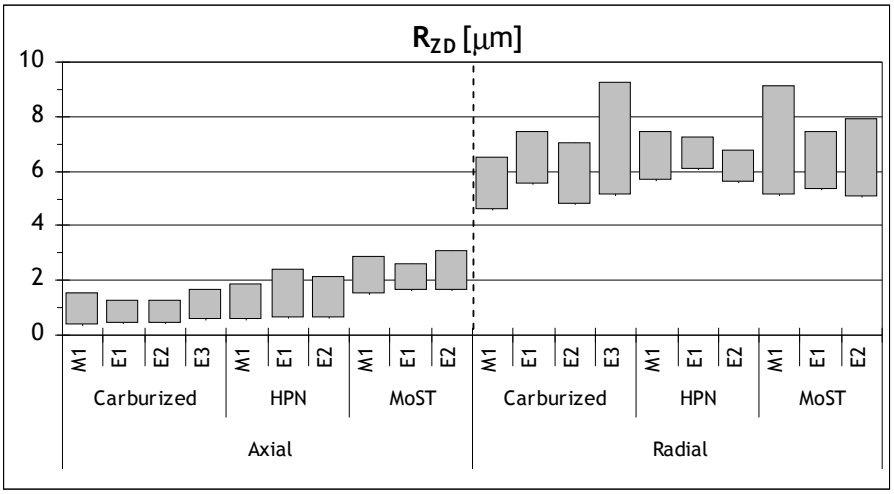


Figure 4.2 – R_{ZD} calculated from the roughness measurements made in axial and radial directions on the teeth flanks of each tested gear after grinding and heat treatment.

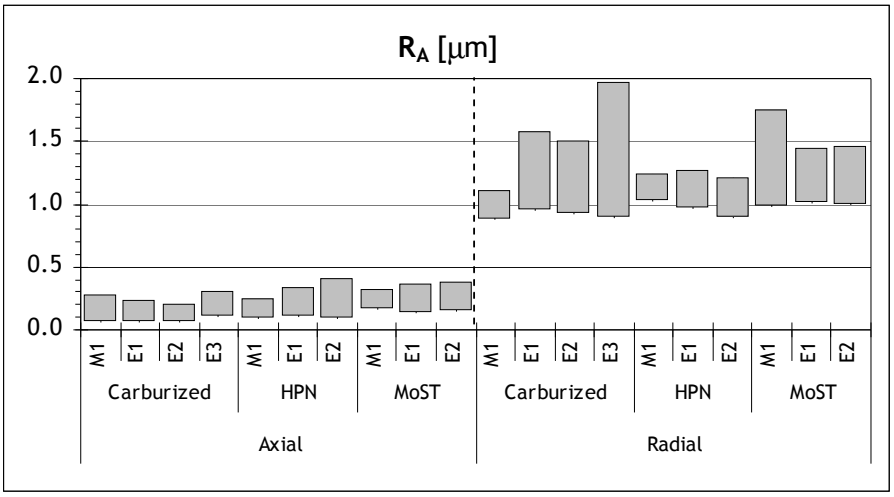


Figure 4.3 – R_a calculated from the roughness measurements made in axial and radial directions on the teeth flanks of each tested gear after grinding and heat treatment.

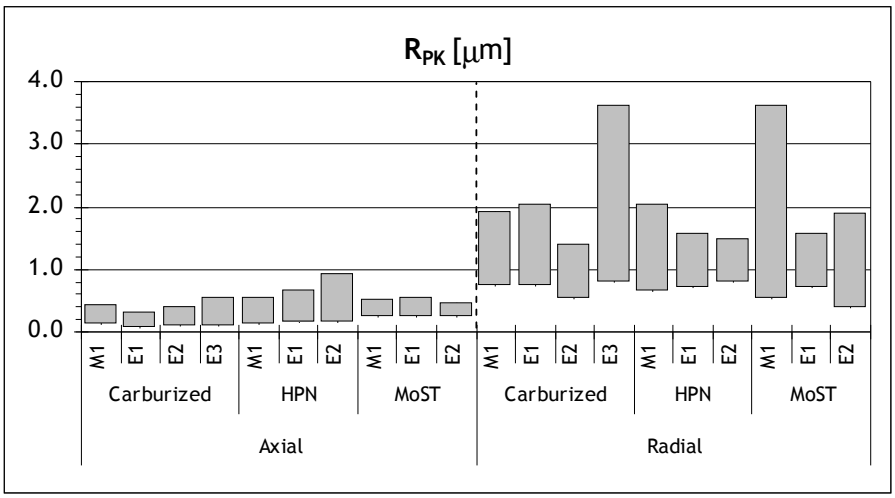


Figure 4.4 – R_{PK} calculated from the roughness measurements made in axial and radial directions on the teeth flanks of each tested gear after grinding and heat treatment.

4.3 Gear micropitting test procedure

Gear micropitting tests were based on the DGMK-FZG micropitting short test procedure (abbreviated as GFKT-C/8.3/90) [15], which is a short term test able to classify candidate lubricants in terms of gear micropitting, analogous to FVA-FZG-micropitting test [14].

The codification of the tests is showed in Table 4.6 . Test reference refers to the material type (C – case hardened, N – nitrided and Mo – MoS2/Ti coating) and to the lubricant (M – mineral and E – ester).

Table 4.7 shows the operating conditions used during the gear micropitting tests. Dip lubrication was used.

The GFKT micropitting test procedure specifies that the test should be performed on load stages K7 and K9. However, taking into account that the test gears had a very high initial roughness (see Table 4.4), tests were performed on load stages K6, K8 and K9, as indicated on Table 4.7. It was expected that decreasing one load stage might contribute to a better assessment and understanding of gear micropitting behaviour with different lubricants.

The test procedure can be resumed as follow:

1. Load stage K3 (running-in);
2. Collection of a lubricant sample for analysis;
3. Load stage K6;
4. Collection of a lubricant sample for analysis;
5. Dismounting gears, for weight and roughness measurement, surface photography;
6. Mounting gears with fresh lubricant;
7. Load stage K8;
8. Repeating step 4, step 5 and step 6;
9. Load stage K9;
10. Repeating step 4 and step 5.

After each load stage (except K3) the test gears were dismounted, cleaned in ultrasonic bath and weighted. Afterwards, the teeth flanks were inspected and photographed and the surface roughness of the teeth flanks was measured. The oil samples collected during the tests were analyzed by Ferrometry. Surface topography measurements were performed and some tooth flanks of the nitrided gears were examined by scanning electron microscopy (SEM).

Table 4.6 – Micropitting tests codification. Test references, materials and lubricants combinations.

Material	*Lubricant*	*Test Reference*
20 MnCr 5 case hardened	Mineral 1	C-M1
	Ester 1	C-E1
	Ester 2	C-E2
	Ester 3	C-E3
34 CrNiMo 6 high pressure nitrided	Mineral 1	N-M1
	Ester 1	N-E1
	Ester 2	N-E2
20 MnCr 5 case hardened + MoS_2/Ti	Mineral 1	Mo-M1
	Ester 1	Mo-E1
	Ester 2	Mo-E2

Table 4.7 - Operating conditions of gear micropitting tests (* at pitch point).

		K3 running in		K6		K8		K9	
		pinion	wheel	pinion	wheel	pinion	wheel	pinion	wheel
Oil temperature	[°C]	80		90					
Torque	[Nm]	28.8	43.2	98.9	148.4	171.6	257.4	215.6	323.4
Rotational speed	[rpm]	2250	1500	2250	1500	2250	1500	2250	1500
Tangential speed	[m/s]	8.3							
Hertzian contact pressure*	[MPa]	514		953		1256		1408	
Power	[kW]	6.8		23.3		40.4		50.8	
Duration	[h]	1		16		16		16	
N. of cycles	[10^3]	135	90	2160	1440	135	90	2160	1440

4.4 Gear micropitting results

The pinion performs 1.5 times more cycles than the wheel, so micropitting appears first on the pinion. For that reason, the results presented in this work are all referred to the pinion, except the mass loss that has been measured both on pinion and wheel. Post test analysis included visual inspection, examination by scanning electron microscopy[4], surface topography measurements of the teeth flanks, assessment of the micropitting area, mass loss of the gear (pinion and wheel), ferrometric analysis of the lubricant samples and surface roughness measurement of the teeth flanks, below and above the pitch line.

Detailed information about the several aspects evaluated during the gear micropitting test is gathered in Appendix C – Gear micropitting tests data sheets.

4.4.1 Mass loss

The mass loss results give a global perspective of the severity of wear during each load stage.

The measurements of pinion and wheel mass loss during each load stage and for each material/lubricant combination are presented in Figure 4.5. Each bar shows pinion mass loss (lower part of the bar) and the wheel mass loss (dashed part). Each colour corresponds to a specific lubricant (M1: black, E1: red, E2: blue and E3: green). Generally, the mass loss of the pinion and wheel increased with the load stage.

During running-in and load stage K6, the carburized gears lubricated by E2 and E3 gear oil had almost the same mass loss value. The carburized gear tested using lubricant E1 was the material-lubricant combination that had the highest mass loss value till load stage k6 while test C-M1 had the lowest mass loss during the same period. All the nitrided gears showed similar values of mass loss and the same happened with the coated gears. The tests of nitrided gears and the one with the carburized gear lubricated with mineral oil showed the best results during the first two load stages.

Total mass loss after load stage K8 was close to 10 mg (test of the nitrided gears and using the material/lubricant combinations C-M1, C-E2 and Mo-M1).

[4] SEM analysis was made only for nitrided gears.

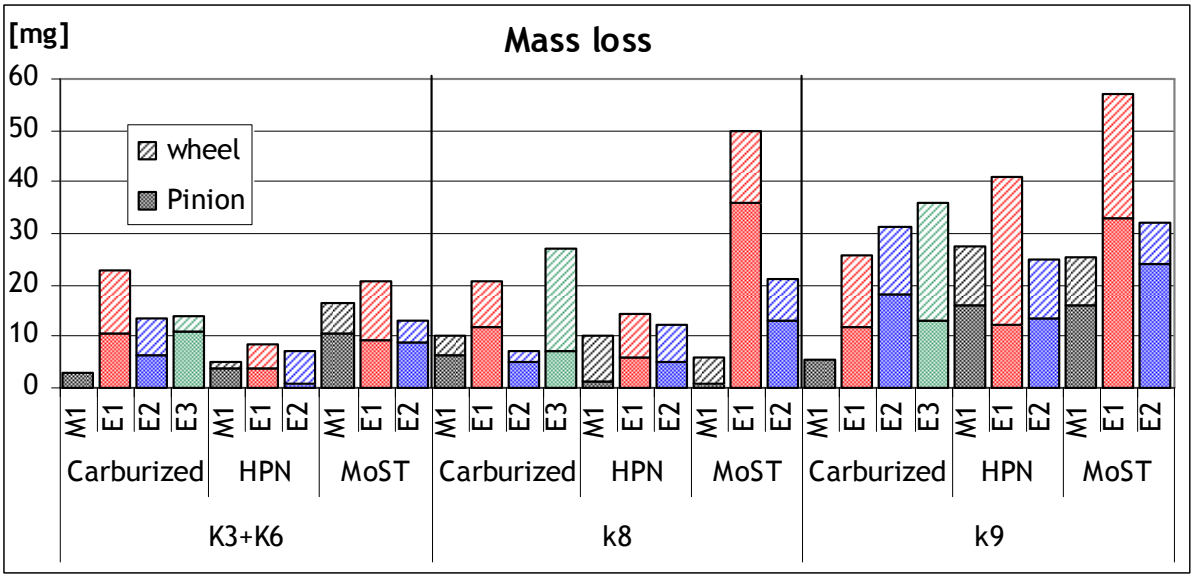


Figure 4.5 – Mass loss results.

Total mass loss after load stage K8 was close to 10 mg for both materials. After load stage K9 the carburized steel had the higher value of mass loss while the high pressure nitrided steel had a mass loss value slightly smaller. Once again, E1 lubricant allowed high values of mass loss. E3 ester lubricant also conducted to a significant mass loss value.

After load stage k9, only the carburized gear lubricated with the mineral oil didn't show a significant increase of the mass loss value. Gears from the other material-lubricant combinations had mass loss values around 30 mg, except the nitrided and the coated gear lubricated with E1 ester oil, which presented higher mass loss values.

For more detailed information about mass loss results see Appendix C – Gear micropitting tests data sheets.

4.4.2 Ferrometry

Oil samples collected during gear micropitting tests were analyzed by Direct Reading Ferrography, also designated as Ferrometry. For each lubricant sample, the ferrometric parameters *DL*(large wear particles index) and *DS* (small wear particles index) were measured and the corresponding concentration of wear particles index - *CPUC* (representing the total amount of wear particles contained in a lubricant sample) and the severity wear particles index - *ISUC* (related to the severity of the wear particles contained in a lubricant sample) were determined.

Figure 4.6 and Figure 4.7 present the evolutions of the *CPUC* and *ISUC* indexes, respectively during the gear micropitting tests.

Figure 4.6 show that during the running-in (load stage K3) the carburized gear lubricated with ester oils E1 and E3 generated higher wear particle concentration than the others material-lubricant combinations.

After load stage K6, once again the carburized gear lubricated with E1 and E3 lubricant had the highest *CPUC* index values, fallowed by the C-E2 combination. During this load stage, E1 ester generated a higher wear particle concentration with all materials. *CPUC* index of coated gears did not have the evolution shown on the mass loss results (where the coated gears had similar or higher values of mass loss), because the wear particles from

MoS_2/Ti coating are not ferromagnetic and are not detectable on the device used to measure *DL* and *DS* indexes. Probably, detected wear particles belonged to the ferromagnetic base material.

During load stages K8 and k9, the carburized gears (coated or not) lubricated with mineral gear oil presented the smallest *CPUC* values. The other material-lubricant combinations had similar values on load stage K8. On load stage K9, the carburized gear generated smaller wear particle concentration when lubricated with the mineral oil, while the nitrided gear generated less wear particles when the esters were used.

Figure 4.7 shows that during the first two load stages, the carburized gears lubricated by the ester oils (E1 and E3 on load stage K3 and the three esters on load stage K6) generated more severe wear particles while the other material lubricant combinations had similar results. On load stages K8 and K9 the carburized gears revealed the same tendency observed during load stages K3 and K6. The highest *ISUC* index value corresponding to nitrided gears was obtained with M1 lubricant and to the ester E1 when coated gears were tested.

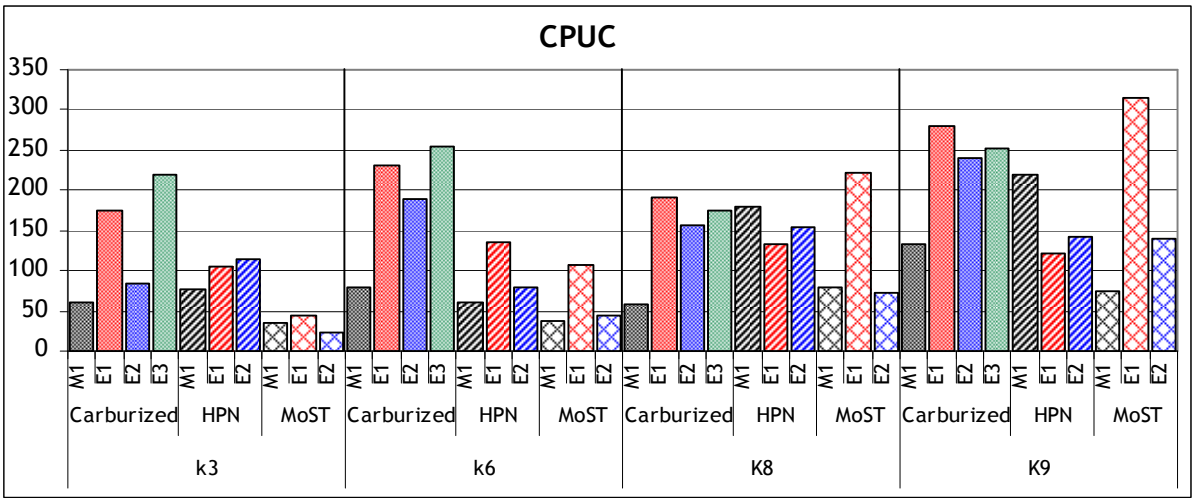


Figure 4.6 - Evolution of the *CPUC* index during the gear micropitting tests.

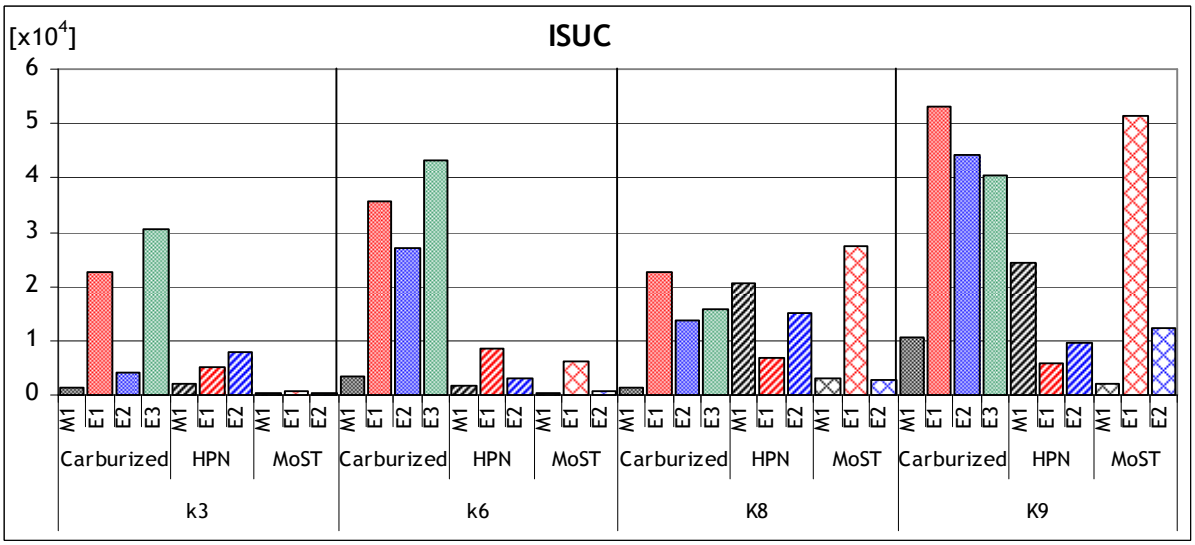


Figure 4.7 – Evolution of the *ISUC* index during the gear micropitting tests.

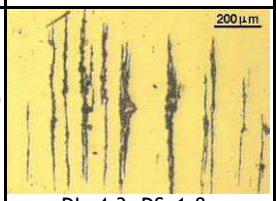
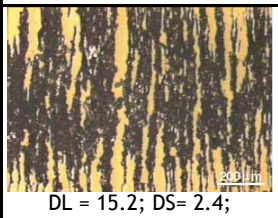
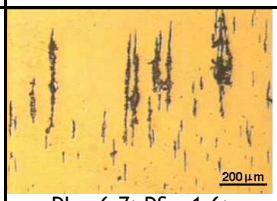
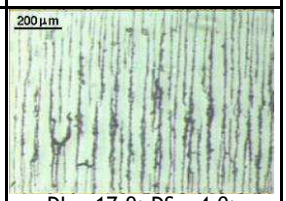
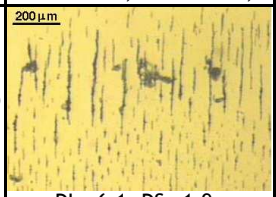
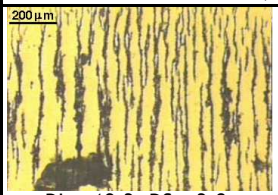
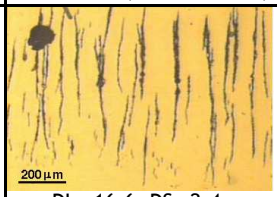
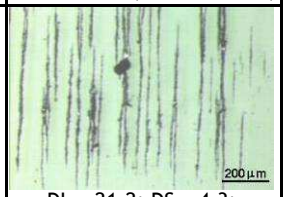
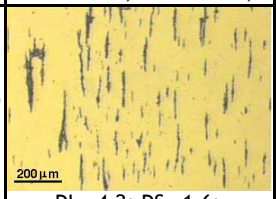
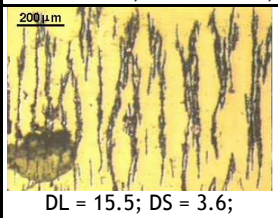
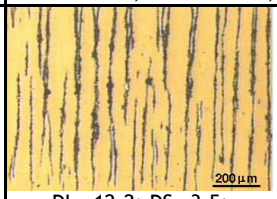
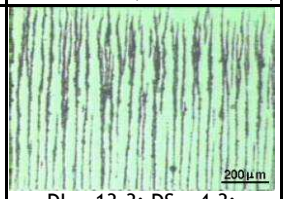
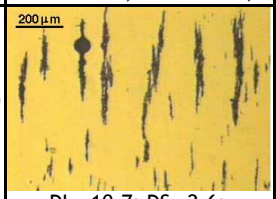
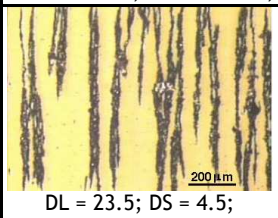
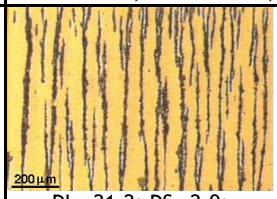
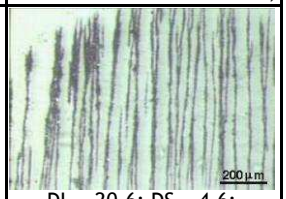
4.4.3 Analytical Ferrography

Table 4.8, Table 4.9 and Table 4.10 present pictures of the ferrograms and ferrometry values from the lubricant samples collected during gear micropitting tests of each material (carburized steel, high pressure nitrided steel and carburized steel of the MoS_2/Ti coated, respectively).

Concerning to the wear particles type, the evolution is the same in all tests. After running-in wear particles of large size and fatigue particles of smaller size were detected (see Figure 4.8). Next two load stages (K6 and K8) only produced small wear particles (see Figure 4.9) while during the last load stage (K9) large wear particles reappeared.

The ferrograms from Table 4.8 show that when carburized gears were tested, the reference mineral oil allowed a significantly smaller wear particle concentration at all load stages, confirming the results of the *CPUC* and *ISUC* indexes (see Figure 4.6 and Figure 4.7). On the other hand, an opposite tendency was observed on the tests of the nitrided gears, the mineral oil promoting a higher wear particle concentration during load stage K9 (see Table 4.9, Figure 4.6 and Figure 4.7).

Table 4.8 - Ferrograms obtained after each load stage of micropitting tests with carburized gears. (Magnification = 100 x; *d*=0.1).

	Lubricants			
	Mineral 1	**Ester 1**	**Ester 2**	**Ester 3**
Load stage K3	 DL=4.3; DS=1.8; CPUC=61.0; ISUC=1.5E3;	 DL = 15.2; DS= 2.4; CPUC = 176.0 ISUC = 2.3E4;	 DL = 6.7; DS = 1.6; CPUC = 83.0; ISUC = 4.2E3;	 DL = 17.9; DS = 4.0; CPUC = 219.0; ISUC = 3.0E4;
Load stage K6	 DL =6.1; DS =1.9; CPUC=80.0; ISUC=3.4E3;	 DL = 19.3; DS = 3.8; CPUC = 231.0; ISUC = 3.6E4;	 DL =16.6; DS =2.4; CPUC = 190.0; ISUC = 2.7E4;	 DL = 21.2; DS = 4.3; CPUC = 255.0; ISUC = 4.3E4;
Load stage K8	 DL =4.2; DS =1.6; CPUC=58.0; ISUC=1.5E3;	 DL = 15.5; DS = 3.6; CPUC = 191.0; ISUC = 2.3E4;	 DL =12.2; DS =3.5; CPUC = 157.0; ISUC = 1.4E4;	 DL = 13.3; DS = 4.3; CPUC = 176.0. ISUC = 1.6E4;
Load stage K9	 DL =10.7; DS =2.6; CPUC=133.0; ISUC=1.1E4;	 DL = 23.5; DS = 4.5; CPUC = 280.0; ISUC = 5.3E3;	 DL =21.2; DS =2.9; CPUC = 241.0; ISUC =4.4E4;	 DL = 20.6; DS = 4.6; CPUC = 252.0; ISUC = 4.0E4;

The three lubricants had similar results during the first two load stages (K3 and K6) of the coated gears tests. During load stage K8 and K9, E1 ester oils displayed a significantly higher concentration of wear particles (see Table 4.10), witch is consistent with the mass loss results (see Figure 4.5) and the evolution of the *ISUC* and *CPUC* wear particles indexes (see Figure 4.6 and Figure 4.7).

In general, the ferrograms show the same tendency that was observed on the evolution of wear particle indexes (see Figure 4.6 and Figure 4.7).

Some friction polymers were detected in two tests with ester oil (test N-E2: load stage K8; test Mo-E1: load stages k6, K8 and K9). Figure 4.10 shows an example of a friction polymer found in the oil sample collected after load stage K8 in the test of nitrided gears lubricated by E2 ester oil.

Table 4.9 - Ferrograms obtained after each load stage of micropitting tests with nitrided gears. (Magnification = 100 x; *d*=0.1).

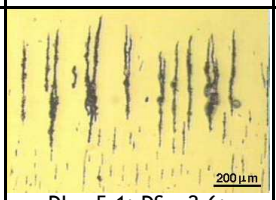
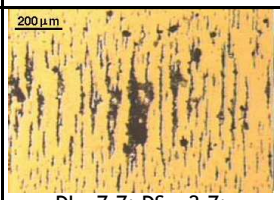
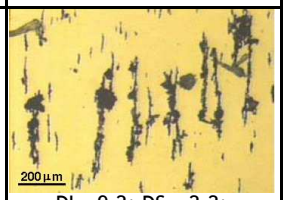
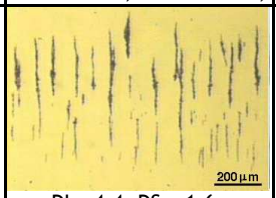
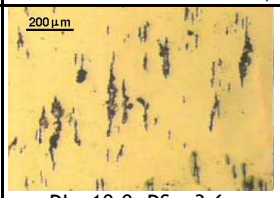
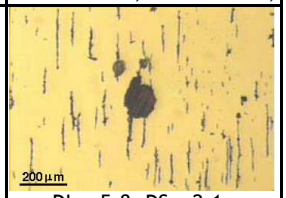
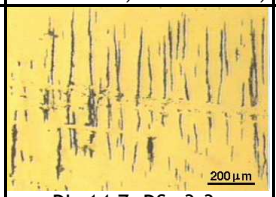
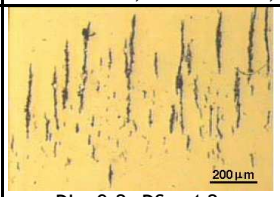
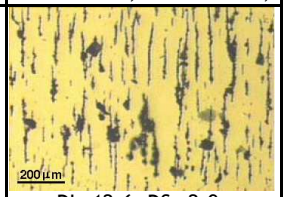
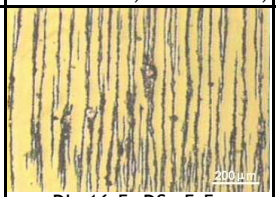
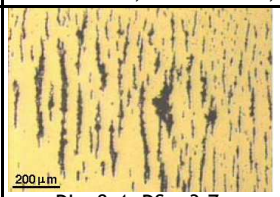
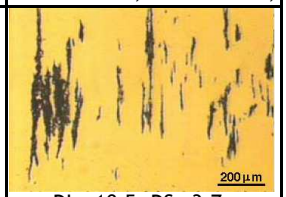
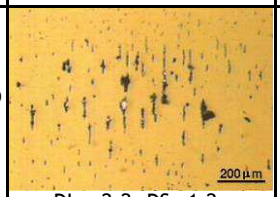
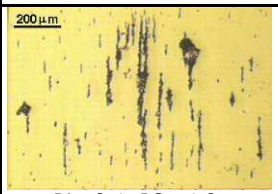
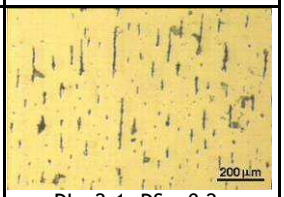
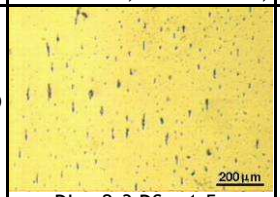
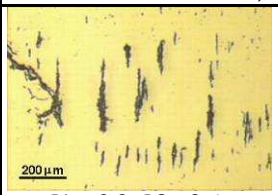
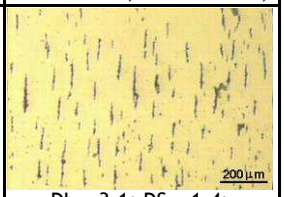
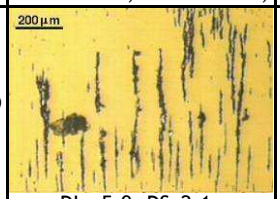
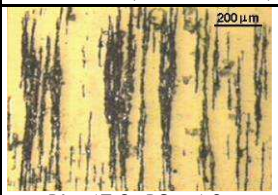
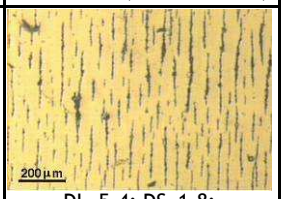
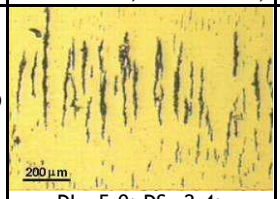
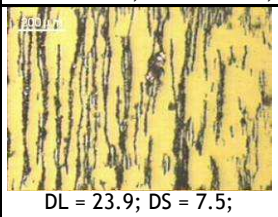
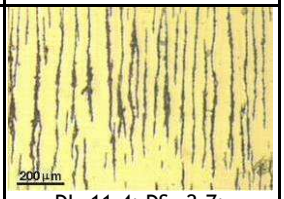
	Lubricants		
	Mineral 1	**Ester 1**	**Ester 2**
Load stage K3	 DL = 5.1; DS = 2.6; CPUC = 77.0; ISUC = 1.9E3;	 DL= 7.7; DS = 2.7; CPUC = 104.0 ISUC = 5.2E3;	 DL= 9.2; DS = 2.2; CPUC = 114.0; ISUC = 8.0E3;
Load stage K6	 DL= 4.4; DS = 1.6; CPUC = 60.0; ISUC = 1.7E3;	 DL= 10.0; DS = 3.6; CPUC = 136.0; ISUC = 8.7E3;	 DL = 5.8; DS = 2.1; CPUC = 79.0; ISUC = 2.9E3;
Load stage K8	 DL=14.7; DS =3.3; CPUC = 180.0; ISUC =2.1E4;	 DL= 9.2; DS = 4.2; CPUC = 134.0; ISUC = 6.7E3;	 DL=12.6; DS =2.9; CPUC = 155.0; ISUC = 1.5E4;
Load stage K9	 DL=16.5; DS =5.5; CPUC = 220.0; ISUC =2.4E4;	 DL= 8.4; DS = 3.7; CPUC = 121.0; ISUC = 5.7E3;	 DL =10.5; DS =3.7; CPUC = 142.0; ISUC = 9.7E3;

Table 4.10 - Ferrograms obtained after each load stage of micropitting tests with coated gears. (Magnification = 100 x; *d*=0.1).

	Lubricants		
	Mineral 1	**Ester 1**	**Ester 2**
Load stage K3	 DL = 2.2; DS= 1.2; CPUC = 34.0; ISUC = 3.4E2;	 DL= 3.1; DS = 1.3; CPUC = 44.0 ISUC = 7.9E2;	 DL= 2.1; DS = 0.2; CPUC = 23.0; ISUC = 4.4E2;
Load stage K6	 DL = 2.3 DS = 1.5; CPUC = 38.0; ISUC = 3.0E2;	 DL = 8.3; DS = 2.4; CPUC = 107.0; ISUC = 6.3E3;	 DL = 3.1; DS = 1.4; CPUC = 45.0; ISUC = 7.7E2;
Load stage K8	 DL =5.9; DS=2.1; CPUC = 80.0; ISUC =3.0E3;	 DL= 17.3; DS = 4.9; CPUC = 222.0; ISUC = 2.8E4;	 DL=5.4; DS=1.8; CPUC = 72.0; ISUC = 2.6E3;
Load stage K9	 DL =5.0; DS =2.4; CPUC = 74.0; ISUC =1.9E3;	 DL = 23.9; DS = 7.5; CPUC = 314.0; ISUC = 5.1E4;	 DL=11.4; DS =2.7; CPUC = 141.0; ISUC = 1.2E4;

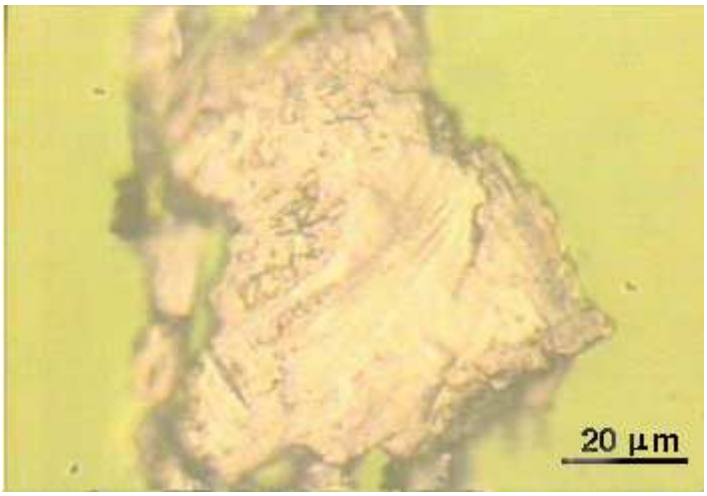


Figure 4.8 - Example of a large size wear particle found in the lubricant sample collected after load stage K3 of the C-M1 micropitting test (magnification 1000x).

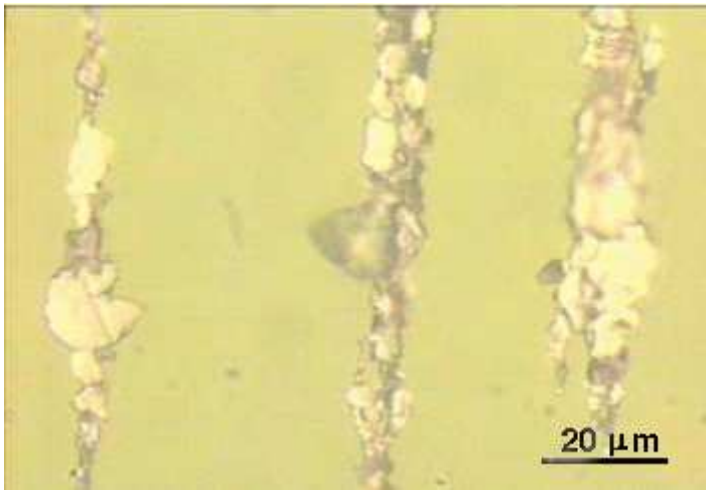


Figure 4.9 - Example of small wear particles found in the lubricant sample collected after load stage K6 of the C-M1 micropitting test (magnification 1000x).

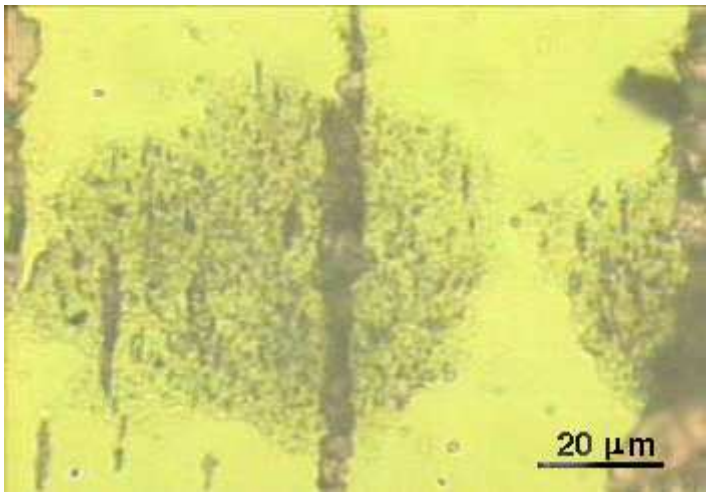


Figure 4.10 - Friction polymer detected in N-E2 micropitting test after load stage K8 (magnification 1000x).

4.4.4 Visual inspection

Assessment of micropitting failure is a difficult task to perform by visual inspection. It is often reported that with gears mounted on the shafts, it is almost impossible to detect micropitting. Light of high intensity is needed to distinguish the grey stained area that micropitting resembles. That same difficulty was experienced in these tests.

During teeth inspection after each load stage, after dismounting and cleaning, teeth surface were photographed with a high resolution camera and the micropitting area was measured. Table 4.11, Table 4.12 and Table 4.13 display representative pictures of pinion teeth for each material (carburized steel, high pressure nitrided steel and carburized steel with the MoS_2/Ti coating, respectively). The micropitting area is surrounded by a red line for better recognition and the corresponding values are presented as a percentage of the total flank area. Each row of these tables corresponds to a particular lubricant and each column corresponds to a specific load stage.

All lubricants had similar behaviours during the micropitting tests of the carburized gears. However, E2 and E3 biodegradable esters displayed the lowest percentage of micropitting area after load stage k9 (see Table 4.11).

High pressure nitrided steel was the gear material that performed better concerning the percentage of teeth flanks area with micropitting. Table 4.12 shows that from running-in until load stage K8, the pinions didn't show any evidence of micropitting. After load stage K9, gears lubricated with M1 and E1 lubricants displayed a small micropitting area (M1: 13% and E1: 5%) while gears tested with the E2 lubricant still didn't show any evidence of micropitting.

On the micropitting tests performed with coated gears mineral oil had always a lower value of micropitted area, while both esters had very similar behaviours as may be seen in Table 4.13.

Three body abrasion marks were also visible on the teeth flanks of carburized and nitrided pinions, mainly above the pitch line and after load stage k9, possibly generated by the micropitting wear particles released during the tests.

Table 4.11 - Visual inspection: Carburized steel.

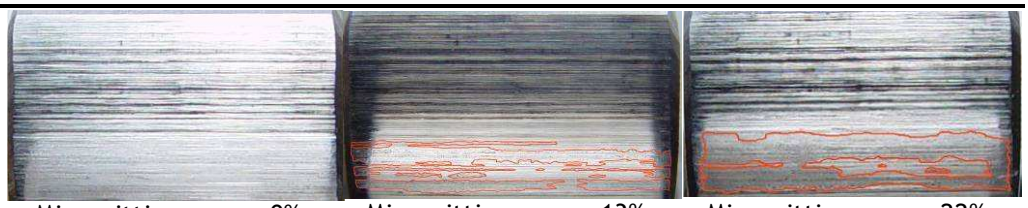
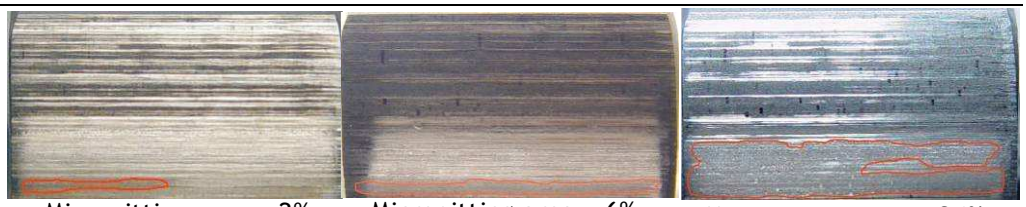
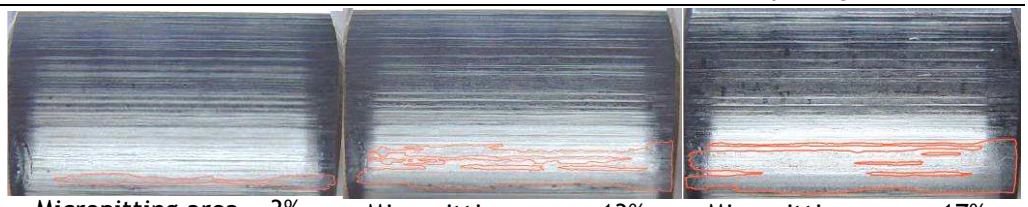
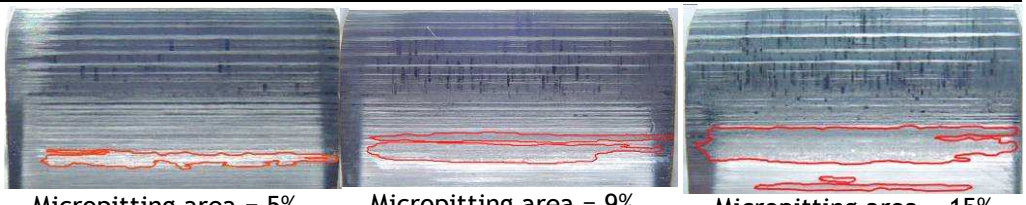
Load stage	K6 T_{wheel}=148Nm	K8 T_{wheel}=257Nm	K9 T_{wheel}=323Nm
C-M1	 Micropitting area = 0%	Micropitting area = 13%	Micropitting area = 22%
C-E1	 Micropitting area = 2%	Micropitting area = 6%	Micropitting area = 24%
C-E2	 Micropitting area = 3%	Micropitting area = 13%	Micropitting area = 17%
C-E3	 Micropitting area = 5%	Micropitting area = 9%	Micropitting area = 15%

Table 4.12 - Visual inspection: High pressure nitrided steel.

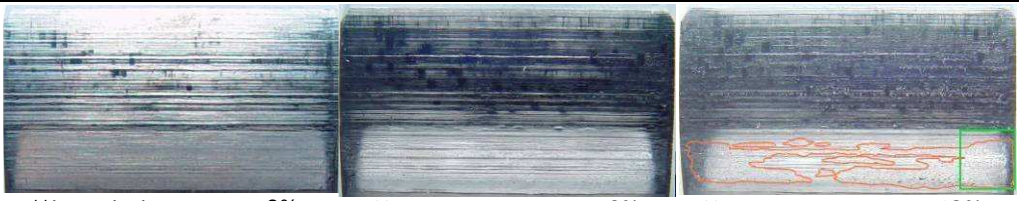
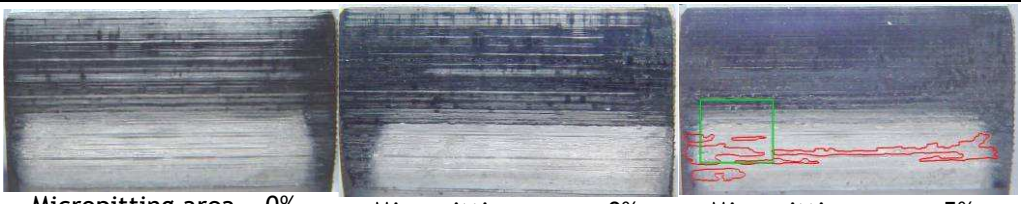
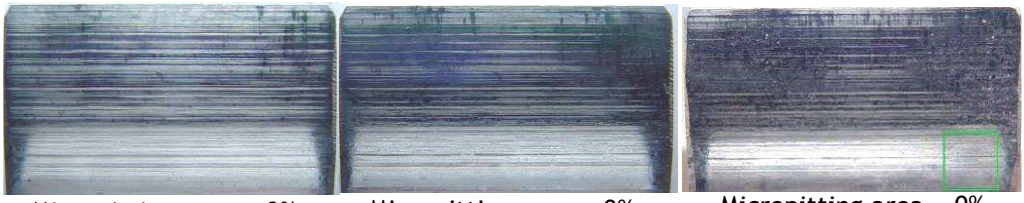
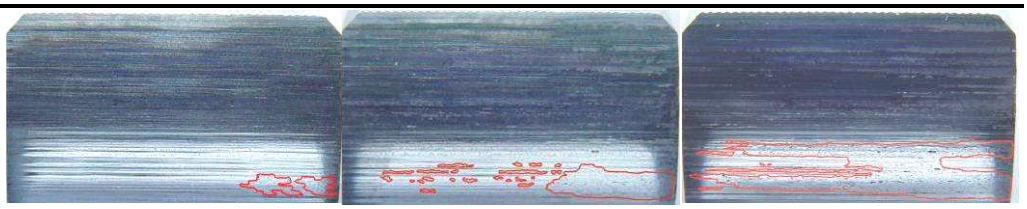
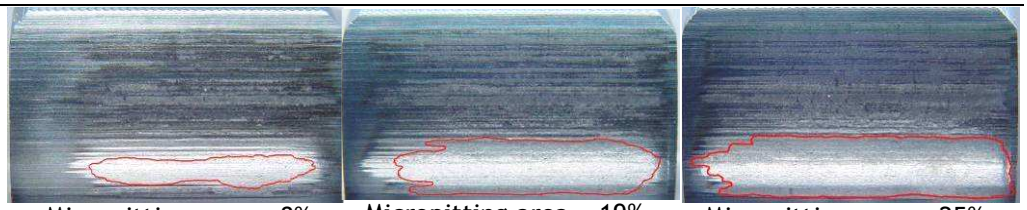
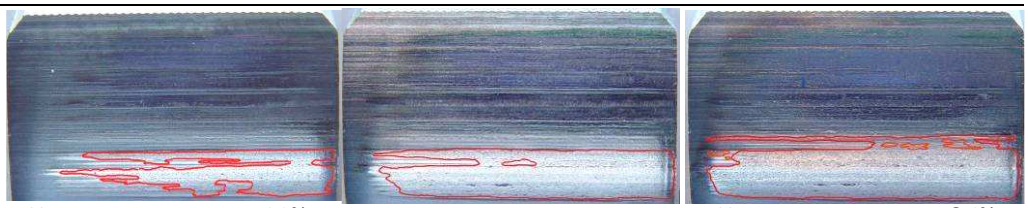
Load stage	K6 T_{wheel}=148Nm	K8 T_{wheel}=257Nm	K9 T_{wheel}=323Nm
N-M1	 Micropitting area = 0%	Micropitting area = 0%	Micropitting area = 13%
N-E1	 Micropitting area = 0%	Micropitting area = 0%	Micropitting area = 5%
N-E2	 Micropitting area = 0%	Micropitting area = 0%	Micropitting area = 0%

Table 4.13 - Visual inspection: Carburized steel with a MoST coating.

Load stage	K6 T_{wheel}=148Nm	K8 T_{wheel}=257Nm	K9 T_{wheel}=323Nm
Mo-M1	 Micropitting area = 2%	Micropitting area = 6%	Micropitting area = 18%
Mo-E1	 Micropitting area = 8%	Micropitting area = 19%	Micropitting area = 25%
Mo-E2	 Micropitting area = 11%	Micropitting area = 19%	Micropitting area = 24%

4.4.5 Surface roughness

Surface roughness of the teeth flanks was measured in the radial and axial directions, in both cases below and above pitch line, as shown in Figure 4.11. Roughness measurements were performed using a Hommelwerk T4000 device, covering a total measurement length of L_t=**4.8 mm** and a cut-off filter λ_c=**0.8 mm**, and they were digitally filtered [16].

The roughness measurements made in the axial direction revealed to be more useful to evaluate gear micropitting and its evolution during the tests, since in that direction the initial roughness is very small, thus micropitts formation became very clear.

Figure 4.12 shows the roughness profiles of each material-lubricant combination measured below pitch line on the axial direction after load stages K8 and K9, allowing the comparison of micropitting evolution during each test. In each figure, there are three graphs corresponding to the different tested gear materials (see Table 4.6). For each material, there are one coloured roughness profile corresponding to each lubricant (M1: black, E1: red, E2: blue and E3: green) and a grey line corresponding to the roughness profile measured on the new surface.

Below each roughness profile graph, there is a table (Table 4.14 and Table 4.15) with the roughness parameters witch significantly evolved. The evaluation of the variation of these roughness parameters is a good way to quantify the main changes in the roughness profiles showed in Figure 4.11 and Figure 4.12.

For detailed information about measured roughness profiles and roughness parameters Appendix C – Gear micropitting tests data sheets.

After load stage K8 (see Figure 4.12) the roughness profiles of the carburized and of the coated gears, whatever the lubricant, present a significant number of dip valleys corresponding to micropitts, while the nitrided gears show very few valleys and an almost flat surface, indicating that gear micropitting didn't occur. This result is in agreement with the visual inspection of the tooth flanks and with the micropitting area results reported in Table 4.11, Table 4.12 and Table 4.13.

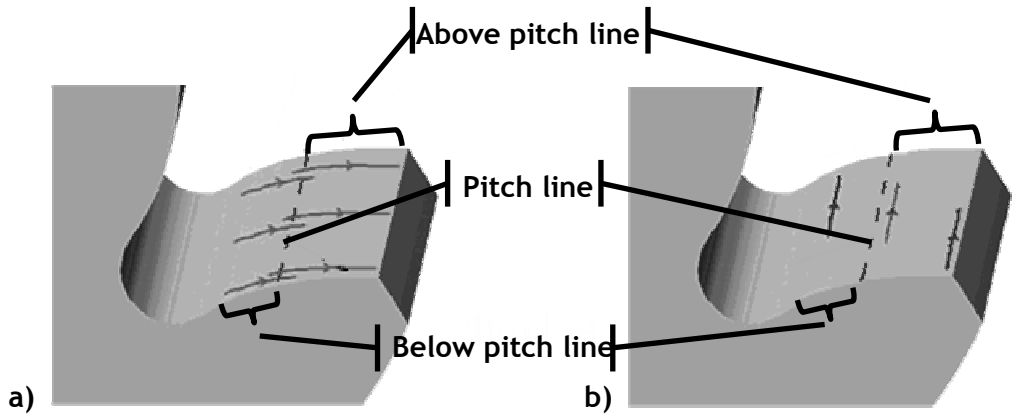


Figure 4.11 - Roughness measurements location (a- radial direction; b- axial direction).

The roughness parameters presented in Table 4.14 also give the same indication. The R_{vk} roughness parameter, related to the depth of the surface roughness valleys and, thus, to micropitts, shows a very significant increase after load stage K8 in the cases of the carburized gears and the coated ones, from 0.4 up to 1.6μm in the case of the carburized gears lubricated with the E2 ester oil and from 0.6 to 2.2 μm in the case of the coated gears lubricated with the same lubricant. The roughness profiles and the R_{VK} evolution also indicate that the micropitts in the coated gears seems to be deeper. In the case of nitrided gears the R_{vk} parameter didn't have a significant increase.

After load stage K9 (see Figure 4.13), only the roughness profile measured in the nitrided gear lubricated with the ester E2 didn't show dip valleys, meaning that micropitting didn't occur, the corresponding R_{vk} parameter didn't have a significant evolution (see Table 4.15) in agreement with the visual inspection of the tooth flanks and the micropitting area results reported in Table 4.12. All the other material/lubricant combinations lead to micropitting. The roughness profiles confirm this fact because the number and the valleys depth increase in all roughness profiles. As expected, the roughness parameter values also increase (see Table 4.15).

The values of the $R_{Z\text{-}D}$ and R_{VK} roughness parameters (see Table 4.15) indicate that reference mineral oil caused deeper valleys in the tests with all gear materials. Micropitting is much more visible with many deep valleys on the roughness profiles from tests with coated gears (the higher values of $R_{Z\text{-}D}$ and R_{Vk} confirm this fact – see Table 4.15).

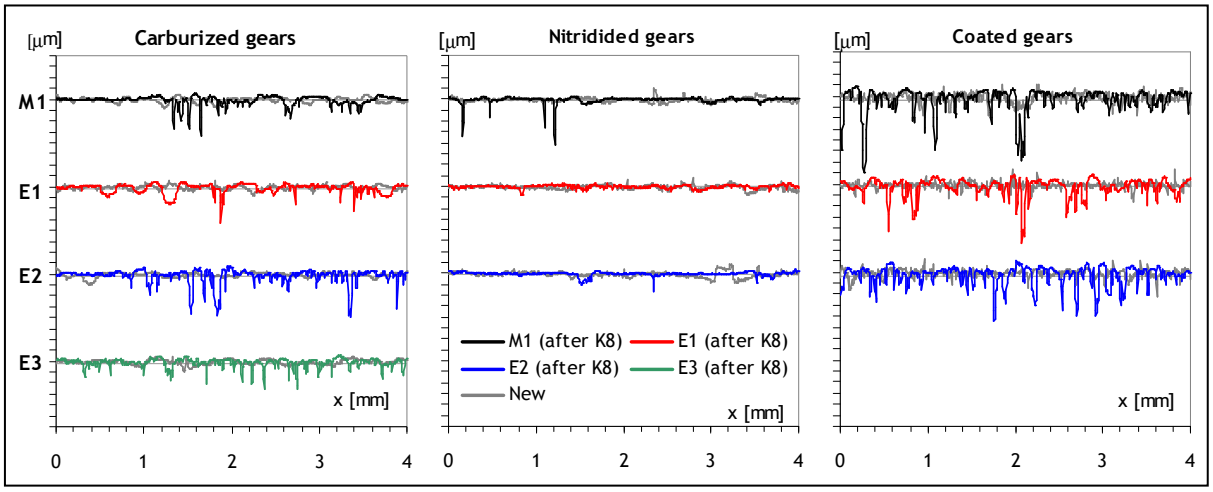


Figure 4.12 - Pinion roughness profiles measured after load stage K8 along the axial direction and below pitch line.

Table 4.14 - R_{ZD} and R_{VK} roughness parameters calculated from the measurements made after load stage k8 along the axial direction, below pinion pitch line (values in μm).

		Carburized steel		Nitrided steel		MoS_2/Ti coating	
		$R_{Z\text{-}D}$	R_{VK}	$R_{Z\text{-}D}$	R_{VK}	$R_{Z\text{-}D}$	R_{VK}
Initial		1.0	0.4	1.0	0.3	2.1	0.6
After K8	M1	2.3	1.1	1.4	0.5	3.3	1.8
	E1	2.8	1.2	0.8	0.4	4.5	2.2
	E2	3.0	1.6	0.8	0.5	4.0	1.9
	E3	1.7	0.8				

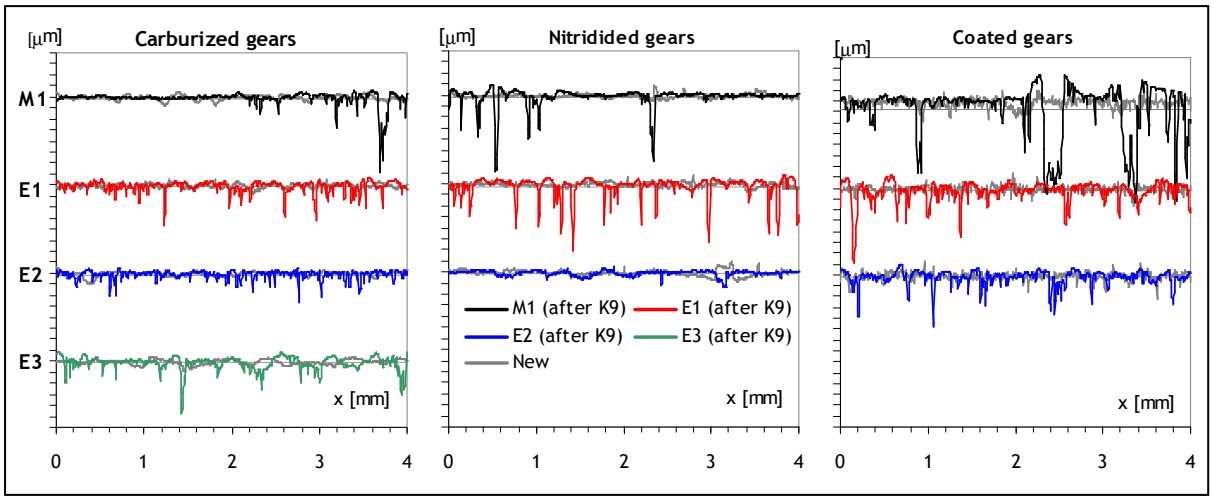


Figure 4.13 - Pinion roughness profiles measured after load stage K9 along the axial direction and below pinion pitch line.

Table 4.15 - R_{ZD} and R_{VK} roughness parameters calculated from the measurements made after each load stage k9 along the axial direction, below pinion pitch line (values in μm).

		Carburized steel		Nitrided steel		MoS_2/Ti coating	
		R_{Z-D}	R_{VK}	R_{Z-D}	R_{VK}	R_{Z-D}	R_{VK}
Initial		1.0	0.4	1.0	0.3	2.1	0.6
After K9	M1	2.6	2.1	3.5	2.2	6.3	4.5
	E1	2.5	0.9	3.1	1.5	3.7	1.6
	E2	2.1	0.8	0.8	0.5	3.7	1.4
	E3	2.9	1.1				

4.4.6 Surface topography

In order to have more precise information about the morphology and depth of the micropitts, surface topography measurements of teeth flanks were performed below the pitch line, as shown in Figure 4.14.

The topography measurements were performed on the same device used to measure the surface roughness. Each measurement is composed by 200 roughness profiles measured in axial direction (see Figure 4.11) using a total measurement length L_t=12 mm. Figure 4.15, Figure 4.16 and Figure 4.17 present the topography measurements (2x12 mm) made in the carburized, nitrided and coated gears, respectively. More detailed topography results are collected in Appendix C – Gear micropitting tests data sheets.

Figure 4.15 clearly shows that the tooth from the carburized gear lubricated with mineral gear oil presents more micropitts and deeper than the teeth flanks lubricated with the ester oils. On the flanks tested with the esters oil is also possible to identify several micropitts however, their number, size and depth are smaller that those ones observed with M1 lubricant.

Figure 4.16 show that nitrided gears displayed the best performance concerning to the micropitting formation. The gear lubricated by the mineral oil have several micropitts (some of them with a significant depth) however, their number and size are smaller than those displayed by the other gear materials. On the flank tested with E1 ester oil, the amount of micropitts is smaller than those observed with the M1 lubricant. On the micrographs corresponding to the E2 gear oil, only a few micropitts appeared and the most part of the grinding marks still are visible.

The topography measurements presented in Figure 4.17 indicate that the worst microppitting results were obtained by the coated gears. As it happened with the other gear materials, the tooth flanks lubricated with the ester oils present less concentration of large micropitts and the best performance was achieved by E2 lubricant. The central part of tooth lubricated by ester E1 seems to have suffered severe wear, which is in agreement with the mass loss results (see Figure 4.5).

Table 4.16 presents some representative unfiltered roughness profiles selected from the topography measurements (see Appendix C – Gear micropitting tests data sheets). The profiles were filtered and Table 4.17 display the roughness parameters calculated from each one.

Some representative areas (2 x 2 mm) were selected from each topography measurement of pinion teeth (see Appendix C – Gear micropitting tests data sheets). Table 4.18 displays the micropitts with a depth greater than 5 μm in those areas and the corresponding relative area in percentage of the total area (4 mm^2). The value 5 μm was chosen because after the gear micropitting tests the R_{max} parameter corresponding to the measurements made in radial direction is always grater than 5 μm, while in the cases where there is no micropitting, it doesn't exceed this value.

Table 4.16, Table 4.17 and Table 4.18 confirms that the nitrided gears display less micropitts. All the tooth flanks lubricated with mineral gear oil presents more and deeper micropitts than the teeth flanks lubricated with the ester oils.

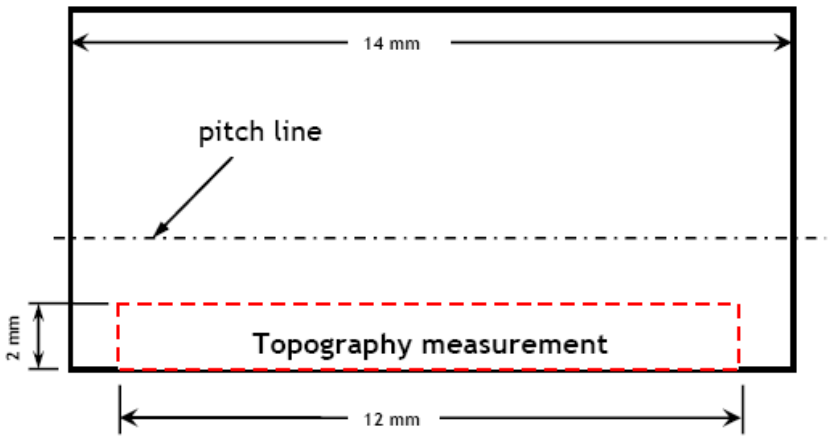


Figure 4.14 - Topography measurements location.

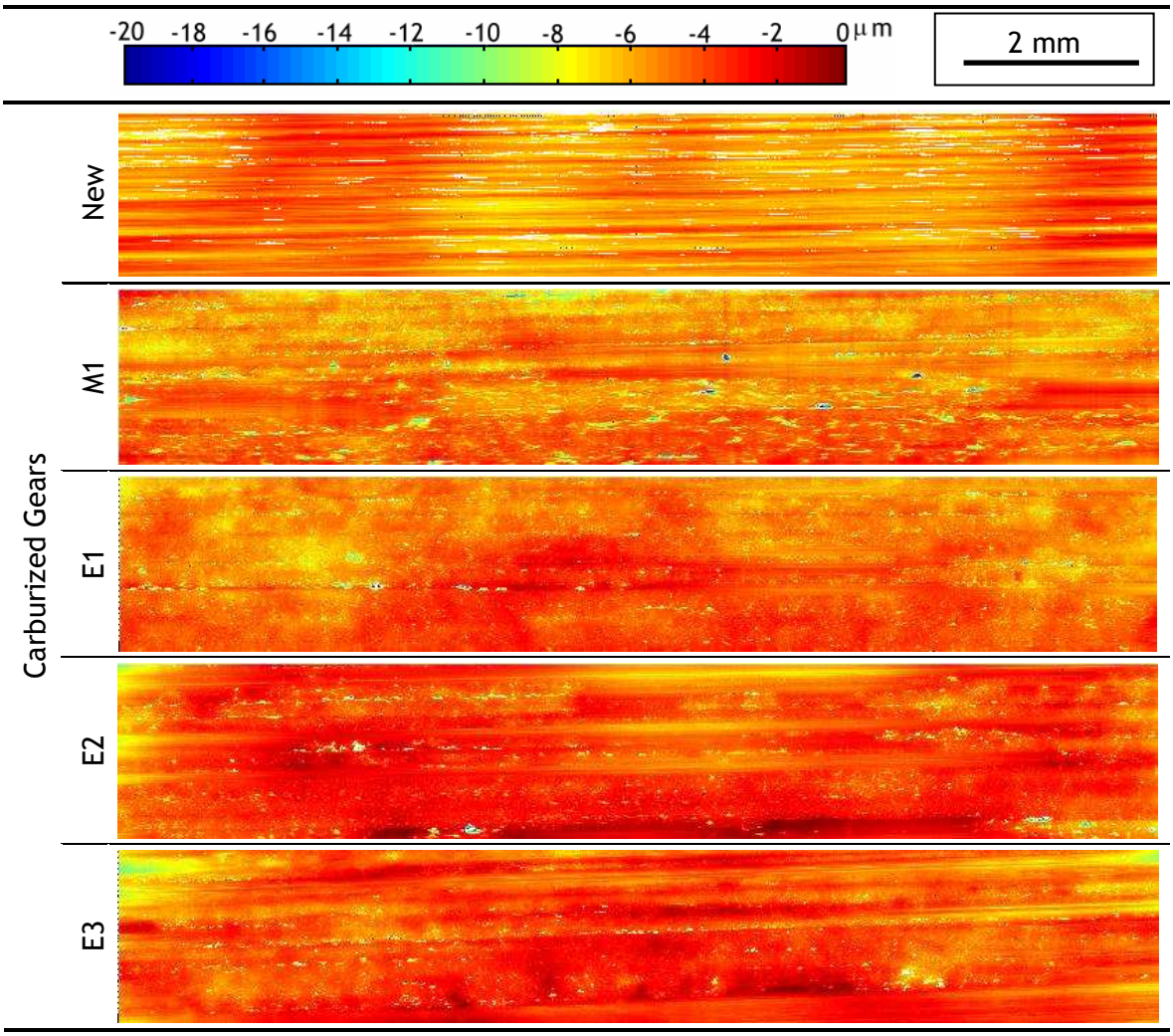


Figure 4.15 – Topography measurements in the carburized gears.

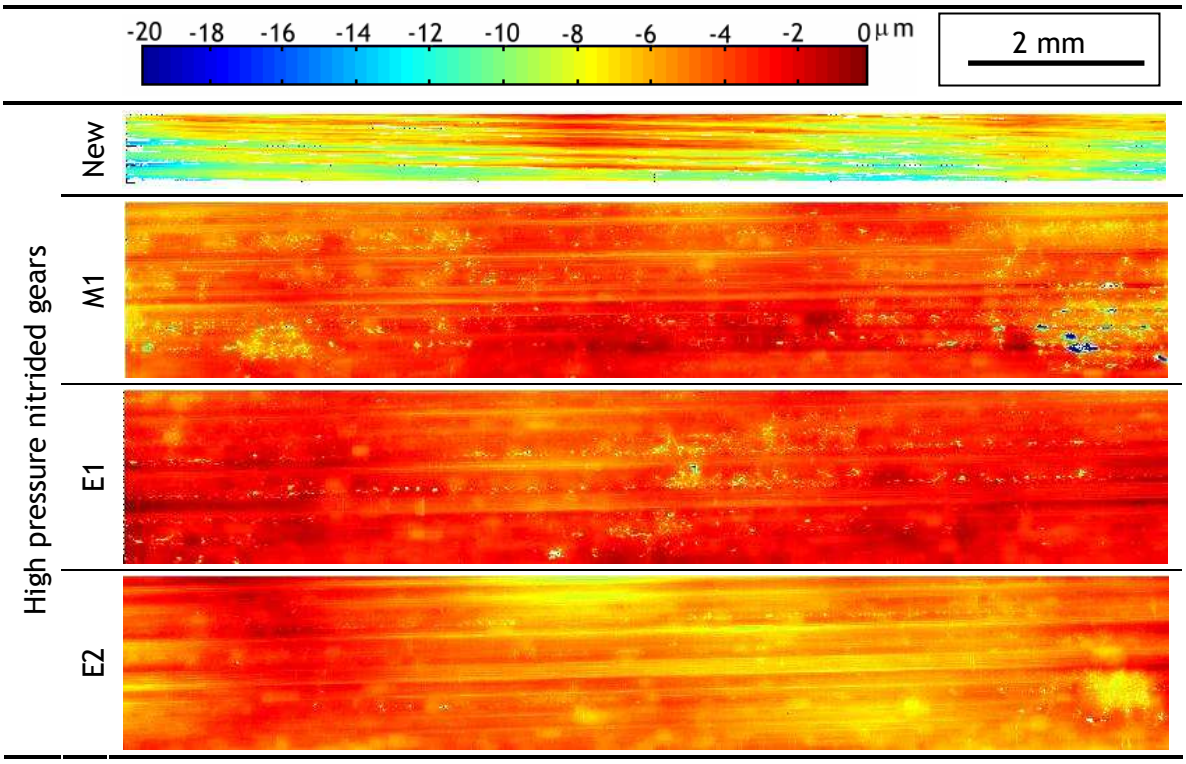


Figure 4.16 - Topography measurements in the high pressure nitrided gears.

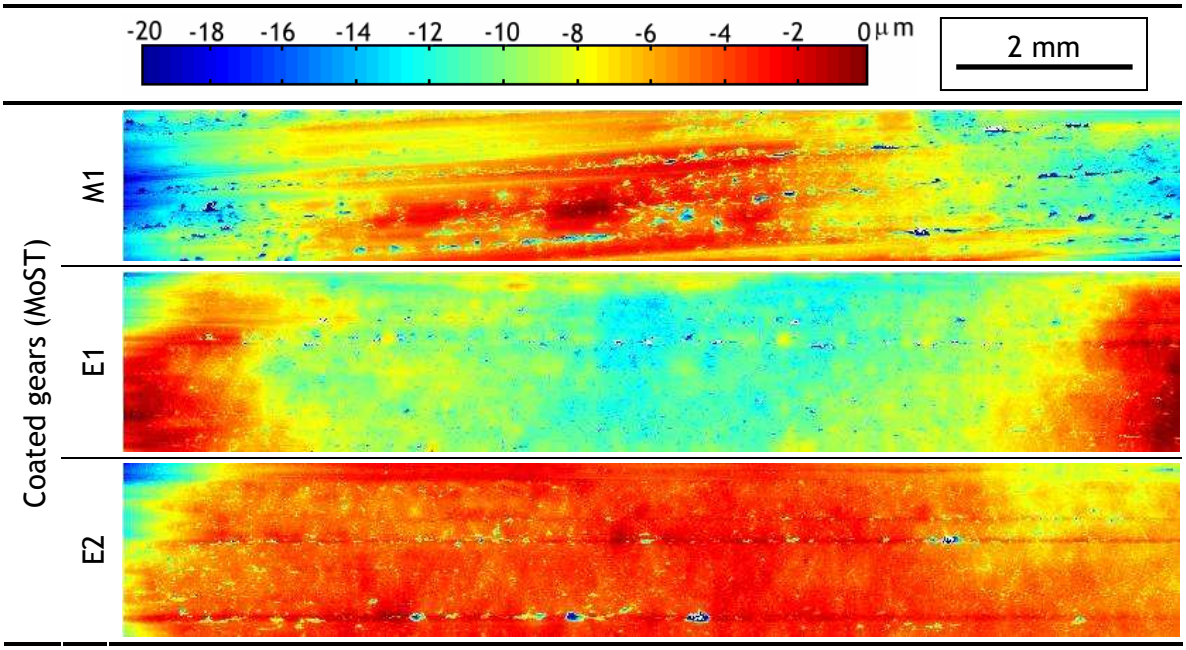


Figure 4.17 - Topography measurements in the coated gears.

Table 4.16 – Representative unfiltered roughness profiles selected from the topography measurements after load stage K9 (vertical axis units: μm; horizontal axis units: mm).

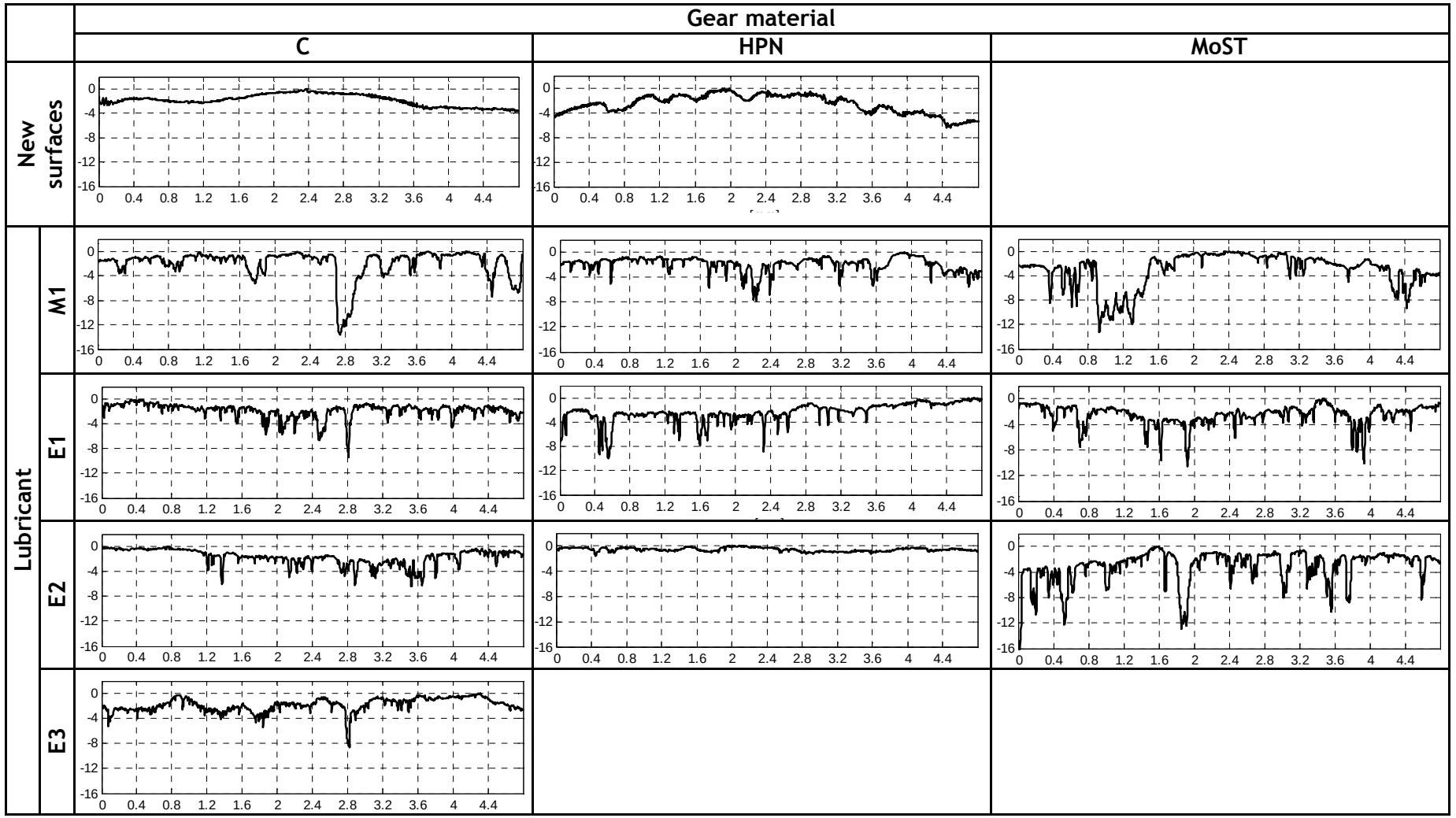


Table 4.17 – Roughness parameter corresponding to the profiles presented in Table 4.16 (values in μm).

Material	Test	R_{max}	R_{Z-D}	R_{pk}	R_{vk}
C	New	0.8	0.6	0.1	0.2
	M1	11.9	6.1	1.7	4.1
	E1	8.2	5.1	0.2	2.5
	E2	5.1	3.9	0.3	2.4
	E3	6.6	4.0	0.3	1.5
HPN	New	1.8	1.7	0.1	0.6
	M1	5.8	4.7	0.1	2.4
	E1	7.1	4.8	0.2	3.2
	E2	1.3	0.9	0.1	0.3
MoST	M1	10.8	5.9	1.8	3.6
	E1	8.2	6.1	0.7	3.1
	E2	10.6	8.4	0.3	5.4

4.4.7 SEM analysis of the teeth flanks of the nitrided steel gears

The teeth flanks of the nitrided gears presented in Table 4.12 were examined by scanning electron microscopy (SEM)[5]. In order to have more precise information about the morphology and depth of the micropitts, surface topography measurements were performed on the areas where SEM micrographs were taken.

Table 4.19 presents a summary of the results from SEM observations and topography measurements. The first row on Table 4.19 shows representative micrographs (magnification: 100X) corresponding to the areas marked with a green square on the photos from Table 4.12 obtained after load stage K9. The second row displays the micrographs corresponding to the areas marked by green squares on the lower magnification ones. The last row displays the topography measurements corresponding to the micrographs from the second row.

The SEM micrographs, taken below the pitch line, clearly show that the tooth flank lubricated with mineral gear oil presents more and deeper micropitts than the teeth flanks lubricated with the ester oils. On the flank tested with E1 ester oil it is also possible to identify several micropitts however, their number and size are smaller that those observed with M1 lubricant. On the micrographs corresponding to E2 gear oil, only a few micropitts appeared and most of the grinding marks are still visible. These facts are in agreement with the micropitting area results. In terms of morphology and depth, the micropitts from the surface lubricated with mineral lubricant are larger and deeper reaching a maximum depth of 20μm while the micropitts found in the micrographs corresponding to E1 and E2 ester gear oils only reached 10 and 7μm respectively.

[5] The SEM observations were performed at CEMUP – Centro de Materiais da Universidade do Porto, Porto, Portugal (financing contracts ref. REEQ/1062/CTM/2005 and REDE/1512/RME/2005 of 'FCT - Fundação para a Ciência e Tecnologia'). The author want to thank Dr. Carlos Sá from CEMUP for the support concerning SEM analysis.

Table 4.18 – Micropitts deeper than 5 µm.

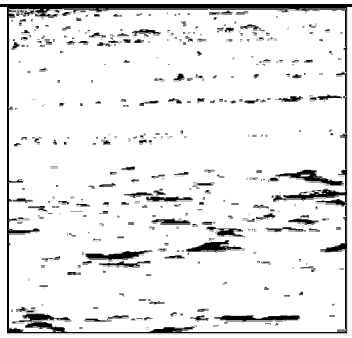
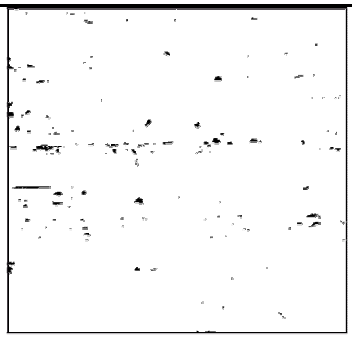
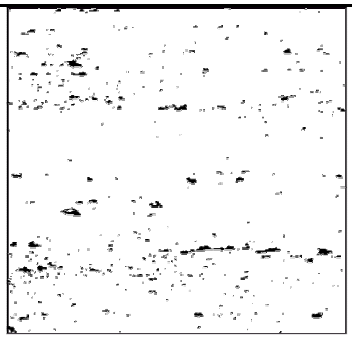
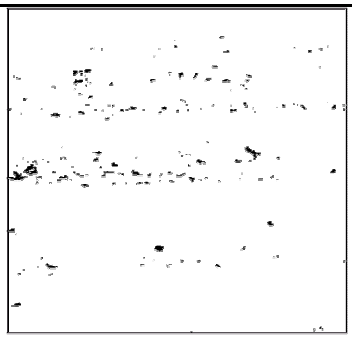
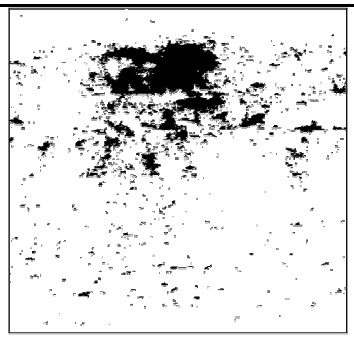
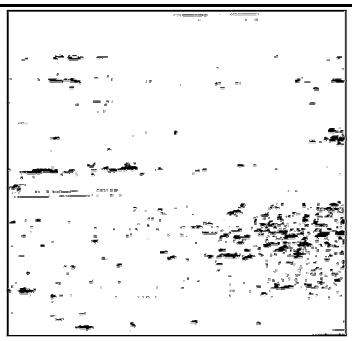
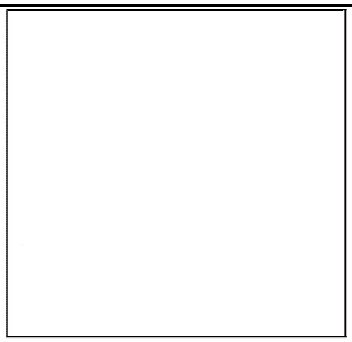
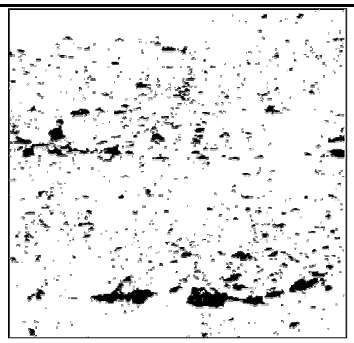
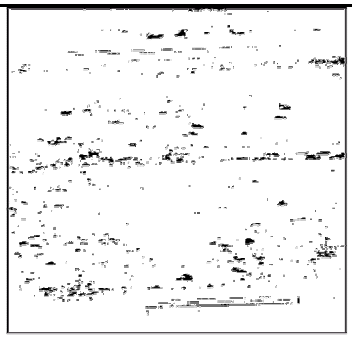
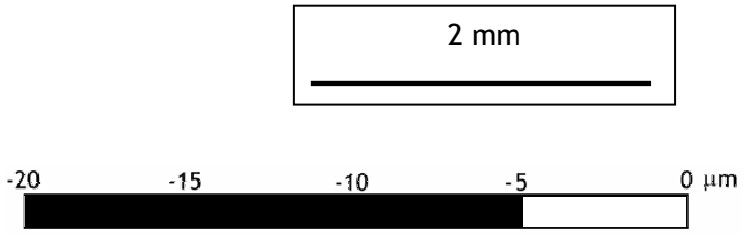
Lubricant	Gear material: C	Gear material: HPN	Gear material: MoST
M1	 5.2 %	 0.8 %	 16.2%
E1	 3.0 %	 0.8 %	 8.7 %
E2	 2.6 %	 0.0%	 5.7 %
E3	 2.4 %		

Table 4.19 - SEM micrographs and topography measurements (H. P. Nitrided gears).

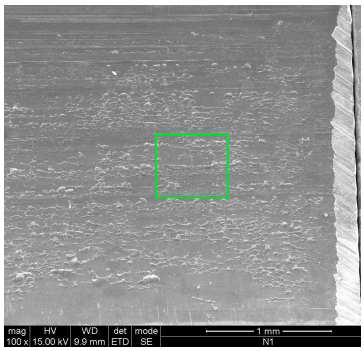
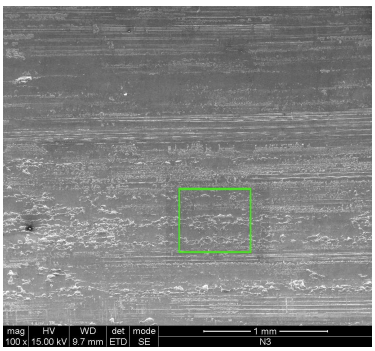
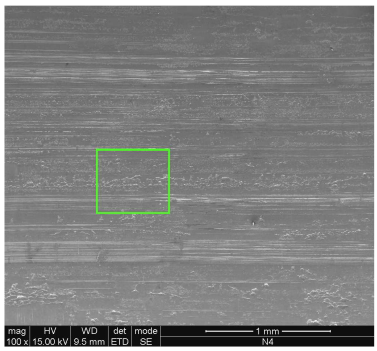
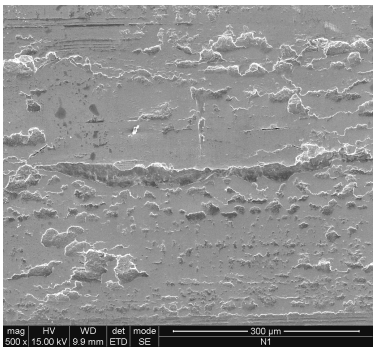
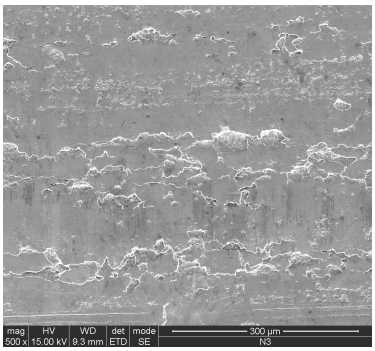
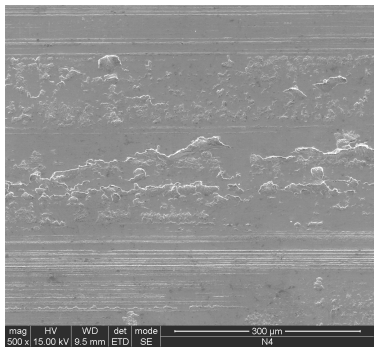
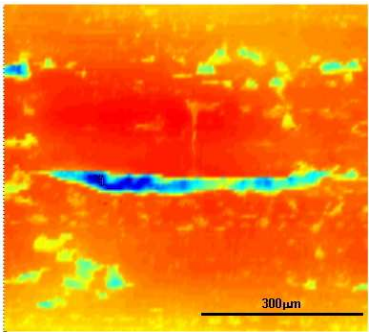
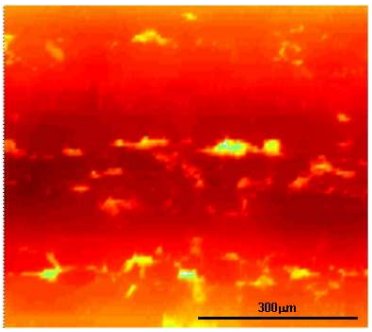
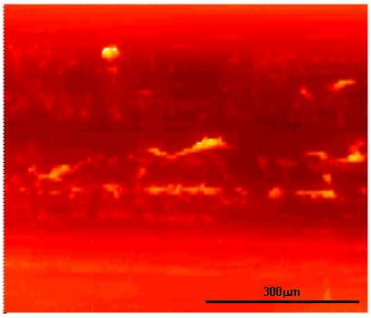
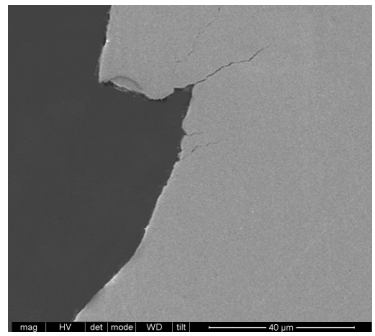
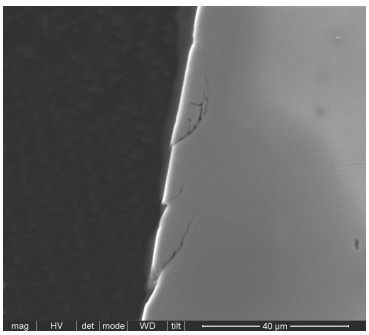
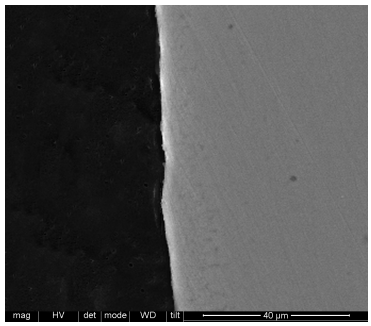
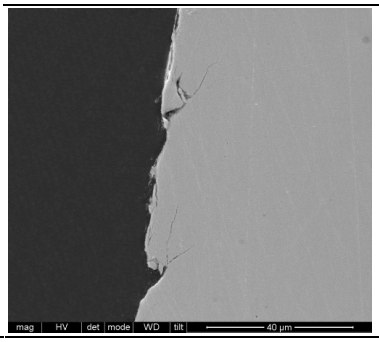
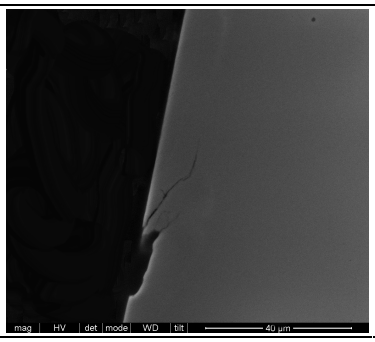
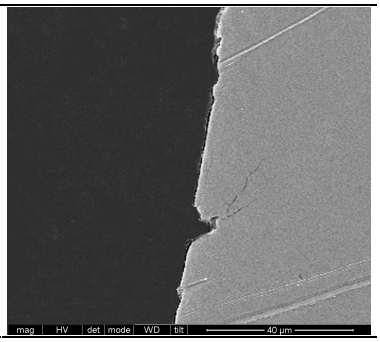
	Mineral 1	Ester 1	Ester 2
100X			
500X			
Depth			

Table 4.20 presents a summary of the results from SEM observations of the cut teeth after polished. These micrographs indicate that mineral oil M1 tend to generate more and deeper cracks than the ester oils. With the ester oil E2, only were found cracks in the presented micrograph while on the pinion teeth lubricated with fluids M1 and E1, several groups of cracks were visible.

Table 4.20 - SEM micrographs of cut teeth (H. P. Nitrided gears).

	Mineral 1	Ester 1	Ester 2
3000X			
			

4.5 Discussion on gear micropitting tests

4.5.1 Mass loss

Figure 4.18 presents the cumulative results of mass loss measured during the gear micropitting tests. This figure shows that till load stage K8 the material-lubricant combinations C-M1, C-E2 and Mo-M1 and all the nitrided gears had similar evolutions, the other combinations (C-E1, C-E3 and Mo-E2) had higher mass loss and the coated gear lubricated with the E1 ester oil displayed the greatest mass loss value.

After load stage K9 the mass loss had a very significant increase, except in the case of carburizing steel gears lubricated by mineral gear oil.

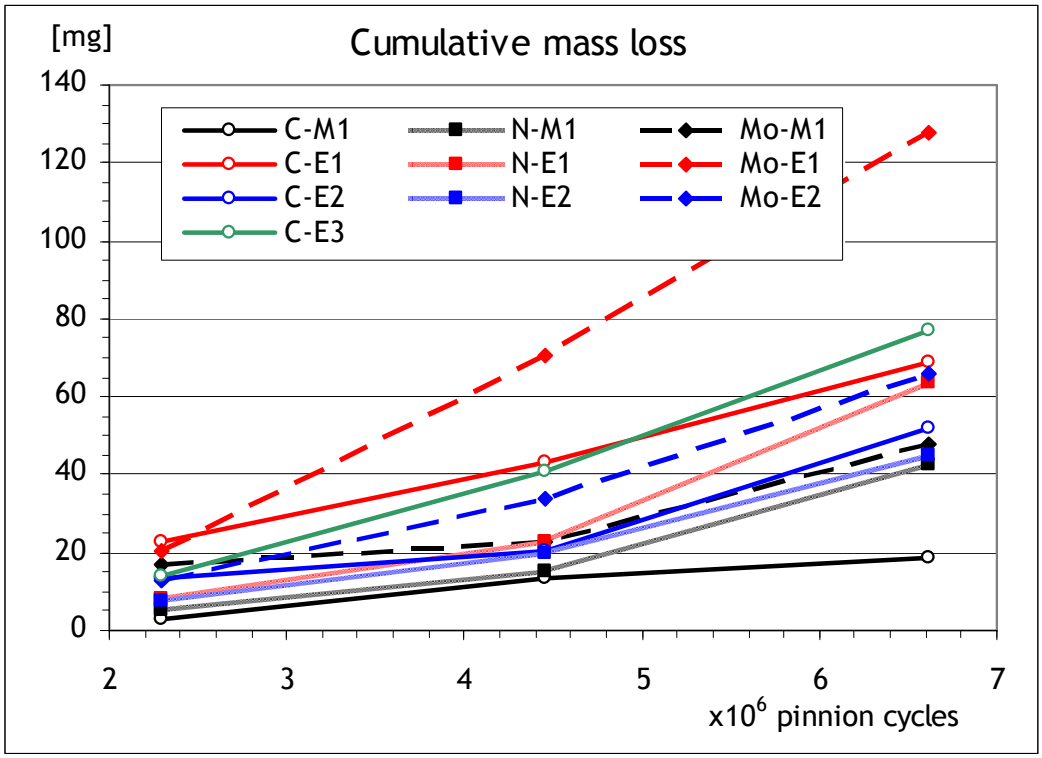


Figure 4.18 - Cumulative mass loss for the three lubricants during gear micropitting tests.

4.5.2 Ferrometry

Figure 4.19 presents the cumulative *CPUC* index results obtained during gear micropitting tests. Cumulative *CPUC* values of carburized and nitrided gears show the same tendency revealed by mass loss results (see Figure 4.18). In general, the rate of wear particle generation increased with the applied torque, as happened with mass loss. *CPUC* index of coated gears didn't have the evolution shown by the mass loss results (where Mo-E combination had higher values of mass loss), because the wear particles from MoS_2/Ti coating are not ferromagnetic and are not detectable on the device used to measure *DL* and *DS* indexes.

The *CPUC* index represents the total amount of wear particles inside a lubricant sample and should follow the mass loss trend of each gear during the test. Such good correlation is shown in Figure 4.20 that presents the cumulative mass loss results *vs* the wear particle concentration index. However this figure shows that the relation between the CPUC and mass loss obtained in the tests with the coated gears is different from the relation obtained with the other two gear materials. This happens for the same reason that was previously described to explain the difference between mass loss and the *CPUC* index evolution in the tests with MoS_2/Ti coating.

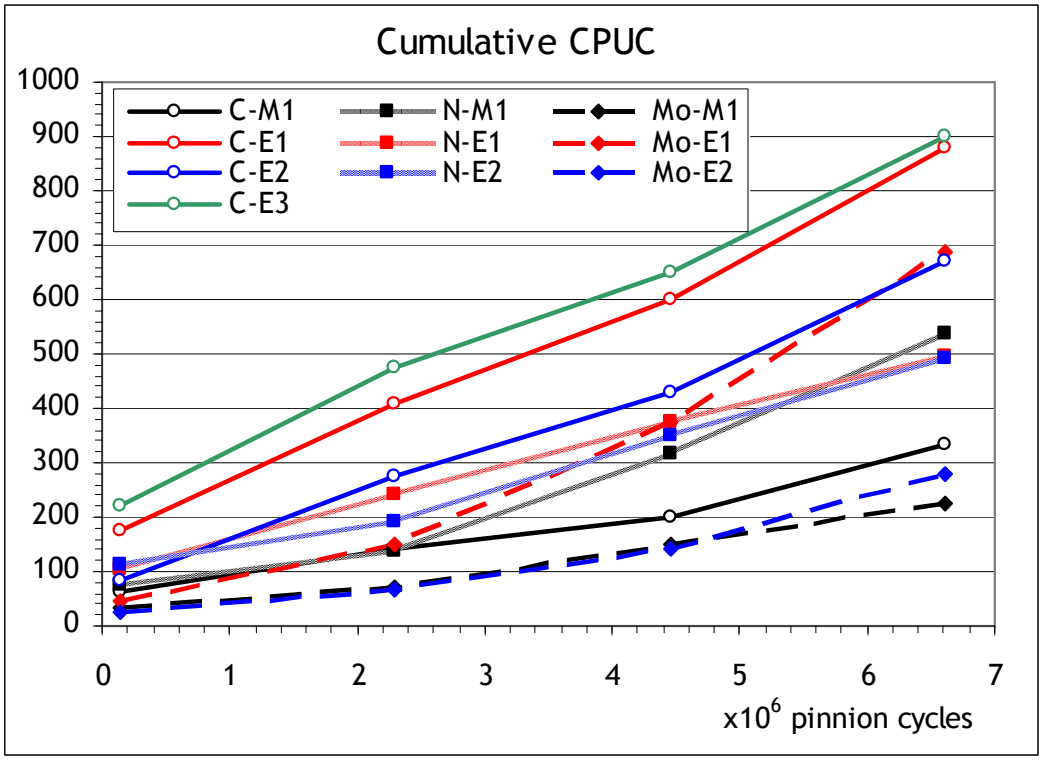


Figure 4.19 - Cumulative *CPUC* ferrometric index during micropitting test (*d*=0.1).

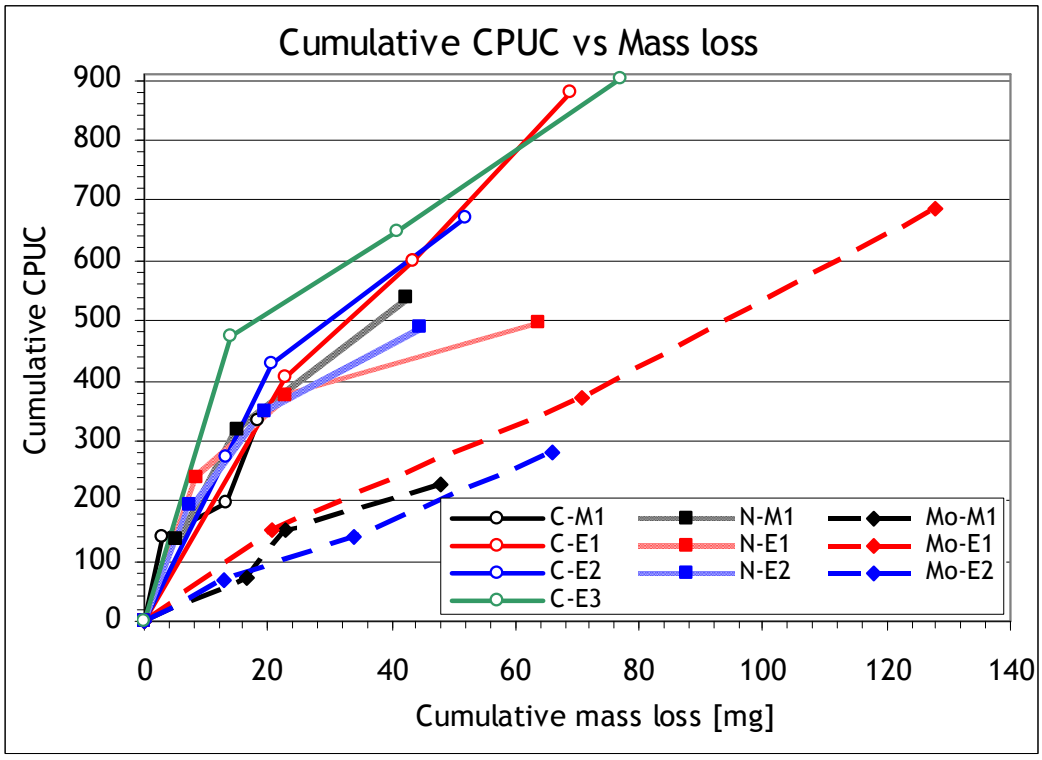


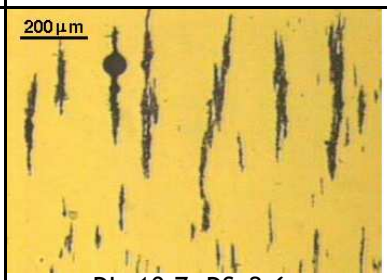
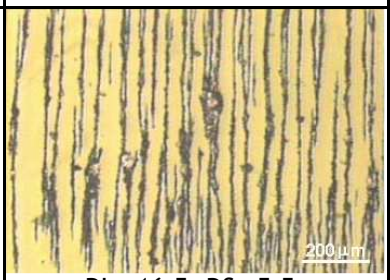
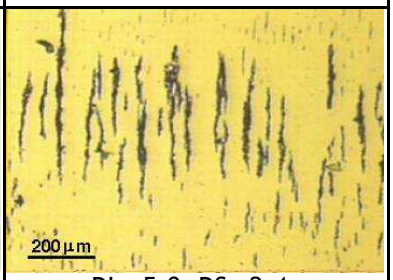
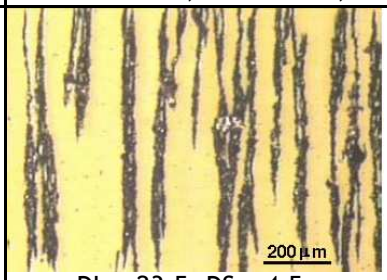
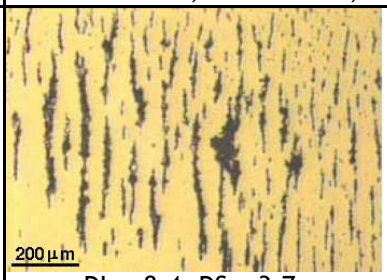
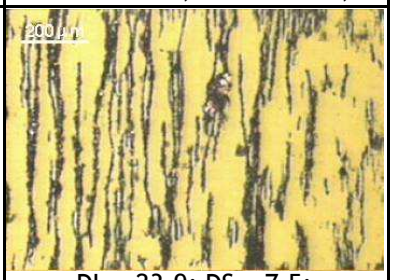
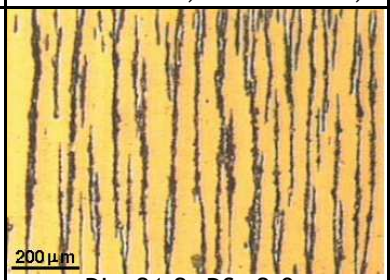
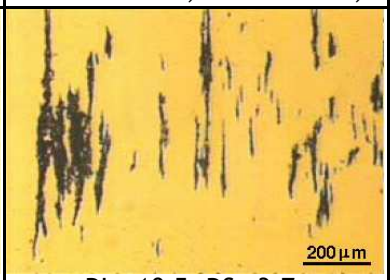
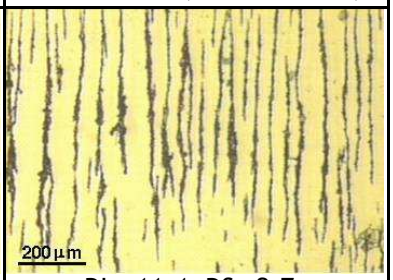
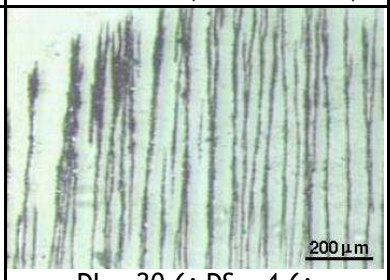
Figure 4.20 - Cumulative *CPUC* vs. cumulative mass loss during gear micropitting tests.

4.5.3 Analytical Ferrography

Table 4.21 shows pictures of the ferrograms and ferrometry values from the lubricant samples collected at the end of the load stage K9 of each gear micropitting test.

It is clear that during load stage K9 the combinations carburized steel/mineral oil and nitriding steel/ester oil showed the best performance, generating less wear particles and of smaller size than the other possible combinations. This is confirmed by the ferrograms and by the large particles (*DL*) and *CPUC* indexes.

Table 4.21 - Analytical ferrography after load stage 9 (d=0.1; magnification: 100X).

		Gear material		
Lubricants		**Carburized steel**	**Nitrided steel**	**MoS_2/Ti coating**
	Mineral 1	 DL=10.7; DS=2.6; CPUC=133.0; ISUC=1.1E4;	 DL =16.5; DS =5.5; CPUC = 220.0; ISUC =2.4E4;	 DL =5.0; DS =2.4; CPUC = 74.0; ISUC =1.9E3;
	Ester 1	 DL = 23.5; DS = 4.5; CPUC = 280.0; ISUC = 5.3E3;	 DL = 8.4; DS = 3.7; CPUC = 121.0; ISUC = 5.7E3;	 DL = 23.9; DS = 7.5; CPUC = 314.0; ISUC = 5.1E4;
	Ester 2	 DL =21.2; DS =2.9; CPUC = 241.0; ISUC =4.4E4;	 DL =10.5; DS =3.7; CPUC = 142.0; ISUC = 9.7E3;	 DL =11.4; DS =2.7; CPUC = 141.0; ISUC = 1.2E4;
	Ester 3	 DL = 20.6; DS = 4.6; CPUC = 252.0; ISUC = 4.0E4;		

During load stage K9 the carburized steel and the MoS_2/Ti coating lubricated with the mineral oil, and the H.P. Nitrided steel lubricated by the esters (E1 or E2) showed the best performance, generating less wear particles of smaller sizes than the other possible material-lubricant combinations, as shown by the *CPUC* indexes determined and by the large particles index (*DL*) measured. The ferrograms clearly confirm these results

4.5.4 Lubricant film thickness

The specific lubricant film thickness (Λ)is given by the following expression [30]:

$$\Lambda = \frac{h_{0T}}{\sigma} \tag{4.1}$$

The lubricant film thickness (h_{0T}) is strongly dependent on the lubricant properties, in particular the dynamic viscosity (η), piezoviscosity (α), and thermoviscosity (β),as proposed by the following [30, 31]:

$$h_{0T} = \phi_T . h_0 \tag{4.2}$$

where the thermal correction factor (ϕ_T) is given by

$$\phi_T = \left\{1 + 0.1\left[\left(1 + 14.8 V_S^{0.83}\right) L^{0.64}\right]\right\}^{-1} \qquad \left(0 < \phi_T \leq 1\right), \tag{4.3}$$

the sliding rate (V_S) is defined by

$$V_S = \frac{\left|U_1 - U_2\right|}{U_1 + U_2} \tag{4.4}$$

the thermal parameter (*L*) is given by

$$L = \frac{\beta_0 . \eta_0 . \left(U_1 + U_2\right)^2}{K_f} \tag{4.5}$$

and the lubricant film thickness (h_0) is given by:

$$h_0 = 0{,}975 \frac{\left[\alpha . \eta_0 \left(U_1 + U_2\right)\right]^{0{,}727} . R_X^{0{,}364} . \left(b . E^*\right)^{0{,}091}}{F_{bt}^{0{,}091}} \tag{4.6}$$

In Figure 4.21, the lubricant film thicknesses plotted along the meshing line, for mineral and ester oils, during load stage K9.

The film thickness obtained with the E1, E2 and E3 biodegradable esters is 30%, 21% and 23% lower than the one obtained with mineral gear oil, respectively. This is due to the higher piezoviscosity and thermoviscosity coefficients of mineral lubricant and to the lower viscosity of E1 and E3 ester oils (see Table 4.22). This explains the lower mass loss of the gears lubricated with the mineral oil, in comparison to the gears lubricated with ester based lubricants.

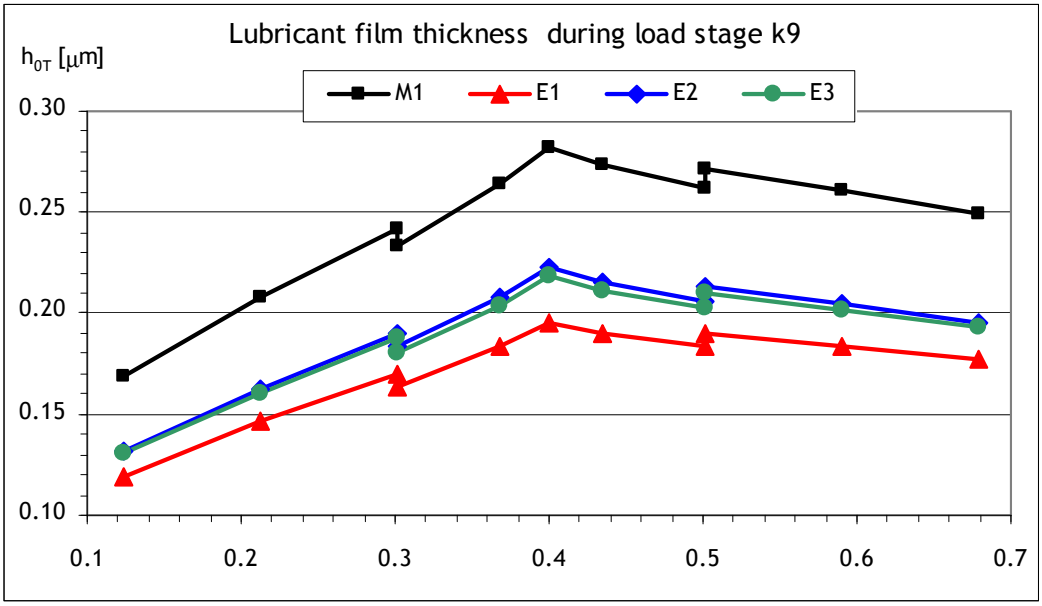


Figure 4.21 - Lubricant film thickness along the gear meshing line.

Table 4.22 - Viscosity and piezoviscosity coefficient of the four lubricants at operating temperature.

Lubricant	$\nu_{90°C}$ [cSt]	$\beta_{90°C}$ [cSt/°C]	$\alpha_{1.4GPa,90°C}$ [Pa^{-1}]
Mineral 1	19,34	0,0297	1,58x10-8
Ester 1	18,57	0,0253	9,68x10-9
Ester 2	21,63	0,0253	9,68x10-9
Ester 3	20,24	0,0253	9,68x10-9

4.5.5 Micropitting area

Figure 4.22 displays the evolution of the micropitting area during the gear tests.

Carburized steel gears (coated or not) always generated higher micropitting area and their values were similar for both lubricants. On the test performed with the carburized gears, all the lubricants caused similar percentages of micropitted area. However, the ester oils E2 and E3 seem to allow a lower increasing rate. The MoS_2/Ti coating of carburized gears showed an increase of micropitted area of gears lubricated with esters, while the coated gears lubricated by the mineral fluid had a slightly better performance.

High pressure nitrided steel was the gear material that performed better concerning to the percentage of teeth flanks area with micropitting. The three lubricants (M1, E1 and E2) suffered no micropitting till the end of load stage K8 when lubricating this material. In the last load stage (K9) the pinions lubricated by M1 and E1 gear oils displayed a moderate micropitting area, 13% in the case of gear M1 and 5% in the case of gear E1. The gear E2 suffered no micropitting during the tests.

As expected, high surface hardness materials, such as carburized steel, are much more sensible to gear micropitting than low surface hardness ones.

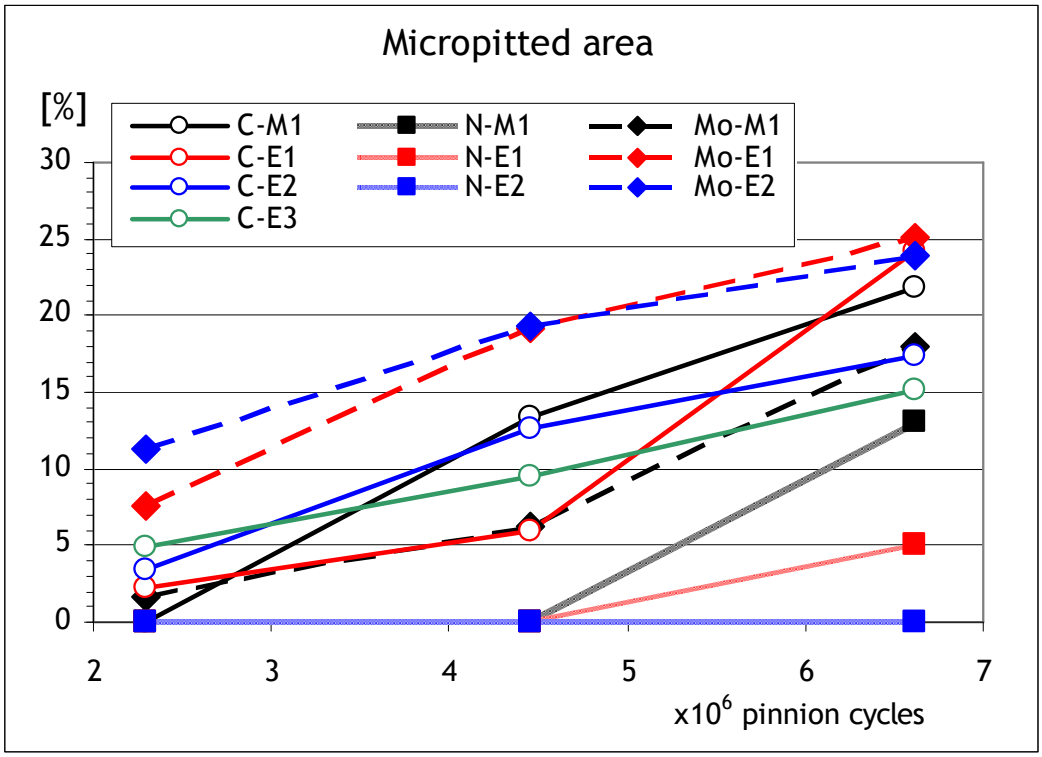


Figure 4.22 - Evolution of the micropitted area during gear micropitting tests.

4.5.6 SEM and surface topography

SEM analysis and surface topography measurements show that whatever the gear material, the teeth flanks lubricated with the mineral gear oil M1 had more micropitts and deeper than those ones lubricated with the ester oils. Concerning to the biodegradable ester gear oils, E2 lubricant had less micropitts and less deep than E1.

Table 4.18 displays the micropitts with a depth greater than 5 μm in those areas and the corresponding relative area in percentage of the total area (4 mm^2). The value 5 μm was chosen because after the gear micropitting tests the R_{max} parameter corresponding to the measurements made in radial direction is always grater than 5 μm, while in the cases where there is no micropitting, it doesn't exceed this value.

Figure 4.23 a summary of the values of percentage of area of micropitts with a depth greater than 5 μm presented in Table 4.18 having into account each gear material.

The nitrided gears showed the best performance, having less micropitts and the coated gear displayed the worst results in terms of micropitting performance.

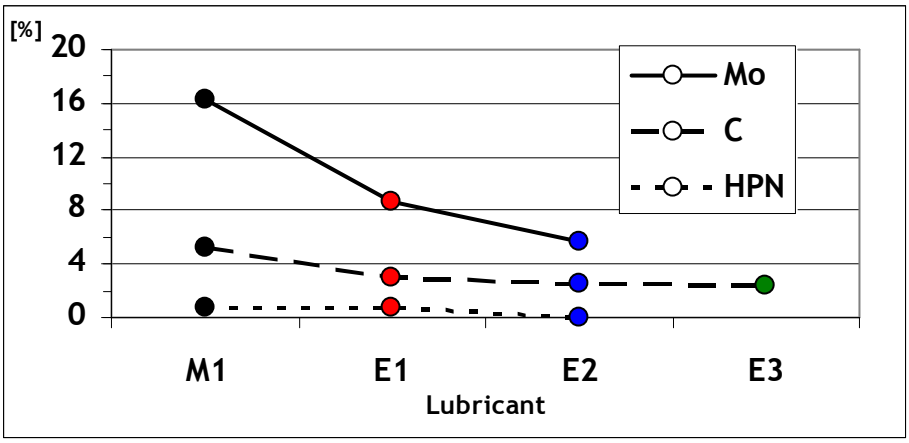


Figure 4.23 – Percentage of area of micropitts with a depth greater than 5 µm presented in Table 4.18 having into account each gear material.

4.5.7 Gear Micropitting Failure Criteria

Both in DGMK [15] and FVA [14] micropitting test procedure, the failure criteria is assessed by the average profile deviation of the teeth flanks after tests. However, in this work, the equipment for measuring the profile deviation is not available, and a different criterion was used.

In the FVA test procedure[14] the micropitting area and the mass loss can also be used to assess the micropitting failure. Although the gears used in this work don't allow the establishment of a micropitting class according to the methods proposed by FVA and DGMK, because non-standard gears with high surface roughness were used, it is possible to compare the micropitting behaviours of the different material-lubricant. Figure 4.24 and Figure 4.25 show the Gear Micropitting Failure Criteria according to FVA, taking into account the results after load stages K8 and K9, respectively, concerning mass loss and micropitting area.

C-M1, N-M1, N-E1 and N-E2 material-lubricant combinations passed the FVA gear micropitting criteria till load stage K8, C-E2 and Mo-M1 stayed very close to the range of failure edge and the other combinations did not satisfy the FVA criteria. In load stage K9 only the combination carburized steel-mineral oil (C-M1) passed the FVA criteria.

According to FVA micropitting test [14], the roughness Ra of tooth flanks measured in radial direction should be $0,5 \pm 0,1\mu m$ and the Ra measured on gears used was $1,1 \pm 0,4\mu m$. Considering the surface roughness of the gears that have been tested, the highest load stage considered should be the load stage K8.

Tanking into account the surface finishing of the tested gears, witch have high surface roughness, load stage K9 of the gear micropitting test procedure is too severe. However, the result obtained by the carburized steel gear lubricated by mineral oil confirms the outstanding capacity of the micropitting additive package contained in this gear oil.

The gears lubricated with ester based lubricant have a micropitting are similar to that of the gears lubricated with the mineral oil, but, in general, they generate more wear and higher mass loss because they have lower film thickness along the meshing line. So it is difficult for the gear lubricated with ester based lubricants to satisfy the FVA micropitting failure criteria which was developed for carburized gears lubricated with mineral oils.

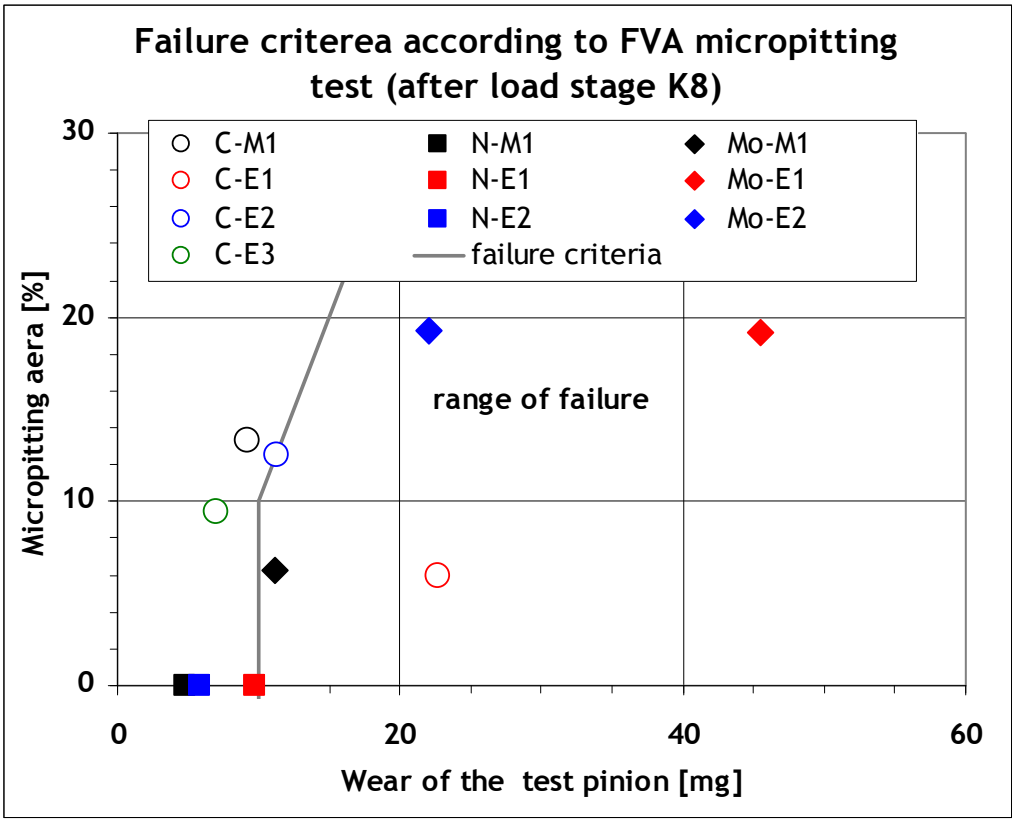


Figure 4.24 - Failure criteria according to FVA [14], after load stage K8.

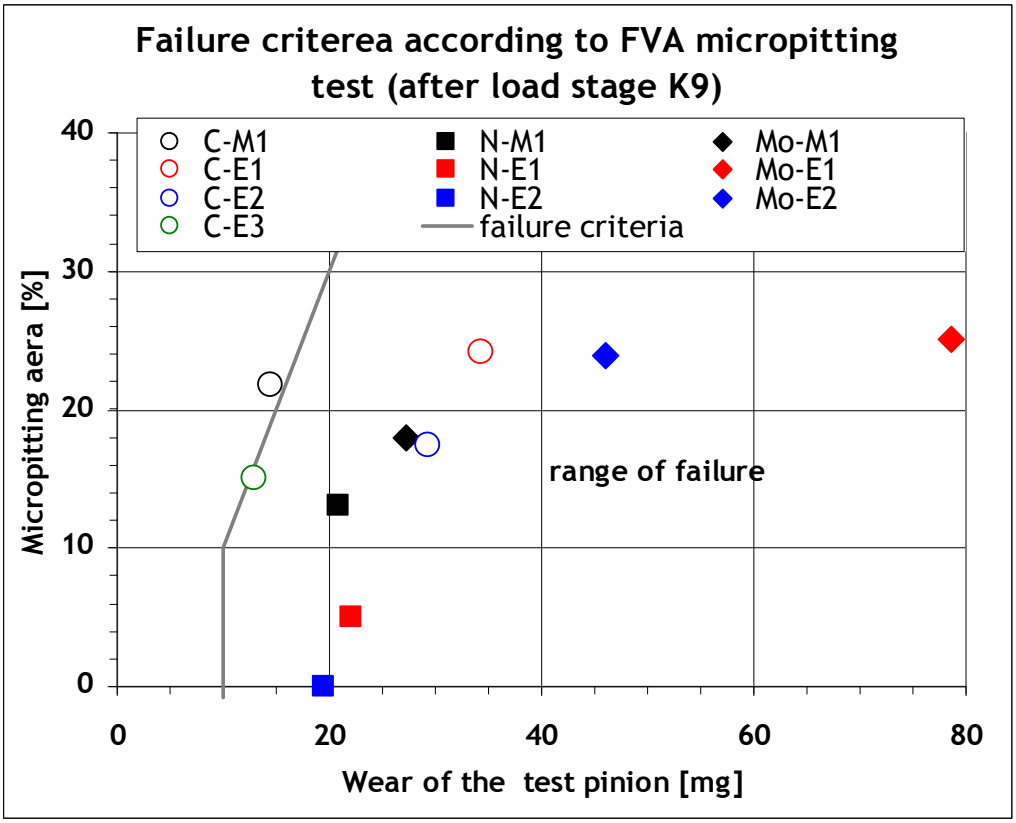


Figure 4.25 - Failure criteria according to FVA [14], after load stage K9.

4.6 Conclusions on gear micropitting tests

The main conclusions that can be stated from the FZG gear micropitting tests are:

- ✓ Tests of the carburized gears:
  - o The gear micropitting performance of the lubricants C-M1 and C-E2 was very good and similar (in terms of micropitting area and mass loss), untill load stage K8;
  - o The mineral oil was the only lubricant that didn't promote a great increase of the mass loss after load stage K9;
  - o Esters E1 and E3 caused higher mass loss.

- ✓ Tests with the high pressure nitrided gears:
  - o The gear micropitting performance of the three lubricants was very good and similar, till load stage K8;
  - o After load stage K9, the mineral oil M1 generated more pits and deeper pits, higher micropitting area, higher severity wear particles, lower mass loss and higher film thickness than the ester oils E1 and E2;
  - o After load stage K9, the micropitting performance of the ester oil E2 was better than E1 (lower micropitting area, less pits and not so deep, lower mass loss).

- ✓ Tests with the MoS_2/Ti surface coating:
  - o In comparison with the carburized gears, the coated gears lubricated by the mineral oil produced less micropitting area and more wear;
  - o E1 gear oil had the worst results in terms of microppited area and mass loss;

- ✓ Micropitting performance:
  - o High pressure nitriding steel with ester oil E2 was the combination that has best micropitting protection;
  - o Carburized steel lubricated with the mineral oil had a greater micropitting resistance;
  - o On the tests of the carburized and the nitrided gears, ester lubricants tended to generate less micropitting (lower micropitting area, less pits and not so deep) than the mineral oil;
  - o Carburized gears lubricated with E2 and E3 lubricants had the smaller increasing rate of micropitting area;
  - o High Pressure Nitrided Steel had better micropitting protection with ester oils E1 and E2;
  - o Gears with the MoS_2/Ti coating and lubricated with ester oils had the worst results in terms of micropitting area;

- ✓ Wear protection:
  - o Reference oil promoted less wear than ester lubricants;
  - o Carburized steel lubricated with the mineral oil had the smaller mass loss;

- ✓ Micropitting test procedure:
    - o The properties chosen to evaluate test results are adequate and allow the analysis of surface evolution along test, although the mass loss and the Ferrometry are correlated and the relation between CPUC and mass loss is different for the gears with a MoST coating.
    - o The tests presented in this report were performed using gears of current quality, allowing a prediction of overall lubricant and gear material behaviour at low costs;

CHAPTER 5

5 GEAR POWER LOSS TESTS

In order to evaluate and compare the energetic performance of the industrial gear oils under study (M1, E1, E2 and E3), gear power loss tests were performed on the FZG test rig using type C gears made of carburized steel (DIN 20MnCr5) and nitrided steel (DIN 34CrNiMo6). The stabilized oil operating temperature is measured for different values of the input torque and input speed.

The protection against wear provided by each lubricant is also compared. Lubricant samples are collected during and at the end of each gear power loss test, and analyzed by Direct Reading Ferrography in order to evaluate the wear particles indexes *CPUC* and *ISUC*.

The gear mass loss and the surface roughness of the teeth flanks were measured at the end of the tests, and the teeth flanks were carefully inspected in order to detect surface failures (micropitting, pitting and scuffing).

An energetic model of the FZG test gearbox was developed, integrating the mechanisms of power dissipation and heat evacuation, and allowing the determination of oil operating temperature in steady state conditions. The X_L parameter in the average friction coefficient equation proposed by Hohn et al.[32] is determined for each lubricant, using an optimization routine that correlates experimental and model results.

5.1 Power loss inside a gearbox

The most important mechanisms of power loss inside any gearbox are the churning losses and the frictional losses [32, 33]. The same occurs in the test box of the FZG gear test rig (see Figure 5.1).

The churning losses are related to the rotational movement of the mechanical components, e.g. gears, rolling bearings and seals, immerged in the viscous oil bath. This form of power loss is quite often called the “No Load Power Loss”, since it is independent of the applied torque [32, 33]. The friction power losses are load dependent and have origin in the contact between bodies, in particular between gear teeth and between rolling elements and raceways in rolling bearings. These losses are dependent of the load, the friction coefficient between the contacting surfaces, the speed, the lubricant properties and the contact geometry and roughness.

In order to attain thermal equilibrium inside a gearbox, the heat generated by friction and churning must be evacuated. This is done by conduction, radiation and convection between the test gearbox and the surrounding environment.



Figure 5.1 – Test box of the FZG gear test rig (opened).

5.2 Test gears

Test gears used in the power loss tests are similar to standard FZG type C gears (see Figure 1.6) made of carburized steel (DIN 20MnCr5) and nitrided steel (DIN 34CrNiMo6) and their geometric characteristics are presented in Table 1.10.

The tested gears had a lower gear accuracy grade than those proposed in the standards [27, 29], having higher surface roughness at the teeth flanks and yielding a lower operating specific film thickness, as shown in Table 5.1. Since all lubricants were tested with similar gears, the results are comparable.

Table 5.2 shows specific film thickness at the beginning of each test (running-in load stage and wheel speed of 1000 rpm). Specific film thickness is different for the four gear oils because they have different piezoviscosity coefficients (see Table 1.1 and Table 4.22).

Table 5.1 - Gear quality grade and average surface roughness (pinion and wheel).

Material and heat treatment	*Gear reference*	*Gear quality grade (ISO 1328)*	*Mean roughness R_a of tooth flanks [μm]*	
			Axial direction	*Radial direction*
Standard gear	ZF®	5	/	0,5
20 MnCr 5 case hardened	C-M1	9	0,18	1,20
	C-E1	9	0,10	1,09
	C-E2	9	0,09	1,09
	C-E3	9	0,15	1,21
34 CrNiMo 6 high pressure nitriding	N-M1	9	0,15	1,14
	N-E2	9	0,20	1,15

Table 5.2 - Specific film thickness between gear teeth: standard *vs* used gears.

Lubricant	*Gear*	$\frac{R_{a1}+R_{a2}}{2}$	$\sqrt{R_{q1}^2+R_{q2}^2}$	*ν@45ºC*	T_1	P_0 [a)]	Λ [b)]		
		[μm]	*[μm]*	*[cSt]*	*[Nm]*	*[Mpa]*	*A*	*I*	*dif (%)*
Mineral 1	Standard	0,50	0,99	114,51	3,3	174	0,589	1,307	/
	C-M1	1,20	2,10	114,51	3,3	174	0,278	0,616	-53
	N-M1	1,14	2,01	114,51	3,3	174	0,290	0,645	-51
Ester 1	Standard	0,50	0,99	80,20	3,3	174	0,394	0,780	/
	C-E1	1,09	2,00	80,20	3,3	174	0,195	0,387	-50
Ester 2	Standard	0,50	0,99	92,64	3,3	174	0,427	0,880	/
	C-E2	1,09	1,93	92,64	3,3	174	0,219	0,452	-49
	N-E2	1,15	2,05	92,64	3,3	174	0.206	0,424	-52
Ester 3	Standard	0,50	0,99	87,44	3,3	174	0,417	0,847	/
	C-E3	1,21	2,16	87,44	3,3	174	0,191	0,388	-54

a) Contact at pitch point (I).

b) Λ – specific film thickness evaluated in: A – beginning of engagement; I – pitch point.

5.3 Gear power loss test procedure

The gear power loss tests were performed on the FZG test rig (see chapter 1.3.1), using type C gears (see Table 1.10 and Figure 1.6) and dip lubrication, and considering wide ranges of the operating conditions, as shown in Table 5.3. The input power ranged from 0.5 kW to 102 kW.

Each power loss test is composed by four different load (torque) stages, as presented in Table 5.3, each one performed at three different rotational speeds. Each torque - speed combination lasted 3 to 4 hours, which is the time necessary to reach a stabilized operating temperature. If the oil temperature reaches 180ºC the test is stopped for safety reasons (damage of the slave gearbox seals).

The first load stage, performed at very low torque (T = 4.95 Nm), is used to evaluate the churning losses while gear running-in occurs. The oil temperature starts at room temperature (≈20ºC), since at low speed (1000 rpm) the stabilized operating temperature is slightly above 40ºC. After 3 hours the speed is increased to 2000 rpm and after another period of 3 hours is increased to 3000 rpm.

At the beginning of the following load stages the oil temperature is set at 40 ºC (±2 ºC) and the wheel speed is set at 1000 rpm. After 4 hours the speed is increased to 2000 rpm and after another period of 4 hours is increased to 3000 rpm.

The temperature of the oil, of the gearbox wall and of the test room was continuously recorded during the tests. Room ventilation (air insufflation and extraction) was used in order to maintain the room temperature almost constant.

The lubricant was not changed during the test. At the end of each load stage, a lubricant sample was collected (approximately 50 ml) and the same volume of fresh lubricant was added, in order to keep the total oil amount constant.

In average, in each power loss test the lubricant worked 48 hours, corresponding to 5.76 million cycles (For more precise information see Appendix D – FZG gear POWER LOSS tests data sheets).

The codification of tests is showed in Table 5.4. Test reference indicates material type (C – case hardened and N – nitrided) and lubricant (M –mineral and E - ester).

Table 5.3 - Operating conditions used in the power loss gear tests (FZG test rig – type C gears).

Test type	*Wheel Torque*	*Wheel Speed*	*Input Power*	*Initial temperature*	*Operating time*	*Number of cycles*	*Lubricant monitoring*
	[Nm]	*[rpm]*	*[kW]*	*[ºC]*	*[hours]*	*[x10^6]*	*samples*
No load tests	4.95 (K_{FZG}=1)	1000	0.52	Room temperature	(3x4) 12	1.44	40 ml
		2000	1.04				
		3000	1.56				
Load tests	105.0 (K_{FZG}=5)	1000	11.00	40 (±2)	(9x4) 36*	1.44	40 ml
		2000	21.99				
		3000	32.99				
	198.8 (K_{FZG}=7)	1000	20.81			1.44	40 ml
		2000	41.63				
		3000	62.44				
	323.4 (K_{FZG}=9)	1000	33.87			1.44	540 ml
		2000	67.73				
		3000	101.60				
Total					48*	5.76*	

General operating conditions:	
Oil volume [litre]	1,5
Oil temperature control	free
Max. oil temperature [ºC]	180
Type of lubrication	Dip lubrication
Monitoring during test	Wheel speed. Temperature – oil, gearbox wall and room. Room ventilation – air insufflation and extraction.
Monitoring after test	Lubricant analysis: Ferrometry, viscosity and density. Gear analysis: mass loss, surface roughness and visual inspection.

*For more precise information see Appendix D – FZG gear POWER LOSS tests data sheets.

Table 5.4 – Gear power loss tests codification. Material and lubricant combinations and test references.

Material	*Lubricant*	*Test Reference*
20 MnCr 5 case hardened	Mineral 1	C-M1
	Ester 1	C-E1
	Ester 2	C-E2
	Ester 3	C-E3
34 CrNiMo 6 high pressure nitrided	Mineral 1	N-M1
	Ester 2	N-E2

5.4 Results

The results presented include stabilized temperatures, mass loss, ferrometry, analytical ferrography, visual inspection and surface roughness measurements. Visual inspection and surface roughness measurements reports to pinions, since they perform 33% more stress cycles than wheels.

5.4.1 Carburized gears

5.4.1.1 Operating temperature

Figure 5.2 shows the evolution of the oil bath temperature during each test using carburized gears.

For very low torques, designated as “no load tests”, the oil sump temperature depends mainly on the oil viscosity at the operating temperature. At low speed, 1000 rpm, the operating temperatures are small (43 ºC to 47ºC), and thus the mineral oil heats more than the ester oils because it has higher viscosity at those temperatures (see Table 1.1 and Figure 1.1). At high speed, 3000 rpm, the operating temperature of the lubricants M1, E1 and E2 is very similar (≈85ºC), because these oils have identical viscosities at those temperatures, as shown Figure 1.1. E2 lubricant has the highest temperature.

In the tests with input power ranging from 11.0 kW to 101.6 kW (see Table 5.3) the operating temperature of the oils M1, E1 and E3 at 1000 and 2000 rpm was very similar, the main differences being found at 3000 rpm. The reference mineral oil attained the highest temperature during the last load stage; E1 lubricant maximum temperature occurred for wheel torques of 105 and 199 N.m (see Figure 5.2). The operating temperature of the E2 ester oil was always smaller than the temperature of the other lubricants (except in the case of the 105 Nm torque at 3000 rpm), as shown in Figure 5.2. This indicates that the friction power loss in the contact between the gear teeth and the corresponding friction coefficient are considerably smaller in the case of the ester oil E2, taking into consideration that the “no-load power losses” are similar for the four oils.

At high speed (3000 rpm) and high torque (323 Nm) (input power: 101.6 kW), the operating temperature of the reference mineral oil was significantly higher than the operating temperature of the ester fluids (more than 17 ºC).

Figure 5.3 shows the stabilised oil temperature and the room temperature, measured at the end of each test period. In general, the four lubricants had similar stabilization temperatures during the first load stages. Then, M1 lubricant tends to stabilize at higher temperature and the ester E2 always stabilized at the lower operating temperature.

A particular situation occurred under the input torque of 105.0 at low speed (1000 rpm) the E1 ester oil generates lower power loss than the mineral oil, while the opposite occurs at high speed (3000 rpm). This situation is related to balance between friction and churning power losses in each case, and will be analyzed later on.

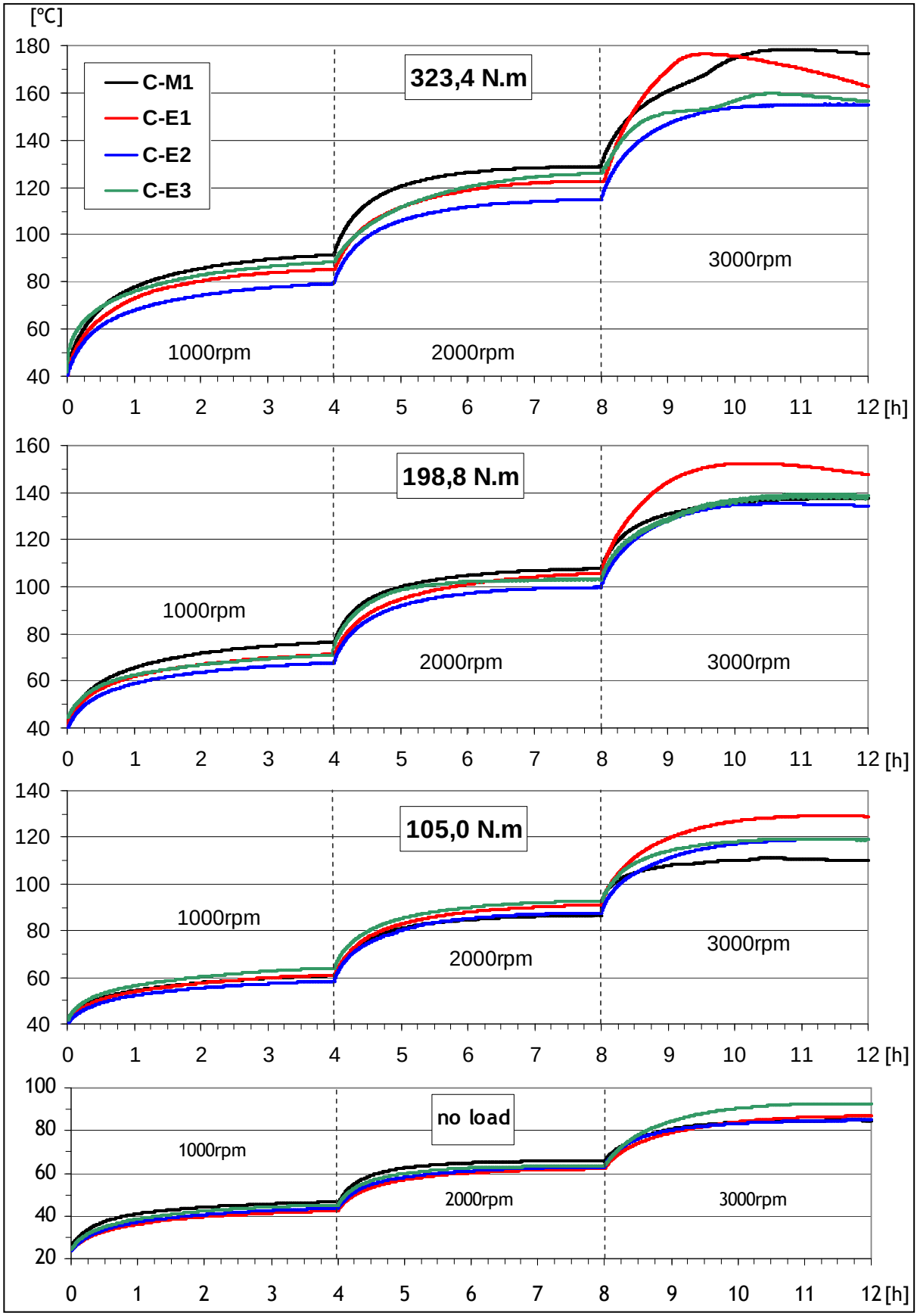


Figure 5.2 - Oil sump temperature during tests with carburized gears (vertical - temperature in °C, horizontal - time in hours, gear wheel speed and torque indicated).

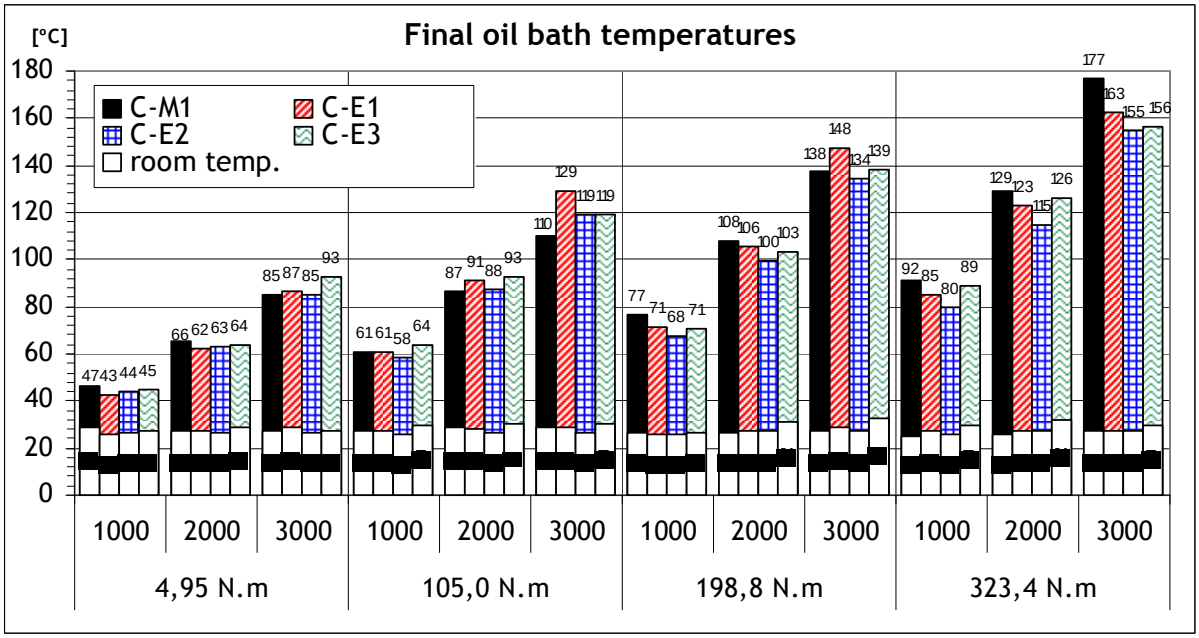


Figure 5.3 - Stabilized oil bath temperature *vs*. input speed and input torque measured during the tests with the carburized gears.

In Figure 5.4 the stabilized oil bath temperature of the four oils is plotted against the input power, at constant speed. In all cases, the oil temperature increases when the input power increases, as expected. Thus, as long as the input power increases the stabilized oil bath temperature also increases, no matter if the input speed increases and the torque decreases or vice-versa.

In general, for low input power all fluids presented similar stabilized temperatures while for high input power the ester fluids tends to stabilize at lower temperature.

Figure 5.5 shows the influence of the input torque on the stabilized oil bath temperature, at constant speed. When the torque increases the stabilized oil bath temperature also increases, almost in a linear way, reaching a maximum value at 3000 rpm. The stabilization temperatures of the four lubricants at 1000 rpm and 2000 rpm are similar. The results at 3000 rpm suggest that the increasing rate of the stabilization temperature with the load is smaller for the esters at high speed.

Figure 5.6 shows the stabilized oil temperature plotted against the input speed at constant torque. The oil temperature is strongly affected by the operating speed because the speed affects both the frictional and the churning losses inside the FZG test gearbox. At the highest load, the mineral oil had always the highest stabilization temperature while E2 ester had the lowest one.

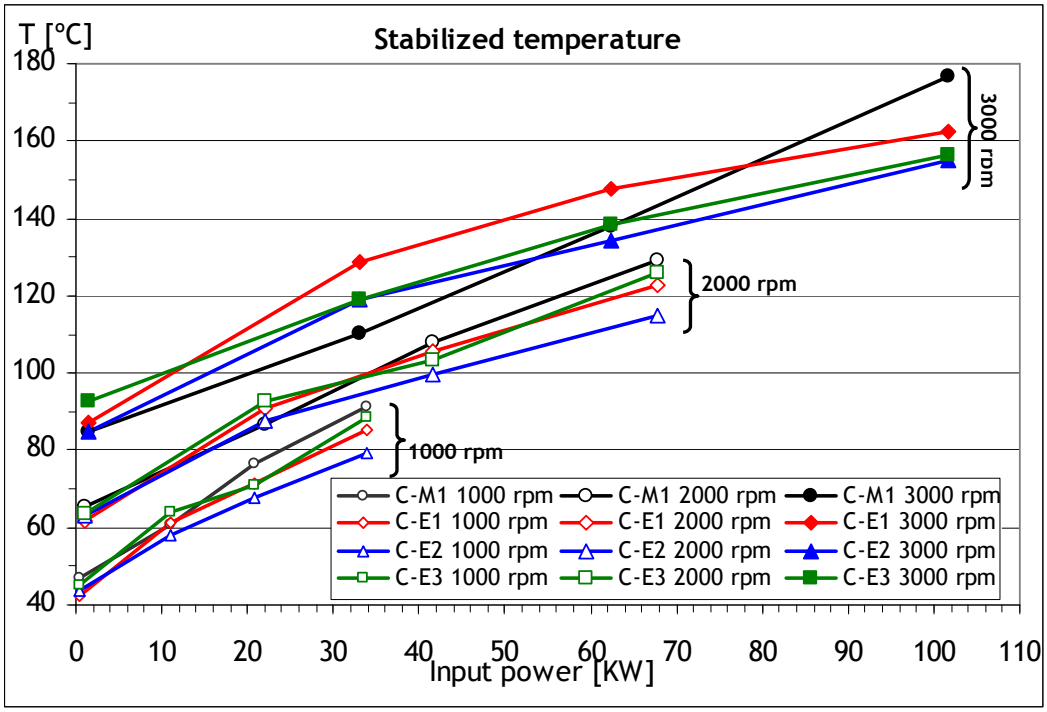


Figure 5.4 - Stabilized oil sump temperature vs. input power.

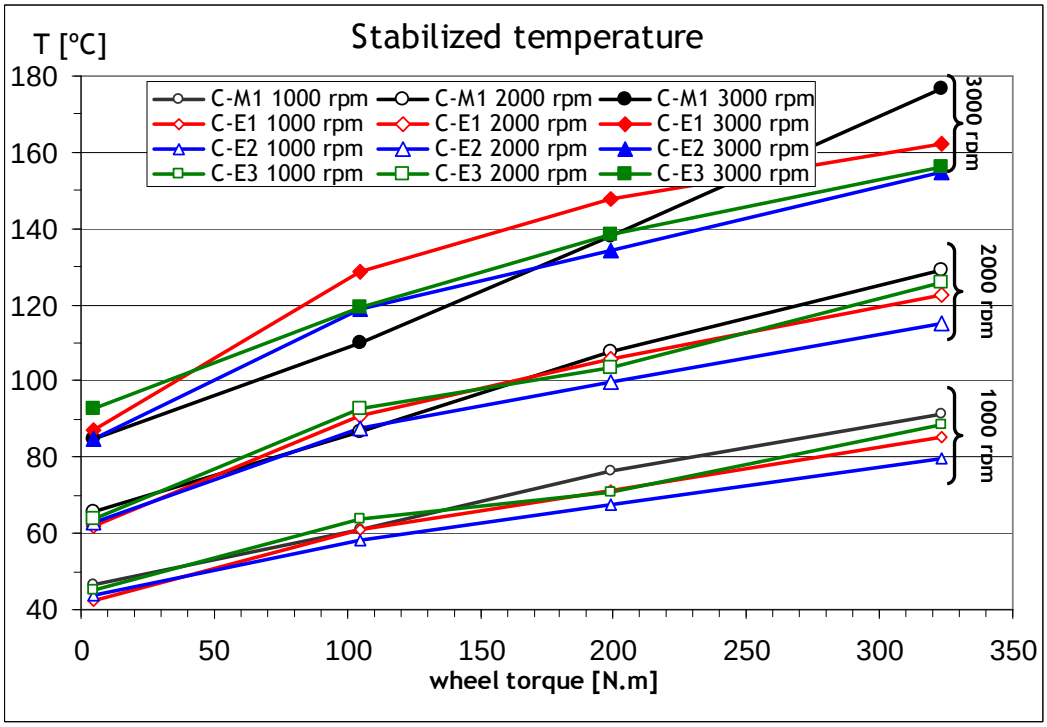


Figure 5.5 - Stabilized oil sump temperature *vs.* wheel torque.

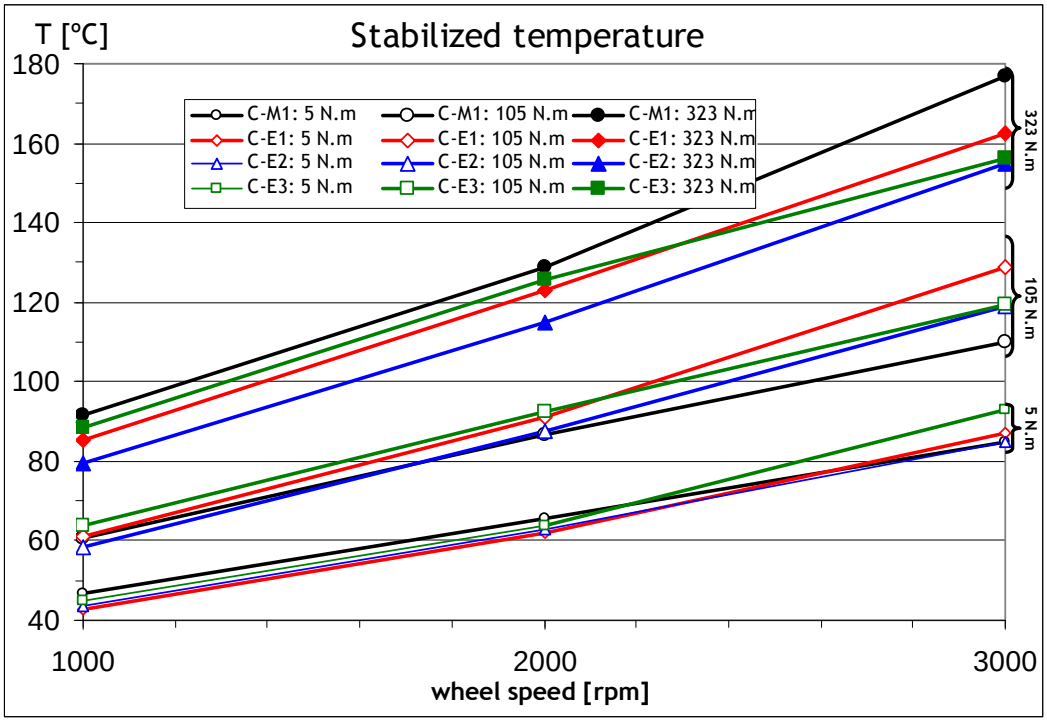


Figure 5.6 - Stabilized oil sump temperature *vs.* wheel speed.

5.4.1.2 Mass loss

Gear mass loss gives a global perspective of wear severity during each power loss test. Figure 5.7 presents the mass loss (g per 10^6 cycles) of the gear pair measured at the end of the test, showing that the E2 ester oil caused a significantly lower mass loss than the other tested lubricants (85% less than lubricants M1 and E3). A very high mass loss was registered for test C-E1 because a scuffing failure occurred. This result is not valid and can not be compared with the results of the other two lubricants.

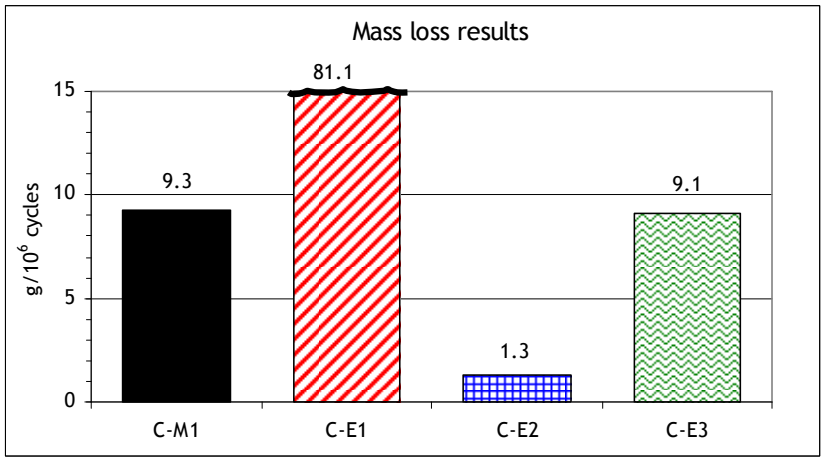


Figure 5.7 - Gear mass loss measurements expressed in g per 10^6 cycles (carburized gears).

5.4.1.3 Oil analysis after test

Oil samples of lubricants M1, E1, E2 and E3 were collected at pre-defined moments during the power loss tests performed in the FZG machine. These oils samples were analyzed after the tests in order to determine:

- The evolution of the ferrometric indexes (*DL*, *DS*, *CPUC*, *ISUC*)[34].
- The variation of lubricant viscosity[6, 35].

5.4.1.3.1 Ferrometry

Each lubricant sample was analyzed by Direct Reading Ferrography (or Ferrometry) in order to measure the ferrometric parameters *DL* (large wear particles index) and *DS* (small wear particles index). Afterwards, the values of *DL* and *DS* were used to evaluate the concentration of wear particles index - *CPUC* and the severity of wear particles index – *ISUC* (see chapter 0).

The *CPUC* index grows when the sum of small and large particles (*DL* + *DS*) increases, while the *ISUC* index grows when the difference between large and small particles (*DL* - *DS*) increases. It's important to remember that the lubricant is not replaced after each load stage.

The evolution of the ferrometric indexes *DL* and *DS* during each test are presented in Figure 5.8. In general, the values of *DL* and *DS* increased throughout the tests, although the most significant particle generation occurs during running-in, that is, during the first load stage.

All lubricants had similar evolutions of the large wear particles index. *DL* index of mineral lubricant started with the highest value but then had a lower increase. The E2 ester also had lower increase while, the ester oils E1 and E3 seemed to have higher increase, indicating that these lubricants could generate more wear particles at high loads. The dilution of the last lubricant sample of E1 fluid is different (see Appendix D – FZG gear POWER LOSS tests data sheets and Table 5.5). This sample has a very high wear particle concentration due to a scuffing failure than occurred during the test (it's marked with an "*" because values must be multiplied by 10 to be comparable to the remaining results).

It is interesting to notice that both M1 and E2 lubricants produced similar *DS* indexes during the test, and the *DL* index of the mineral oil is 65% higher than that of the E2 gear oil.

The evolution of the ferrometric indexes *CPUC* and *ISUC* during each test are presented in Figure 5.9. Both indexes were presented using a logarithmic scale because the last point of E1 lubricant is very high. The three lubricants M1, E1 and E3 had very similar results concerning both indexes (E1 oil had a significant higher value in the last oil sample due the occurrence of a scuffing failure). All lubricant had similar results in the case of the *ISUC* index, the E1 and E3 ester lubricants showed a higher increase. Taking into to account load stages K5, K7 and K9, the *CPUC* and the *ISUC* indexes corresponding to E2 lubricant are 36% and 62% smaller than those ones corresponding to the other three tested lubricants. These values reveal that E2 gear oil generated less wear particles and less severe wear particles than all the other tested lubricants (M1, E1 and E3).

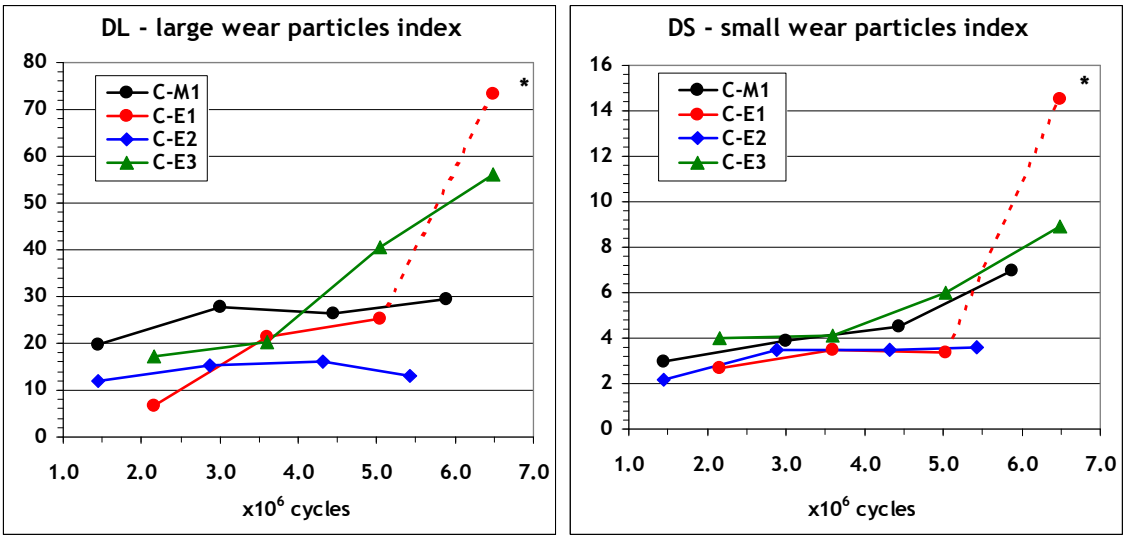


Figure 5.8 - Evolution of *DL* and *DS* wear particles indexes during the power loss tests with carburized gears.

*** - these points were measured using a different dilution so they must be multiplied by 10 to be comparable with the other ones.**

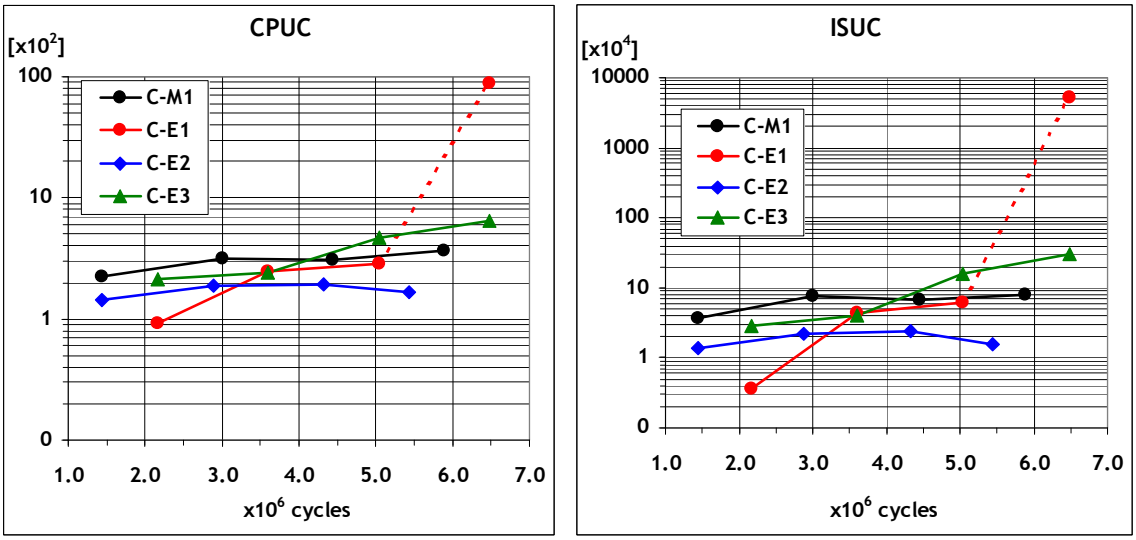


Figure 5.9 - Evolution of *CPUC* and *ISUC* wear particles indexes during the gear power loss tests with the carburized gears.

5.4.1.3.2 Analytical ferrography

Table 5.5 shows analytical ferrograms of the lubricant samples collected during the power loss tests using carburized gears. The ferrograms of the four lubricants are very similar from running-in until load stage K7, showing a significant amount of small size wear particles and some brilliant contact fatigue particles of larger size (see Figure 5.10). An important concentration of wear particles is observed in the ferrogram corresponding to the last load stage of the test performed with mineral oil. The ferrogram of the last load stage of the E1 lubricant is not comparable with the other ones because it has a different dilution.

The lubricant samples collected during the test performed with the ester oils E1 and E2 contained several friction polymers, as shown in Figure 5.11 and Figure 5.13 (ferrogram corresponding to samples collected after load stage k7).

On the E1 ester oil sample of the last load stage, the wear particles are involved with friction polymers (see Figure 5.13). This happened probably due the high temperatures reached during the last load stage (see Figure 5.3).

Significant amounts of non-metallic compounds, probably due to lubricant oxidation, were noticed on the ferrogram corresponding to the mineral oil sample collected after load stage K9, shown in Figure 5.14.

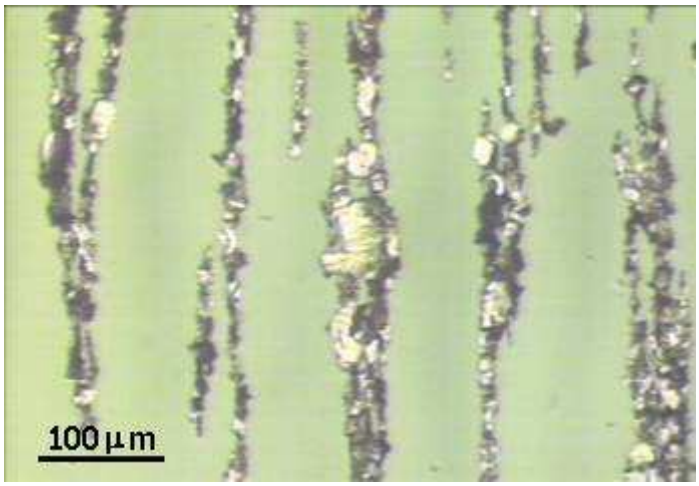


Figure 5.10 - Example of small size wear particles and some brilliant contact fatigue particles of larger size present in the M1 gear oil sample collected after load stage k7 (Magnification = 200x, *d*=0.1).

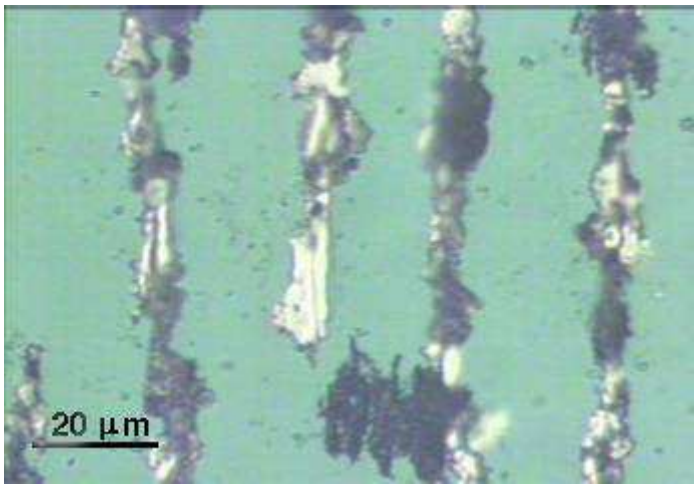
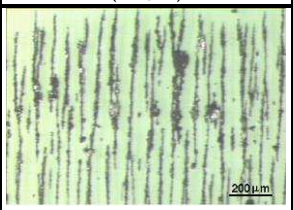
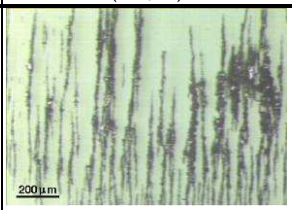
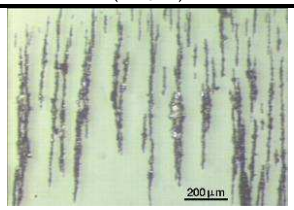
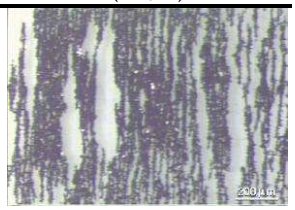
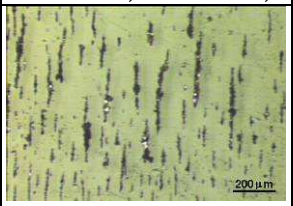
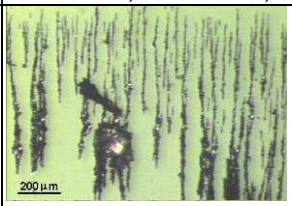
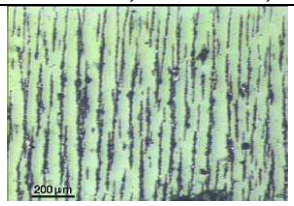
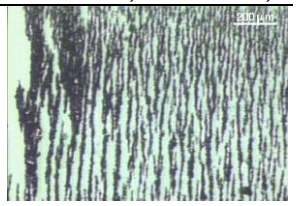
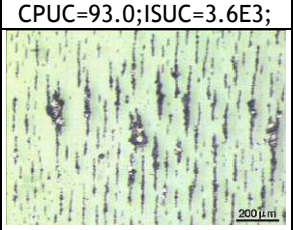
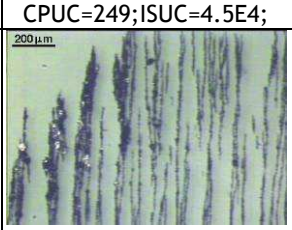
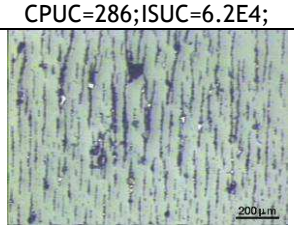
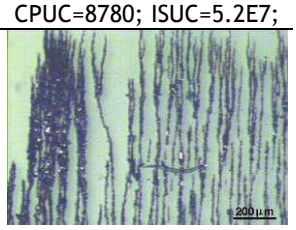
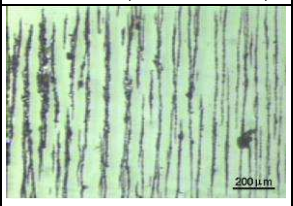
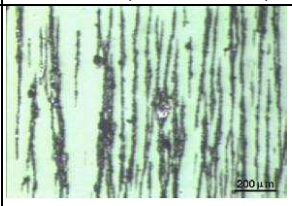
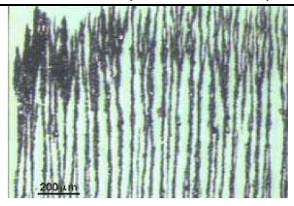
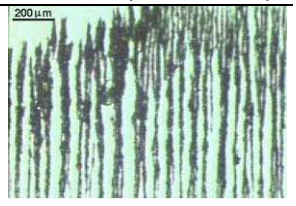


Figure 5.11 - Friction polymers detected in the E1 ester oil sample collected after load stage k7 (Magnification 1000X; *d*=0.1).

Table 5.5 - Ferrogram pictures of the lubricant samples collected during the tests with the carburized gears (Magnification = 100x).

Test	running-in	Load tests		
	T_{wheel}=4.5 Nm (K_{FZG}=1)	T_{wheel}=105.0 Nm (K_{FZG}=5)	T_{wheel}=198.8 Nm (K_{FZG}=7)	T_{wheel}=323.4 Nm (K_{FZG}=9)
C-M1				
	d=0.1; DL=19.6; DS=3.0; CPUC=226; ISUC=3.8E4;	d=0.1; DL=27.9; DS=3.9; CPUC=318; ISUC=7.6E4;	d=0.1; DL=26.5; DS=4.5; CPUC=310; ISUC=6.8E4;	d=0.1; DL=29.4; DS=7.0; CPUC=364; ISUC=8.2E4;
C-E1				
	d=0.1; DL=6.6;DS=2.7; CPUC=93.0;ISUC=3.6E3;	d=0.1; DL=21.4;DS=3.5; CPUC=249;ISUC=4.5E4;	d=0.1; DL=25.2;DS=3.4; CPUC=286;ISUC=6.2E4;	d=0.01; DL=73.3;DS=14.5; CPUC=8780; ISUC=5.2E7;
C-E2				
	d=0.1; DL=12.0; DS=2.0; CPUC=142; ISUC=1.4E4;	d=0.1; DL=15.4; DS=3.5; CPUC=189; ISUC=2.2E4;	d=0.1; DL=16.0; DS=3.5; CPUC=195; ISUC=2.4E4;	d=0.1; DL=13.1; DS=3.6; CPUC=167; ISUC=1.6E4;
C-E3				
	d=0.1; DL=17.2; DS=4.0; CPUC=212; ISUC=2.8E4;	d=0.1; DL=20.3; DS=4.1; CPUC=244; ISUC=4.0E4;	d=0.1; DL=40.5; DS=6.0; CPUC=650; ISUC=3.1E5;	d=0.1; DL=56.1; DS=8.9; CPUC=650; ISUC=3.1E5;

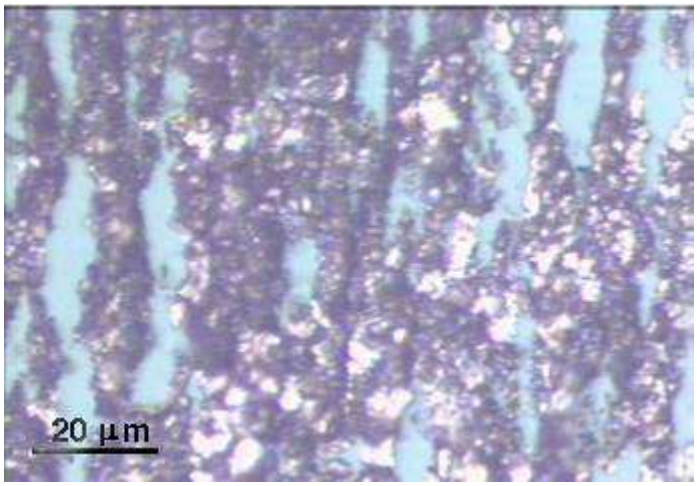


Figure 5.12 - Small wear particles involved by friction polymers (E1 lubricant after load stage 9; Magnification 1000X; *d*=0.01).

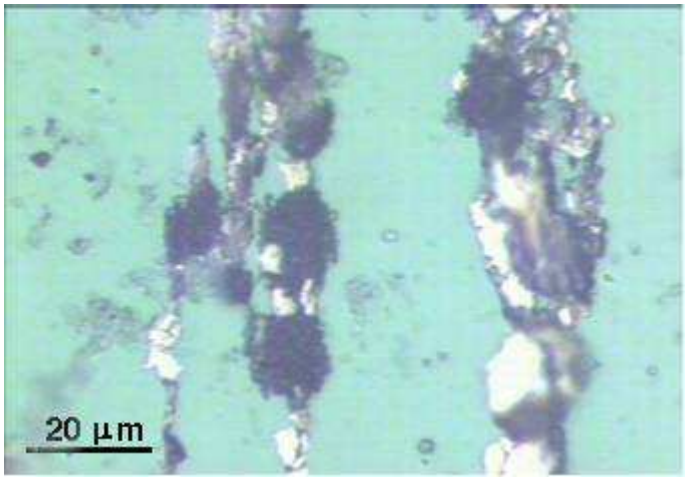


Figure 5.13 - Friction polymers detected in the E2 ester oil sample collected after load stage k7 (Magnification 1000X; *d*=0.1).

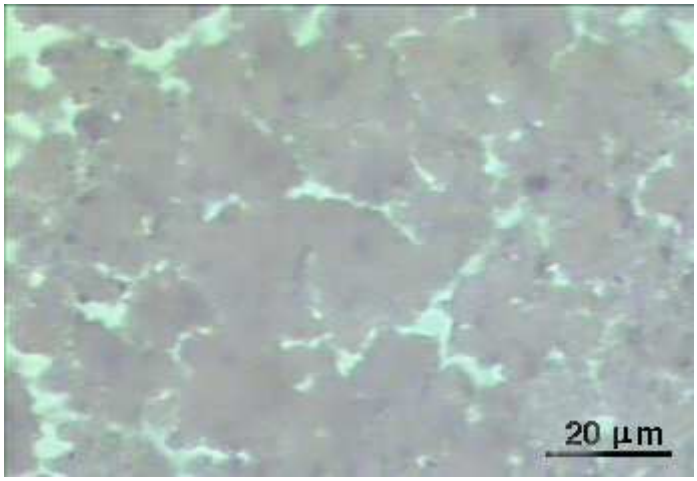


Figure 5.14 - Non-metallic compounds found in the M1 mineral oil sample after load stage K9 (Magnification 1000X; *d*=0.1).

5.4.1.3.3 After test kinematic viscosity

The kinematic viscosity of the four oils was measured at 40 and 100 ºC, before and after the gear power loss tests, using an Engler viscosimeter and in accordance to standard IP 212/92 [36], as presented in Table 5.6.

Table 5.6 – Lubricant viscosity before and after test (with carburized gears).

Test reference	*Lubricant*	*Temp. [ºC]*	*kinematic viscosity [cSt]*		
			Fresh oil	*Used oil*	*Variation*
C-M1	Mineral 1	40	150.0	165.7	10.5 %
		100	14.6	13.8	-5.5 %
C-E1	Ester 1	40	99.4	102.4	3.0 %
		100	14.6	14.1	-3.4 %
C-E2	Ester 2	40	114.5	119.9	4.7 %
		100	17.0	17.4	2.4 %
C-E3	Ester 3	40	108.3	103.2	-4.7 %
		100	15.9	16.2	1.9 %

The viscosity at 40ºC of the mineral oil had a significant increase (more than 10%), indicating that this lubricant suffered an important oxidation, as the analytical ferrography results also indicate – see Figure 5.14. This oxidation is probably due the high temperatures reached by the lubricant (178 ºC). It's viscosity at 100ºC decreased slightly.

The variations in kinematic viscosity at 40 and at 100ºC of the ester oils (E1, E2 and E3) were always below ±10%, indicating that they didn't suffered significant oxidation during the test time.

5.4.1.4 Visual inspection

After dismounting and cleaning, the teeth surfaces were photographed with high resolution. Figure 5.15 shows the flank of a gear pinion tooth after manufacturing, the grinding marks being perfectly identifiable. Figure 5.16, Figure 5.17, Figure 5.18 and Figure 5.19 show the flank of a carburized gear pinion tooth after the power loss tests using the reference mineral oil M1 and the E1, E2 and E3 ester oils, respectively.

The gear flank lubricated with mineral oil and ester E3 (see Figure 5.16 and Figure 5.19) suffered significant wear and shows smooth aspect, mainly above the pitch line. Only a few grinding marks are still visible. Micropitting occurred below the pitch line (the micropitting area is surrounded by a red line for easier reading).

A scuffing failure occurred during E1 lubricant test. It caused a significant degradation of the active teeth flanks. Figure 5.17 presents a pinion tooth surface, showing scuffing marks at the top and base. The appearance of the tooth base (without scuffing marks) is similar to the ones of tests of M1 and E2 lubricants. It indicates that before the scuffing failure, the teeth flank evolution was similar to the one observed with the other two fluids.

The gear flank lubricated with ester oil E2 also shows micropitting below the pitch line (see Figure 5.18), but the grinding marks are still perfectly visible and the tooth flank shows only moderate wear. This fact shows that this ester oil promotes less wear compared to the remaining lubricants under analysis, agreeing with the mass loss results (see Figure 5.7).



Figure 5.15 - Flank of a carburized gear pinion tooth after manufacturing, showing grinding marks.

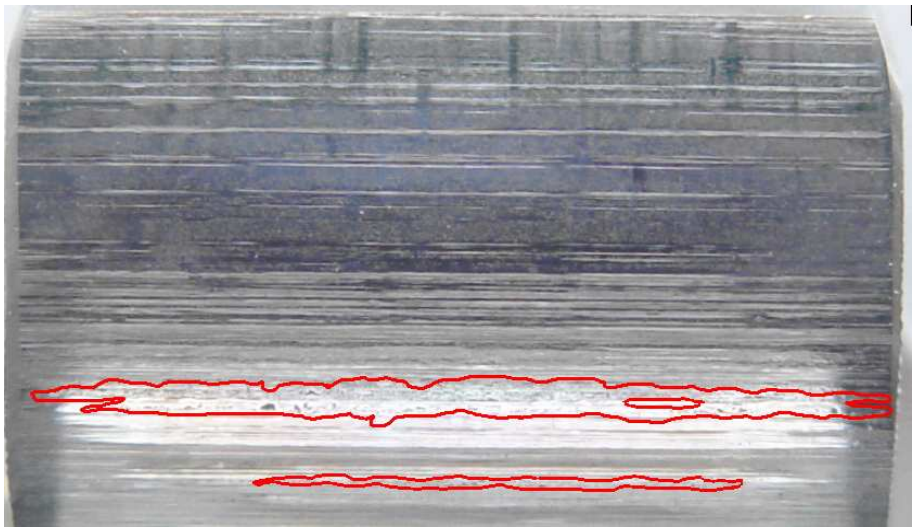


Figure 5.16 - Flank of a carburized gear pinion tooth after test using the reference mineral oil.

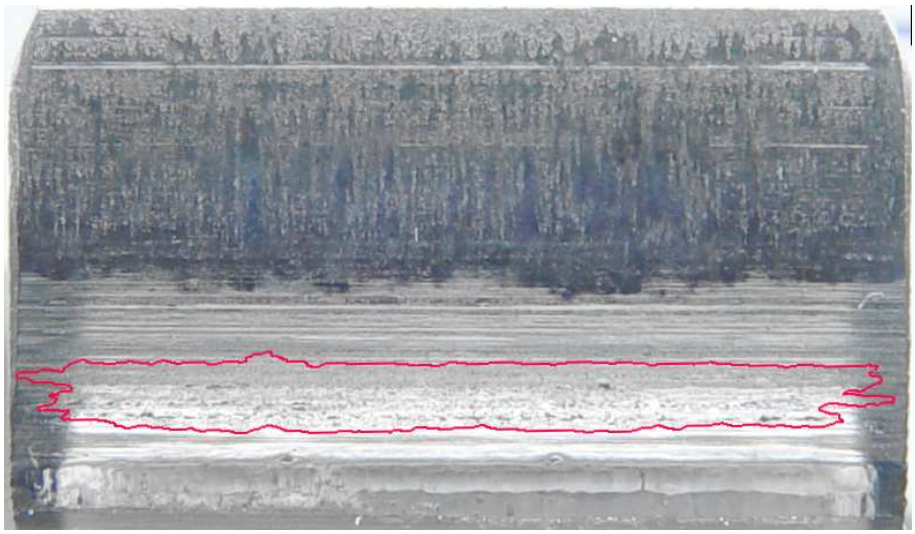


Figure 5.17 - Flank of a carburized gear pinion tooth after test using the E1 lubricant (scuffing marks are observed above the pitch line.

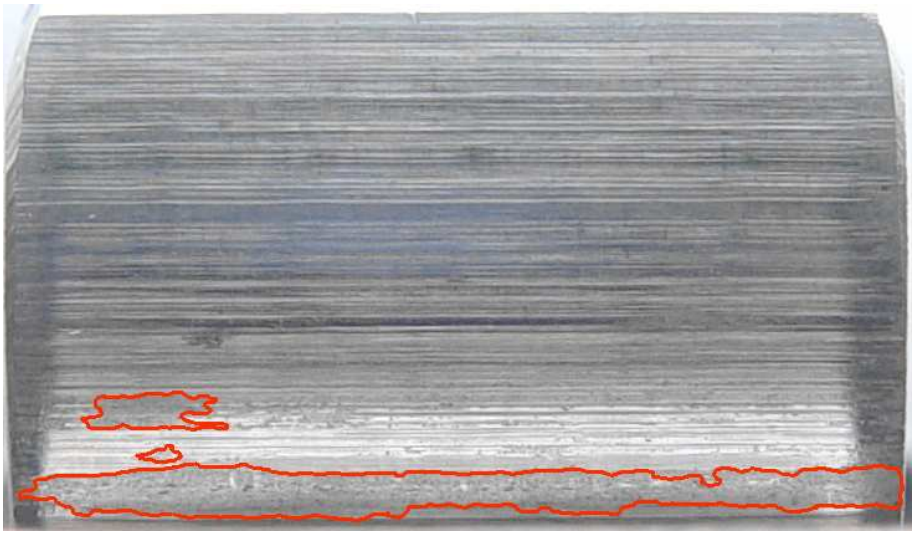


Figure 5.18 - Flank of a carburized gear pinion tooth after test using the E2 lubricant.

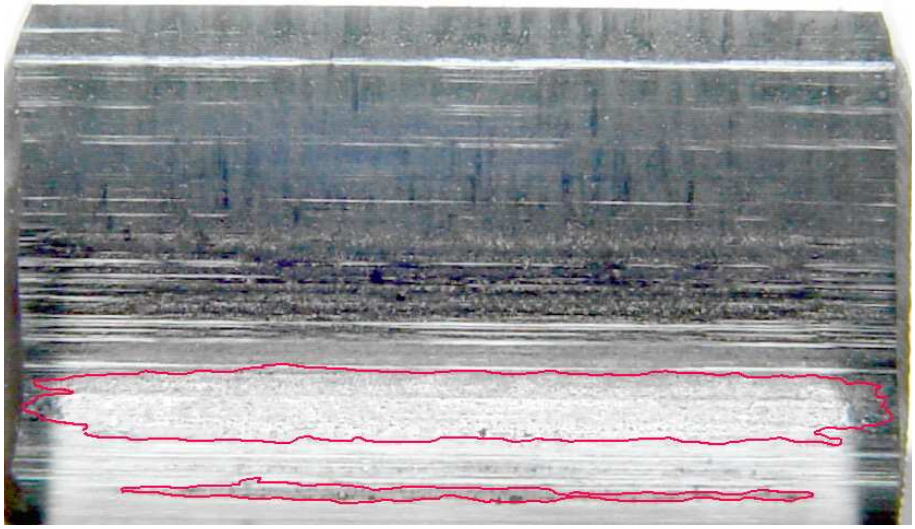


Figure 5.19 - Flank of a carburized gear pinion tooth after test using the E3 lubricant.

5.4.1.5 Surface roughness

Several roughness measurements were made in axial and radial directions, in both cases below and above pitch line (see Figure 4.11). The roughness measurements were performed using a Hommelwerk T4000 device, using a total measurement length L_t=4.8 mm and a cut-off filter λ_c=0.8 mm, and they were digitally filtered [16].

The measurements made above the pitch line in the radial direction give a good indication of surface wear and the measurements made below the pitch line in the axial direction put into evidence the depth of micropitts.

The roughness profiles of the teeth flanks measured in the axial direction, above and below the pitch line, are presented in Figure 5.20 and Figure 5.21 respectively, after manufacturing and after test using the mineral and ester oils. The corresponding surface roughness parameters are presented in Table 5.7.

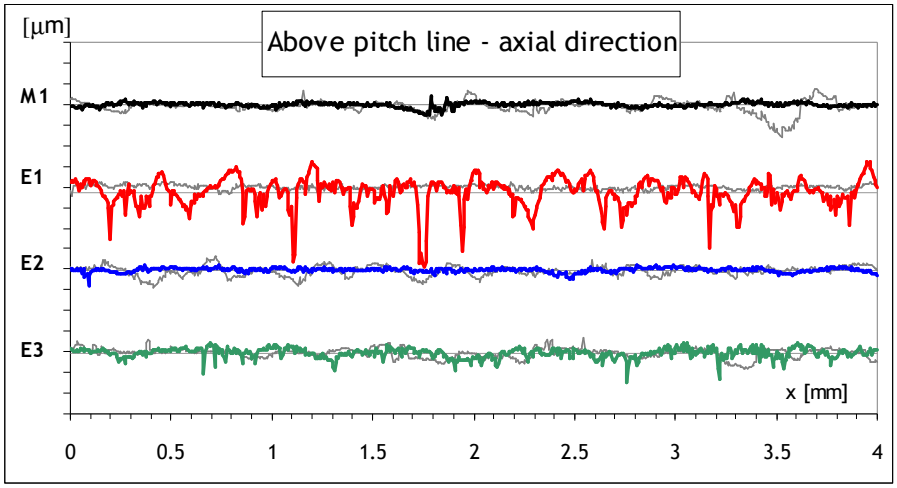


Figure 5.20 - Roughness profiles measured in axial direction above pitch line (carburized gears).

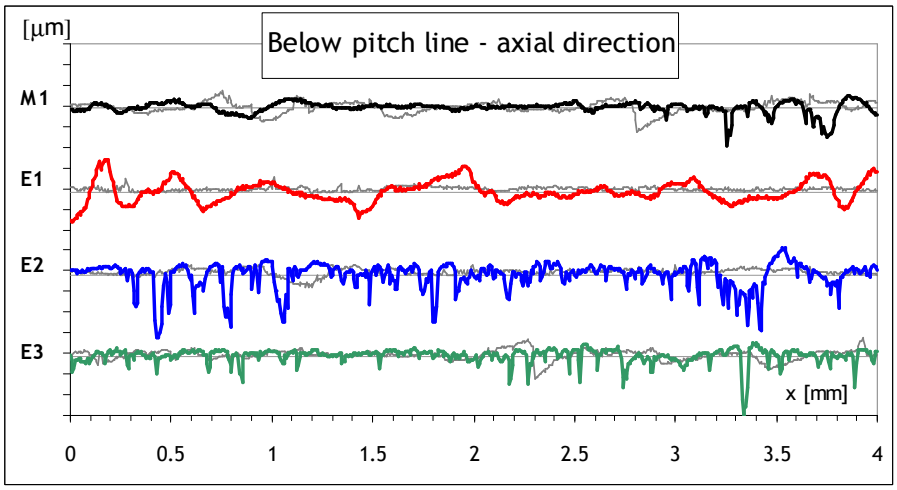


Figure 5.21 - Roughness profiles measured in axial direction below pitch line (carburized gears).

Table 5.7 - Average roughness parameters measured in axial direction [µm].

Test ref.	Lubricant		above pitch line			below pitch line		
			$R_{z\text{-}D}$	R_{pk}	R_{vk}	$R_{z\text{-}D}$	R_{pk}	R_{vk}
C-M1	**Mineral 1**	Initial	1,15	0,26	0,42	0,91	0,22	0,51
		Final	0,85	0,15	0,38	0,84	0,17	0,40
		Variation	-27%	-44%	-8%	-8%	-24%	-21%
C-E1	**Ester 1**	Initial	0,49	0,08	0,13	0,44	0,17	0,12
		Final	3,76	0,40	1,39	1,47	0,50	0,46
		Variation	661%	392%	1005%	230%	204%	286%
C-E2	**Ester 2**	Initial	0,69	0,14	0,19	0,68	0,14	0,32
		Final	0,70	0,08	0,31	2,04	0,23	0,93
		Variation	0%	-38%	63%	199%	66%	188%
C-E3	**Ester 3**	Initial	0,67	0,24	0,22	0,75	0,20	0,29
		Final	2,10	0,14	0,79	2,03	0,18	0,78
		Variation	215%	-40%	263%	169%	-7%	171%

Above the pitch line and in the axial direction, the surface roughness of the tooth flanks decreased significantly after being tested using M1, E2 and E3 oils, as shown in Figure 5.20 and in Table 5.7. The R_{pk} parameter, related to the surface roughness peaks, decreased more than 35% in the three cases, meaning that those roughness peaks were worn out during gear operation. The profile measured at the end of the test of E1 lubricant (presented in Figure 5.20) and the great increase of the roughness parameters, clearly show that a scuffing failure occurred in this test, with the consequent degradation of the surface geometry ($R_{Z\text{-}D}$ increased 661% - see Table 5.7).

The surface roughness of the tooth flanks below the pitch line shows the same tendency concerning wear of the roughness peaks. However, micropitting occurred in this zone, generating micropitts visible in the roughness profiles, as shown in Figure 5.21, and also the increase of the R_{vk} roughness parameter presented in Table 5.7 (exception for mineral oil, R_{vk} decreasing 21%), what could indicate a greater size or number of micropitts for the ester fluids. However, the smooth aspect showed by the gear lubricated by mineral oil and his higher mass loss value lead to believe that, in case of the reference lubricant, the micropitts effect was attenuated the surface wear). Figure 5.21 shows measurements made at the teeth lubricated by E1 fluid. The roughness parameters had a very significant increase (as happened above pitch line) due the occurrence of scuffing.

Figure 5.22 and Figure 5.23 present the roughness profiles measured in the axial direction, above and below the pitch line, respectively, after manufacturing and after test with the mineral and ester oils. The corresponding surface roughness parameters are presented in Table 5.8.

Surface roughness measured in radial direction is considerably larger than in the axial direction due to the grinding direction (axial). Figure 5.22 and Figure 5.23 indicate that roughness profiles became flatter. $R_{Z\text{-}D}$ decreased in all cases (see Table 5.8) confirming this evolution. Surface roughness of the teeth flanks decreased during the tests of all four lubricants.

The E3 ester caused the highest reduction of R_{pk} above and below pitch line (see Table 5.8). Roughness profiles were smoother as well as teeth flanks aspect (see Figure 5.19). These facts confirm that E3 lubricant provides a smoothing effect on surfaces.

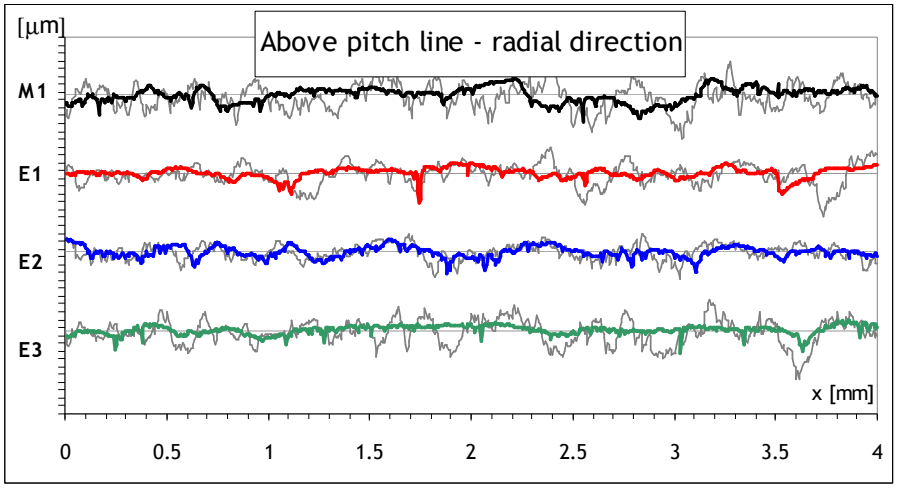


Figure 5.22 - Roughness profiles measured in radial direction above pitch line (carburized gears).

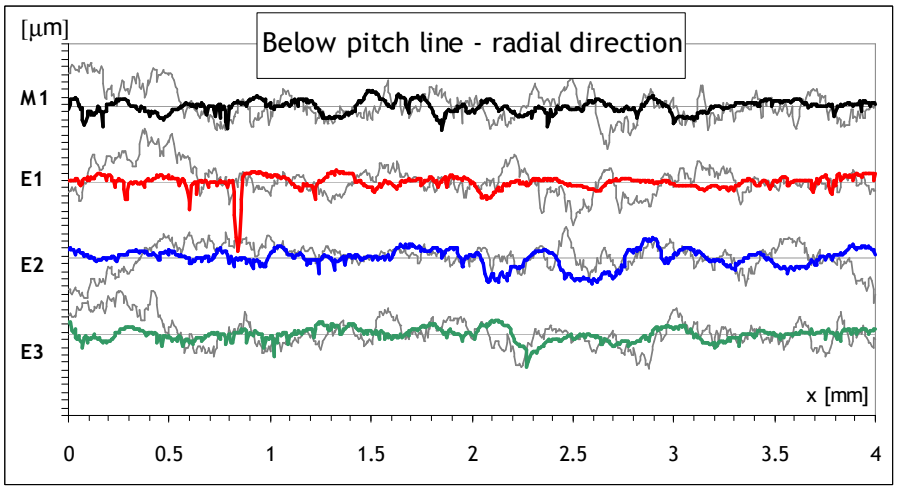


Figure 5.23 - Roughness profiles measured in radial direction below pitch line (carburized gears).

Table 5.8 - Average roughness parameters measured in radial direction [µm].

Test ref.	Lubricant		above pitch line			below pitch line		
			$R_{z\text{-}D}$	R_{pk}	R_{vk}	$R_{z\text{-}D}$	R_{pk}	R_{vk}
C-M1	**Mineral 1**	Initial	7,16	1,27	1,85	6,65	1,25	1,50
		Final	3,00	0,36	1,21	4,18	0,72	1,31
		Variation	-58%	-72%	-35%	-37%	-42%	-13%
C-E1	**Ester 1**	Initial	5,81	1,15	2,40	6,51	1,67	1,74
		Final	3,41	0,74	1,22	5,62	0,97	1,77
		Variation	-41%	-36%	-49%	-14%	-42%	2%
C-E2	**Ester 2**	Initial	4,44	0,54	1,20	5,99	1,58	2,09
		Final	3,41	0,99	1,04	3,86	0,84	1,98
		Variation	-23%	84%	-13%	-36%	-47%	-5%
C-E3	**Ester 3**	Initial	6,41	1,13	2,26	6,94	1,70	1,78
		Final	3,24	0,48	1,23	3,64	0,66	1,27
		Variation	-50%	-58%	-46%	-48%	-61%	-29%

5.4.2 High pressure nitrided gears

5.4.2.1 Operating temperature

Figure 5.24 shows the evolution of the oil bath temperature during tests of the carburized gears. This figure show that at 1000 and at 2000 rpm the E2 ester lubricant has a lower operating temperature, whatever the load. At higher speeds (3000 rpm) different behaviours were observed and the results are not conclusive. Probably, more time would be necessary to reach the stabilization temperature at this speed.

Figure 5.25 displays the stabilised oil temperature and the room temperature, measured at the end of each test period of carburized and nitrided gears. At 1000 and 2000 rpm, the ester oil E2 always stabilized at lower temperature for both gear materials. The difference between these two gears oils tend to increase with the load. At 3000 rpm, the results from ester oil E2 lubricating the nitrided gears are not conclusive, as mentioned before.

Stabilized oil bath temperature during tests of nitrided gears is plotted against the input power in Figure 5.26, at constant speed and for the M1 and E2 oils. In both cases, the oil temperature increased when the input power increased, as expected. Thus, using nitrided gears the stabilized oil bath temperature will increase as long as the input power increases, no matter if the input speed increases and the torque decreases or vice-versa, as it also happens with the carburized gears.

Figure 5.27 shows the influence of the input torque on the stabilized oil bath temperature during tests of nitrided gears at constant speed. When the torque increases the stabilized oil bath temperature also increases, almost in a linear way, reaching a maximum value at 3000 rpm.

Stabilized oil temperature obtained with the nitrided gears is plotted against the input speed at constant torque in Figure 5.28. Once again, the oil temperature is strongly affected by the operating speed because the speed affects both the frictional and the churning losses inside the FZG test gearbox. Having into account the results from wheel speeds of 1000 and 2000 rpm, the stabilization temperature of the ester oil E2 is the lowest one. The difference between the temperature reached by this lubricant and the mineral one tend to increase with the load and to decrease with speed.

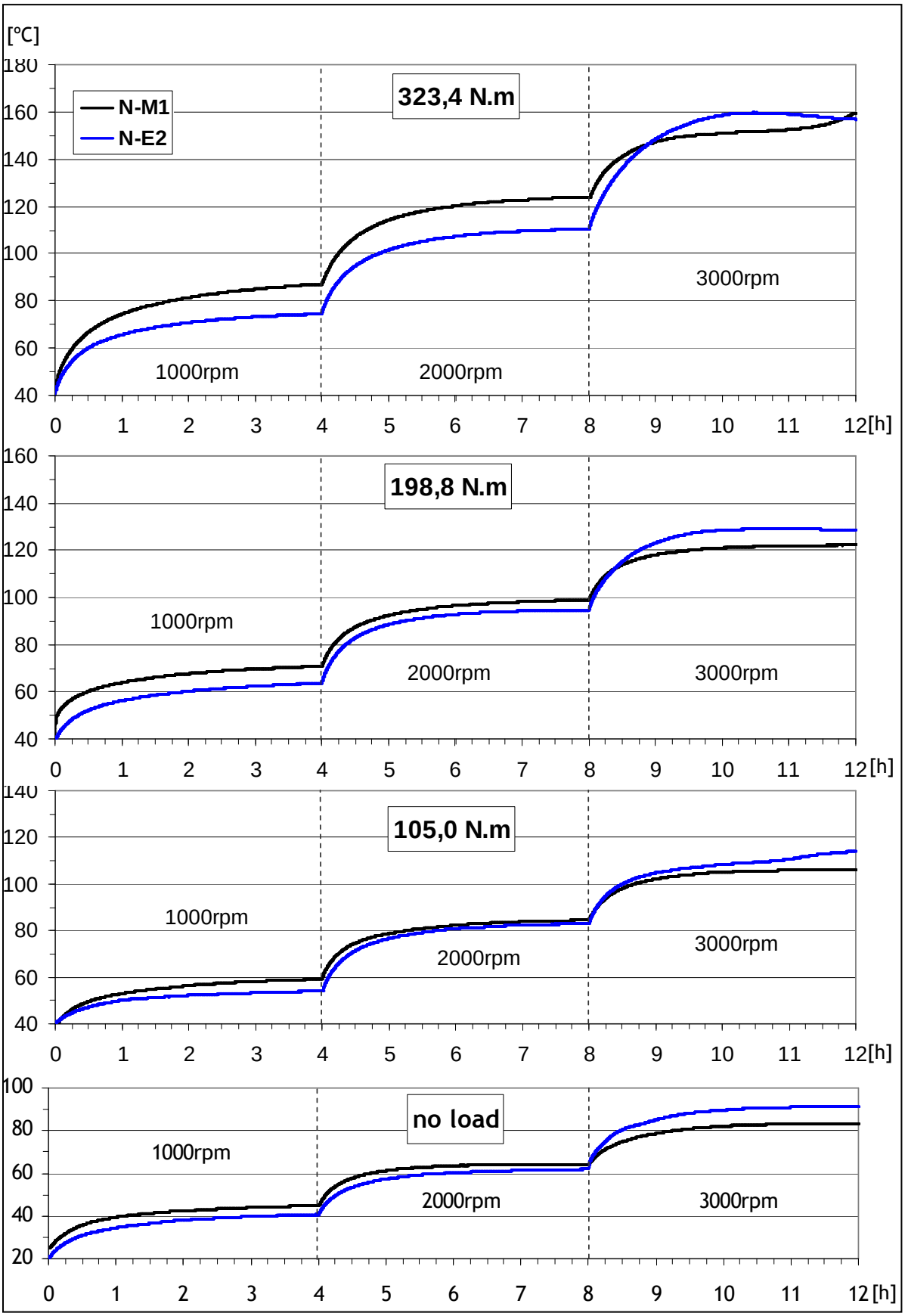


Figure 5.24 - Oil sump temperature during tests with nitrided gears (vertical - temperature in °C, horizontal - time in hours, gear wheel speed and torque indicated).

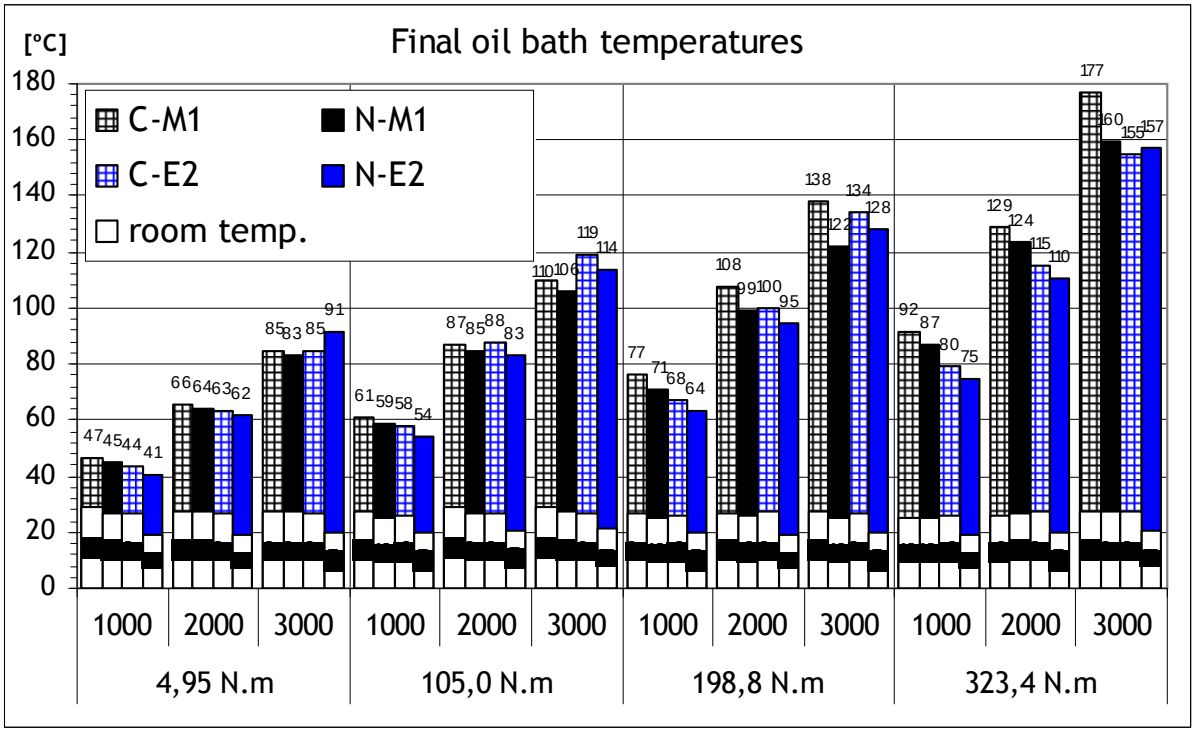


Figure 5.25 - Stabilized oil bath temperature *vs.* input speed and input torque measured during the tests with the carburized and nitrided gears.

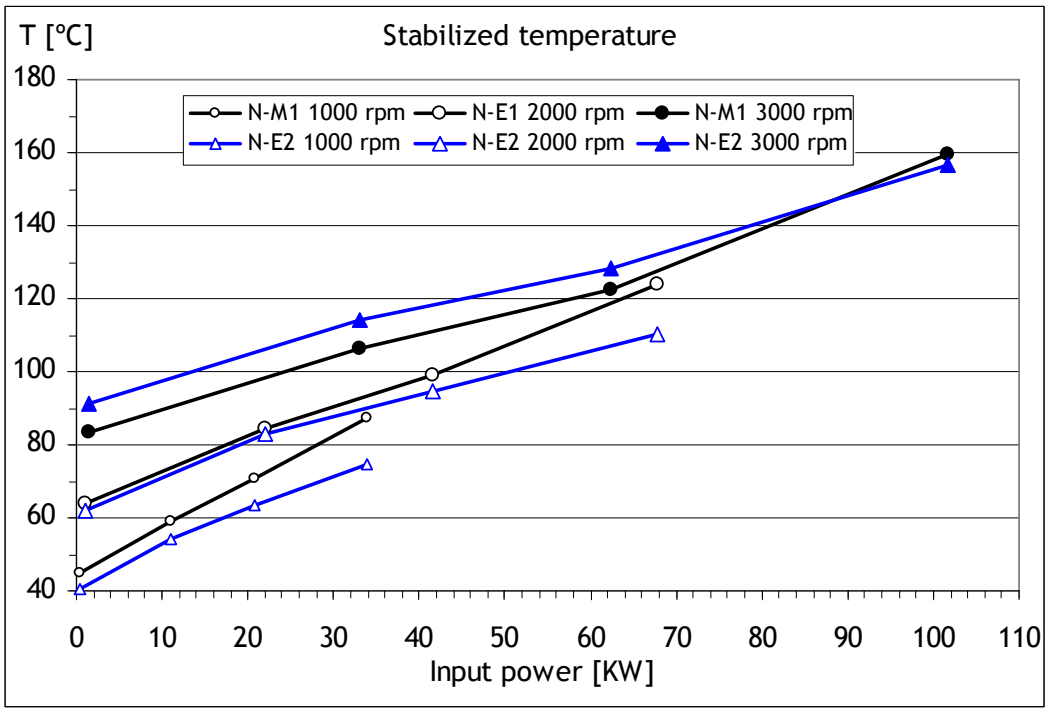


Figure 5.26 - Stabilized oil sump temperature vs. input power (nitrided gears).

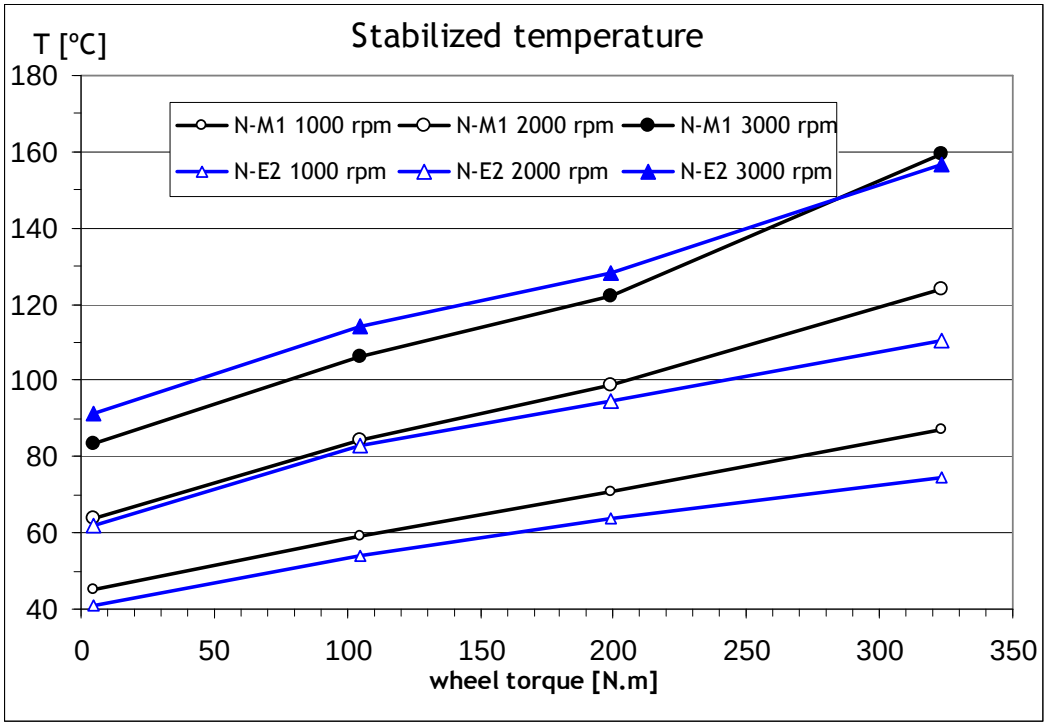


Figure 5.27 - Stabilized oil sump temperature *vs.* wheel torque (nitrided gears).

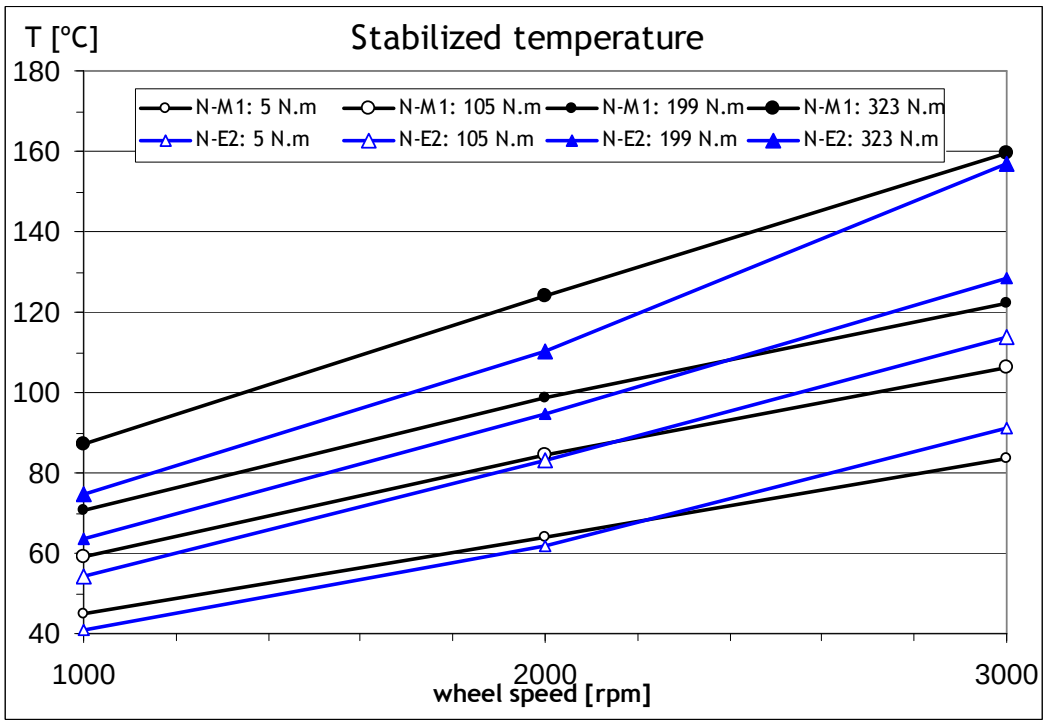


Figure 5.28 - Stabilized oil sump temperature *vs.* wheel speed (nitrided gears).

5.4.2.2 Mass loss

Figure 5.7 presents the mass loss (g per 10^6 cycles) of the gear pair measured at the end of the tests of nitrided gears, showing that the E2 ester oil caused a significantly lower mass loss than the other tested lubricant (59% less than lubricant M1).

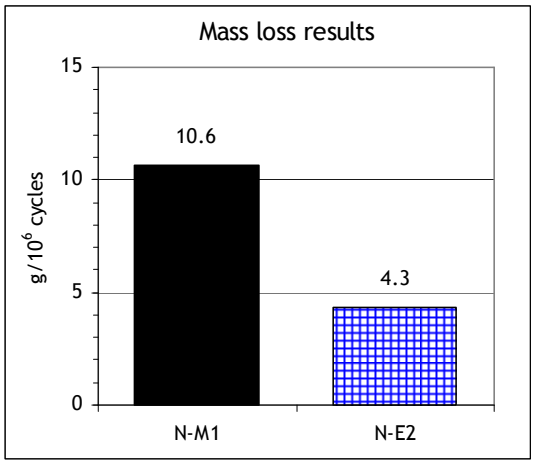


Figure 5.29 - Gear mass loss measurements expressed in g per 10^6 cycles (nitrided gears).

5.4.2.3 Oil analysis after test

5.4.2.3.1 Ferrometry

The evolution of the ferrometric indexes *DL* and *DS* during each test of the high pressure nitrided gears are presented in Figure 5.30. Figure 5.31 displays the corresponding *CPUC* and *ISUC* wear particle indexes. The indexes obtained from the lubricant samples collected during the power loss tests of the nitrided gears had similar tendencies. In general, their values increased along the tests, although the most significant particle generation occurred during running-in. The E2 ester oil generated less wear particles than the mineral one during the first load stage, confirming the mass loss results.

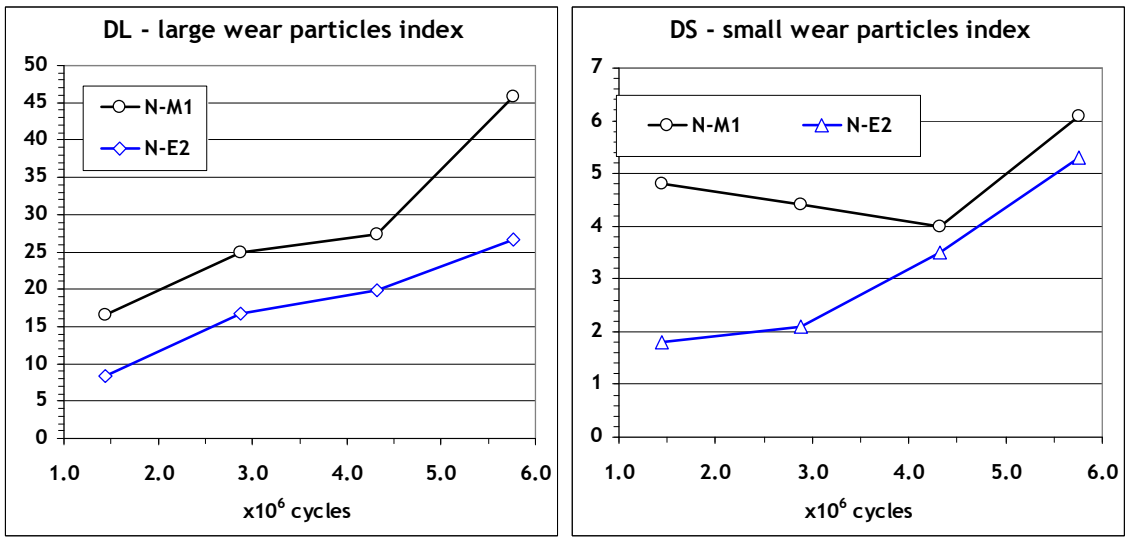


Figure 5.30 - Evolution of *DL* and *DS* wear particles indexes during the power loss tests of nitrided gears.

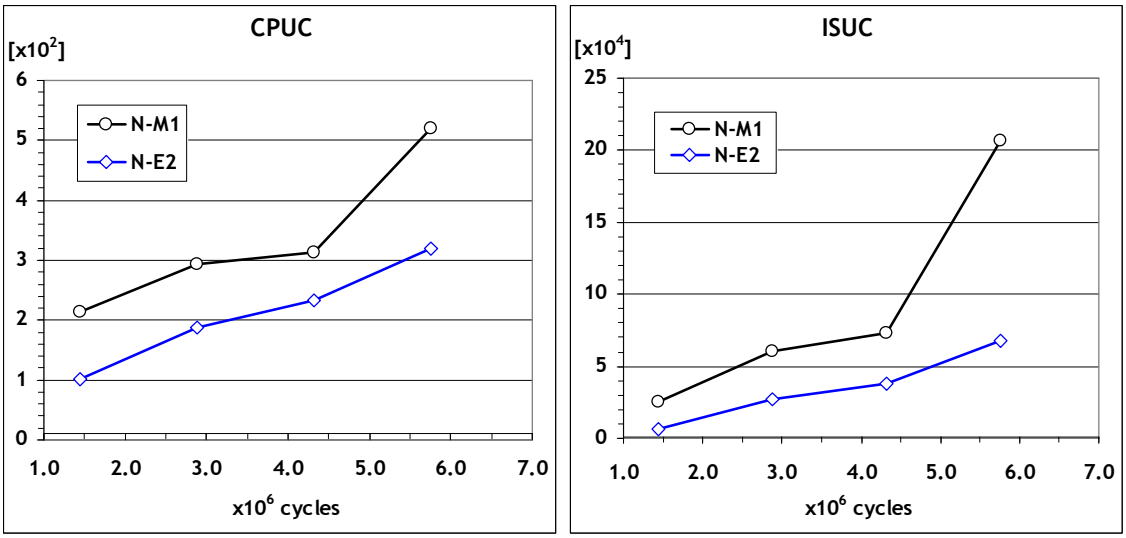
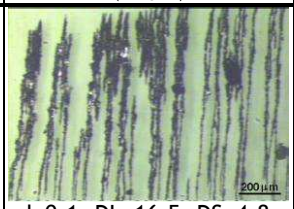
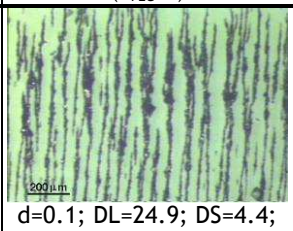
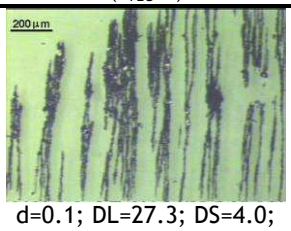
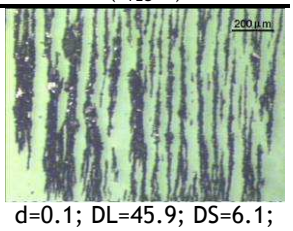
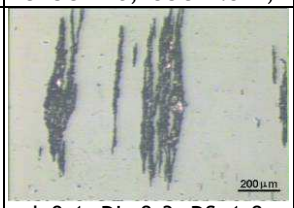
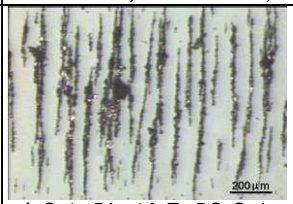
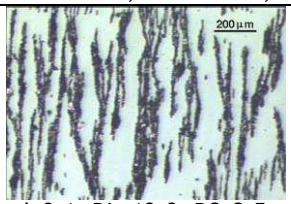
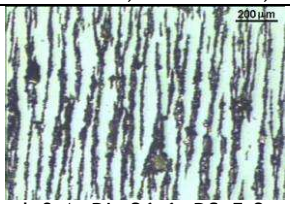


Figure 5.31 - Evolution of *CPUC* and *ISUC* wear particles indexes during the gear power loss tests of nitrided gears.

5.4.2.3.2 Analytical ferrography

Table 5.9 shows analytical ferrograms of the lubricant samples collected during the power loss tests of the high pressure nitrided gears and the corresponding wear particles indexes. The ferrograms collected after load stages K1 and K5 show that the ester E2 generated a significantly lower concentration of wear particles during the first two load stages. The ferrograms of both lubricants (M1 and E2) corresponding to load stages K7 and K9 were similar.

Table 5.9 - Ferrogram pictures of the lubricant samples collected during the tests of the high pressure nitrided gears (Magnification = 100x).

Test	running-in	Load tests		
	T_{wheel}=4.5 Nm (K_{FZG}=1)	T_{wheel}=105.0 Nm (K_{FZG}=5)	T_{wheel}=198.8 Nm (K_{FZG}=7)	T_{wheel}=323.4 Nm (K_{FZG}=9)
N-M1	 d=0.1; DL=16.5; DS=4.8; CPUC=213; ISUC=2.5E4;	 d=0.1; DL=24.9; DS=4.4; CPUC=293; ISUC=6.0E4;	 d=0.1; DL=27.3; DS=4.0; CPUC=313; ISUC=7.3E4;	 d=0.1; DL=45.9; DS=6.1; CPUC=520; ISUC=2.1E5;
N-E2	 d=0.1; DL=8.3; DS=1.8; CPUC=101; ISUC=6.6E3;	 d=0.1; DL=16.7; DS=2.1; CPUC=188; ISUC=2.8E4;	 d=0.1; DL=19.8; DS=3.5; CPUC=233; ISUC=3.8E4;	 d=0.1; DL=26.6; DS=5.3; CPUC=319; ISUC=6.8E4;

5.4.2.4 Visual inspection

After dismounting and cleaning the teeth surface of nitrided gears, they were photographed with high resolution. Figure 5.32 shows the flank of a gear pinion tooth after manufacturing, the grinding marks being perfectly identifiable. Figure 5.33 and Figure 5.34 show the flank of a carburized gear pinion tooth after the power loss tests using the reference mineral and the E2 ester oil, respectively. The aspect of the teeth flanks lubricated with M1 and E2 fluids is similar. Both pinions suffered significant wear and show a smooth aspect, in particular above the pitch line, and only a few grinding marks are still visible. Micropitting occurred below the pitch line and several pitts of large dimensions are visible.

Figure 5.35 displays the flank of a nitrided gear wheel tooth where a spall was found after test using the reference mineral oil. The formation of this spall at the wheel tooth and the several pitts of large dimensions at the pinion teeth indicate that probably the load stage K9 is too severe, taking into account the mechanical properties of the high pressure nitrided gears (surface hardness, …) and the high number of cycles performed ($5{,}76 \times 10^6$ wheel cycles, see Table 5.3).

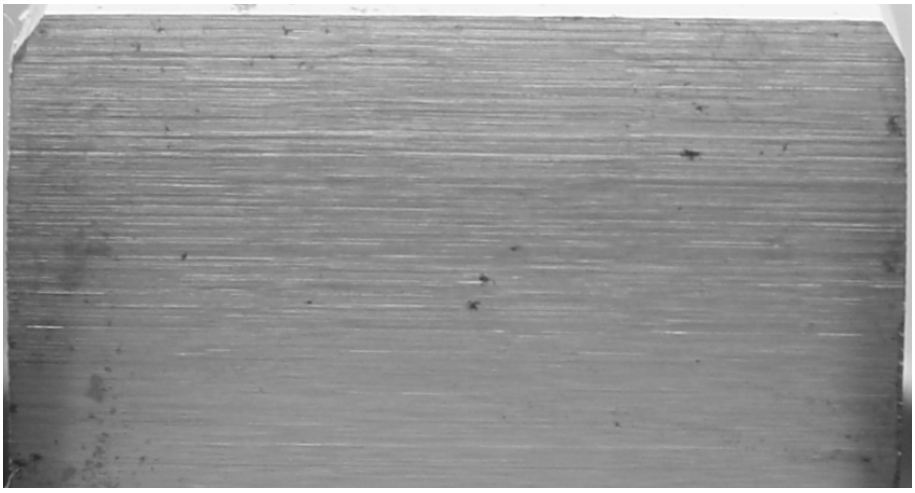


Figure 5.32 - Flank of a nitrided gear pinion tooth after manufacturing, showing grinding marks.



Figure 5.33 - Flank of a nitrided gear pinion tooth after test using the reference mineral oil.

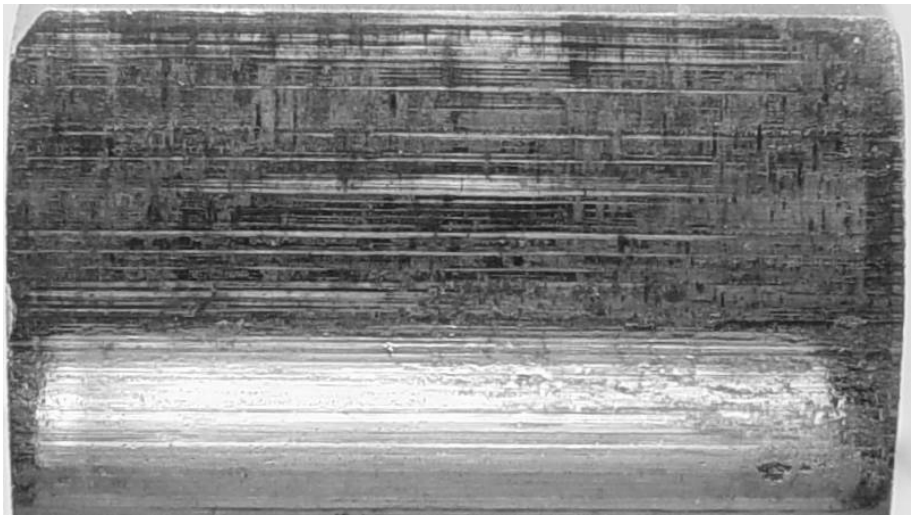


Figure 5.34 - Flank of a nitrided gear pinion tooth after test using the E2 ester oil.



Figure 5.35 - Flank of a nitrided gear wheel tooth after test using the reference mineral oil M1.

5.4.2.5 Surface roughness

The roughness profiles of the teeth flanks were measured in the axial direction, above and below the pitch line, and are presented at Figure 5.36 and Figure 5.37 respectively, after manufacturing and after tests using mineral and ester oils. The corresponding surface roughness parameters are presented in Table 5.10. Surface roughness of the tooth flanks, above the pitch line in the axial direction, decreased significantly after tests with both oils, as shown at Figure 5.36 and Table 5.10. The R_{pk} parameter, related to the surface roughness peaks, decreased more than 70%, meaning that roughness peaks were worn out during gear operation. Below pitch line, the surface roughness of the tooth flanks shows the same tendency concerning wear of the roughness peaks. However, in the case of the mineral gear oil, micropitting occurred in this zone, generating micropitts visible in the roughness profiles, as shown in Figure 5.37, and also in the increase of the R_{vk} roughness parameter, as presented in Table 5.10.

Figure 5.38 and Figure 5.39 present roughness profiles measured in the axial direction, above and below the pitch line, respectively, after manufacturing and after tests using mineral and ester oils. These figures and the variation of the $R_{Z\text{-}D}$ roughness parameter (greater than 40% - see Table 5.11) show that surface roughness in the radial direction decreased significantly with both lubricants, mainly due to the wear of the asperity peaks.

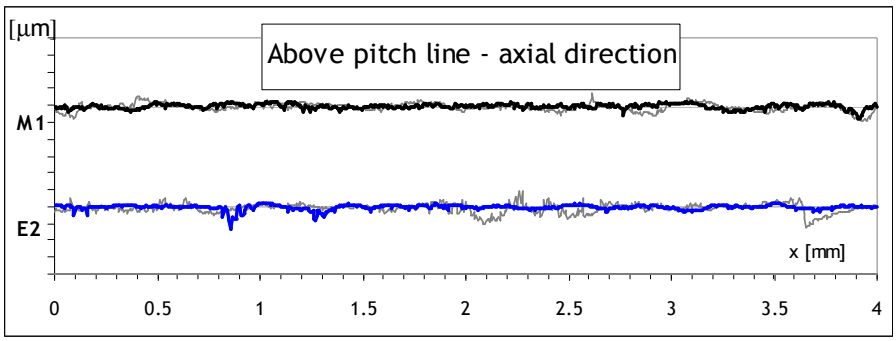


Figure 5.36 - Roughness profiles measured in axial direction above pitch line (nitrided gears).

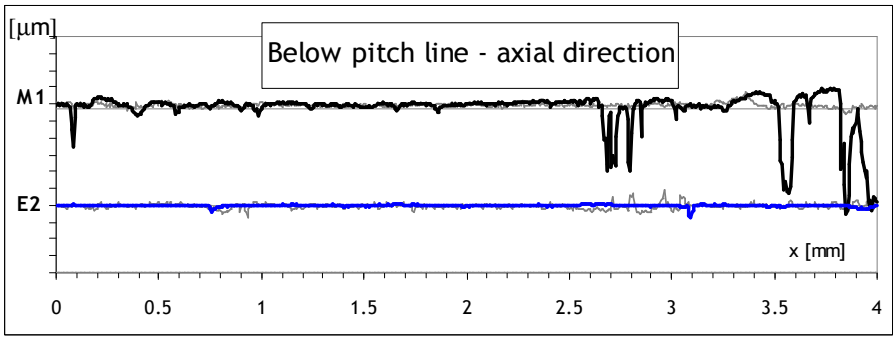


Figure 5.37 - Roughness profiles measured in axial direction below pitch line (nitrided gears).

Table 5.10 – Average roughness parameters measured in axial direction [µm].

Test ref.	Lubricant		above pitch line			below pitch line		
			$R_{Z\text{-}D}$	R_{pk}	R_{vk}	$R_{Z\text{-}D}$	R_{pk}	R_{vk}
N-M1	**Mineral 1**	Initial	1,20	0,31	0,56	0,93	0,28	0,28
		Final	1,16	0,09	0,65	3,96	0,49	3,99
		Variation	-3%	-70%	16%	327%	76%	1336%
N-E2	**Ester 2**	Initial	1,08	0,27	0,32	0,98	0,33	0,24
		Final	0,56	0,06	0,21	0,34	0,04	0,16
		Variation	-49%	-78%	-34%	-66%	-87%	-34%

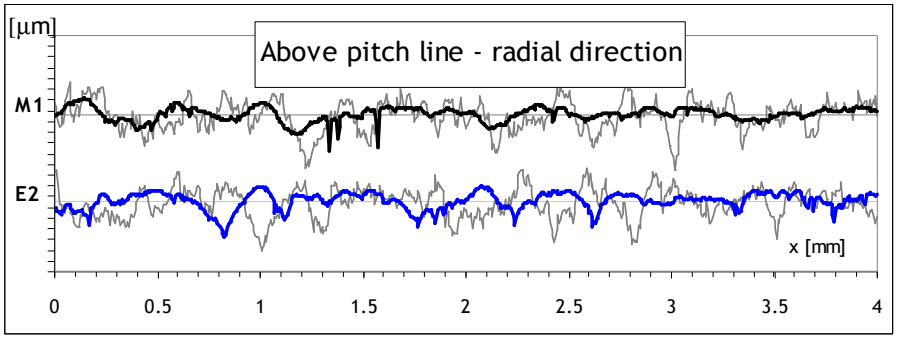


Figure 5.38 - Roughness profiles measured in radial direction above pitch line (nitrided gears).

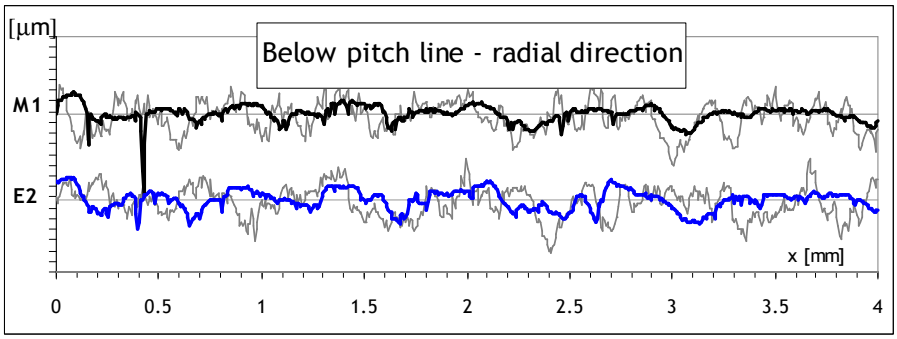


Figure 5.39 - Roughness profiles measured in radial direction below pitch line (nitrided gears).

Table 5.11 - Average roughness parameters measured above pitch line in radial direction [µm].

Test ref.	Lubricant		above pitch line			below pitch line		
			$R_{Z\text{-}D}$	R_{pk}	R_{vk}	$R_{Z\text{-}D}$	R_{pk}	R_{vk}
N-M1	**Mineral 1**	Initial	6,30	1,12	1,94	6,01	0,66	1,58
		Final	2,83	0,35	1,21	3,33	0,29	1,17
		Variation	-55%	-69%	-38%	-45%	-57%	-26%
N-E2	**Ester 2**	Initial	6,91	1,87	1,59	7,13	1,86	1,68
		Final	0,33	0,06	0,12	0,39	0,06	0,13
		Variation	-95%	-97%	-92%	-94%	-97%	-92%

5.5 Power loss model

The most important mechanisms of power dissipation inside any gearbox, such as the test gearbox of the FZG gear test rig, are the churning losses and the frictional losses [32, 33].

The churning losses are related to the rotational movement of the mechanical components, e.g. gears, rolling bearings and seals, immerged in the viscous oil bath. This form of power loss is very often designated as “No Load Power Loss”, since it is independent of the applied torque [32, 33]. The churning losses inside a gearbox have three main origins:

- The churning of the rotating gear set immerged in the oil bath;
- The churning of the rotating rolling bearings immerged in the oil bath;
- Friction between other moving components and the oil bath, e.g. oil seals.

Since there is no torque applied, the friction between the gear teeth is very small and doesn’t affect the overall power loss. The *No Load Power Loss* depends on the following parameters [32, 33]:

1. The rotational speed of the gearbox;
2. The viscosity of the lubricant oil at the operating temperature;
3. The volume of lubricating oil;
4. The gearbox geometry and internal arrangement (dimensions, number of gears, type and number of rolling bearings, seals, …);
5. The surrounding temperature ,which influences the heat evacuation.

The frictional losses are related to the friction between moving parts transmitting load, mainly the rolling bearings and the gear teeth. They depend on the load transmitted and on the friction coefficient between the contacting surfaces [32, 33].

The total power loss is obtained adding the churning and the friction losses.

For a given gearbox geometry (for instance the gearbox of the FZG test rig shown in Figure 5.1), input speed, applied torque and lubricating oil, the power dissipated heats the oil bath increasing its temperature. Simultaneously, some heat is evacuated to the air and to the steel plate supporting the FZG test gearbox. This is done by conduction, radiation and convection between the test gearbox and the surrounding environment.

The final oil bath temperature depends on the balance between the heat generated and heat evacuated. After a long operating period both the temperature of the oil and of the test rig tend to an equilibrium state [32, 33].

The different mechanisms of power loss and heat evacuation are presented in Figure 5.40. The thermal balance of FZG test box results in an equilibrium temperature, since all the parameters of the equilibrium equation depend on the oil temperature, directly or indirectly

$$P_{fr}+P_{M1}+P_{spl}+P_{M0}+P_{sl}=Q_{cn}+Q_{rad}+Q_{cnv} \quad (5.1)$$

The temperature dependence of the equilibrium equation terms is non-linear, implying an iterative solution method.

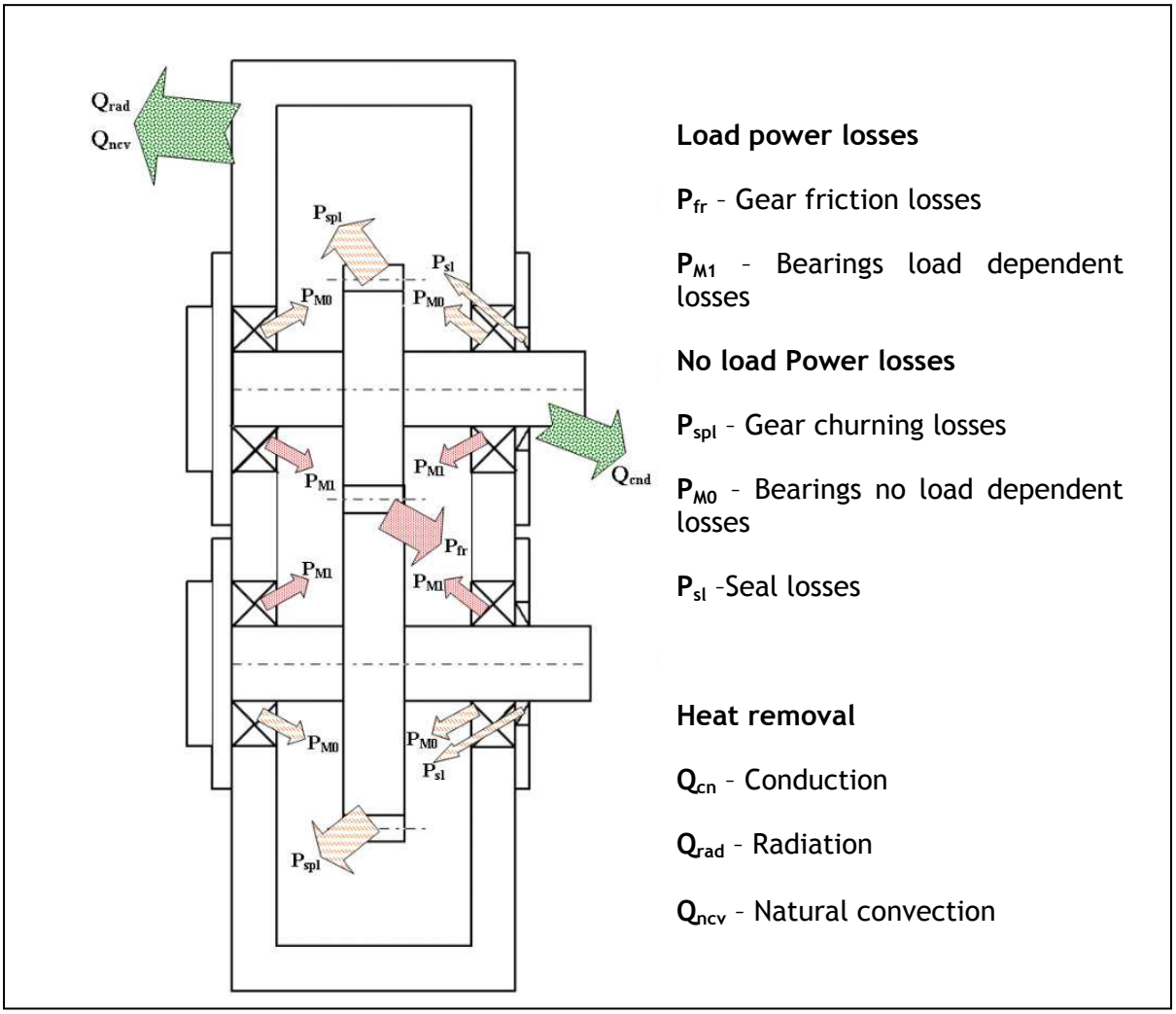


Figure 5.40 – Forms of power loss and heat evacuation of the FZG test box.

5.5.1 Load dependent power losses

5.5.1.1 Gear friction losses

The gear friction losses depend mainly on the geometric conditions of the gearing, the number of teeth, the input power and the friction coefficient [32, 33].

$$P_{fr} = \pi \cdot \left(\frac{1}{z_1} + \frac{1}{z_2} \right) \cdot \left(1 - \left(\frac{g_f - g_a}{p_b} \right) + \left(\frac{g_f}{p_b} \right)^2 + \left(\frac{g_a}{p_b} \right)^2 \right) \cdot P_{in} \cdot \mu_m \qquad (5.2)$$

The friction coefficient is the most important factor in this study, because it is the only parameter influenced by the operating conditions. The original friction coefficient used is proposed by Michaelis et al [32],

$$\mu_m = 0{,}048 \cdot \left(\frac{F_{bt}/b}{\upsilon_{\Sigma c} . \rho_c} \right)^{0,2} \cdot \eta_{oil}{}^{-0.05} \cdot Ra^{0,25} \cdot X_L \qquad (5.3)$$

where X_L=1 for mineral oils, and oil viscosity is calculated as defined in Table 1.1.

5.5.1.2 Bearing friction losses

The load dependent power losses in bearings depend on the type of bearing, the combined applied load (axial and radial), the bearing diameter and the friction coefficient. The friction coefficient for the FZG test box rolling bearings is constant [37].

$$P_{M1} = \frac{\pi}{30} . N . \left(\sqrt{F_r^2 + F_a^2} . f_1 . D \right) \qquad (5.4)$$

5.5.2 No load power losses

5.5.2.1 Gear churning losses

The churning losses from gears are independent of load, and the most influencing parameters are the gear diameter, rotating speed, immersion area of gears, gear width and oil viscosity and density. The test box design also has a significant influence on the churning losses, as well as the fluid flow regime. Changenet et al [33] proposed an expression dependent on Froud (“F_R”) and Reynolds (“Re”) non-dimensional numbers.

$$P_{spl} = \frac{\pi}{30} . N . \left(\frac{1}{2} . \rho . \left(\frac{\pi . N}{30} \right)^2 . A_i . \left(\frac{d_P}{2} \right)^3 \right) . \left(\left(\frac{2.h}{d_P} \right)^{0,45} . \left(\frac{V_{oil}}{d_P} \right)^{0,1} . F_R{}^{-0,6} . Re^{-0,21} \right) \qquad (5.5)$$

5.5.2.2 Bearings churning losses

The calculation of no load power losses in bearings [37] is mainly dependent on the rotating speed, bearing diameter, type of bearing and lubricant viscosity at the operating temperature.

$$P_{M0} = \frac{\pi}{30} \cdot N \cdot \left(f_0 \cdot 10^{-7} \cdot \left(N \cdot \eta_{oil} \right)^{\frac{2}{3}} \cdot D^3 \right) \cdot 10^{-3} \qquad (5.6)$$

5.5.2.3 Seals power losses

The seals power losses are independent of applied load and represent the friction losses in the contact between seal leaps and shafts. These power losses depend mainly on the rotating speed and shaft diameter [32].

$$P_{sl} = 7{,}69 \cdot 10^{-6} \cdot d_i^2 \cdot N \tag{5.7}$$

5.5.3 Heat removal from the test box

The heat removal from the test box is done by radiation, free and forced convection and conduction. All these forms of heat removal depend on the wall gearbox temperature that in the case of FZG test box, it's almost the same as the oil temperature.

5.5.3.1 Convection

The room where the test rig stands is equipped with forced ventilation (air insufflation and air extraction), allowing to keep the room temperature constant, although the air velocity is to low to guarantee forced convection.

The natural convection heat removal was splited in two parts, one referring to the vertical walls convection and another referring to the horizontal walls convection [33].

The convection coefficient for vertical walls is:

$$h_v = 11.06 \cdot h_{ca}{}^{-0.1} \cdot \left(\frac{Tw - Ta}{Ta} \right)^{0.3} \tag{5.8}$$

where h_{ca} is the height of gearbox.

The convection coefficient for horizontal walls (test box cover) is:

$$h_h = 12.87 \cdot L_{ca}{}^{-0.04} \cdot \left(\frac{Tw - Ta}{Ta} \right)^{0.32} \tag{5.9}$$

where L_{ca} is the characteristic dimension of horizontal wall (mean value of width and length).

The power removed by convection in vertical and horizontal walls is:

$$Q_{ncv} = h_v \cdot A_v \cdot (Tw - Ta) + h_h \cdot A_h \cdot (Tw - Ta) \tag{5.10}$$

5.5.3.2 Radiation

The amount of power removed by radiation is determined from Stefan Boltzman law, but for simplicity a heat radiation coefficient (α_{rad}) is defined [32].

$$\alpha_{rad} = 0.23 \cdot 10^{-6} \cdot \varepsilon \cdot \left(\frac{Tw + Ta}{2} \right)^3 \tag{5.11}$$

The power removed by radiation is determined from the following expression.

$$Q_{rad} = \alpha_{rad} \cdot A_{rad} \cdot (Tw - Ta) \tag{5.12}$$

5.5.3.3 Conduction

Conduction is the form of heat removal in the FZG test box of higher calculation difficult. This happens because the heat conduction is bi-directional and the base plate of FZG test box has a complex shape. To accurately calculate the power removed by conduction, a complex simulation of the FZG test rig is required. Michaelis et al.[38] proposed the substitution of heat conduction by increasing the test box radiation and convection area by a factor (f_{cn}) of 1.5 to 2.5 times the area of contact between the test box and the base plate.

$$Q_{cn} = \left(Q_{rad} + Q_{ncv}\right) \cdot \left(fcn \cdot \frac{A_{base}}{A_{rad}} \right) \tag{5.13}$$

The "f_{cn}" factor for the used test rig was determined from the results of the no load tests. In those tests only the no-load power losses occurred, allowing the calculation of the "f_{cn}" value that best describes the used FZG test rig. The value calculated was $f_{cn} = 2.5$.

5.5.4 FZG test gearbox simulation

5.5.4.1 Structure of the thermal balance model for the FZG test gearbox

The thermal balance model for the FZG test gearbox was implemented using Matlab®. The program structure is shown in Figure 5.41. This program structure is valid for the adjustment of any type of parameters, and in this work is used for the adjustment of conduction parameter, churning losses, friction coefficient and for the determination of equilibrium temperatures for any operating conditions.

Parameters were adjusted using the least squares method and Newton's non-linear method. The target function for minimization is the difference between generated and evacuated power in the test box, that is, the thermal balance equation of the FZG test box.

The input values depend on the type of parameter that must be optimized. For the friction coefficient, the input values are the final temperature of tests, the operating conditions (speed and torque), the lubricant properties (in function of temperature) and geometrical data about the gears and test box, as well as initial values for all parameters.

For determining the stabilization temperature, the input values are the parameters of $\boldsymbol{X_L}$ factor (see equation 5.3), the operating conditions (speed and torque), the lubricant properties (as a function of temperature) and geometrical data of gears and test box, as well as initial values for temperature.

5.5.4.2 Calculation of the friction coefficient

The stabilization temperatures attained in the power loss tests differed substantially for the oils tested. This difference is due to their physical and tribological properties. The most relevant tribological property for the friction power loss is the friction coefficient between the flanks of the contacting teeth.

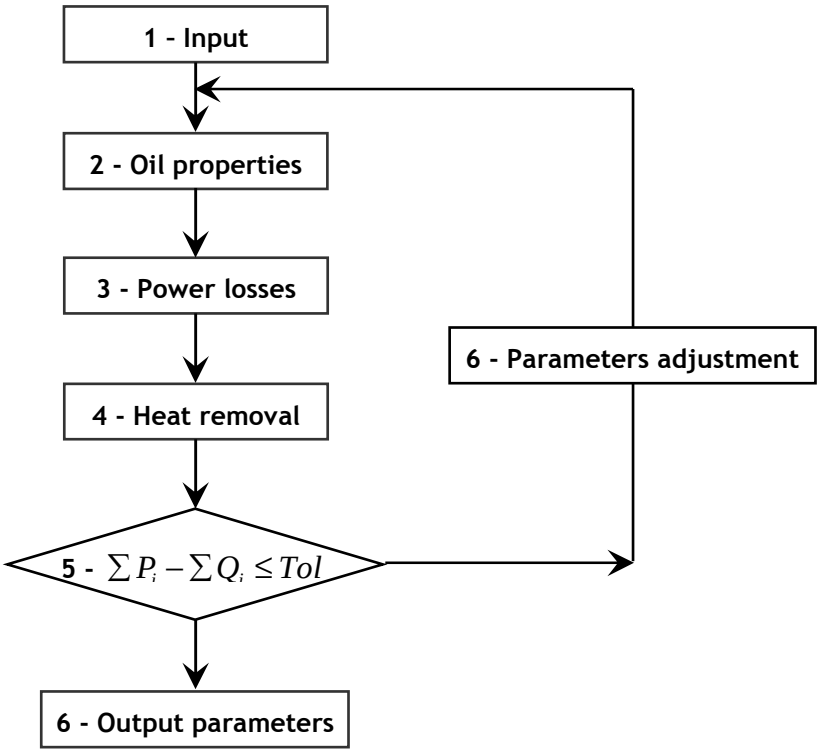


Figure 5.41 - Program structure for friction coefficient parameters optimization.

The friction coefficient expression proposed by Michaelis et al. [32] states that

$$\mu_m = 0{,}048 \cdot \left(\frac{F_{bt}/b}{\upsilon_{\Sigma c} . \rho_c} \right)^{0,2} \cdot \eta_{oil}{}^{-0.05} \cdot Ra^{0,25} \cdot X_L \qquad (5.14)$$

It depends on the applied load, oil viscosity, velocity sum and the equivalent surface roughness. The X_L parameter is equal to 1 for additive free mineral oils. One of the aims of this work is to optimize the X_L parameter, for each one of the tested lubricants, in order to realistically represent their behaviour during the power loss tests performed using the FZG test rig.

5.5.4.2.1 Carburized gears

Figure 5.42, Figure 5.43, Figure 5.44 and Figure 5.45 show stabilization temperatures measured during the power loss tests with carburized gears and the corresponding numerical values, respectively for the reference mineral and ester oils (M1, E1, E2 and E3), considering the X_L parameter equal to 1. For the reference mineral oil, the correlation between experimental and numerical stabilization temperatures is quite low. The difference between experimental and numerical values increases when the load increases. At the highest load stage the gap is above 30ºC. The correlation also gets worse when the rotating speed increases, although the temperature difference in this case is much smaller then the one observed with load.

The results from ester oils are similar, although the differences between experimental and numerical temperatures are much higher than for reference mineral oil. These results indicate that $X_L < 1$ for the four oils and must be adapted to each lubricant. The X_L parameter may have other values in order to take into account the presence of additives (e.g. extreme pressure, anti-wear, friction modifiers, viscosity index improvers …) or because the base oil has a different nature (synthetic ester, polialpheolefins …).

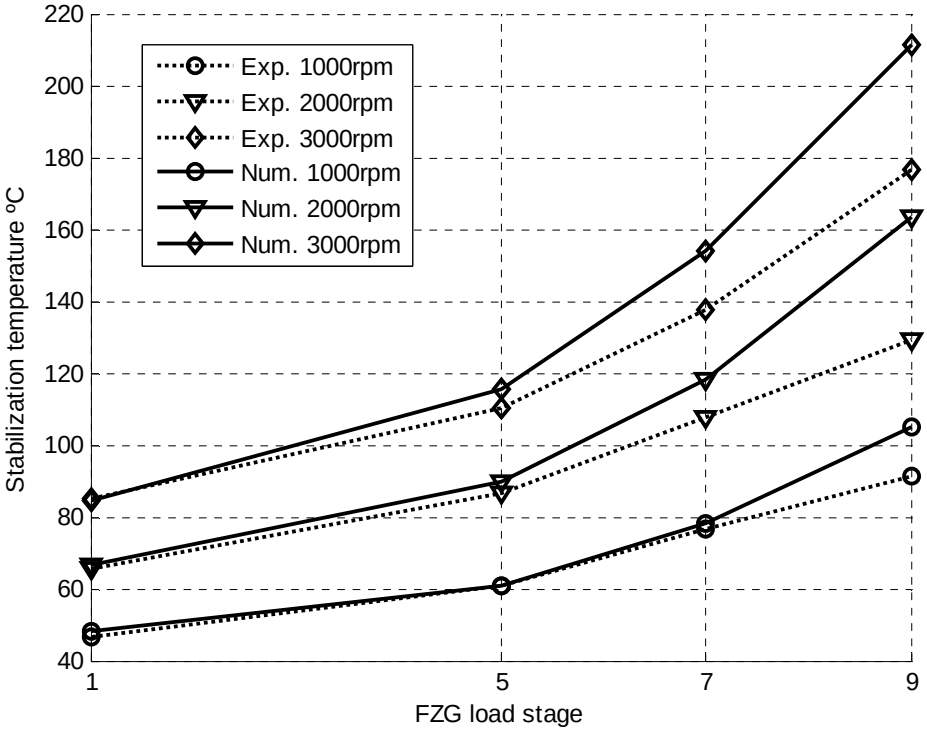


Figure 5.42 – Stabilization temperature for reference mineral oil: experimental vs. numerical values (carburized gears, X_L=1).

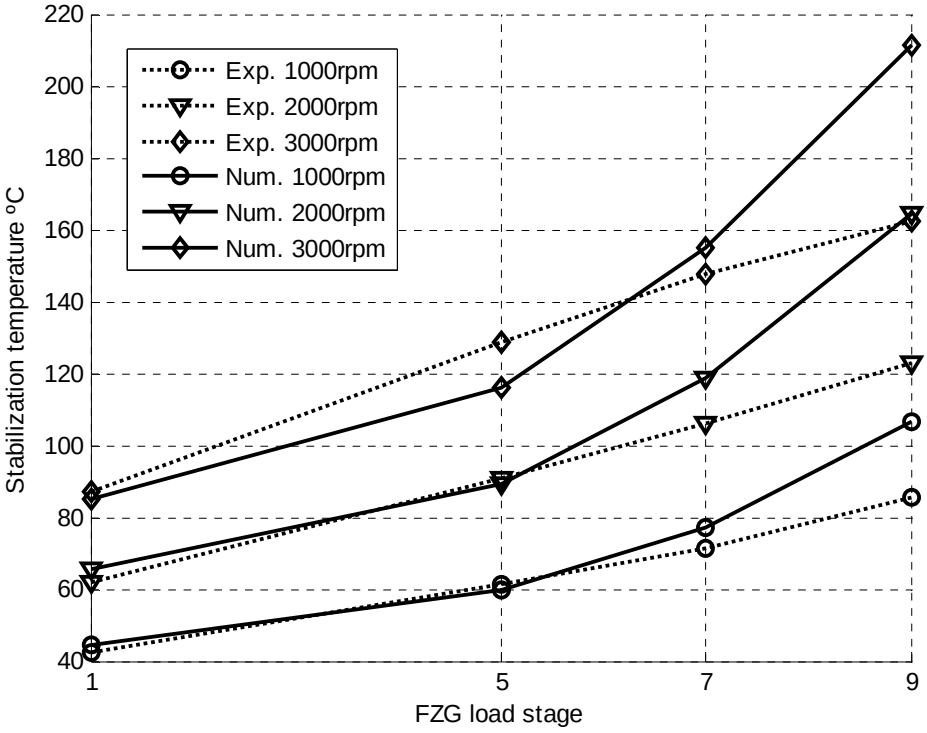


Figure 5.43 - Stabilization temperature for ester oil E1: experimental vs. numerical values (carburized gears, X_L=1).

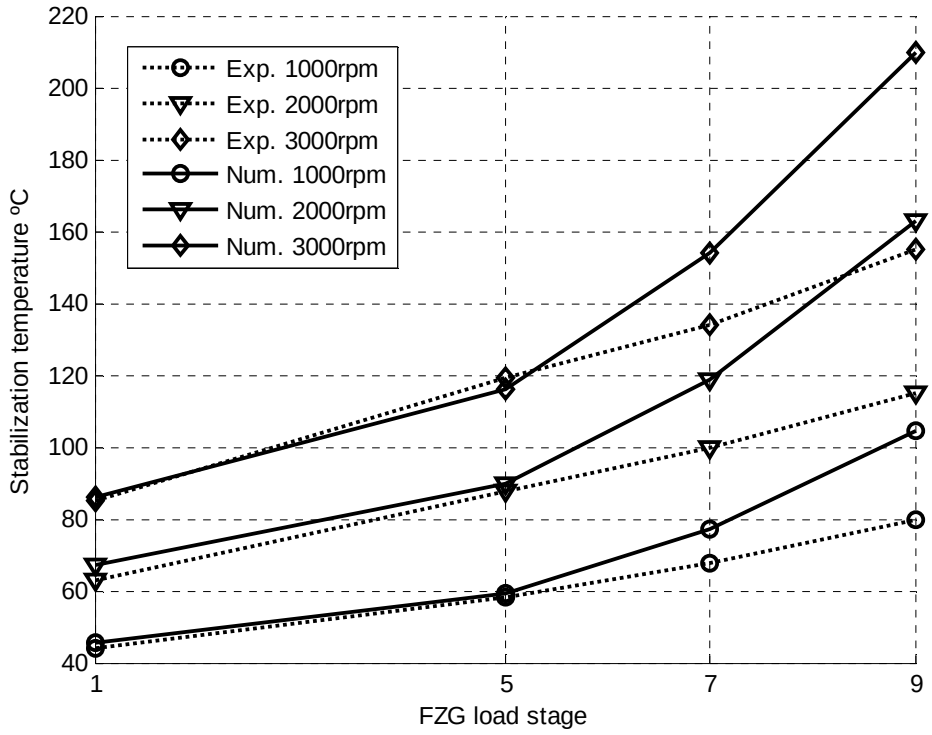


Figure 5.44 – Stabilization temperature for ester oil E2: experimental vs. numerical values (carburized gears, X_L=1).

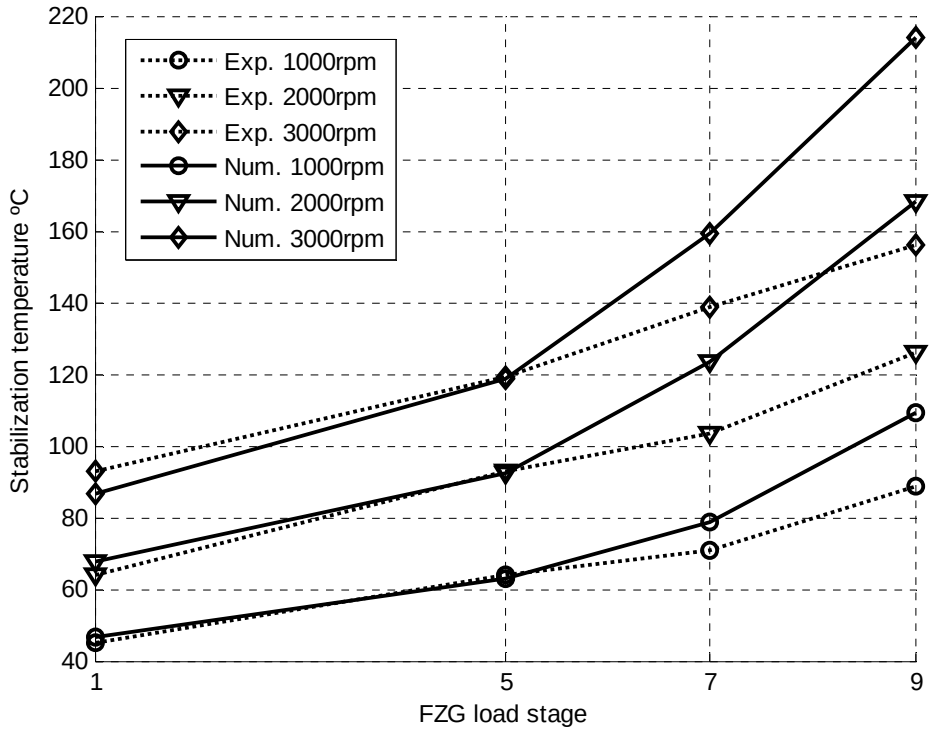


Figure 5.45 – Stabilization temperature for ester oil E3: experimental vs. numerical values (carburized gears, X_L=1).

These previous correlations indicate that the X_L parameter in the friction coefficient must be corrected, in order to take into account the type of oil (base oil and additives) and the applied load. A systematic work was performed to optimize the correlation between experimental and numerical data. The X_L parameter was optimized for the four oils, combining a constant and one, two or three variables. These variables ("***var***" in expression (5.15)) were the load - F_{bt}, the oil viscosity - η, and the rolling speed - $v_{\Sigma c}$. Basically this factor multiplies the base friction coefficient by a constant and/or modifies the exponent of each variable,

$$X_L = \frac{c}{(\mathrm{var}_1)^{c_1} \cdot \ldots \cdot (\mathrm{var}_n)^{c_n}} \tag{5.15}$$

The expression for X_L parameter that gave the best correlation for the four oils, within the range of operating conditions tested, is represented by

$$\mu_m = \frac{1}{(F_{bt}/b)^{c_1}} \tag{5.16}$$

5.5.4.2.2 High pressure nitrided gears

Figure 5.42 and Figure 5.44 show the stabilization temperatures measured during the power loss tests of high pressure nitrided gears and the corresponding numerical values, respectively for oils M1 and E2, considering the X_L parameter equal to 1. The experimental results corresponding to the nitrided gears and E2 oil at 3000 rpm were not considered because they were not conclusive as mentioned before (see chapter 5.4.2.1)

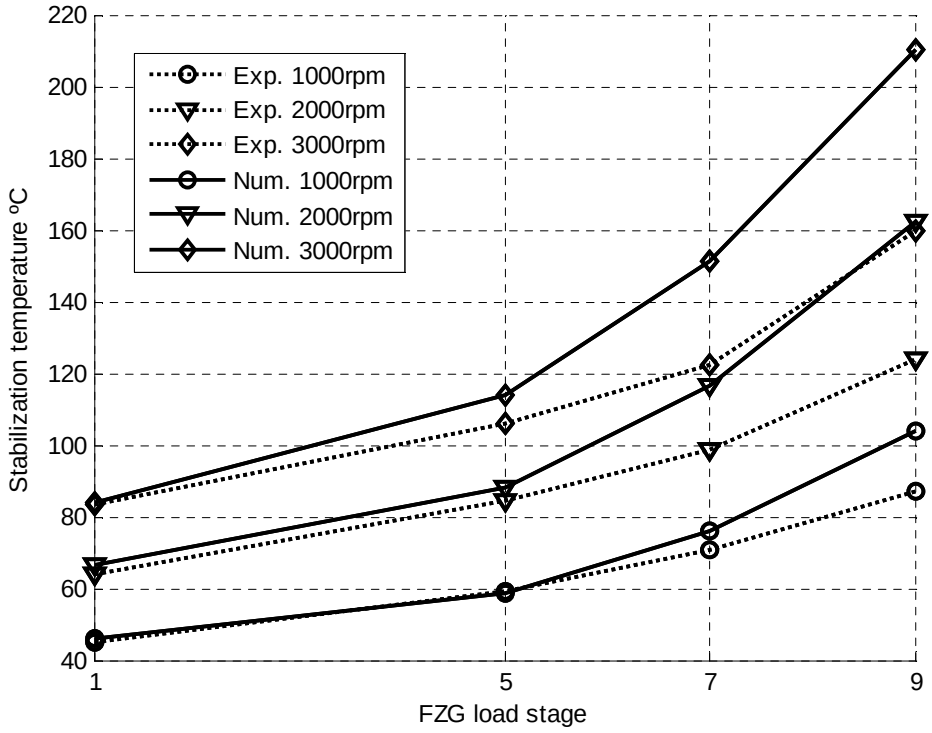


Figure 5.46 – Stabilization temperature for reference mineral oil: experimental vs. numerical values (nitrided gears, X_L=1).

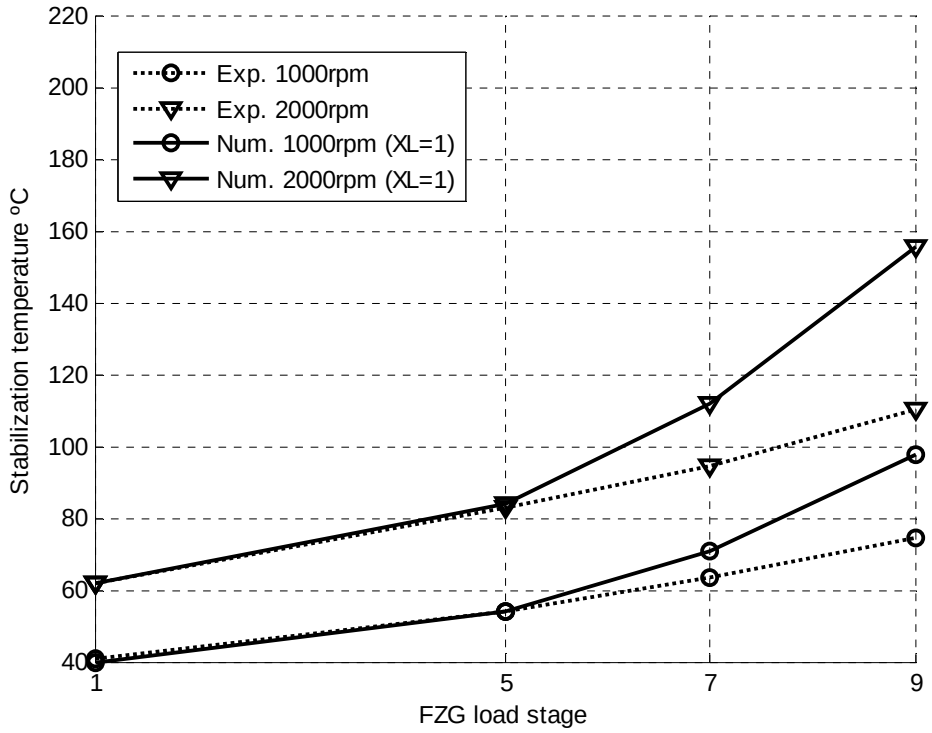


Figure 5.47 – Stabilization temperature for ester oil E2: experimental vs. numerical values (nitrided gears, X_L=1).

As for the carburized gears, the correlation between experimental and numerical stabilized temperatures of the nitrided gears is quite low. The difference between experimental and numerical values increases when the load increases. The gap at the highest load stage is above 40ºC.

As mentioned earlier, these results indicate that $\boldsymbol{X_L < 1}$ for the two oils and must be adapted to each lubricant and material, in order to take into account the presence of additives, or because the base oil has a different nature, or because materials have different friction coefficients.

These previous correlations indicate that the $\boldsymbol{X_L}$ parameter in the friction coefficient must be corrected in order to take into account the type of oil (base oil and additives), the applied load and the material. A systematic work was performed to optimize the correlation between experimental and numerical data and the $\boldsymbol{X_L}$ parameter was optimized for the two oils (M1 and E2) and for both gear materials (carburizing and nitriding steel). Once again, the expression for $\boldsymbol{X_L}$ parameter that gave the best correlation for the different combinations of lubricant and gear material was expression (5.16).

5.5.4.3 Updated friction coefficients

5.5.4.3.1 Carburized gears

The values of c_1 in expression (5.16) for the carburized gears and for each gear oil are presented in Table 5.12.

Table 5.12 – Values of c_1 of each lubricant (obtained from the tests with carburized gears).

Test ref.	**Lubricant**	c_1
C-M1	Mineral 1	0,0612
C-E1	Ester 1	0,0738
C-E2	Ester 2	0,1055
C-E3	Ester 3	0,0995

Figure 5.48, Figure 5.49, Figure 5.50 and Figure 5.51 show the experimental and numerical stabilization temperatures of the four gear oils corresponding to each load stage. The correlation factors for the calculated stabilization temperatures using the new X_L parameters are 99.60, 97.22, 98.61 and 98.72% for lubricants M1, E1, E2 and E3 respectively.

Figure 5.52 presents the numerical stabilization temperatures at each load stage for both lubricants (room temperature= 25ºC). In the first 5 load stages the four lubricants have similar stabilization temperatures. However, the ester gear oils tend to stabilize at a slightly higher temperature at 2000 and 3000 rpm due to their higher viscosities at those temperature (see Figure 1.1). From load stage K6 to load stage K10 the ester lubricants always stabilize at lower temperature (particularly, E2 and E3 esters) and the difference between them increase when of the load and the rotation speed icrease.

Figure 5.53, Figure 5.54, Figure 5.55 and Figure 5.56 show the updated friction coefficients ("Updt") calculated at the stabilization temperatures (shown in Figure 5.52) for the four oils, comparing them with the standard Michaelis expression ("Std", $X_L = 1$). The friction coefficient decreases significantly, mainly at high loads.

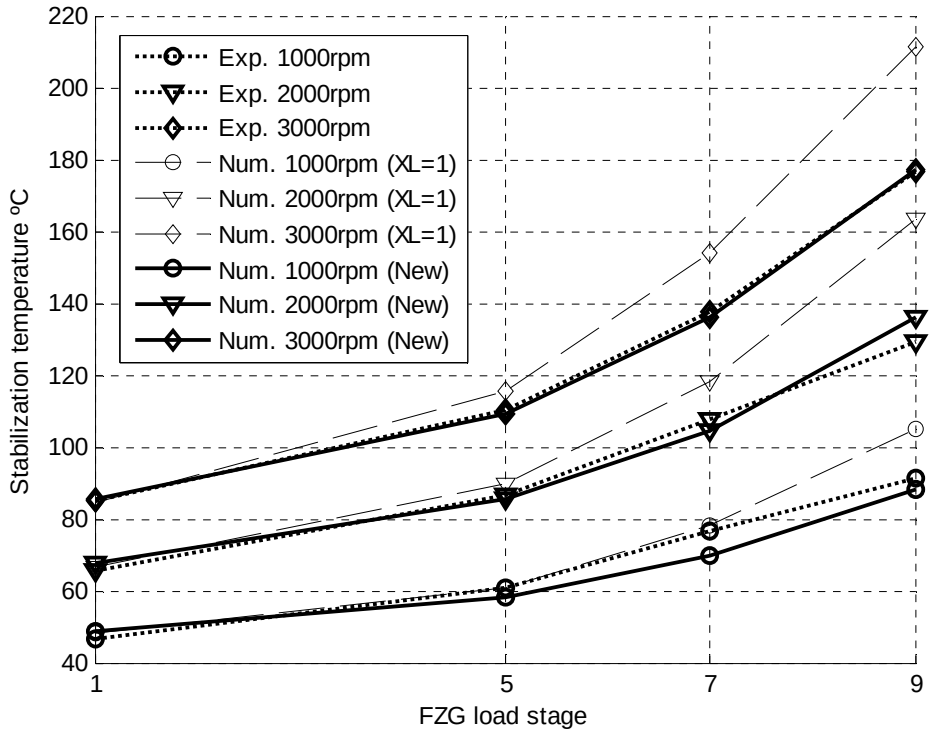


Figure 5.48 - Experimental vs. numerical stabilization temperature of the reference mineral oil, for each load stage and operating speed (carburized gears).

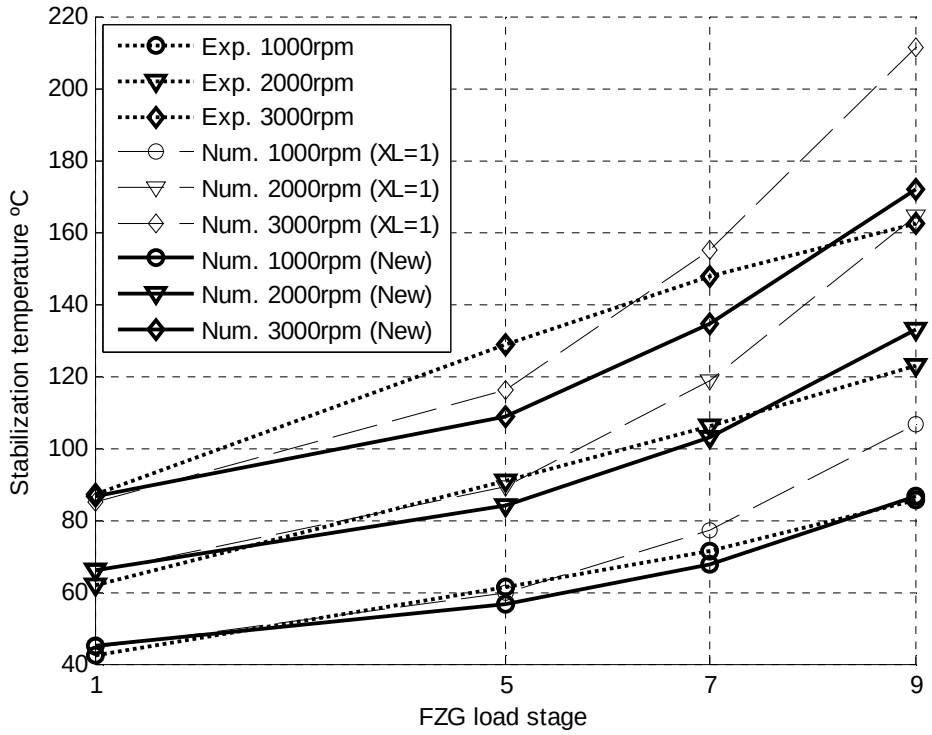


Figure 5.49 - Experimental vs. numerical stabilization temperature of the E1 ester oil, for each load stage and operating speed (carburized gears).

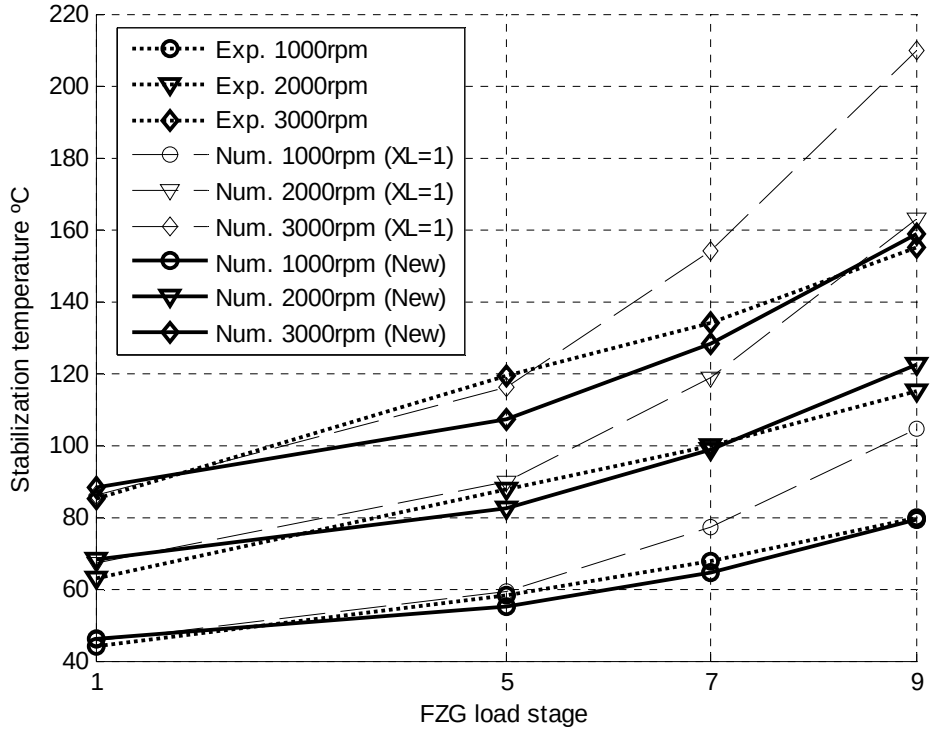


Figure 5.50 - Experimental vs. numerical stabilization temperature of the E2 ester oil, for each load stage and operating speed (carburized gears).

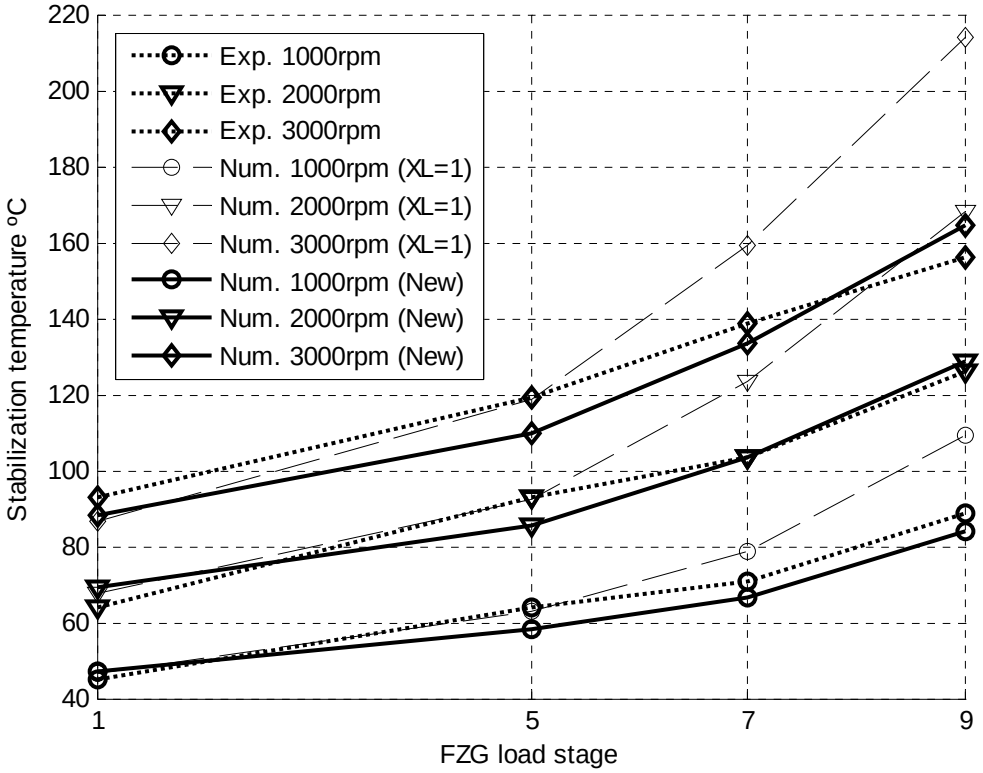


Figure 5.51 - Experimental vs. numerical stabilization temperature of the E3 ester oil, for each load stage and operating speed (carburized gears).

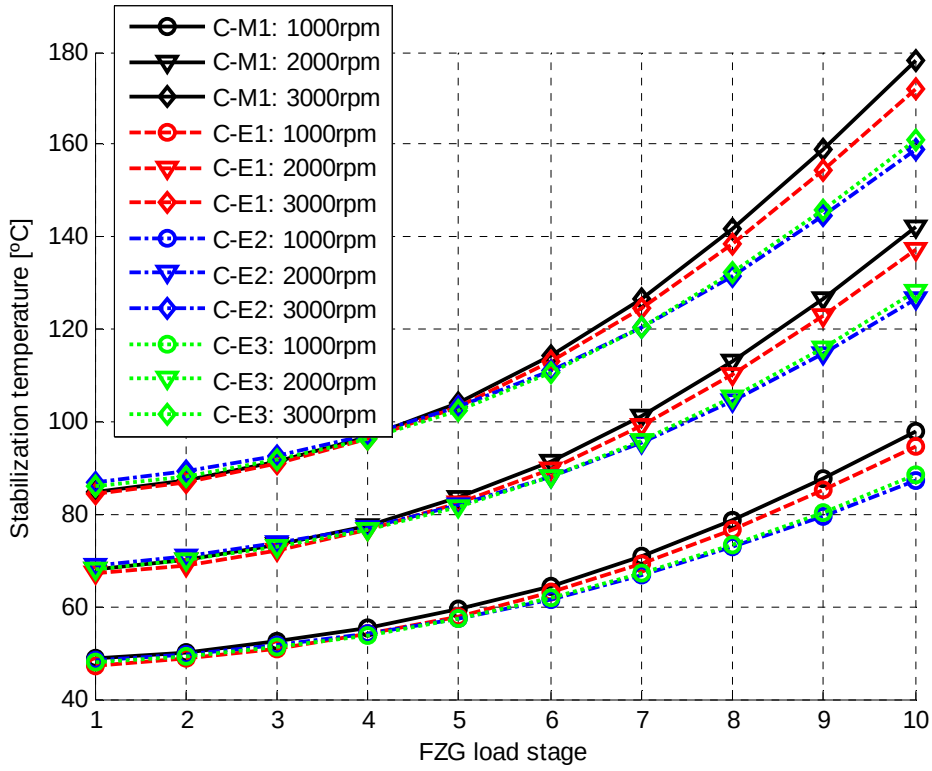


Figure 5.52 - Numerical stabilization temperature for each load stage for the four lubricants (Carburized gears; Troom=25°C).

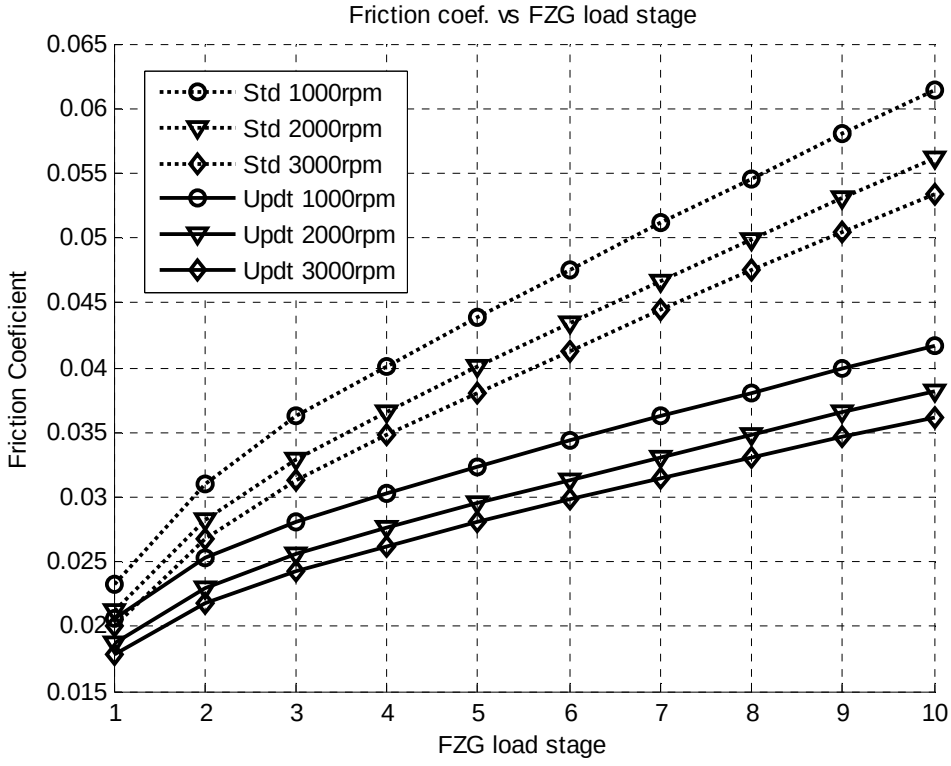


Figure 5.53 - Updated vs. Standard friction coefficient for reference mineral oil (carburized gears).

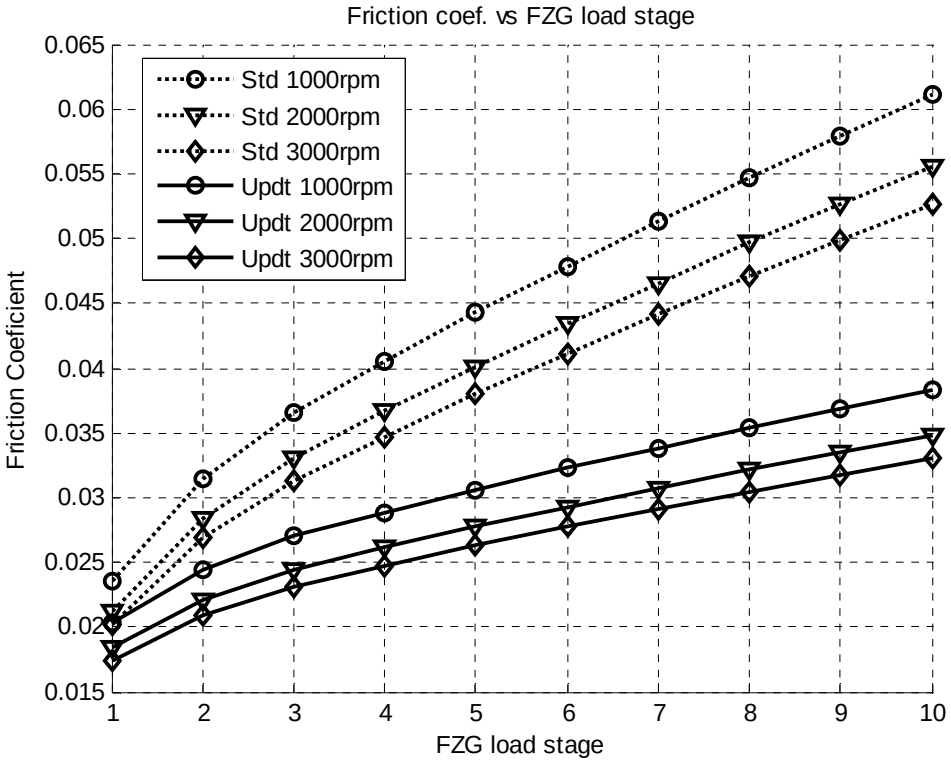


Figure 5.54 - Updated vs. Standard friction coefficient for the E1 ester oil (carburized gears).

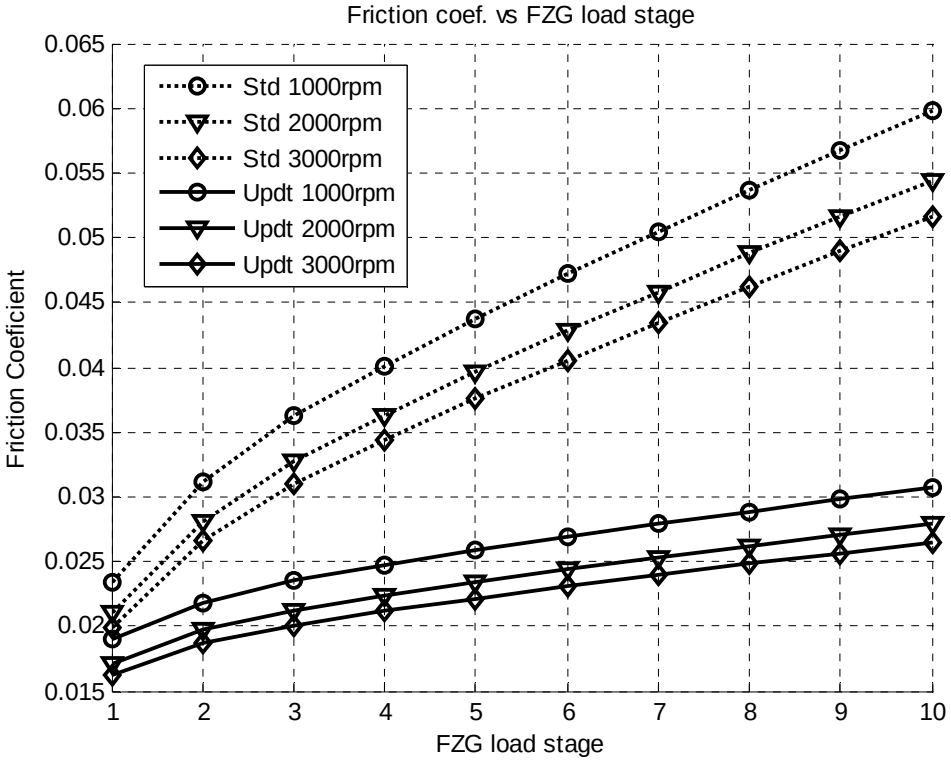


Figure 5.55 - Updated vs. Standard friction coefficient for the E2 ester oil (carburized gears).

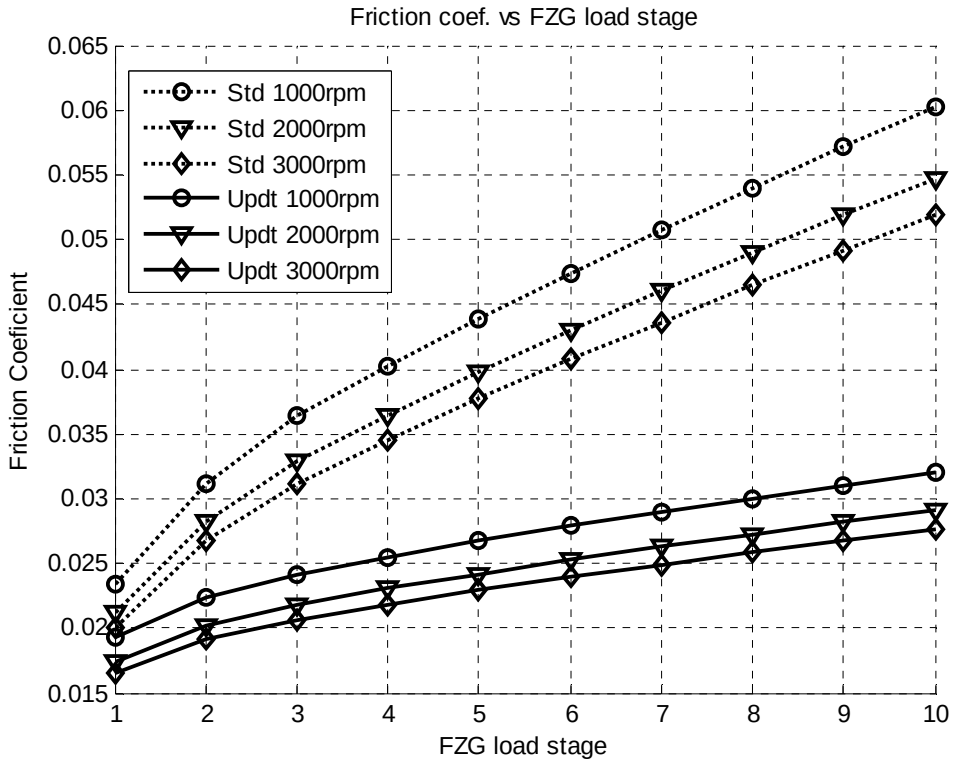


Figure 5.56 - Updated vs. Standard friction coefficient for the E3 ester oil (carburized gears).

5.5.4.3.2 High pressure nitrided gears

The values of c_1 in expression (5.16) for the high pressure nitrided gears and for lubricants M1 and E2 are presented in Table 5.13.

Table 5.13 – Values of c_1 of each lubricant (obtained from the tests of the nitrided gears).

Test ref.	**Lubricant**	C_1
N-M1	Mineral 1	0,0942
N-E2	Ester 2	0,1035

Figure 5.57 and Figure 5.58 show the experimental and numerical stabilization temperatures corresponding to each load stage, for the nitrided gears lubricated by M1 and E2 lubricants. The correlation factors for the stabilization temperatures using the new X_L parameters are 99.43 and 99.06% for lubricants M1 and E2, respectively.

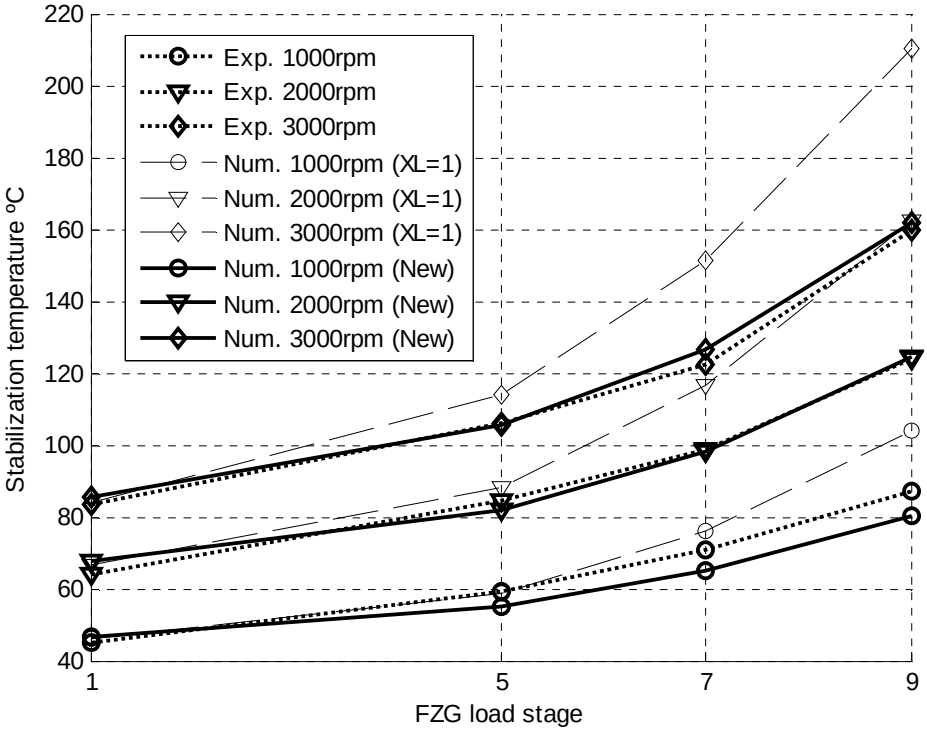


Figure 5.57 - Experimental vs. numerical stabilization temperature of the reference mineral oil, for each load stage and operating speed (nitrided gears).

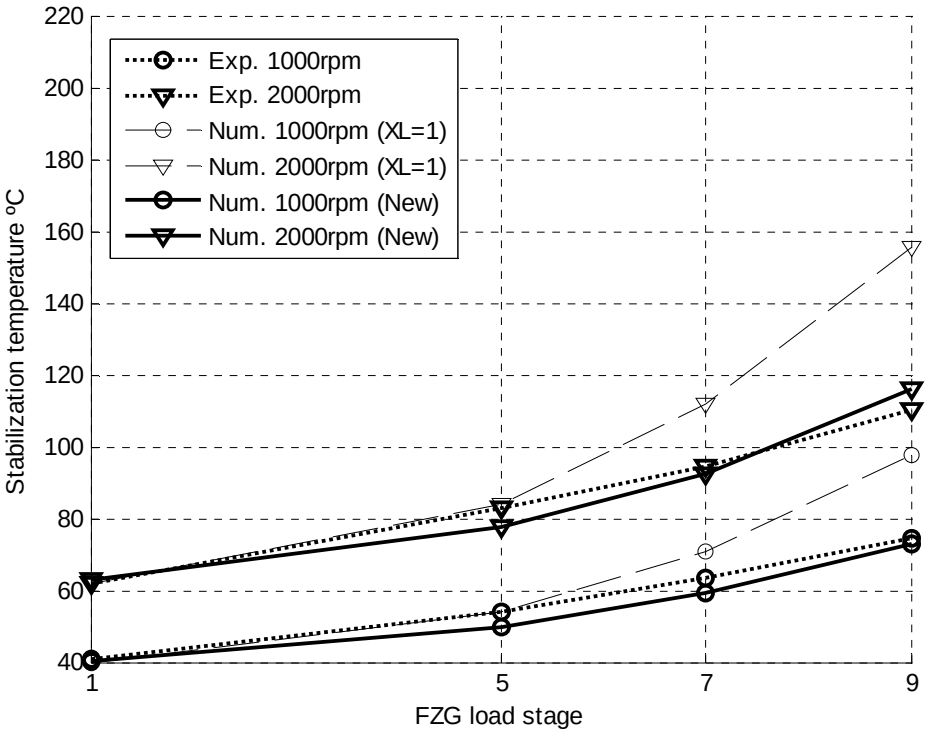


Figure 5.58 - Experimental vs. numerical stabilization temperature of the E2 ester oil, for each load stage and operating speed (nitrided gears).

Figure 5.59 presents the numerical stabilization temperatures at each load stage for lubricants M1 and E2 and for both gear materials (room temperature= 25ºC). When lubricating the nitrided gears, both lubricants display very similar stabilization temperatures.

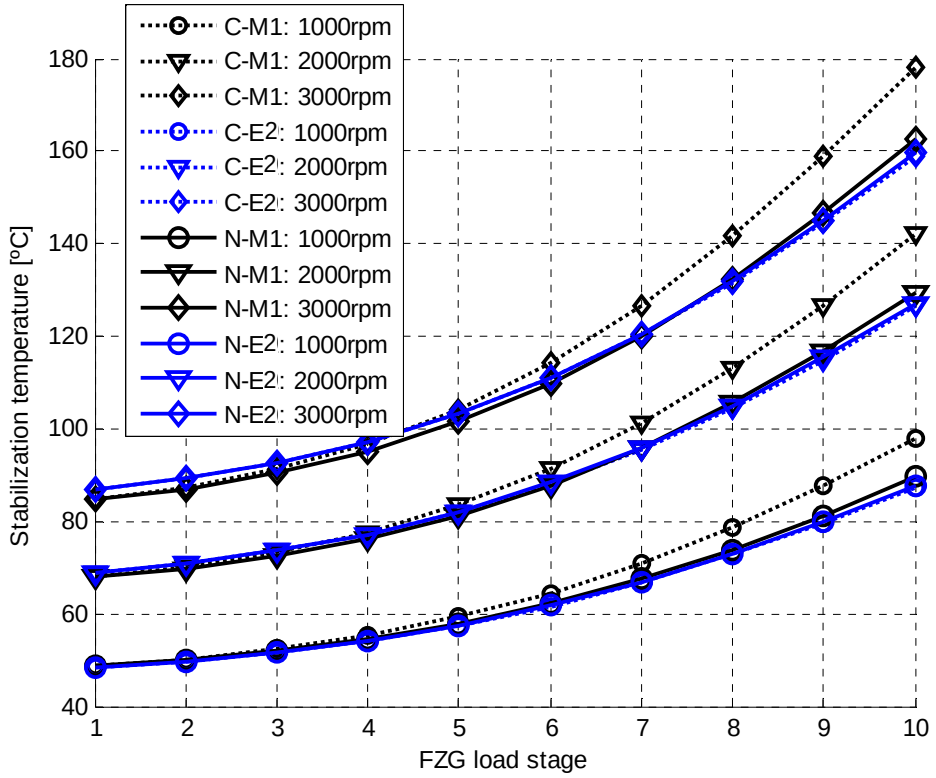


Figure 5.59 - Numerical stabilization temperature for each load stage for the lubricants M1 and E2 (carburized gears and nitrided gears; Troom=25ºC).

Figure 5.59 show that the stabilization temperature of the mineral oil when lubricating nitrided gears are significantly lower than when carburized gear are used. The difference between temperatures corresponding to the two gear materials increase with the increasing load. On the other hand, temperatures corresponding to the ester oil E2 are very similar for both materials, indicating that the operating temperature of this lubricant at the different load stages is not influenced by the gear material (unlike it happens with mineral lubricant).

Figure 5.60 and Figure 5.61 show the updated friction coefficients ("Updt") calculated at the stabilization temperatures (shown in Figure 5.59) for the two oils, comparing them with the standard Michaelis expression ("Std", $X_L = 1$). The friction coefficient decreases significantly, mainly at high loads.

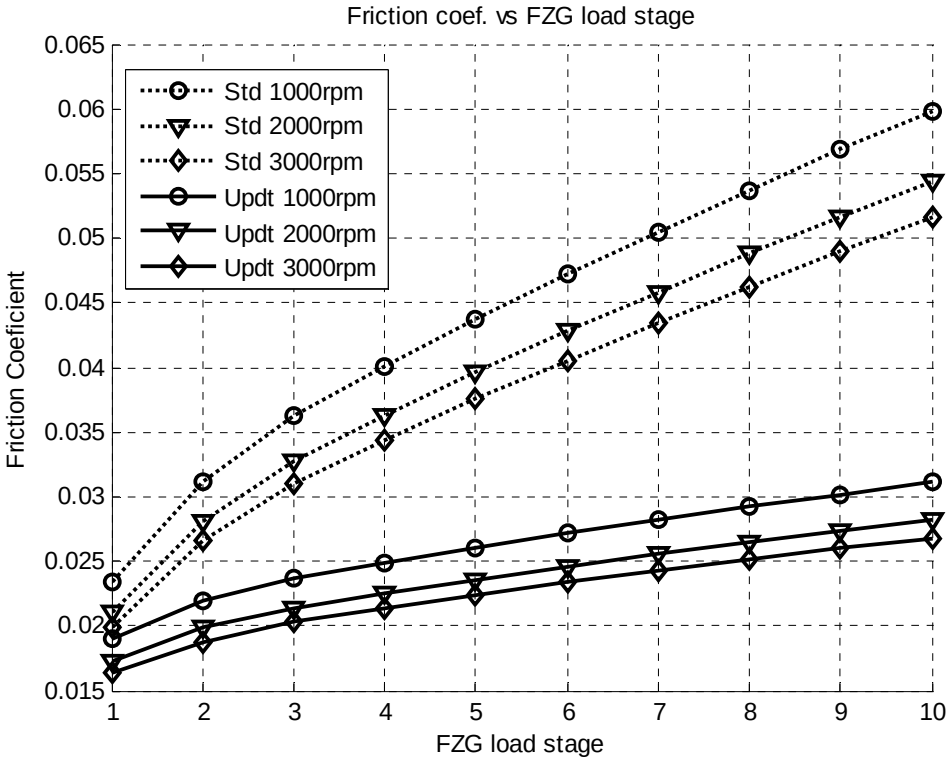


Figure 5.60 - Updated vs. Standard friction coefficient for reference mineral oil (nitrided gears).

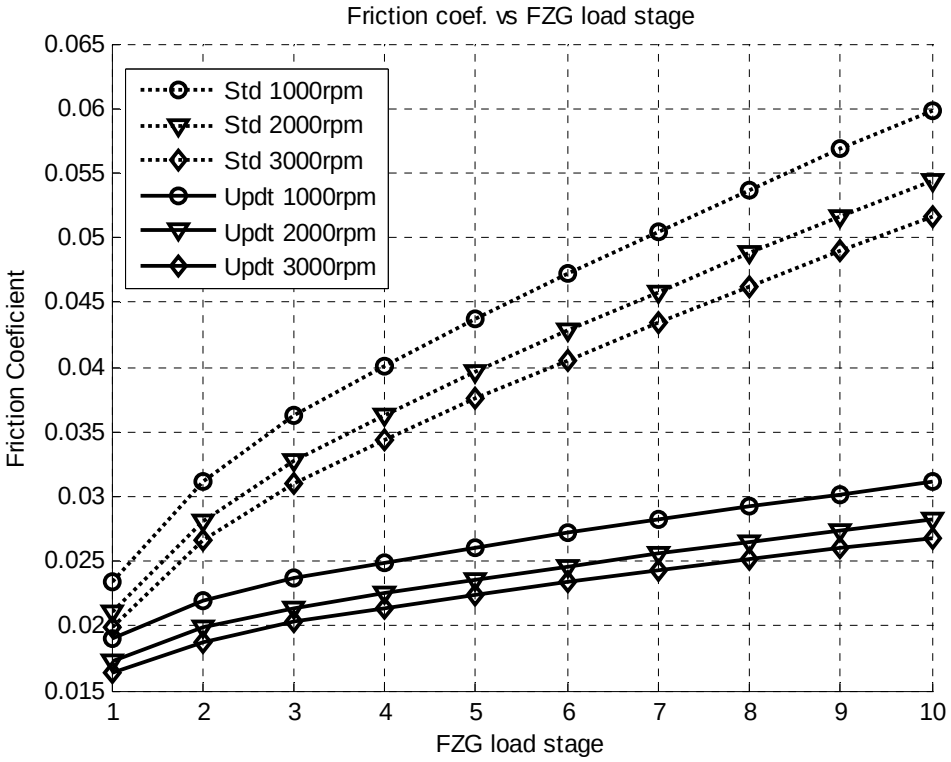


Figure 5.61 - Updated vs. Standard friction coefficient for the E2 ester oil (nitrided gears).

5.5.4.4 Friction coefficient comparison

All tested oils promote a significant reduction of the friction coefficient in comparison to a standard additive free mineral oil. The friction coefficient expressions for the mineral and ester lubricants are given by the following expression:

$$\mu_m = 0.048.\left(\frac{F_{bt}/b}{\upsilon_{\Sigma c}.\rho_c}\right)^{0.2}.\eta_{oil}{}^{-0.05}.Ra^{0.25}.\frac{1}{\left(F_{bt}/b\right)^{c_1}} \qquad (5.17)$$

The values of c_1 corresponding to each are shown in Table 5.12 and Table 5.13, for carburized gears and high pressure nitrided gears, respectively.

5.5.4.4.1 Carburized gears

The comparison between the four lubricants clearly shows that ester oils allow smaller friction coefficients than the reference mineral oil, as shown in Figure 5.62. This difference is shown in Figure 5.63 where the friction reduction promoted by the ester oils increases with the increasing temperature and contact pressure. For contact pressures above 0.8 GPa (load stage k5 and following) the friction reduction was an 5%, 17% and 20% with esters E1, E3 and E2, respectively. This difference in friction coefficient is directly reflected in the power loss due to teeth friction, which is the most relevant form of heat generation at higher loads in the FZG test box, as it will be shown in the following paragraphs.

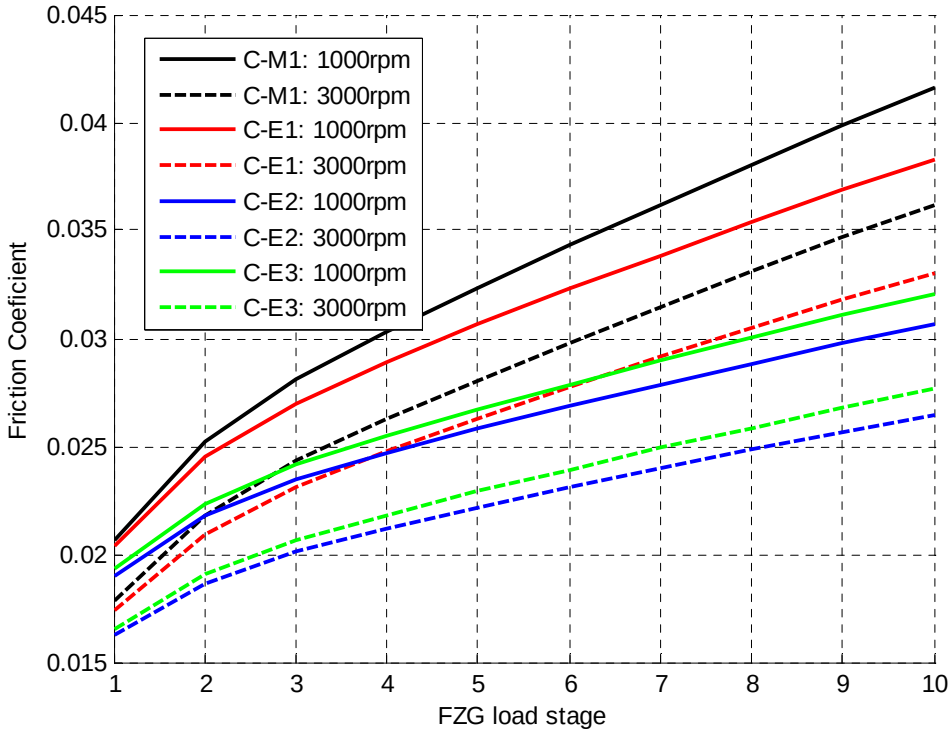


Figure 5.62 - Friction coefficient at stabilization temperatures with carburized gears.

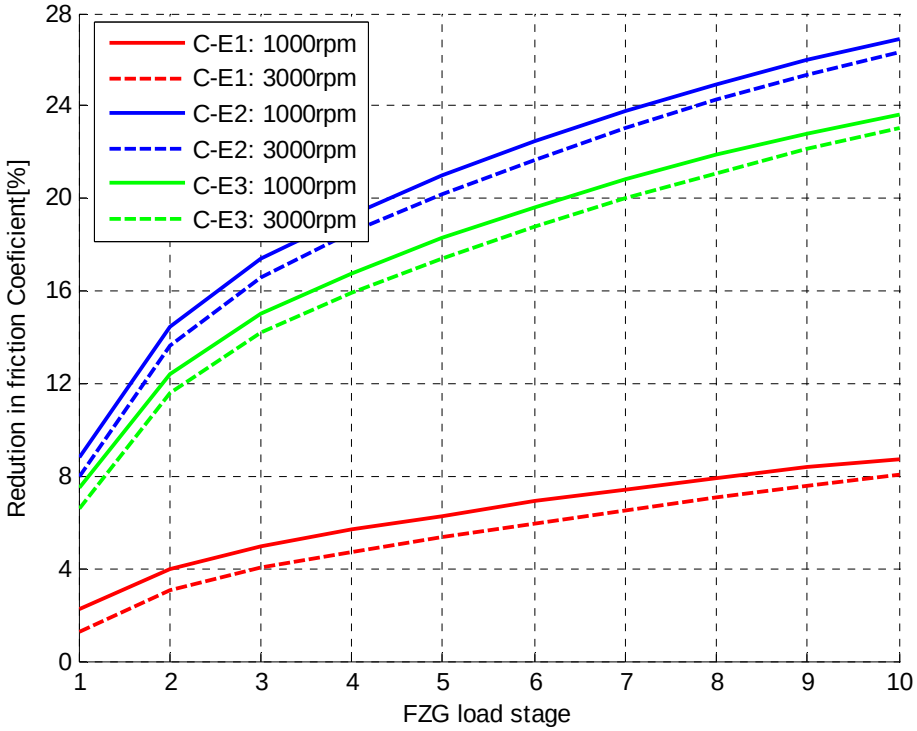


Figure 5.63 - Friction coefficient reduction at stabilization temperatures provided by the ester oils in comparison to the reference mineral oil with carburized gears at stabilization temperatures.

Figure 5.64, Figure 5.65, Figure 5.66 and Figure 5.67 present the power loss distribution of the mineral and esters oils, for each FZG load stage (at stabilization temperatures – see Figure 5.52; room temperature= 25ºC; wheel speed =2000 rpm). The gear churning losses (P_{spl}) are the most important mechanism of power loss at low torque (48 % - 50% in FZG load stage k1), while the gear friction losses (P_{fr}) are the most relevant mechanism of power loss at high torque (68 % - 76% in FZG load stage k10), whatever the lubricant considered. The power loss due to the rolling bearings and seals is very similar for the four lubricants, decreasing in percentage of the overall power loss as the torque increases.

The power losses associated with each lubricant are compared in Figure 5.68, for a wheel speed of 2000 rpm and at stabilization temperatures, showing that the power losses in the bearings and the churning losses in the gears are very similar for the four gear oils. The major difference in power loss is related to the friction power loss between gear teeth, which is significantly smaller in the case of the ester oil, mainly at high torque.

The seal losses have the same value for the four oils, since the model only depends on the speed and seal diameter.

Figure 5.69 presents the global efficiency of FZG test gearbox for the four lubricants at different load stages and at two different speeds. The evolution of the global efficiency is very similar for the four oils. However, the biodegradable lubricants display a slightly better global efficiency for higher loads.

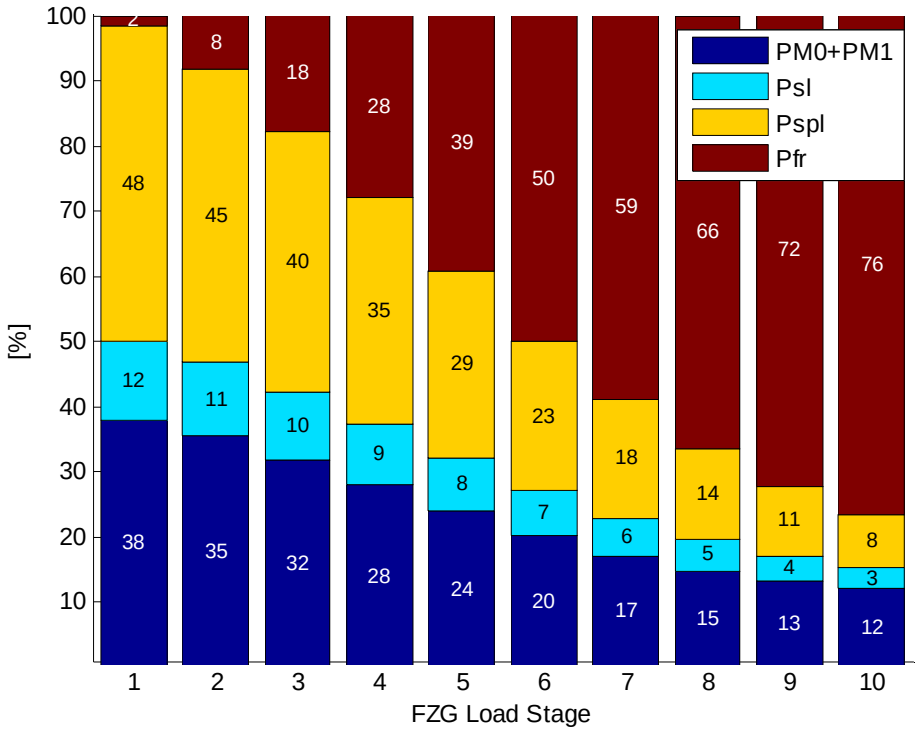


Figure 5.64 - Power losses distribution as function of load at 2000 rpm for reference mineral oil (M1) with carburized gears and at stabilization temperatures.

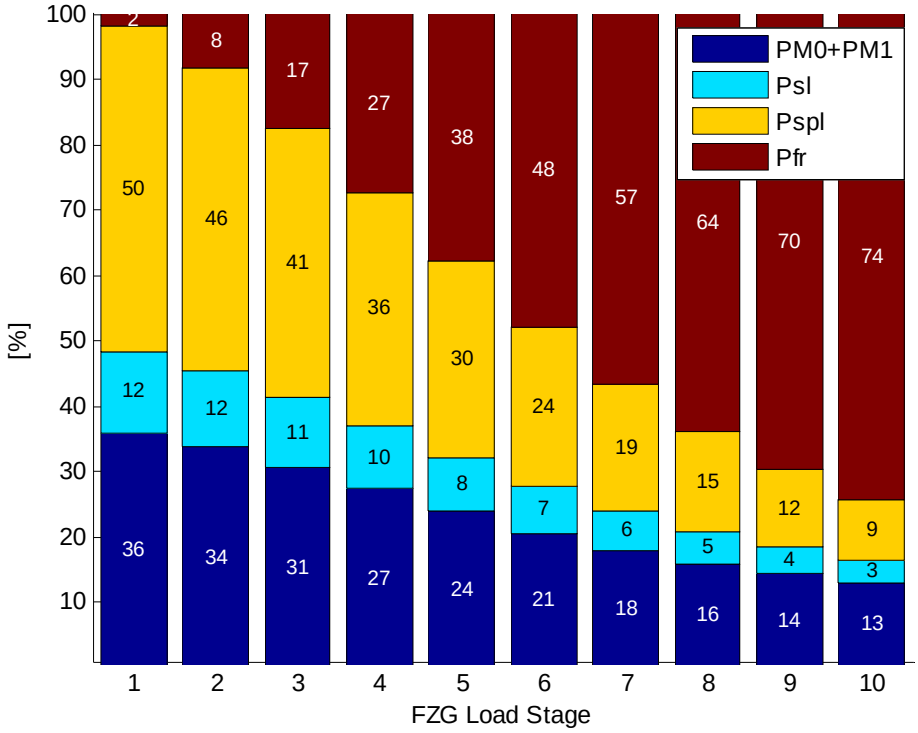


Figure 5.65 - Power losses distribution as function of load at 2000 rpm for Ester E1 with carburized gears and at stabilization temperatures.

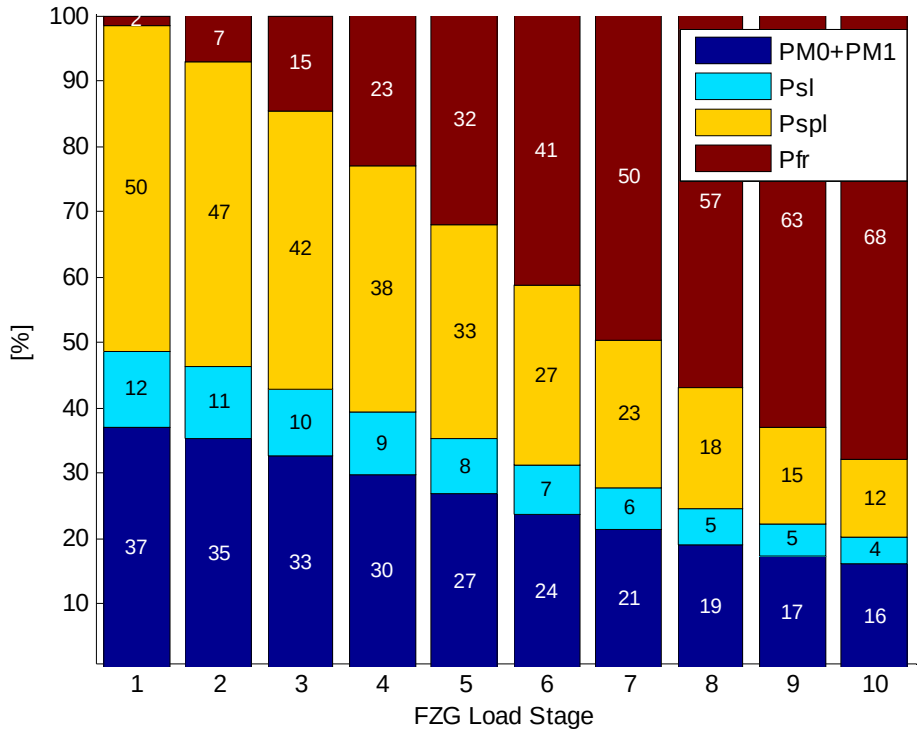


Figure 5.66 - Power losses distribution as function of load at 2000 rpm for Ester E2 with carburized gears and at stabilization temperatures.

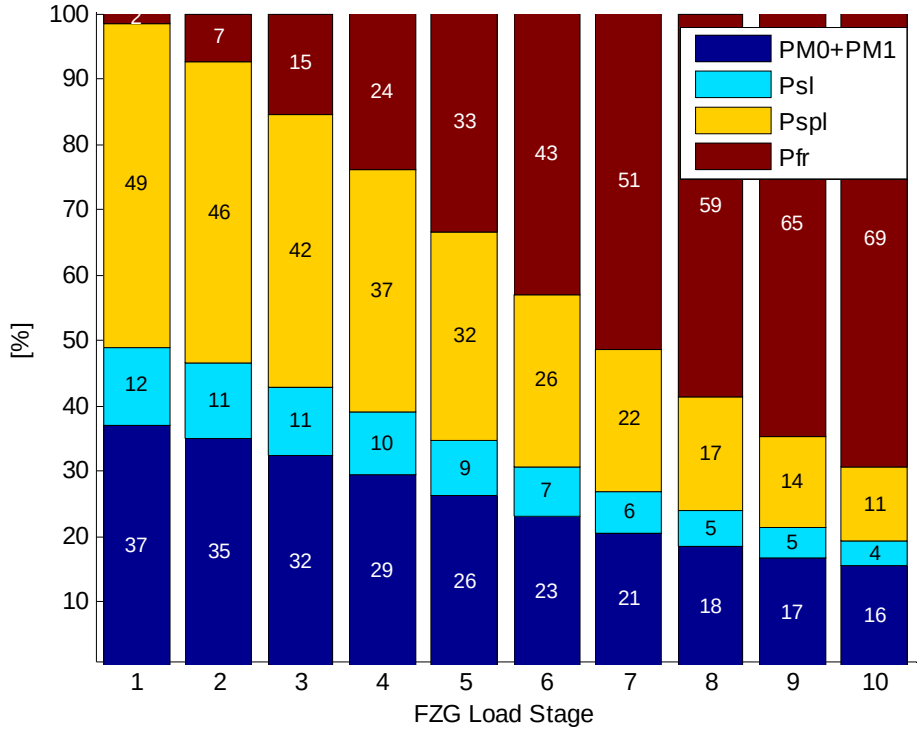


Figure 5.67 - Power losses distribution as function of load at 2000 rpm for Ester E3 with carburized gears and at stabilization temperatures.

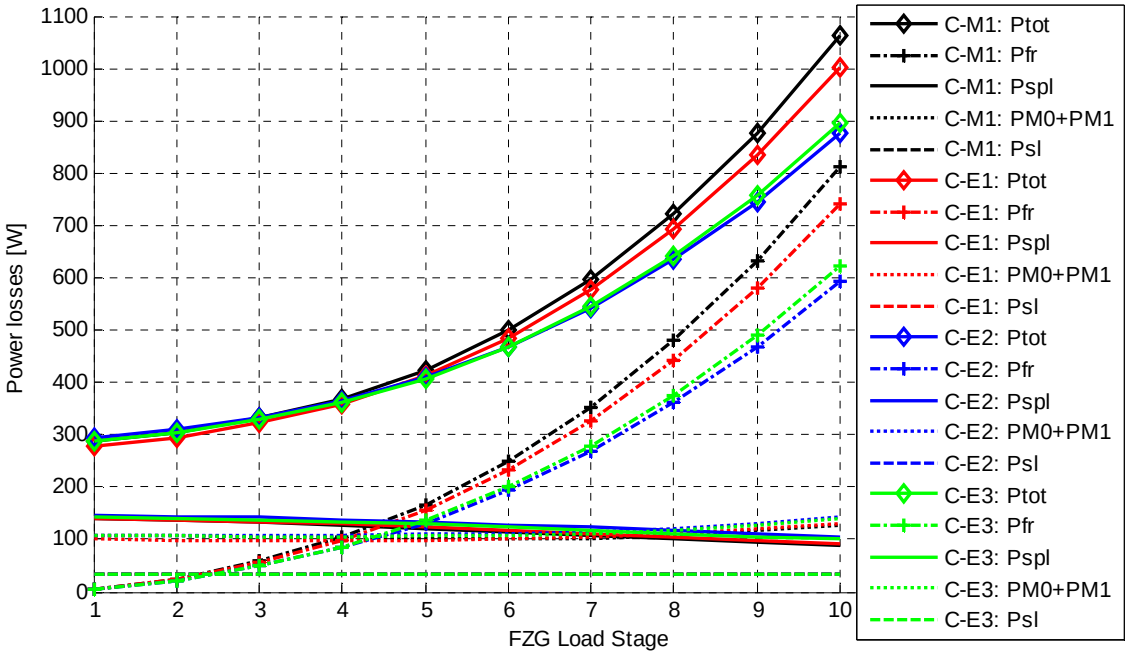


Figure 5.68 - Power losses as function of load at 2000 rpm and with carburized gears at stabilization temperatures.

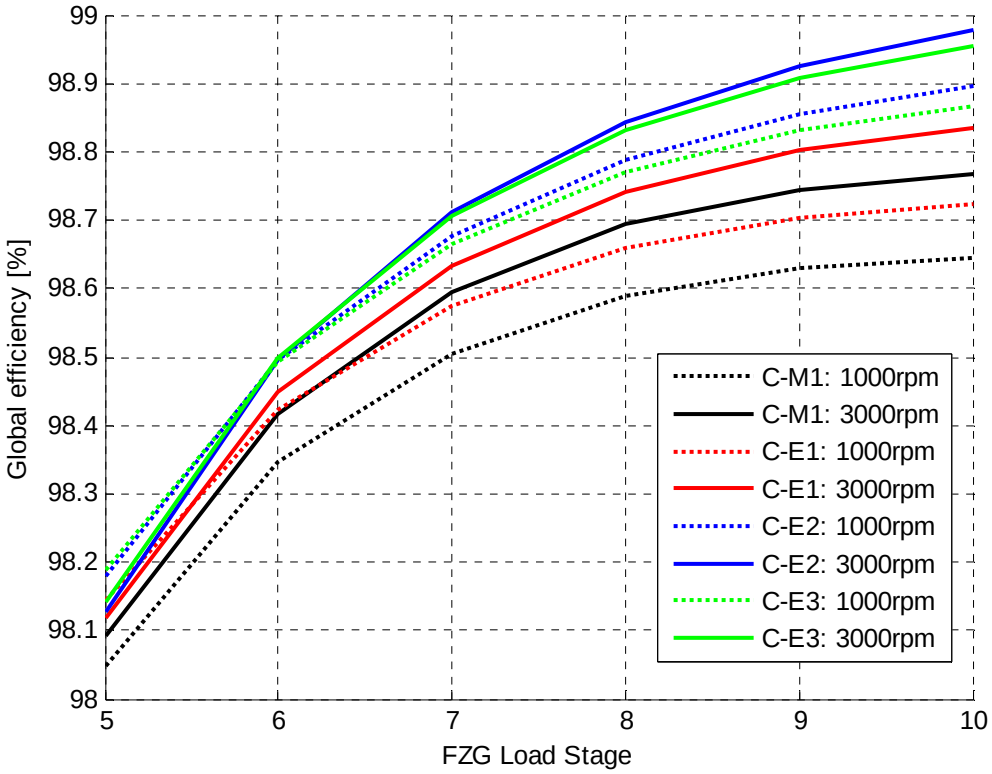


Figure 5.69 – Global efficiency vs FZG Load stage (with carburized gears at stabilization temperatures).

5.5.4.4.2 High pressure nitrided gears

Figure 5.70 displays the friction coefficients of M1 and E2 gear oils when lubricating the carburized and the high pressure nitrided gears. This figure manifestly demonstrates that the friction coefficient of ester E2 is smaller than the one of mineral oil M1 (for both gear materials). It also shows that friction coefficient of the ester is not affected by gear material, while the one of mineral gear oil is significantly smaller for nitrided gears, when compared to the carburized ones.

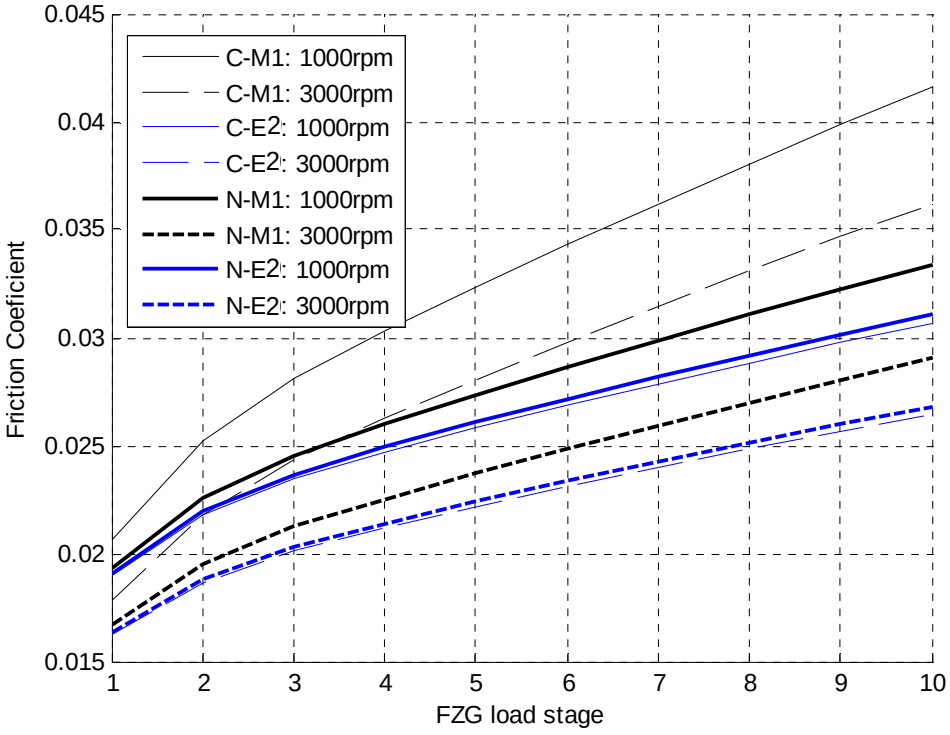


Figure 5.70 - Friction coefficient at stabilization temperatures of nitrided and of carburized gears.

This difference in friction coefficient is presented in Figure 5.71, showing that the friction reduction promoted by each combination of material-lubricant in relation to the carburized gear lubricated by the mineral oil. The reduction in friction coefficients increases with the load.

For contact pressures higher than 0.8 GPa (load stage k5 and following) the friction reduction was above 19% with esters E1 and above 15% for the nitrided gears lubricated by the mineral oil. This difference in friction coefficient is directly reflected in the power loss due to teeth friction, which for the higher loads is the most relevant form of heat generation in the FZG test box.

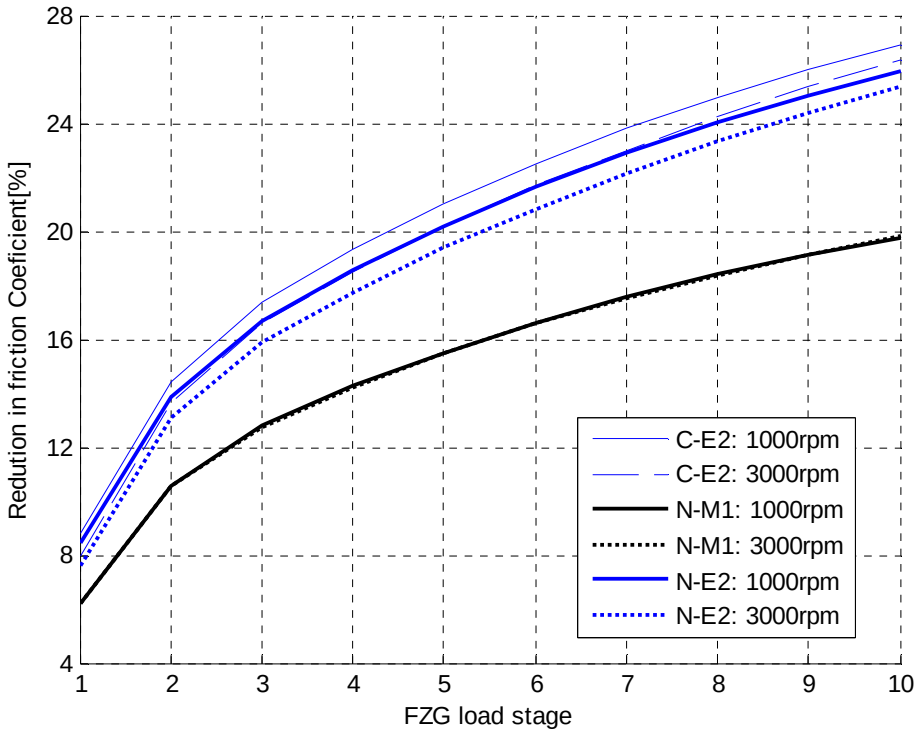


Figure 5.71 - Friction coefficient reduction at stabilization temperatures provided by the E2 ester oil with both materials and by the mineral oil with the nitrided steel in comparison to the mineral oil with the nitrided and the carburized gears (at stabilization temperatures).

Figure 5.72 and Figure 5.73 present the power loss distribution of the mineral oil and ester E2, for each FZG load stage (at stabilization temperatures – see Figure 5.59; room temperature= 25ºC; wheel speed =2000 rpm). The gear churning losses (P_{spl}) are the most important mechanism of power loss at low torque (48 % - 50% in FZG load stage k1), while the friction losses (P_{fr}) are the most relevant mechanism of power loss at high torque (68 % - 71% in FZG load stage k10). The power loss due to the rolling bearings and seals is very similar for both lubricants, decreasing in percentage of the overall power loss as the torque increases.

The power losses associated with both lubricants (M1 and E2) are compared in Figure 5.74, for a wheel speed of 2000 rpm and at stabilization temperatures, showing that the power losses in the bearings and the churning losses of gears are very similar for both oils. The major difference in power loss is related to the friction power loss between gear teeth, which are significantly smaller in the case of the ester oil, mainly at high torque. The seal losses have the same value for both gear oils, since the model only depends on the speed and seal diameter.

Figure 5.75 presents the global efficiency of FZG test gearbox for the carburized and nitrided gears lubricated with M1 and E2 lubricants at different load stages at two different speeds. The evolution of the global efficiency is very similar for the E2 ester, lubricating carburized and nitrided gears, and for the reference mineral lubricant and nitrided gears. The carburized gear lubricated with the mineral oil displayed a slightly worse global efficiency.

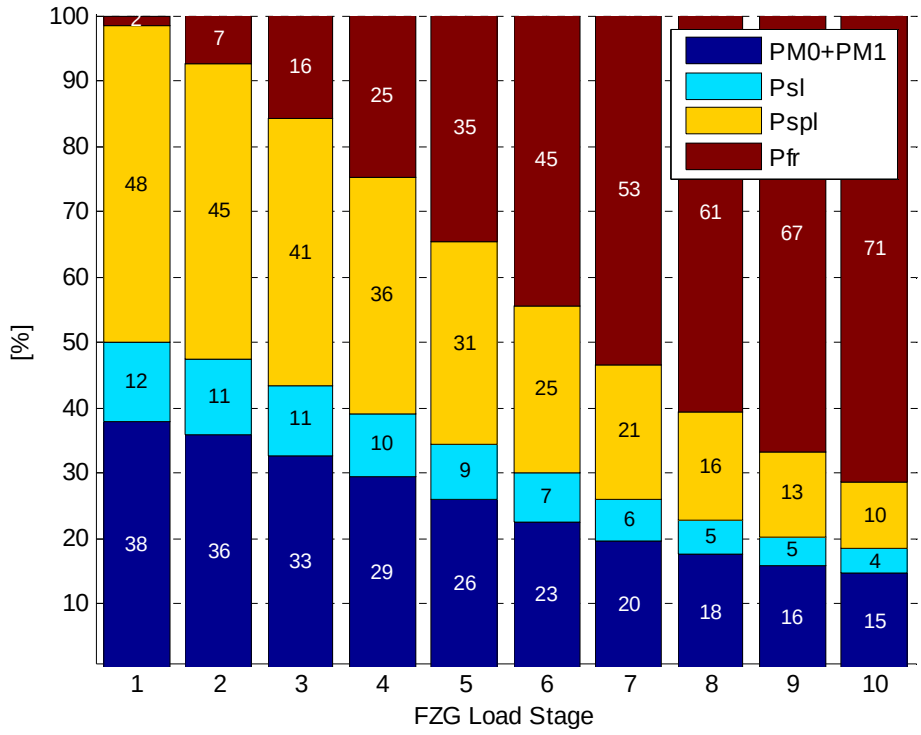


Figure 5.72 - Power losses distribution as function of load at 2000 rpm for reference mineral oil (M1) with nitrided gears (at stabilization temperatures).

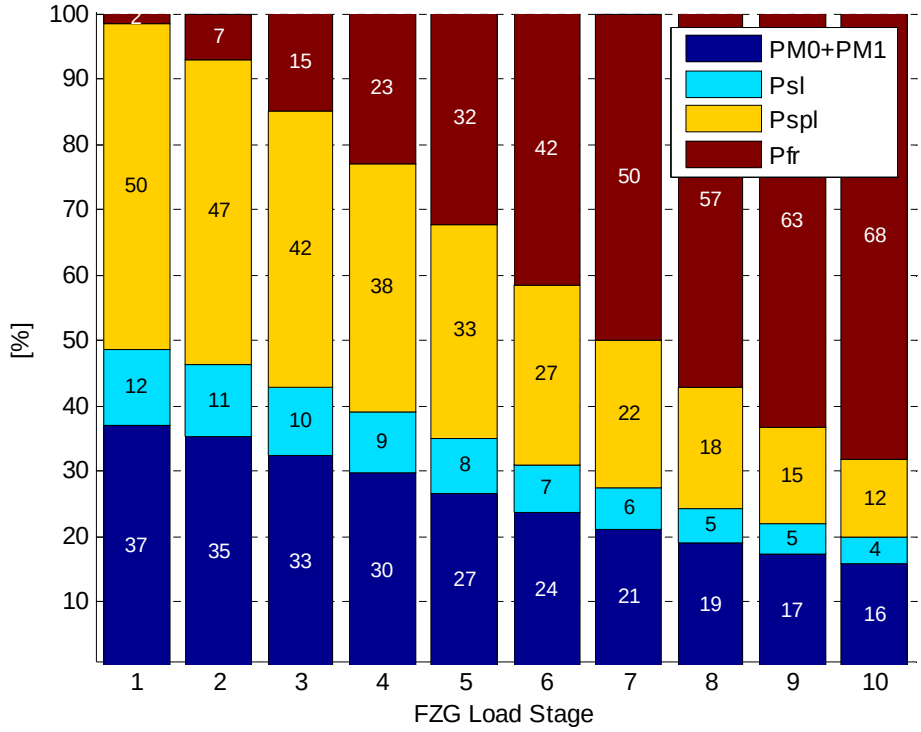


Figure 5.73 - Power losses distribution as function of load at 2000 rpm for Ester E2 with nitrided gears (at stabilization temperatures).

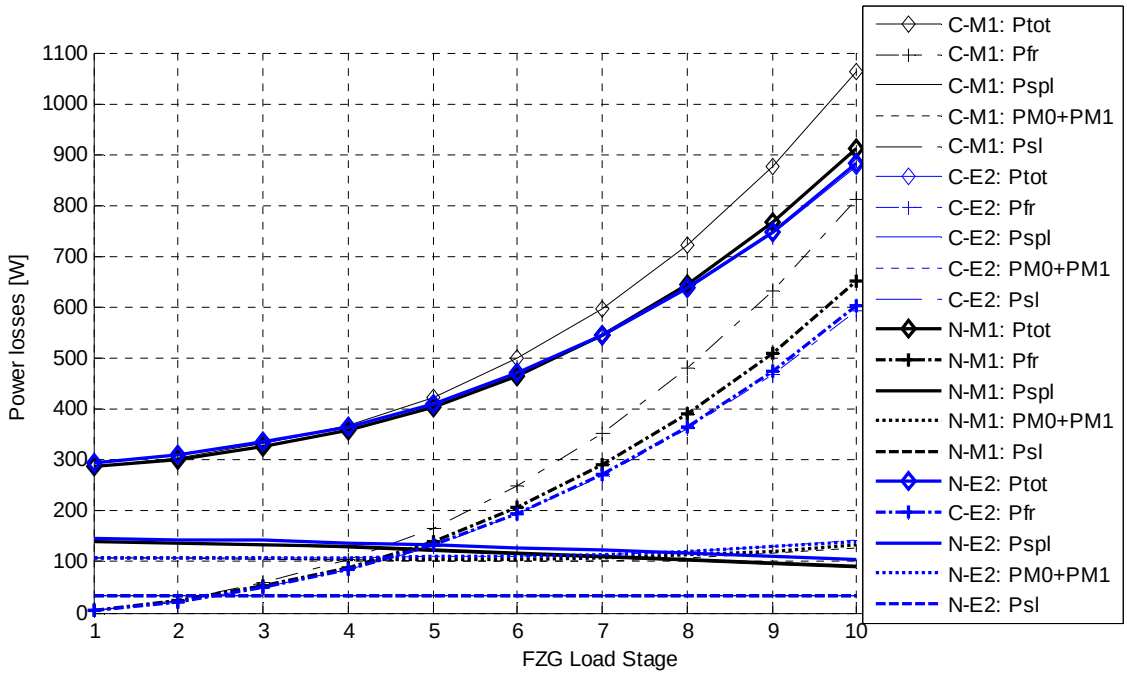


Figure 5.74 - Power losses as a function of load at 2000 rpm and with nitrided of the carburized gears at stabilization temperatures.

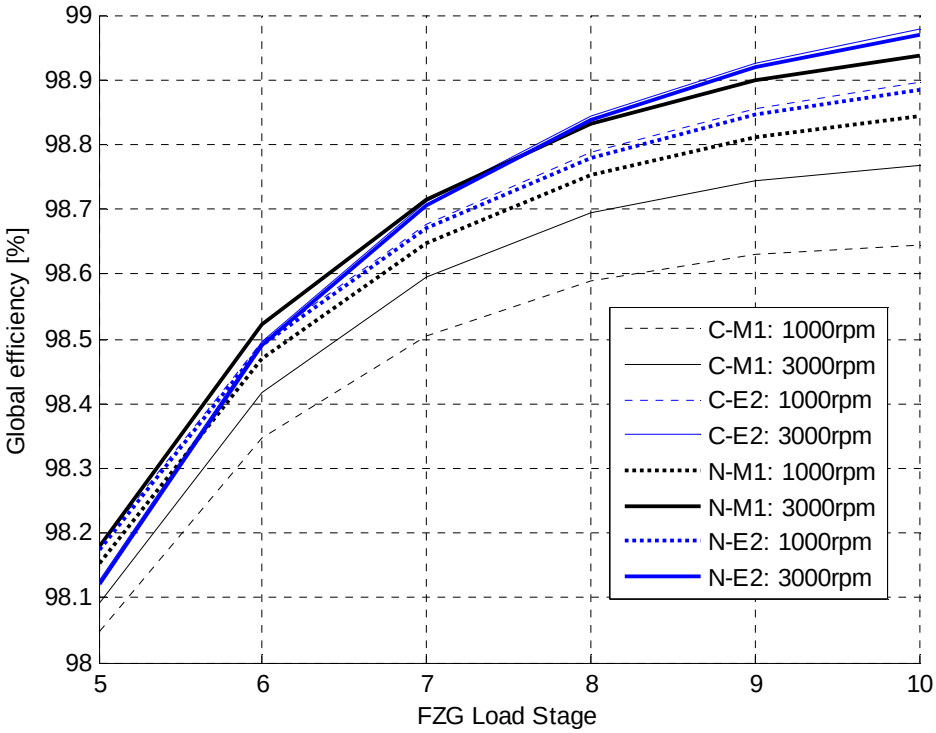


Figure 5.75 - Global efficiency vs FZG Load stage (of the nitrided and the carburized gears at stabilization temperatures).

5.6 Conclusions on FZG gear power loss tests

The main conclusions from the FZG gear power loss tests are:

- ✓ Power loss tests of carburized gears:
  - o The E2 ester oil promotes much less wear than the other three gear oils (86% reduction of mass loss in comparison with the reference oil). Mass loss promoted by ester oil E3 is slightly lower than the one promoted by the reference mineral oil (reduction of 2%);
  - o The evolution of the wear particle indexes of M1, E1 and E3 lubricants is similar, indicating that wear promoted by those lubricants doesn't vary significantly. All the wear particle indexes are significantly smaller for the E2 biodegradable ester. In relation to the reference fluid (M1), E2 oil generates less wear particles: DL- 45% less, DS- 27% less, CPUC- 42% less and ISUC- 70% less;
  - o The E3 ester creates a smoothing effect on surfaces.

- ✓ Power loss tests of high pressure nitrided gears:
  - o Ester E2 also promotes much less wear than the reference oil when lubricating the nitrided gears (reduction of 59% of mass loss). It also generates less wear particles: DL and CPUC- less 38%, DS- less 35% and ISUC- less 61%.

- ✓ Power loss model of FZG gear box:
  - o The proposed model simulates adequately the heat balance inside the FZG test gear box, for the operating conditions considered, allowing the evaluation of the most important forms of power loss and heat evacuation;
  - o Friction coefficients calculated for the four lubricants are significantly smaller than those predicted by Michaelis equation for an additive free mineral oil. In the case of the M1 mineral oil the friction coefficient is influenced by gear material.
  - o Power losses due teeth friction at FZG load stage 10 represent more than 68% of the total power losses (at 2000 rpm) and are reduced from 812W (reference oil M1) to 595W (E2 ester, less 27%). In comparison to the carburized gears lubricated by mineral oil, teeth friction losses are 651W with N-M1 (less 20%), 742W with C-E1 (less 9%), 595W with C-E2 (less 27%), 603W with N-E2 (less 26%) and 621W with C-E3(less 24%);
  - o For the highest loads, the esters and the mineral oils used with nitrided gears have a slightly better global efficiency than when carburized gears are lubricated with the reference mineral oil.

- ✓ Friction coefficients:
  - o Ester oils have a friction coefficient 5% to 20% smaller (E1 and E2 fluids, respectively) than the reference mineral oil M1, when lubricating carburized gears under contact pressures higher than 0.8 GPa;
  - o Mineral oil and nitrided gear result in a smaller friction coefficient than when carburized gears are used (similar to that of ester oils E2 and E3);
  - o The friction coefficient of the E2 ester oil is almost the same with both gear materials;
  - o The friction coefficient reduction provided by the esters and by the nitrided steel, in relation to the mineral oil tested with the carburized gears increases when the temperature increases, mainly with the increasing contact pressure.

- ✓ Stabilization temperatures
  - o Stabilization temperature is similar for both lubricants operating at low loads (pinion torque up to 48 N.m);
  - o E2 lubricant has the lowest stabilization temperature operating with carburized gears at higher loads (pinion torque higher than 48 Nm), followed by ester E3. The operating temperature of the ester E1 is slightly lower than the one of the mineral oil, witch is always higher. The difference increases with the increase of the input power (increase of load and/or increase of rotation speed;
  - o The E2 ester oil have similar operation temperatures when lubricating both gear materials;
  - o Mineral oil has a lower stabilization temperature when nitrided gears are used instead of carburized ones (similar to esters E2 and E3).

CHAPTER 6

6 DISCUSSION AND CONCLUSIONS

6.1 Discussion

6.1.1 Four ball wear tests

The Four-Ball wear test results indicate that the best results concerning to wear preventive properties were achieved by E2 biodegradable lubricant. The Lubricants M1 and E1 displayed similar behaviour in wear protection, slightly below gear oil E2. These tests also showed that beside the anti-wear additives, lubricant film thickness (related to lubricant viscosity and piezoviscosity) may have some influence on contact wear [21, 22].

6.1.2 FZG gear scuffing tests

The gear scuffing test results indicate that the ester based biodegradable and non-toxic gear oils (E1 and E2) presented several advantages compared to the reference mineral oil in terms of gear scuffing load carrying capacity: higher FZG scuffing load stage in test FZG A20/16.6/90, the same FZG scuffing load stage in test FZG in test FZG A10/16.6/90 and higher critical oil bath temperatures. Globally, the ester based biodegradable gear oils, showed a very good anti-scuffing performance, above that of the mineral oil in several aspects [21, 22].

6.1.3 FZG gear micropitting tests

FZG gear micropitting tests show that, on the tests of the carburized and the nitrided gears, ester lubricants tended to generate less micropitting (lower micropitting area, less pits and not so deep) than the mineral oil. The analysis of the micropitting tests results indicate that at the same operating temperature, reference oil M1 generates higher film thickness and lower mass loss (less wear) than the ester lubricants [39-41].

In comparison with the carburized gears, the coated gears lubricated by the mineral oil produced less micropitting area and more wear, on the other hand the coated gear lubricated by the ester oils had the worst results in term of micropitting area and mass loss.

6.1.4 FZG gear power loss tests

The power loss tests showed that using carburized gears, the ester oils promote a lower oil bath operating temperature at higher loads (pinion torque higher than 48 Nm). This difference in oil bath stabilization could reach *11%* (19º in the case of the ester E2 at load stage K10 and at 3000 rpm). This difference is very important, since the mineral oil can not operate at so high temperatures as the ester lubricant, because it is very sensitive to oxidation at those temperatures, decreasing the oil life. When nitrided gears are used instead of carburized ones (similar to esters E2 and E3), mineral oil has lower stabilization temperatures while E2 ester oil has similar operation temperatures when lubricating both gear materials.

In what concerns power loss, the reduction promoted by ester oils could reach 262 W (in the case of ester E2 at load stage K10 and at 3000 rpm) in comparison to the mineral oil, for the same operating conditions (using carburized gears). This corresponds to a power loss reduction of *17%*, in comparison to mineral lubricant.

The oil analysis performed and the mass loss measurements show that the wear protection promoted by E2 lubricant is significantly better (86% reduction of mass loss in comparison with the reference oil using carburized gears). The evolution of the wear particle indexes of M1, E1 and E3 lubricants is similar, indicating that wear promoted by those lubricants doesn't vary significantly.

The power loss results also show that ester oils have friction coefficients smaller than the reference mineral oil when lubricating carburized gears [42] (under contact pressures higher than 0.8 GPa) what could explain its better results in micropitting tests (lower micropitting area, less pits and not so deep).

6.2 Conclusions

The main conclusions are:

1. The ester biodegradable lubricants promote a lower operating temperature in comparison with the tested mineral reference lubricant.
2. The ester lubricants allow a substantial reduction in power loss, attaining 17%.
3. The overall efficiency is increased.
4. The wear protection of ester lubricants is slightly better than the conferred by the mineral lubricant.
5. The the ester lubricants promote less micropitting than the reference mineral oil.
6. The mineral lubricant might be replaced by a biodegradable non-toxic ester lubricant with advantage.

The main objective of this work was reached, shoing that was to show that biodegradable and low-toxicity lubricant formulations (base lubricant and additives) derived from renewable resources can be successfully used in mechanical transmissions, since the materials are adapted to the tribologic properties of these lubricants.

6.3 Future works:

This work could be developed in several ways:

Micropitting:

- Modelization of the gear micropitting using mixed lubrication models and multi-axial fatigue criteria (Dang Van).
- Perform topography measurements after each load stage in order to evaluate the overall evolution of the pinion teeth flanks during the tests.
- Evaluate the influence of the lubricant additives in the gear micropitting evolution.

Power loss:

- Perform gear power loss tests measuring the power losses directly.

REFERENCES

1. *Lea, C., Energy savings through use of advanced biodegradable lubricants. Industrial Lubrication and Tribology, 2007.* ***59****(3): p. 132-136.*
2. *Weck, M., O. Hurasky-Schonwerth, and C. Bugiel, Service Behaviour of PVD-Coated Gearing Lubricated with Biodegradable Synthetic Ester Oils. VDI-Berichte, 2002(Nr1665).*
3. *Martins, R., P. Moura, and J. Seabra, Power loss in FZG gears: Mineral oil vs. biodegradable ester and carburized steel vs. austempered ductile iron vs. MoS2-Ti coated steel. VDI Berichte, 2005(1904 II): p. 1467-1486.*
4. *Martins, R., et al., Friction coefficient in FZG gears lubricated with industrial gear oils: Biodegradable ester vs. mineral oil. Tribology International, 2006.* ***39****(6): p. 512-521.*
5. *Pettersson, A., Tribological characterization of environmentally adapted ester base fluis. Tribology Interational, 2003.* ***36****(11).*
6. *Denis, J., J. Briant, and J.C. Hipeaux, "Physico-Chimie des Lubrifiants – Analyses et Essais". Éditions Technip, 1997.*
7. *Denis, J., J. Briant, and J.-C. Hipeaux, Physico-Chimie des Lubrifiants – Analyses et Essais. 1997: Éditions Technip.*
8. *Gold, J.W., et al., Viscosity-Pressure-Temperature Behaviour of Mineral and Synthetic Oils. Journal of Synthetic Lubrication, 2001.* ***18****(1).*
9. *Amaro, R.I., et al., Molybdenum disulphide/titanium low friction coating for gears application. Tribology International, 2005.* ***38****(4): p. 423-434.*
10. *Amaro, R., et al. MoST low friction coating for gears application. in GEARS 2003 - Gears and Transmissions Workshop. 2003. FEUP - Porto - Portugal.*
11. *Renevier, N., et al., Performance of MoS2/metal composite coatings used for dry machining and other applications. Surface Coatings Technology, 2000.* ***123****(1): p. 84-91.*
12. *Winter, H. and K. Michaelis, FZG gear test rig - Desciption and possibilities. In: Coordinate European Council Second International Symposium on The performance Evaluation of Automotive Fuels and Lubricants, 1985.*
13. *DIN 51534 parte 4, Avaliação da capacidade de carga de óleos método standard FZG A/8.3/90. 1990.*
14. *Forschungsvereinigung Antriebstechnik E.V, FVA Research Project Nr. 54/I-IV. 1993.*
15. *DGMK Information sheet, Short Test Procedure for the investigation of the micropitting load capacity of gear lubricants. 2002.*
16. *Mummery, L., Surface Texture Analysi: The Handbook. 1990: Hommelwerke GmbH.*
17. *Olver, A.V., The mechanism of rolling contact fatigue: An update. Proceedings of the Institution of Mechanical Engineers, Part J: Journal of Engineering Tribology, 2005.* ***219****(5): p. 313-330.*
18. *Hohn, B.R. and K. Michaelis, Influence of oil temperature on gear failures. Tribology International, 2004.* ***37****(2): p. 103-109.*
19. *Lipp, et al., Design for rolling contact fatigue.*
20. *DIN 51354 parte 4, Avaliação da capacidade de carga de óleos método standard FZG A/8.3/90. 1990.*

21. *Cardoso, N., et al. Influence of lubricant type in gear scuffing. in Mechanics & materials in design (M2D'2006). 2006. Porto, Portugal.*

22. *Martins, R., N. Cardoso, and J. Seabra, Influence of lubricant type in gear scuffing. Industrial Lubrication and Tribology, 2008 (to be published).* ***6****.*

23. *Castro, J. and J. Seabra, "Power dissipation – temperature scuffing criterion for FZG gears", in VDI-Berichte 1904.2: VDI-EKV International conference on gears. 2005: Munchen.*

24. *Cardis, A. and M. Webster, Gear Oil Micropitting Evaluation, in Gear Technology Vol. 17, No. 5. 2000.*

25. *Klaus, L. and H. Gottfried, "Design for Rolling Contact Fatigue", in International Journal of Power Metallurgy, nº39. 2003*

26. *Winter, H. and P. Oster, Influence of the Lubricant on Pitting and Micro Pitting (Grey Staining, Frosted Areas) Resistance of Case Carburized Gears – Test Procedures, AGMA.*

27. *Forschungsvereinigung Antriebstechnik,E.V. ,FVA Research Project Nr. 54/I-IV,July 1993.*

28. *Antoine, F. and J.-M. Besson, Simplified modellization of gear micropitting. ImechE 2002.* ***216,Part G****.*

29. *DGMK Information sheet; Short Test Procedure for the investigation of the micropitting load capacity of gear lubricants. 2002.*

30. *Gohar, R., Elastohydrodynamics. 1988: Ellis Horwood L.td.*

31. *Dowson, D. and G. R. Higginson, Elastohydrodinamic lubrication. S. I. Editon. 1977: Pergamon Press Ltd.*

32. *Höhn, B.-R., K. Michaelis, and T. Vollmer, Thermal Rating of Gear Drives: Balance Between Power Loss and Heat Dissipation. AGMA Technical Paper, 1996.*

33. *Changenet, C. and M. Pasquier, Power Losses and Heat Exchange in Reduction Gears: Numerical and Experimental results. VDI-Berichte, 2002(1665).*

34. *Hunt, T., Handbook of Wear Debris Analysis and Particle Detection in Liquids, ed. E. Science. 1993.*

35. *Salonen, P., Improved Noise Damping and Reduced Weight in Truck Componentes With KYMENITE ADI, in International ADI and Simulation Conference. 1997: Finland.*

36. *IP 212/92 Standard, Determination of Viscosity of Bitumen Emulsions - Engler Method, in Institute of Petroleum. 1992, UK.*

37. *Eschmann, P., Ball and roller bearings - Theory, design and applications, ed. Wiley. 1985.*

38. *Winter, H. and K. Michaelis. Investigations on the thermal balance of gear drives. in Fifth World Congress on Theory of Machines and Mechanisms. 1979: American Society of Mechanical Engineers.*

39. *Cardoso, N., R. Martins, and J. Seabra. Micropitting performance of nitriding steel gears lubricated with mineral and ester oils. in IBERTRIB 2007. 2007. Bilbao, Spain.*

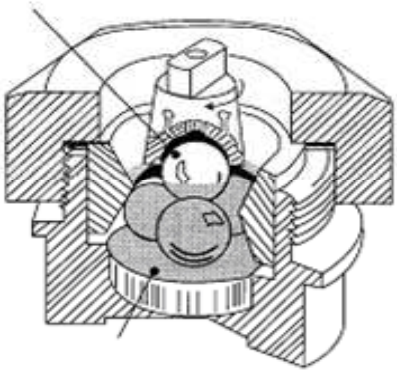
40. *Cardoso, N., R. Martins, and J. Seabra. Micropitting performance of nitriding steel gears lubricated with mineral and ester oils. in Leeds-Lyon 34. 2007 (to be presented). Lyon.*

41. *Martins, R., N. Cardoso, and J. Seabra. Gear micropitting performance of case-hardened and high pressurer nitriding steels. in Leeds-Lyon 33. 2006. Leeds.*

42. Martins, R., N. Cardoso, and J. Seabra. Influence of base oil in gear power loss. in Leeds-Lyon 34. 2007 (to be presented). Lyon.

APPENDIX A – FOUR BALL TESTS DATA SHEETS

Four-Ball Wear Test (ASTM D4172)



CAMERON PLINT
WOKINGHAM BERKSHIRE ENGLAND
SERIAL No: TE 82/7752

Mineral 1 (1)

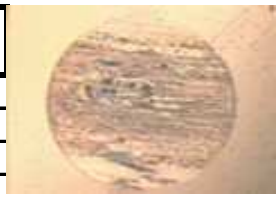
Test Conditions

Temperature	75 ± 2ºC
Speed	1200 ± 60 rpm
Duration	60 ± 1 min
Load	392 ± 2 N [40 ± 0,2 kgf]
Load Arm	10x
Dead weight	4kg

Wear Scar Diameters [µm]

	Direction 1	Direction 2	Average
Ball n°1	372	372	372
Ball n°2	372	372	372
Ball n°3	384	384	384
Upper ball	324		

Ball n°1



Ball n°2



Ball n°3



Upper ball

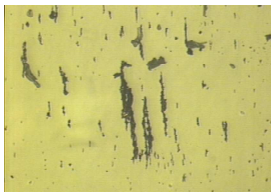


Direct Reading Ferrography

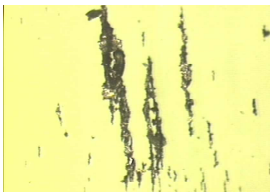
d	1,0
D_L	4,9
D_S	2,7
CPUC	7,6
ISUC	16,7

Analytical Ferrography

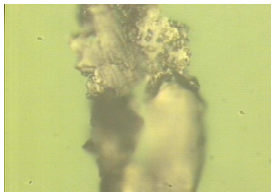
200 x



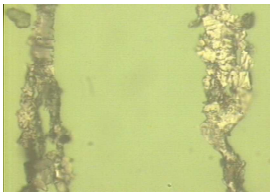
200 x



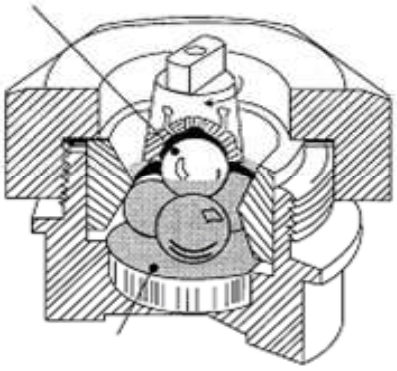
1000 x



1000 x



Four-Ball Wear Test (ASTM D4172)



CAMERON PLINT
WOKINGHAM BERKSHIRE ENGLAND
SERIAL No: TE 82/7752

Mineral 1 (2)

Test Conditions

Temperature	75 ± 2ºC
Speed	1200 ± 60 rpm
Duration	60 ± 1 min
Load	392 ± 2 N [40 ± 0,2 kgf]
Load Arm	10x
Dead weight	4kg

Wear Scar Diameters [µm]

	Direction 1	Direction 2	Average
Ball nº1	408	384	396
Ball nº2	408	396	402
Ball nº3	396	384	390
Upper ball	420		

Ball nº1



Ball nº2



Ball nº3



Upper ball



Direct Reading Ferrography

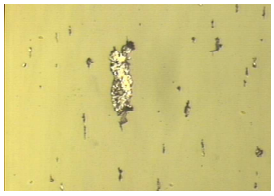
d	1,0
D_L	3,5
D_S	2,4
CPUC	5,9

Analytical Ferrography

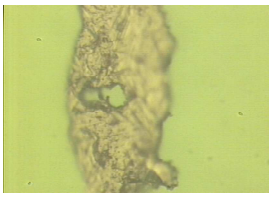


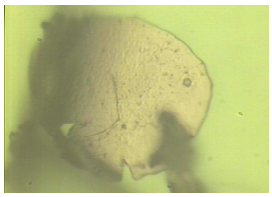


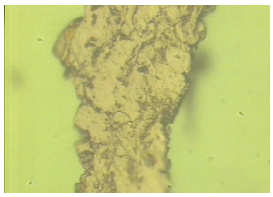


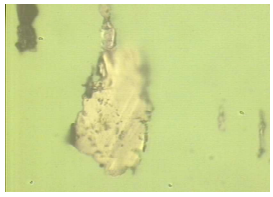


d

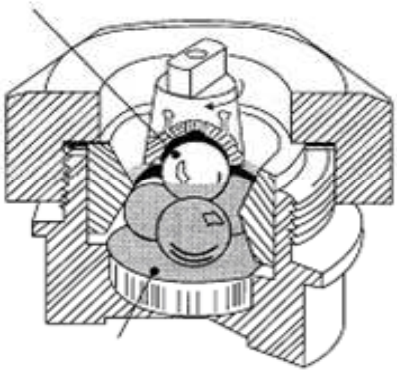








Four-Ball Wear Test (ASTM D4172)



CAMERON PLINT
WOKINGHAM BERKSHIRE ENGLAND
SERIAL No: TE 82/7752

Ester 1 (1)

Test Conditions

Temperature	75 ± 2ºC
Speed	1200 ± 60 rpm
Duration	60 ± 1 min
Load	392 ± 2 N [40 ± 0,2 kgf]
Load Arm	10x
Dead weight	4kg

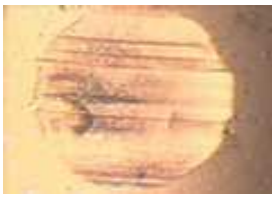
Wear Scar Diameters [µm]

	Direction 1	Direction 2	Average
Ball n°1	408	396	402
Ball n°2	408	408	408
Ball n°3	408	396	402
Upper ball	396		

Ball n°1



Ball n°2



Ball n°3



Upper ball



Direct Reading Ferrography

d	1,0
D_L	6,6
D_S	1,6
CPUC	8,2
ISUC	41,0

Analytical Ferrography

200 x



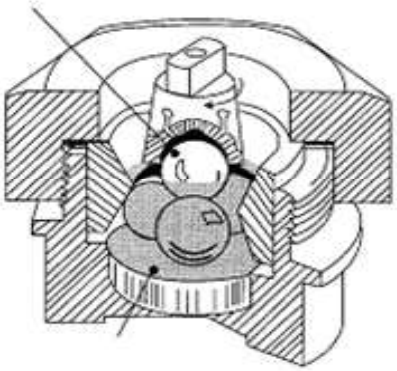
1000 x



1000 x



Four-Ball Wear Test (ASTM D4172)



CAMERON PLINT
WOKINGHAM BERKSHIRE ENGLAND
SERIAL No: TE 82/7752

Ester 1 (2)

Test Conditions

Temperature	75 ± 2ºC
Speed	1200 ± 60 rpm
Duration	60 ± 1 min
Load	392 ± 2 N [40 ± 0,2 kgf]
Load Arm	10x
Dead weight	4kg

Wear Scar Diameters [μm]

	Direction 1	Direction 2	Average
Ball n°1	396	384	390
Ball n°2	408	384	396
Ball n°3	396	396	396
Upper ball	360		

Ball n°1



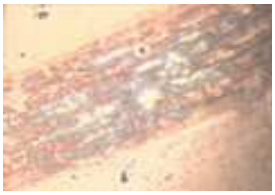
Ball n°2



Ball n°3



Upper ball



Direct Reading Ferrography

d	1,0
D_L	
D_S	
CPUC	#VALUE!
ISUC	#VALUE!

Analytic Ferrography

200 x



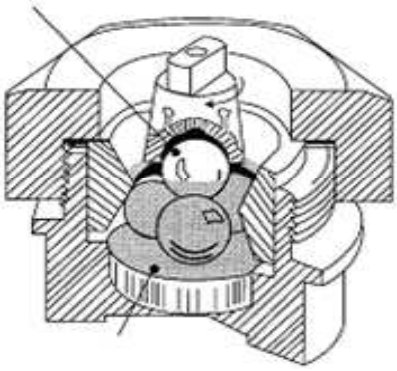
1000 x



1000 x



Four-Ball Wear Test (ASTM D4172)



CAMERON PLINT
WOKINGHAM BERKSHIRE ENGLAND
SERIAL No: TE 82/7752

Ester 2 (1)

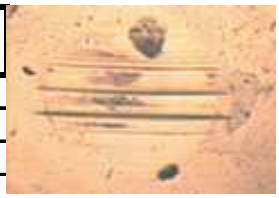
Test Conditions

Temperature	75 ± 2ºC
Speed	1200 ± 60 rpm
Duration	60 ± 1 min
Load	392 ± 2 N [40 ± 0,2 kgf]
Load Arm	10x
Dead weight	4kg

Wear Scar Diameters [µm]

	Direction 1	Direction 2	Average
Ball n°1	372	372	372
Ball n°2	360	360	360
Ball n°3	360	360	360
Upper ball	276		

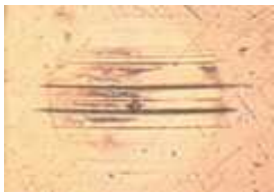
Ball n°1



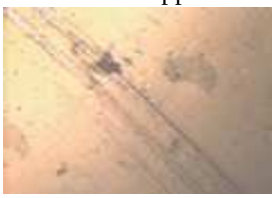
Ball n°2



Ball n°3



Upper ball

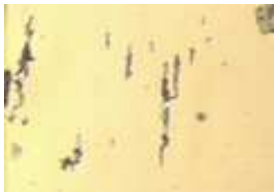


Direct Reading Ferrography

d	1,0
D_L	3,7
D_S	2,7
CPUC	6,4
ISUC	6,4

Analytic Ferrography

200 x



200 x

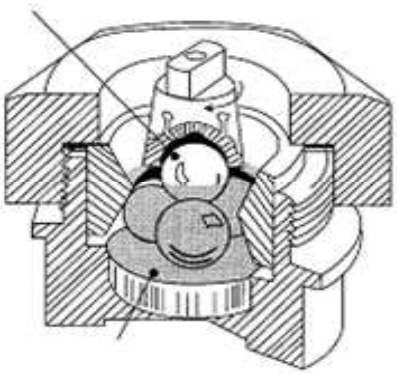


1000 x





Four-Ball Wear Test (ASTM D4172)



CAMERON PLINT
WOKINGHAM BERKSHIRE ENGLAND
SERIAL No: TE 82/7752

Ester 2 (2)

Test Conditions

Temperature	75 ± 2°C
Speed	1200 ± 60 rpm
Duration	60 ± 1 min
Load	392 ± 2 N [40 ± 0,2 kgf]
Load Arm	10x
Dead weight	4kg

Wear Scar Diameters [μm]

	Direction 1	Direction 2	Average
Ball n°1	324	348	336
Ball n°2	348	348	348
Ball n°3	336	348	342
Upper ball	252		

Ball n°1



Ball n°2



Ball n°3



Upper ball



Direct Reading Ferrography

d	1,0
D_L	2,3
D_S	0,6
CPUC	2,9
ISUC	4,9

Analytical Ferrography

200 x



200 x



1000 x



1000 x



APPENDIX B – GEAR SCUFFING TESTS DATA SHEETS

FZG gear scuffing test of M1 gear oil using A20 gear

Test reference: FZG A20/16.6/90 **Oil reference: M1**

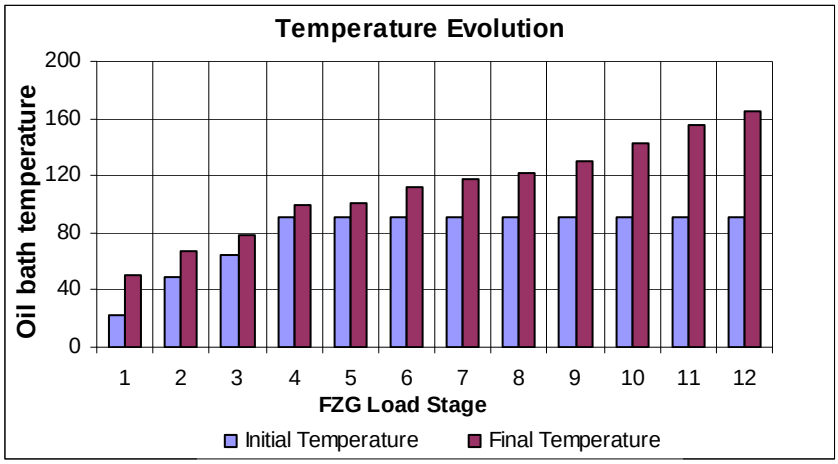
Gear type: A20 **Gear reference: 2A-2 Side: A**

Gear material: Carburized steel (DIN 20MnCr5)

K_{FZG} =11 **Mass loss = 0,414 g**

Oil bath temperature ate the end of each load stage

K_{FZG}	Oil Temp. [°C]	
	Beginning	End
1	22.8	50.5
2	48.4	66.7
3	64.7	78.8
4	90.5	99.7
5	90.5	100.4
6	90.3	111.2
7	90.5	117.3
8	90.5	121.6
9	90.5	130.6
10	90.5	143.2
11	90.5	155.5
12	90.5	164.9



Pinion surface roughness [µm]

			R_{max}	R_{Z-D}	R_a	R_q	M_{r1}	R_{pk}	R_k	Rvk	Mr2	Vo
Initial	axial		1.46	0.89	0.14	0.20	12.92	0.26	0.38	0.36	85.48	26.84
	radial											
Final	axial	good	1.53	1.14	0.15	0.22	8.86	0.14	0.37	0.50	81.29	44.66
		damaged	3.21	2.57	0.40	0.51	7.18	0.31	1.24	0.73	84.08	61.91
	radial	good	5.96	4.34	0.71	0.92	5.54	0.35	2.33	1.55	85.95	109.21
		damaged	2.56	2.24	0.37	0.49	5.80	0.22	1.21	0.86	79.60	88.84

Tooth face changes (face damage)

Zi	R/F	L[mm]	KS:11	R/F	L[mm]	KS:12	R/F	L[mm]	KS:	R/F	L[mm]	KS:	R/F	L[mm]	KS:	R/F	L[mm]	KS:
1 9	F	20		F	20													
2 10	F	20		F	20													
3 11				F	20													
4 12																		
5 13																		
6 14																		
7 15																		
8 16	F	20		F	20													
	Σ	120		Σ	160		Σ	0		Σ	0		Σ	0		Σ	0	

Legend:

- Scooring[6]
- Scuffing[7]

[6] Scoring marks run into the sliding direction of the tooth faces. They occur singly or in zones as light, medium or deep marks (Characteristic: deep scars (grooves) continuing towards the tip of the tooth and having a rougher appearance than the cross-griding marks).

[7] Scuffing marks occur as single, fine marks or strips or area covering part or all of the face width (Characteristic: dull appearance of scuffing areas, their roughness being much greater than the original cross-gridnig pattern. The griding marks are no longer visible).

FZG gear scuffing test of M1 gear oil using A10 gear

Test reference: FZG A10/16.6/90 **Oil reference: M1**

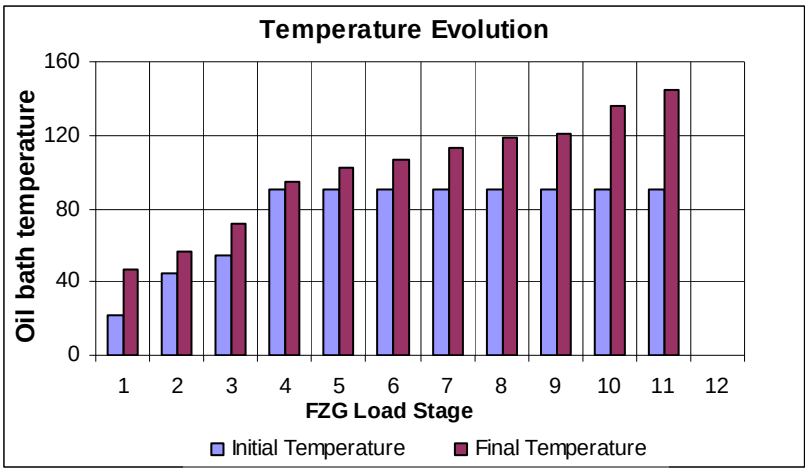
Gear type: A10 **Gear reference: 2A-1 Side: A**

Gear material: Carburized steel (DIN 20MnCr5)

K_{FZG} =11 **Mass loss = 1,049 g**

Oil bath temperature ate the end of each load stage

K_{FZG}	Oil Temp. [°C]	
	Beginning	End
1	21.8	46.6
2	45.1	56.5
3	54.9	71.5
4	90.5	94.2
5	90.5	102.7
6	90.5	106.8
7	90.5	113.5
8	90.3	118.7
9	90.5	120.4
10	90.5	135.9
11	90.5	144.3
12		



Pinion surface roughness [µm]

			R_{max}	R_{Z-D}	R_a	R_q	M_{r1}	R_{pk}	R_k	Rvk	Mr2	Vo
Initial	axial		1.27	0.86	0.14	0.19	11.61	0.20	0.42	0.34	85.33	28.6
	radial		7.98	5.97	0.98	1.26	9.43	1.11	3.08	1.75	86.38	119.7
Final	axial	good	1.17	0.74	0.10	0.14	9.06	0.13	0.32	0.23	89.26	14.8
		damaged	32.78	27.96	6.07	7.39	20.71	12.56	13.78	3.98	90.55	163.4
	radial	good	5.46	3.57	0.60	0.81	7.74	0.64	1.80	1.46	84.60	112.6
		damaged	8.36	4.58	0.73	1.11	7.36	1.36	1.79	2.15	78.56	232.6

Tooth face changes (face damage)

Zi	R/F	L[mm]	KS:9	R/F	L[mm]	KS:10	R/F	L[mm]	KS:11	R/F	L[mm]	KS:	R/F	L[mm]	KS:	R/F	L[mm]	KS:
1	R			R			F	10										
9																		
2				R			F	10										
10																		
3				R			F	2										
11																		
4	R			F	0,5		F	0,5										
12																		
5							F	10										
13																		
6	R			F	0,5		F	10										
14																		
7	R			R			F	10										
15																		
8	R			F	1		F	10										
16																		
	Σ	0		Σ	4		Σ	125		Σ	0		Σ	0		Σ	0	

Legend:

- Scooring
- Scuffing

FZG gear scuffing test of E1 gear oil using A20 gear

Test reference: FZG A20/16.6/90 **Oil reference: E1**

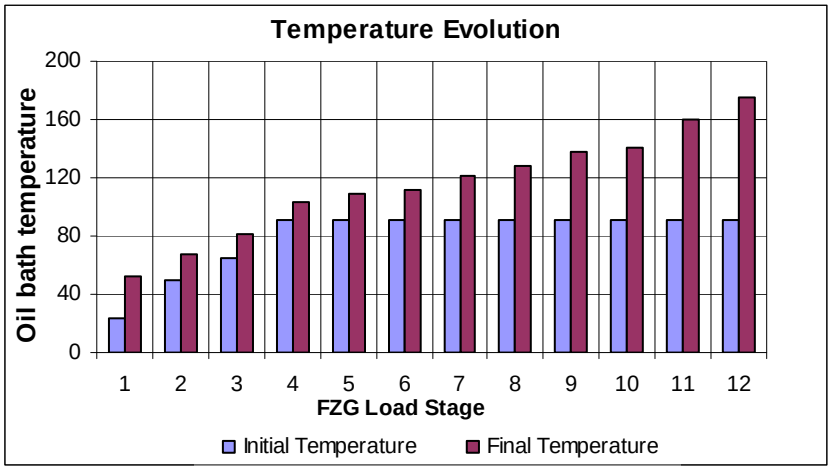
Gear type: A20 **Gear reference: 2A-3 Side: A**

Gear material: Carburized steel (DIN 20MnCr5)

K_{FZG} =12 **Mass loss = 0,081 g**

Oil bath temperature ate the end of each load stage

K_{FZG}	Oil Temp. [°C]	
	Beginning	End
1	23.6	52.5
2	49.7	67.7
3	64.9	81
4	90.5	103
5	90.5	108.6
6	90.5	112.2
7	90.5	120.7
8	90.5	128.1
9	90.5	137.4
10	90.5	140.9
11	90.5	159.7
12	90.5	174.7



Pinion surface roughness [µm]

			R_{max}	R_{Z-D}	R_a	R_q	M_{r1}	R_{pk}	R_k	Rvk	Mr2	Vo
Initial	axial		1.20	0.79	0.14	0.18	12.03	0.21	0.39	0.31	86.18	25.92
	radial											
Final	axial	good	-	-	-	-	-	-	-	-	-	-
		damaged	8.26	6.26	0.94	1.28	4.64	0.38	1.96	2.64	76.61	309.70
	radial	good	-	-	-	-	-	-	-	-	-	-
		damaged	7.32	5.56	0.85	1.15	8.88	0.56	2.08	2.31	81.76	211.73

Tooth face changes (face damage)

Zi	R/F	L[mm]	KS:7	R/F	L[mm]	KS:8	R/F	L[mm]	KS:9	R/F	L[mm]	KS:10	R/F	L[mm]	KS:11	R/F	L[mm]	KS:12
1																		
9							F	2		F	2		F	3		F	20	
2																		
10				F	1		F	1		F	1		F	1		F	20	
3																		
11																F	20	
4																		
12																F	20	
5																		
13	F	1		F	1		F	1		F	2		F	2		F	20	
6																		
14	F	2		F	2		F	2		F	2		F	2		F	20	
7																		
15													F	1		F	20	
8																		
16																F	20	
	Σ	6		Σ	8		Σ	12		Σ	14		Σ	18		Σ	320	

Legend:

- Scooring
- Scuffing

FZG gear scuffing test of E1 gear oil using A10 gear

Test reference: FZG A10/16.6/90 **Oil reference: E1**

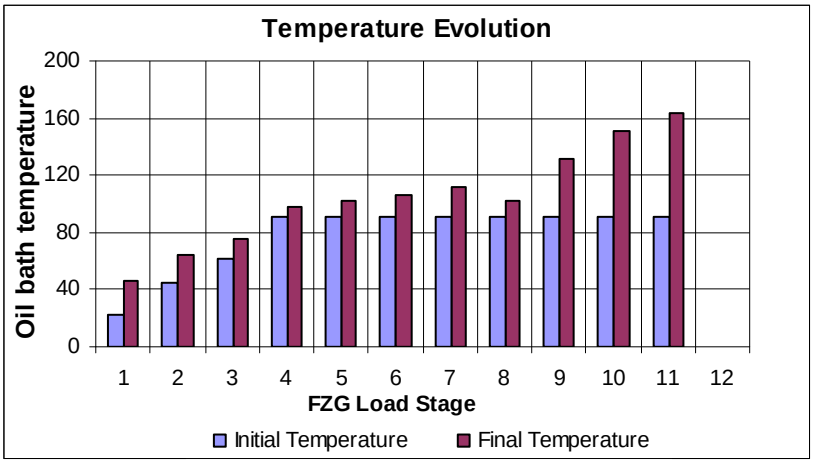
Gear type: A10 **Gear reference: 2A-4 Side: A**

Gear material: Carburized steel (DIN 20MnCr5)

K_{FZG} =11 **Mass loss = 0,181 g**

Oil bath temperature ate the end of each load stage

K_{FZG}	Oil Temp. [°C]	
	Beginning	End
1	21.9	46.1
2	45.3	63.7
3	62	76.1
4	90.5	97.5
5	90.5	102.5
6	90.5	105.7
7	90.5	112.2
8	90.5	101.7
9	90.3	131.2
10	90.5	151.0
11	90.5	164.2
12		



Pinion surface roughness [µm]

			R_{max}	R_{Z-D}	R_a	R_q	M_{r1}	R_{pk}	R_k	Rvk	Mr2	Vo
Initial	axial		0.95	0.67	0.11	0.15	9.91	0.16	0.35	0.21	85.11	17.3
	radial		8.41	5.97	0.97	1.26	10.49	1.25	3.04	1.66	87.31	104.7
Final	axial	good	-	-	-	-	-	-	-	-	-	-
		damaged	7.51	5.89	0.80	1.10	9.03	0.84	2.14	2.11	85.40	160.5
	radial	good	-	-	-	-	-	-	-	-	-	-
		damaged	6.81	5.01	0.66	0.91	6.98	0.68	1.64	1.67	80.16	166.9

Tooth face changes (face damage)

Zi	R/F	L[mm]	KS:7	R/F	L[mm]	KS:8	R/F	L[mm]	KS:9	R/F	L[mm]	KS:10	R/F	L[mm]	KS:11	R/F	L[mm]	KS:
1																		
9													F	10				
2																		
10	R			R			R			R			F	10				
3																		
11													F	10				
4																		
12	R			R			R			R			F	10				
5																		
13													F	10				
6																		
14													F	10				
7																		
15										R			F	10				
8																		
16							R			R			F	10				
	Σ	0		Σ	0		Σ	0		Σ	0		Σ	160		Σ	0	

Legend:

- Scooring
- Scuffing

FZG gear scuffing test of E2 gear oil using A20 gear

Test reference: FZG A20/16.6/90 **Oil reference: E2**

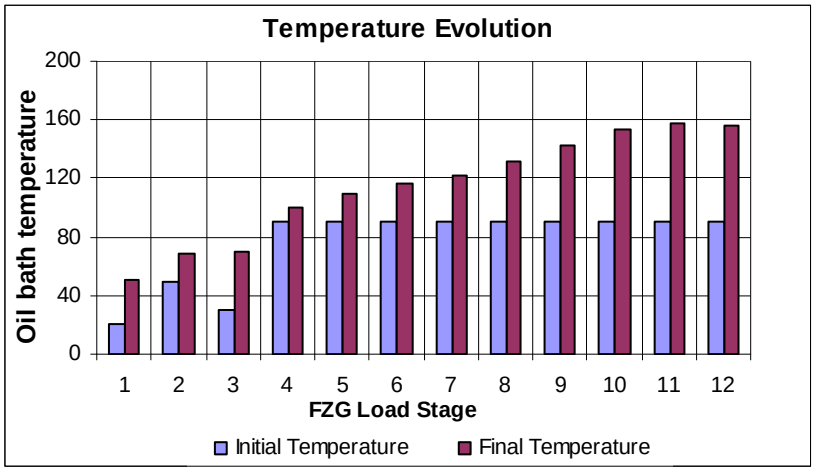
Gear type: A20 **Gear reference: 2A-2 Side: B**

Gear material: Carburized steel (DIN 20MnCr5)

K_{FZG} =12 **Mass loss = 1,888 g**

Oil bath temperature ate the end of each load stage

K_{FZG}	Oil Temp. [°C]	
	Beginning	End
1	20.1	50.5
2	49.1	68.4
3	30.3	70.4
4	90.5	99.5
5	90.5	109.5
6	90.5	116.1
7	90.5	121.8
8	90.5	131.9
9	90.5	142.2
10	90.5	154,0
11	90.5	157.1
12	90.5	156.4



Pinion surface roughness [µm]

			R_{max}	R_{Z-D}	R_a	R_q	M_{r1}	R_{pk}	R_k	Rvk	Mr2	Vo
Initial	axial		1.20	0.79	0.14	0.18	12.03	0.21	0.39	0.31	86.2	25.9
	radial											
Final	axial	good	-	-	-	-	-	-	-	-	-	-
		damaged	8.26	6.26	0.94	1.28	4.64	0.38	1.96	2.64	76.6	309.7
	radial	good	-	-	-	-	-	-	-	-	-	-
		damaged	7.32	5.56	0.85	1.15	8.88	0.56	2.08	2.31	81.8	211.7

Tooth face changes (face damage)

Zi	R/F	L[mm]	KS:7	R/F	L[mm]	KS:8	R/F	L[mm]	KS:9	R/F	L[mm]	KS:10	R/F	L[mm]	KS:11	R/F	L[mm]	KS:12
1	R	3		R	3		F	3		F	4		F	4		F	20	
9																		
2													F	1		F	20	
10																		
3							F	1		F	1		F	1		F	20	
11																		
4																F	20	
12																		
5										F	1		F	2		F	20	
13																		
6																F	20	
14																		
7																F	20	
15																		
8																F	20	
16																		
	Σ	6		Σ	6		Σ	8		Σ	12		Σ	16		Σ	320	

Legend:

- Scooring
- Scuffing

FZG gear scuffing test of E2 gear oil using A10 gear

Test reference: FZG A10/16.6/90 **Oil reference: E2**

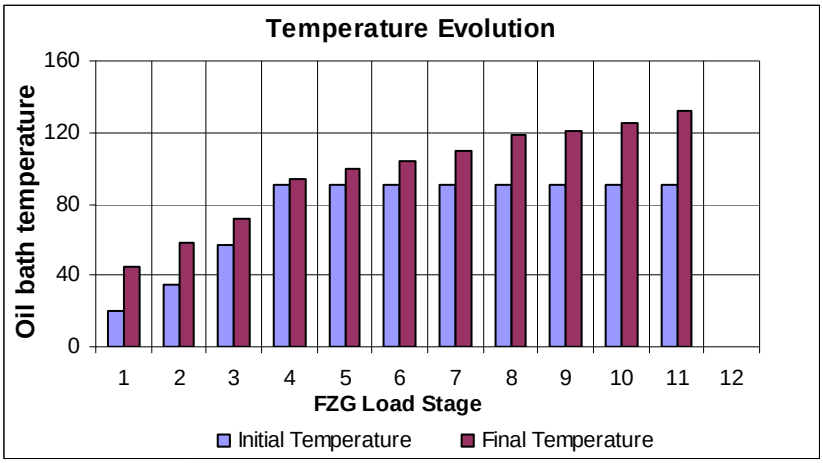
Gear type: A10 **Gear reference: 2A-2 Side: A**

Gear material: Carburized steel (DIN 20MnCr5)

K_{FZG} =11 **Mass loss = 0,075 g**

Oil bath temperature ate the end of each load stage

K_{FZG}	Oil Temp. [°C]	
	Beginning	End
1	19.7	44.8
2	35.0	58.5
3	56.9	71.7
4	90.5	94.1
5	90.5	99.1
6	90.5	103.8
7	90.5	109.6
8	90.5	118.6
9	90.5	120.3
10	90.5	124.9
11	90.5	131.7
12		



Pinion surface roughness [µm]

			R_{max}	R_{Z-D}	R_a	R_q	M_{r1}	R_{pk}	R_k	Rvk	Mr2	Vo
Initial	axial		1.24	0.85	0.13	0.18	9.55	0.27	0.39	0.28	86.0	22.7
	radial		8.00	6.05	1.09	1.39	10.04	1.30	3.75	1.72	89.2	93.6
Final	axial	good	1.35	0.87	0.12	0.17	7.53	0.13	0.38	0.25	85.2	20.6
		damaged	4.68	3.55	0.58	0.75	8.72	0.55	1.91	0.96	85.6	69.5
	radial	good	6.77	4.86	0.92	1.19	9.76	1.53	3.17	1.65	90.9	77.1
		damaged	3.61	2.51	0.45	0.58	5.51	0.50	1.26	1.16	78.5	117.5

Tooth face changes (face damage)

Zi	R/F	L[mm]	KS:9	R/F	L[mm]	KS:10	R/F	L[mm]	KS:11	R/F	L[mm]	KS:	R/F	L[mm]	KS:	R/F	L[mm]	KS:
1																		
9							F	10										
2																		
10							F	10										
3																		
11							F	1										
4																		
12																		
5																		
13	F	1		F	1		F	1										
6																		
14				R			F	6										
7																		
15																		
8																		
16				R			F	10										
	Σ	2		Σ	2		Σ	76		Σ	0		Σ	0		Σ	0	

Legend:

- Scooring
- Scuffing

APPENDIX C – GEAR MICROPITTING TESTS DATA SHEETS

FZG gear micropitting test of carburized gear lubricated by M1 gear oil (C-M1)

Test reference: GFKT-C14/8.3/90 **Oil reference: M1**

Gear type: C14 **Gear reference: 2C-4 Side: A**

Gear material: Carburized steel (DIN 20MnCr5)

Mass loss [mg]

Load stage	running in+k6	K8	K9
Pinion	3	6	5
Wheel	0	4	0
Total	3	10	5

Micropitted area [%]

	running in+k6	K8	K9
1st tooth	0	13	22
5th tooth	0	14	22
Average	0	13	22

Ferrometry

Load stage	K3	K6	K8	K9
d	0.1	0.1	0.1	0.1
DL	4.3	6.1	4.2	10.7
DS	1.8	1.9	1.6	2.6
CPUC	61.0	80.0	58.0	133.0
ISUC	1.5E+03	3.4E+03	1.5E+03	1.1E+04

Surface roughness measurements

Surface roughness parameters [µm]

		Dir.		R_{max}	R_{z-D}	R_a	R_q	M_{r1}	R_{pk}	R_k	R_{vk}	M_{r2}	Vo
Wheel	Initial	Axial		1.30	0.68	0.12	0.17	12.2	0.26	0.33	0.32	86.8	23.0
		Radial		6.98	5.81	0.99	1.23	9.3	0.91	3.18	1.65	88.1	99.0
Pinion	Initial	Axial		1.72	1.23	0.23	0.30	8.7	0.20	0.69	0.53	84.6	42.2
		Radial		6.37	5.23	0.93	1.16	10.7	1.25	3.14	1.04	89.8	53.1
	After running-in + K6	Axial	top	0.95	0.67	0.11	0.14	8.5	0.10	0.35	0.22	86.9	15.5
			bottom	1.72	0.91	0.12	0.17	10.8	0.16	0.30	0.35	83.4	31.1
		Radial	top	4.73	3.97	0.78	0.98	10.1	0.93	2.63	1.38	87.5	82.8
			bottom	5.50	4.30	0.77	0.96	10.9	0.73	2.59	1.30	87.6	82.7
	After K8	Axial	top	0.99	0.63	0.11	0.15	8.1	0.13	0.30	0.30	83.7	26.1
			bottom	3.91	2.27	0.29	0.45	10.0	0.23	0.57	1.10	79.9	111.7
		Radial	top	4.27	3.64	0.71	0.87	7.2	0.52	2.55	1.05	87.1	66.9
			bottom	7.25	5.03	0.75	1.00	10.1	0.88	2.38	1.56	85.0	119.8
	After K9	Axial	top	0.75	0.53	0.08	0.11	10.6	0.08	0.22	0.24	86.6	17.4
			bottom	7.30	2.64	0.28	0.63	16.1	0.28	0.37	2.09	88.0	125.4
		Radial	top	4.11	3.43	0.62	0.76	7.5	0.47	2.16	0.88	87.3	57.1
			bottom	7.66	4.92	0.72	0.97	11.4	0.68	2.20	1.57	85.8	113.3

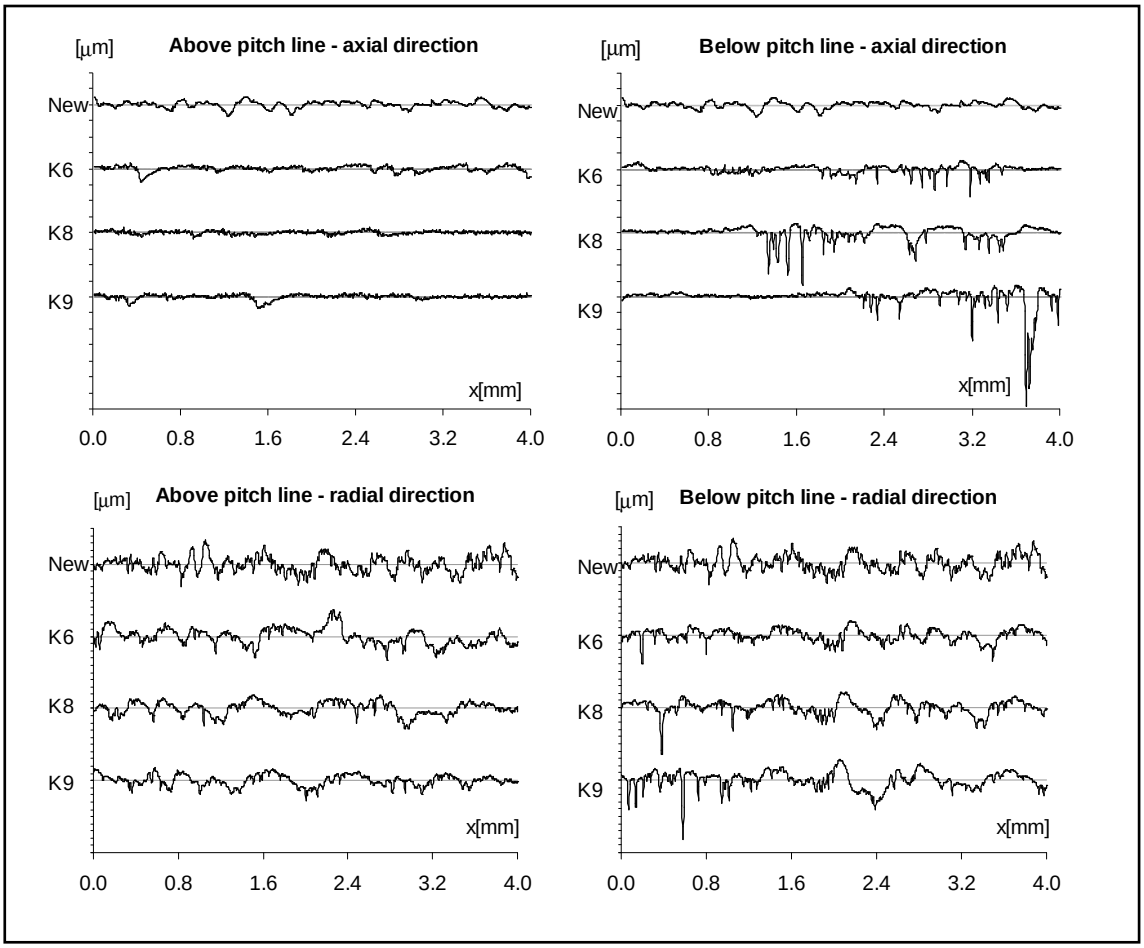
Axial direction pinion roughness parameters variation[%]

	R_{max}	R_{z-D}	R_a	R_q	R_{pk}	R_k	R_{vk}	V_o
$k6_{top}$-original	-45	-46	-53	-52	-48	-49	-59	-63
$k6_{bottom}$- original	0	-26	-48	-42	-22	-56	-34	-26
$k6_{bottom}$-$k6_{top}$	82	36	9	22	51	-13	59	101
$k8_{top}$-$k6_{top}$	5	-6	-5	1	24	-16	37	69
$k8_{bottom}$-$k6_{bottom}$	127	149	138	160	45	86	216	259
$k8_{bottom}$-$k8_{top}$	294	260	173	213	76	91	267	327
$k9_{top}$-$k8_{top}$	-24	-16	-25	-24	-35	-25	-19	-34
$k9_{bottom}$-$k8_{bottom}$	87	17	-3	38	24	-34	89	12
$k9_{bottom}$-$k9_{top}$	870	399	253	471	236	67	759	622

Radial direction pinion roughness parameters variation[%]								
	R_{max}	R_{z-D}	R_a	R_q	R_{pk}	R_k	R_{vk}	V_o
$k6_{top}$-original	-26	-24	-15	-15	-26	-16	33	56
$k6_{bottom}$- original	-14	-18	-17	-17	-42	-17	25	56
$k6_{bottom}$-$k6_{top}$	16	8	-2	-2	-21	-1	-6	0
$k8_{top}$-$k6_{top}$	-10	-8	-10	-12	-44	-3	-24	-19
$k8_{bottom}$-$k6_{bottom}$	32	17	-2	4	20	-8	21	45
$k8_{bottom}$-$k8_{top}$	70	38	7	15	68	-7	49	79
$k9_{top}$-$k8_{top}$	-4	-6	-13	-12	-9	-16	-16	-15
$k9_{bottom}$-$k8_{bottom}$	6	-2	-5	-3	-22	-7	0	-5
$k9_{bottom}$-$k9_{top}$	86	44	17	27	44	2	78	98

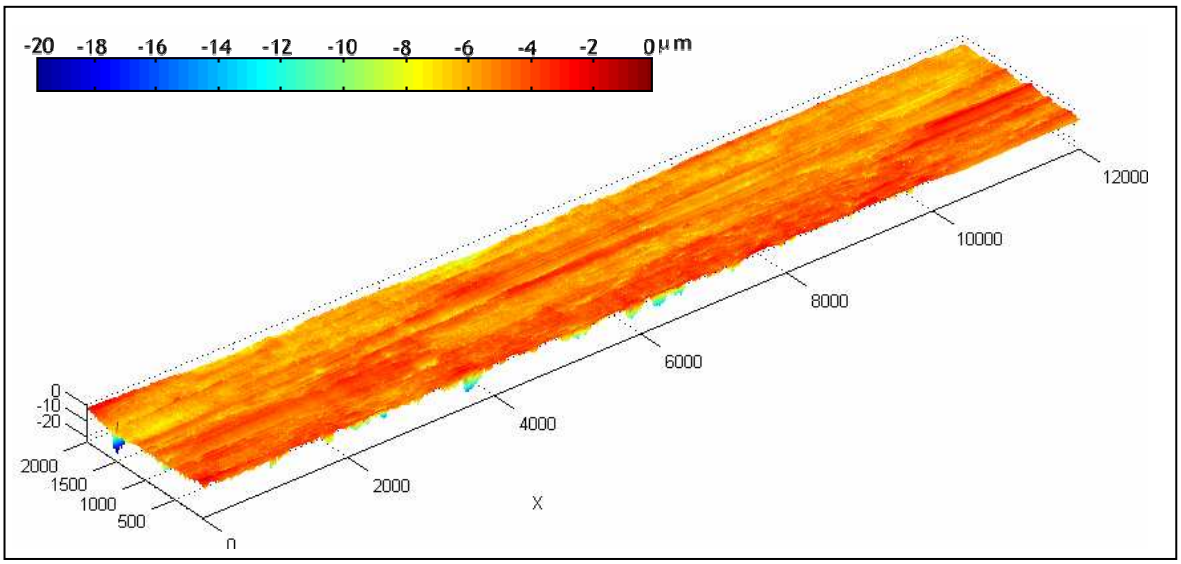
Legend:

top – above pitch line (view Figure 4.11)
bottom - below pitch line (view Figure 4.11)
original – new surface

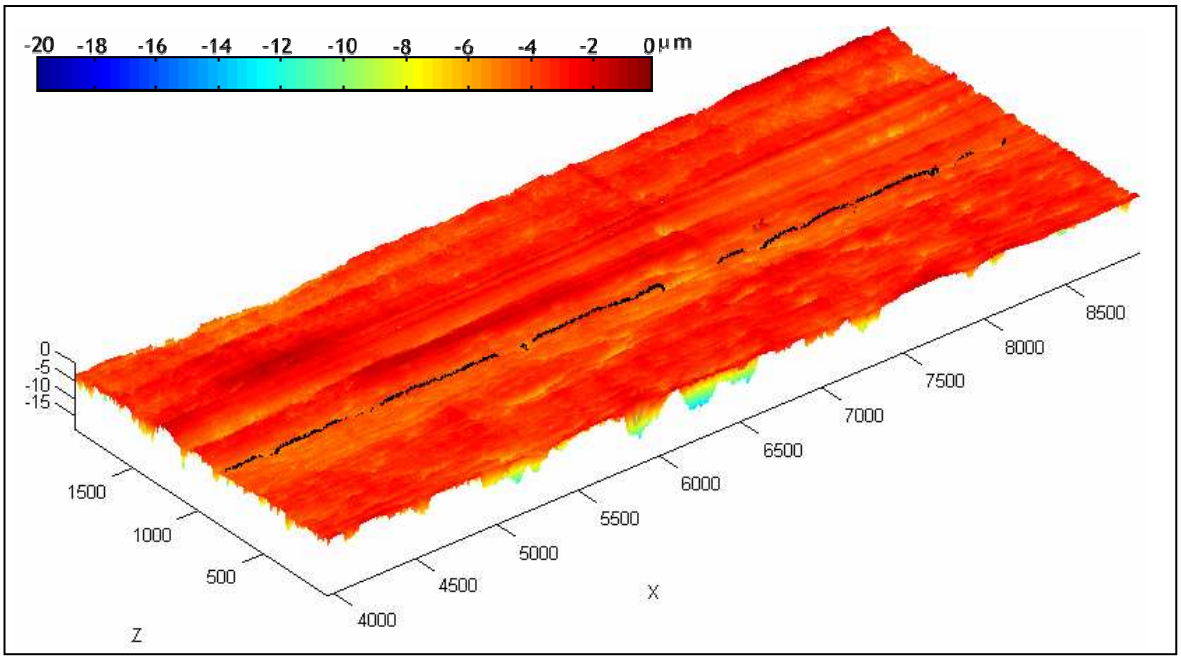


Roughness profiles measured during the gear micropitting tests.

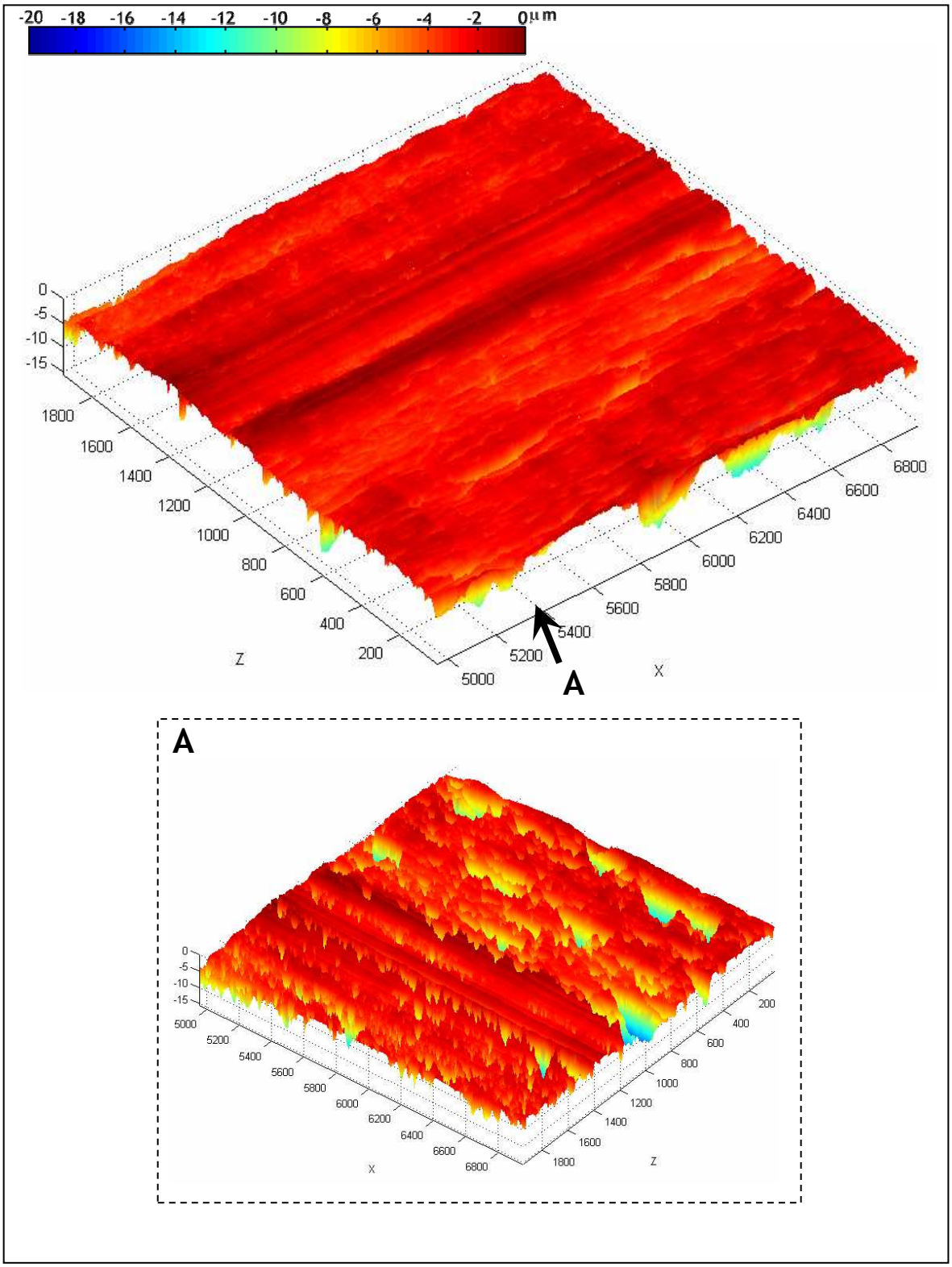
Surface topography measurements



Topography measurement (2X12 mm) made in the pinion of the carburized gear lubricated with the mineral oil (dimensions in µm).



Part of the topography measurement (2X5 mm) made in the pinion of the carburized gear lubricated with the mineral oil (dimensions in µm) and roughness profile presented in Table 4.16.



Part of the topography measurement (2X2 mm) made in the pinion of the carburized gear lubricated with the mineral oil (dimensions in µm).

FZG gear micropitting test of carburized gear lubricated by E1 gear oil (C-E1)

Test reference: GFKT-C14/8.3/90 **Oil reference: E1**

Gear type: C14 **Gear reference: 2C-1 Side: A**

Gear material: Carburized steel (DIN 20MnCr5)

Mass loss [mg]

Load stage	running in+k6	K8	K9
Pinion	11	12	12
Wheel	12	9	14
Total	23	21	26

Micropitted area [%]

	running in+k6	K8	K9
1st tooth	2	6	23
5^{th} tooth	2	6	25
Average	2	6	24

Ferrometry

Load stage	K3	K6	K8	K9
d	0.1	0.1	0.1	0.1
DL	15.2	19.3	15.5	23.5
DS	2.4	3.8	3.6	4.5
CPUC	176.0	231.0	191.0	280.0
ISUC	2.3E+04	3.6E+04	2.3E+04	5.3E+04

Surface roughness measurements

Surface roughness parameters [μm]

		Dir.		R_{max}	R_{z-D}	R_a	R_q	M_{r1}	R_{pk}	R_k	R_{vk}	M_{r2}	Vo
Wheel	Initial	Axial		1.14	0.74	0.13	0.16	8.4	0.15	0.39	0.27	85.1	22.3
		Radial		8.41	6.38	1.14	1.47	9.0	1.56	3.64	1.95	86.9	129.8
Pinion	Initial	Axial		1.36	0.89	0.15	0.20	9.2	0.20	0.49	0.33	87.5	20.4
		Radial		7.58	6.17	1.14	1.40	7.4	1.08	4.15	1.64	87.1	107.6
	After ruing-in + K6	Axial	top	0.98	0.64	0.10	0.14	12.4	0.13	0.28	0.26	86.4	18.0
			bottom	1.92	1.00	0.11	0.18	7.9	0.12	0.28	0.35	82.5	30.5
		Radial	top	5.00	4.00	0.73	0.92	6.4	0.48	2.25	1.61	82.2	144.0
			bottom	7.00	5.18	0.89	1.20	10.9	1.60	2.83	2.16	85.9	152.5
	After K8	Axial	top	2.56	1.52	0.18	0.28	12.2	0.16	0.45	0.67	85.5	51.5
			bottom	4.85	2.83	0.32	0.55	7.6	0.14	0.59	1.15	77.8	124.9
		Radial	top	4.62	3.61	0.64	0.82	6.8	0.41	2.02	1.50	82.9	129.0
			bottom	6.31	4.91	0.82	1.10	9.4	1.47	2.38	2.04	82.7	177.9
	After K9	Axial	top	3.10	1.99	0.24	0.35	9.3	0.16	0.52	0.78	80.4	76.1
			bottom	3.54	2.51	0.28	0.43	7.5	0.14	0.66	0.95	83.3	81.4
		Radial	top	4.81	3.69	0.65	0.83	11.4	0.86	2.14	1.14	85.4	83.1
			bottom	6.27	4.38	0.71	0.93	5.4	0.41	2.32	1.74	84.9	130.8

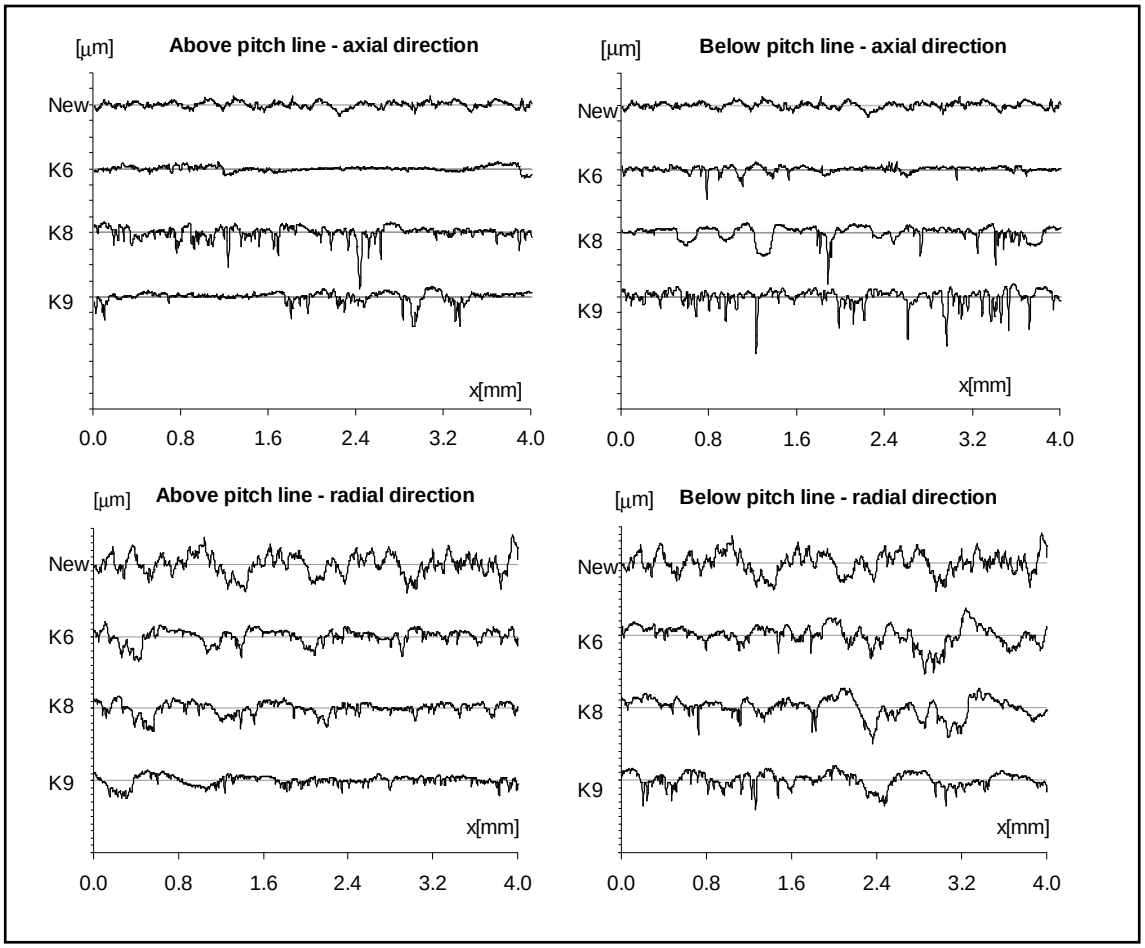
Axial direction pinion roughness parameters variation[%]

	R_{max}	R_{z-D}	R_a	R_q	R_{pk}	R_k	R_{vk}	V_o
$k6_{top}$-original	-28	-28	-36	-32	-35	-44	-21	-12
$k6_{bottom}$- original	41	12	-25	-13	-40	-44	5	50
$k6_{bottom}$-$k6_{top}$	97	55	16	28	-7	0	33	69
$k8_{top}$-$k6_{top}$	162	136	88	107	20	63	156	186
$k8_{bottom}$-$k6_{bottom}$	153	184	183	212	11	115	230	309
$k8_{bottom}$-$k8_{top}$	89	86	76	92	-14	32	71	142
$k9_{top}$-$k8_{top}$	21	31	28	24	4	15	15	48
$k9_{bottom}$-$k8_{bottom}$	-27	-11	-12	-22	7	11	-18	-35
$k9_{bottom}$-$k9_{top}$	14	26	21	20	-11	27	22	7

Radial direction pinion roughness parameters variation[%]								
	R_{max}	R_{z-D}	R_a	R_q	R_{pk}	R_k	R_{vk}	V_o
$k6_{top}$-original	-34	-35	-35	-34	-55	-46	-2	34
$k6_{bottom}$- original	-8	-16	-21	-14	48	-32	32	42
$k6_{bottom}$-$k6_{top}$	40	29	22	30	230	25	35	6
$k8_{top}$-$k6_{top}$	-8	-10	-13	-11	-16	-10	-7	-10
$k8_{bottom}$-$k6_{bottom}$	-10	-5	-8	-9	-8	-16	-5	17
$k8_{bottom}$-$k8_{top}$	37	36	29	34	260	18	37	38
$k9_{top}$-$k8_{top}$	4	2	1	1	109	6	-24	-36
$k9_{bottom}$-$k8_{bottom}$	-1	-11	-14	-15	-72	-3	-15	-27
$k9_{bottom}$-$k9_{top}$	30	19	10	12	-52	8	53	57

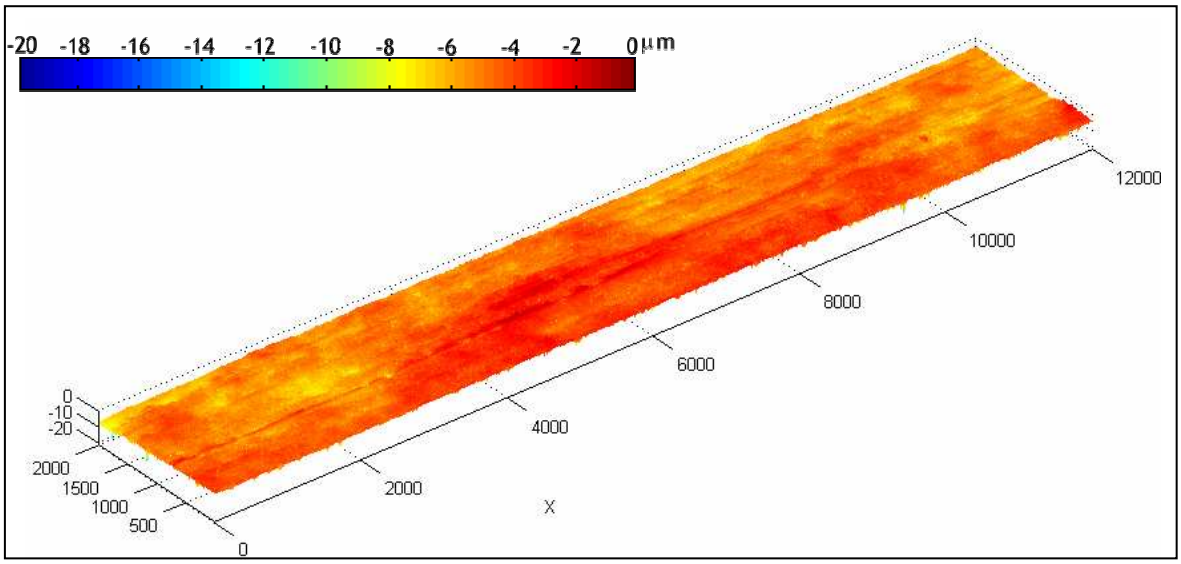
Legend:

top – above pitch line (view Figure 4.11)
bottom - below pitch line (view Figure 4.11)
original – new surface

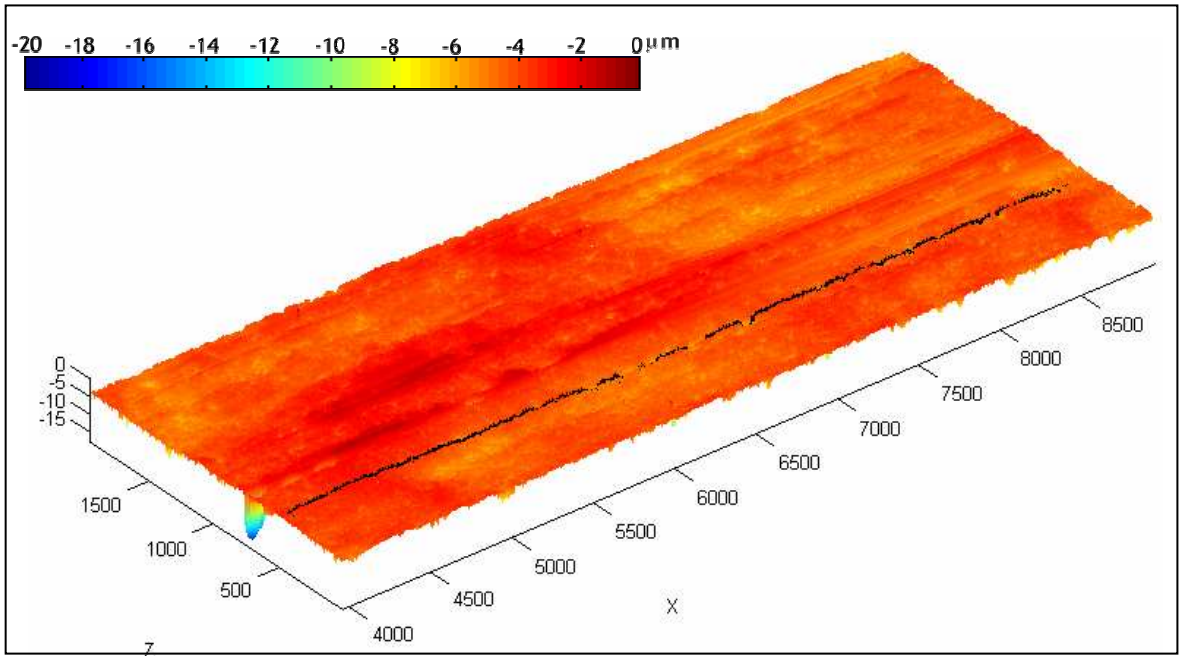


Roughness profiles measured during the gear micropitting tests.

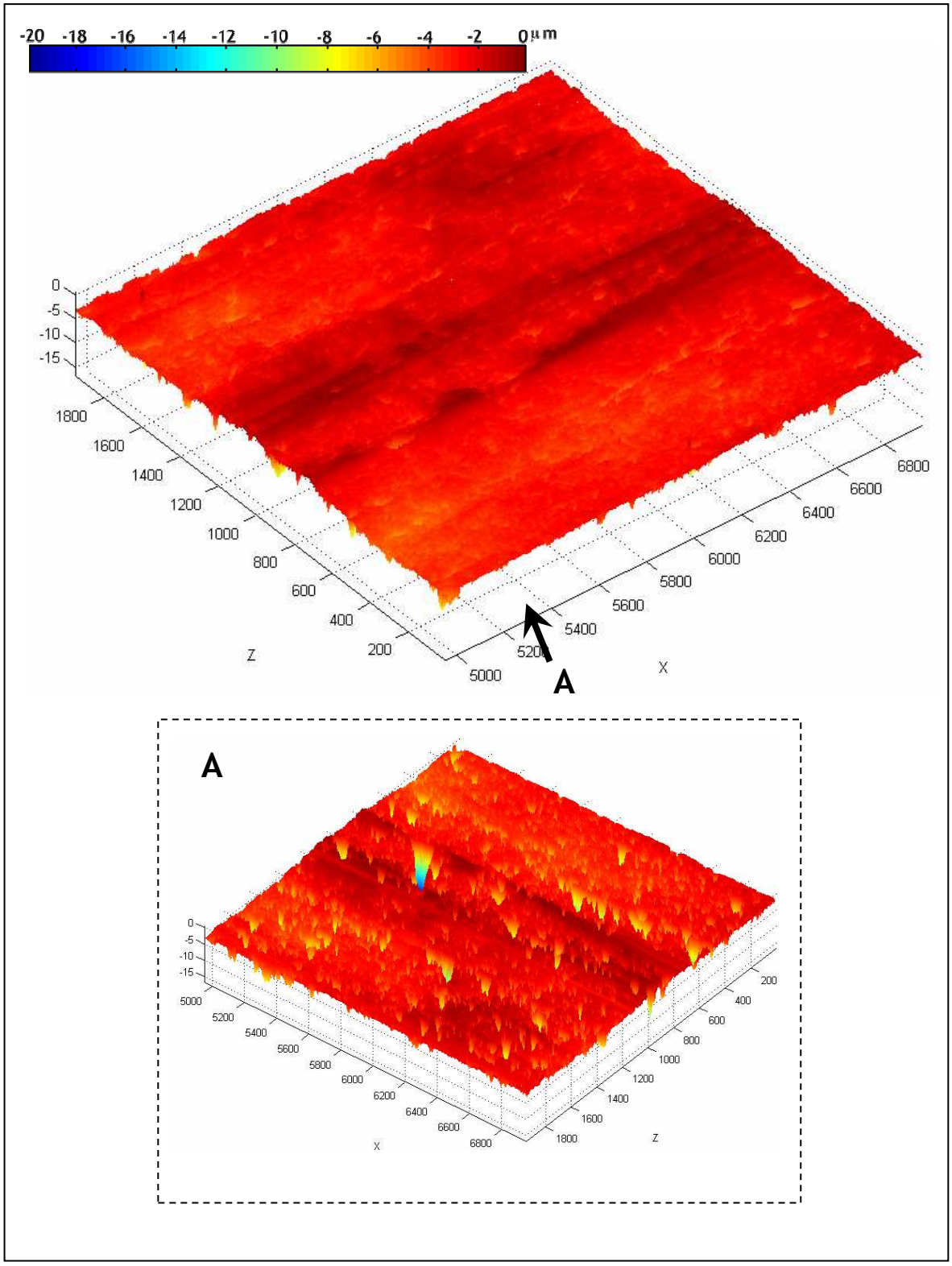
Surface topography measurements



Topography measurement (2X12 mm) made in the pinion of the carburized gear lubricated with ester E1 (dimensions in µm).



Part of the topography measurement (2X5 mm) made in the pinion of the carburized gear lubricated with ester E1 (dimensions in µm) and roughness profile presented in Table 4.16.



Part of the topography measurement (2X2 mm) made in the pinion of the carburized gear lubricated with ester E1 (dimensions in µm).

FZG gear micropitting test of carburized gear lubricated by E2 gear oil (C-E2)

Test reference: GFKT-C14/8.3/90 **Oil reference: E2**

Gear type: C14 **Gear reference: 2C-5 Side: A**

Gear material: Carburized steel (DIN 20MnCr5)

Mass loss [mg]

Load stage	running in+k6	K8	K9
Pinion	6	5	18
Wheel	7	2	13
Total	13	7	31

Micropitted area [%]

	running in+k6	K8	K9
1st tooth	3	11	15
5^{th} tooth	4	14	20
Average	3	13	17

Ferrometry

Load stage	K3	K6	K8	K9
d	0.1	0.1	0.1	0.1
DL	6.7	16.6	12.2	21.2
DS	1.6	2.4	3.5	2.9
CPUC	83.0	190.0	157.0	241.0
ISUC	4.2E+03	2.7E+04	1.4E+04	4.4E+04

Surface roughness measurements

Surface roughness parameters [µm]

		Dir.		R_{max}	R_{z-D}	R_a	R_q	M_{r1}	R_{pk}	R_k	R_{vk}	M_{r2}	Vo
Wheel	Initial	Axial		1.06	0.72	0.13	0.17	9.1	0.15	0.40	0.26	86.5	18.9
		Radial		7.28	5.75	1.04	1.29	6.6	0.85	3.44	1.69	86.5	113.5
Pinion	Initial	Axial		1.45	0.84	0.13	0.18	13.1	0.24	0.35	0.31	86.0	22.4
		Radial		7.51	6.45	1.18	1.47	7.6	1.20	3.89	1.82	84.2	163.7
	After running-in + K6	Axial	top	1.18	0.80	0.12	0.17	8.6	0.09	0.33	0.33	82.0	31.0
			bottom	2.19	1.75	0.21	0.31	7.9	0.13	0.49	0.65	82.7	58.9
		Radial	top	5.24	4.52	0.86	1.07	5.1	0.62	2.64	1.58	80.3	156.1
			bottom	6.96	5.49	1.07	1.37	8.6	1.58	2.88	2.50	77.5	282.4
	After K8	Axial	top	0.83	0.48	0.08	0.11	12.9	0.15	0.24	0.20	86.3	14.8
			bottom	4.13	2.99	0.37	0.58	9.1	0.22	0.57	1.55	79.6	156.6
		Radial	top	4.57	3.86	0.67	0.85	6.4	0.54	1.98	1.40	81.3	131.7
			bottom	6.69	5.11	1.05	1.33	8.8	1.31	3.44	1.93	81.6	175.8
	After K9	Axial	top	2.83	1.29	0.19	0.30	8.8	0.18	0.45	0.71	84.0	56.6
			bottom	3.01	2.14	0.25	0.37	6.7	0.12	0.54	0.83	81.7	75.1
		Radial	top	4.08	3.40	0.57	0.72	7.0	0.43	1.88	1.02	84.2	81.0
			bottom	7.52	5.04	0.81	1.09	7.7	0.80	2.40	1.89	81.5	176.4

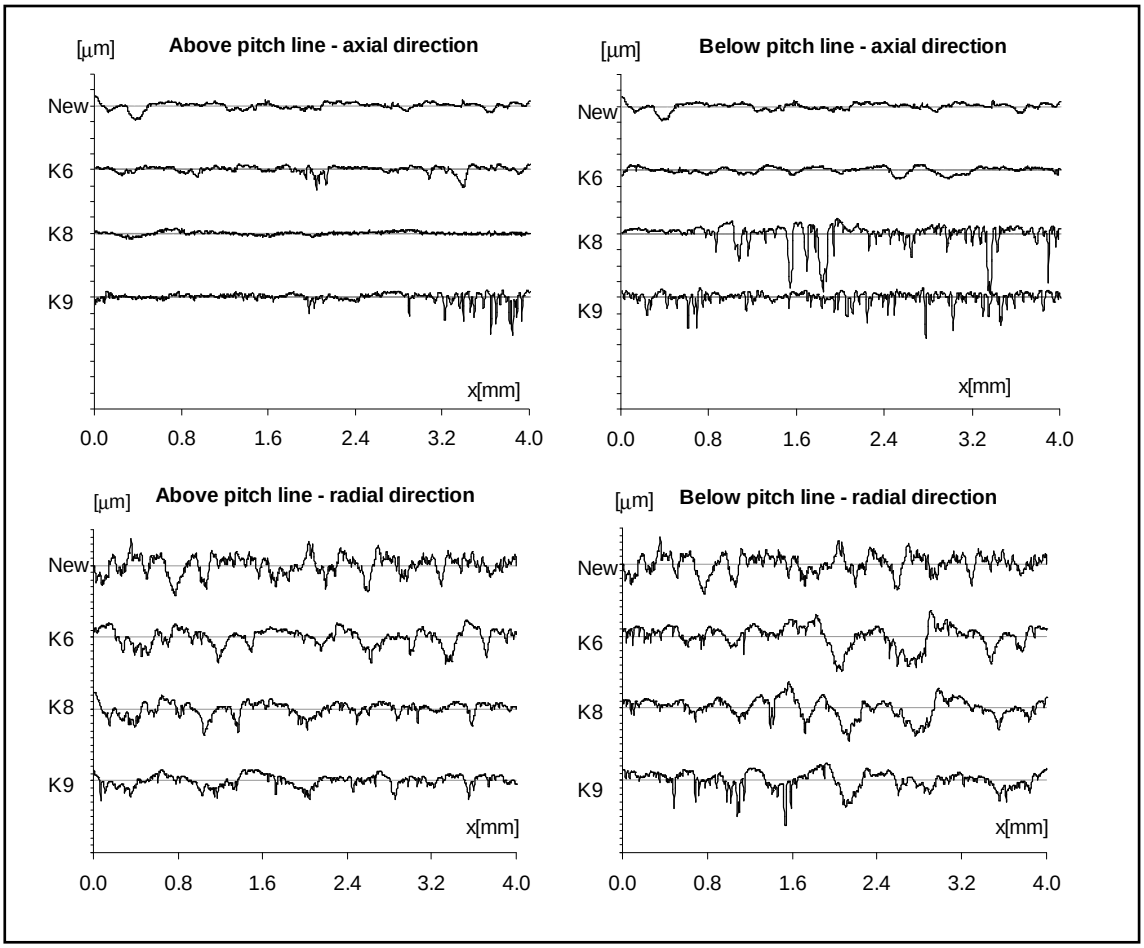
Axial direction pinion roughness parameters variation[%]

	R_{max}	R_{z-D}	R_a	R_q	R_{pk}	R_k	R_{vk}	V_o
$k6_{top}$-original	-19	-5	-3	-7	-64	-6	5	38
$k6_{bottom}$- original	51	109	66	73	-46	41	110	163
$k6_{bottom}$-$k6_{top}$	86	119	71	86	51	50	100	90
$k8_{top}$-$k6_{top}$	-29	-40	-34	-34	75	-27	-38	-52
$k8_{bottom}$-$k6_{bottom}$	89	71	74	88	66	17	138	166
$k8_{bottom}$-$k8_{top}$	396	528	355	431	43	141	665	955
$k9_{top}$-$k8_{top}$	240	170	132	174	16	87	250	282
$k9_{bottom}$-$k8_{bottom}$	-27	-28	-33	-37	-44	-6	-47	-52
$k9_{bottom}$-$k9_{top}$	6	66	31	22	-31	21	16	33

Radial direction pinion roughness parameters variation[%]								
	R_{max}	R_{z-D}	R_a	R_q	R_{pk}	R_k	R_{vk}	V_o
$k6_{top}$-original	-30	-30	-27	-27	-48	-32	-13	-5
$k6_{bottom}$- original	-7	-15	-10	-7	32	-26	37	73
$k6_{bottom}$-$k6_{top}$	33	21	24	28	153	9	58	81
$k8_{top}$-$k6_{top}$	-13	-15	-22	-21	-13	-25	-12	-16
$k8_{bottom}$-$k6_{bottom}$	-4	-7	-1	-3	-17	19	-23	-38
$k8_{bottom}$-$k8_{top}$	46	32	57	56	143	73	38	33
$k9_{top}$-$k8_{top}$	-11	-12	-15	-16	-21	-5	-27	-38
$k9_{bottom}$-$k8_{bottom}$	12	-1	-23	-18	-39	-30	-2	0
$k9_{bottom}$-$k9_{top}$	84	48	44	52	89	27	86	118

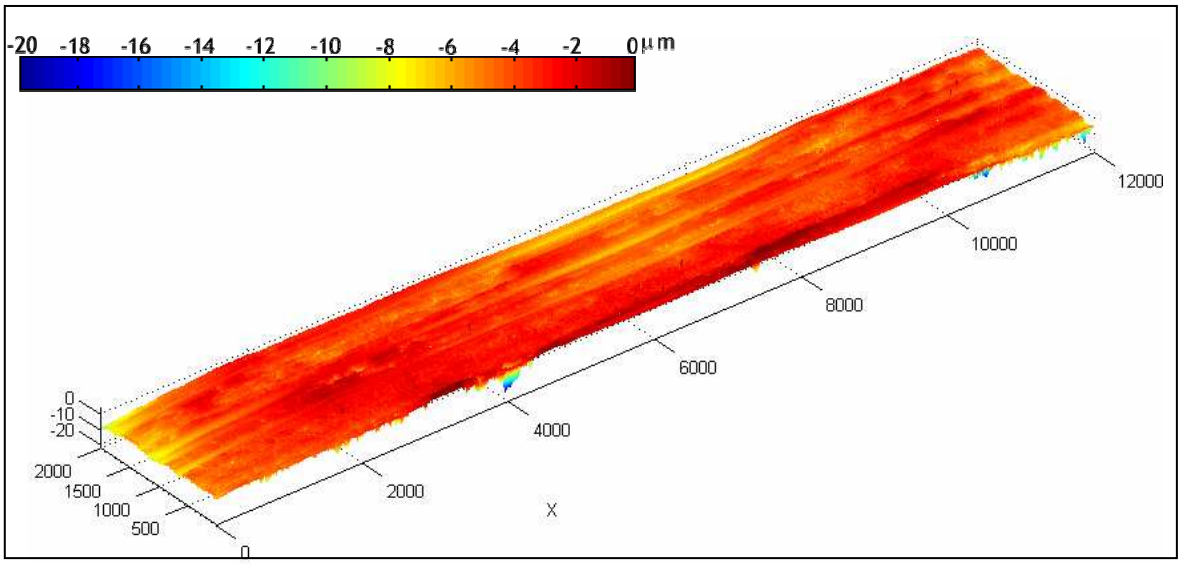
Legend:

top – above pitch line (view Figure 4.11)
bottom - below pitch line (view Figure 4.11)
original – new surface

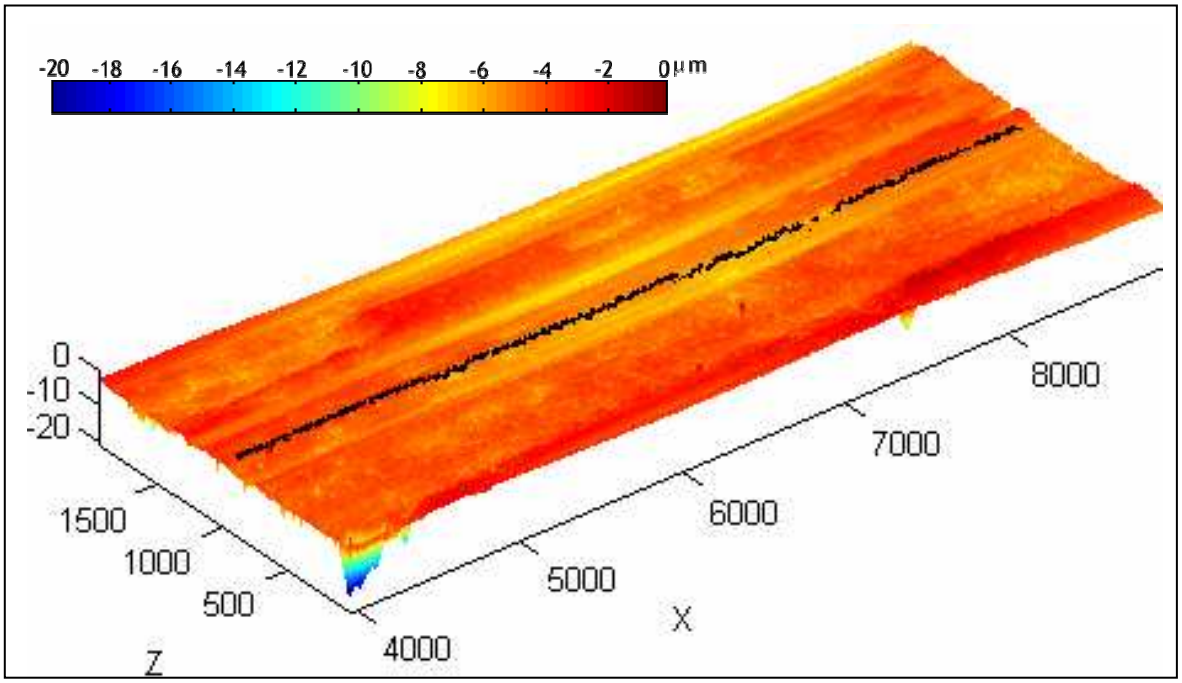


Roughness profiles measured during the gear micropitting tests.

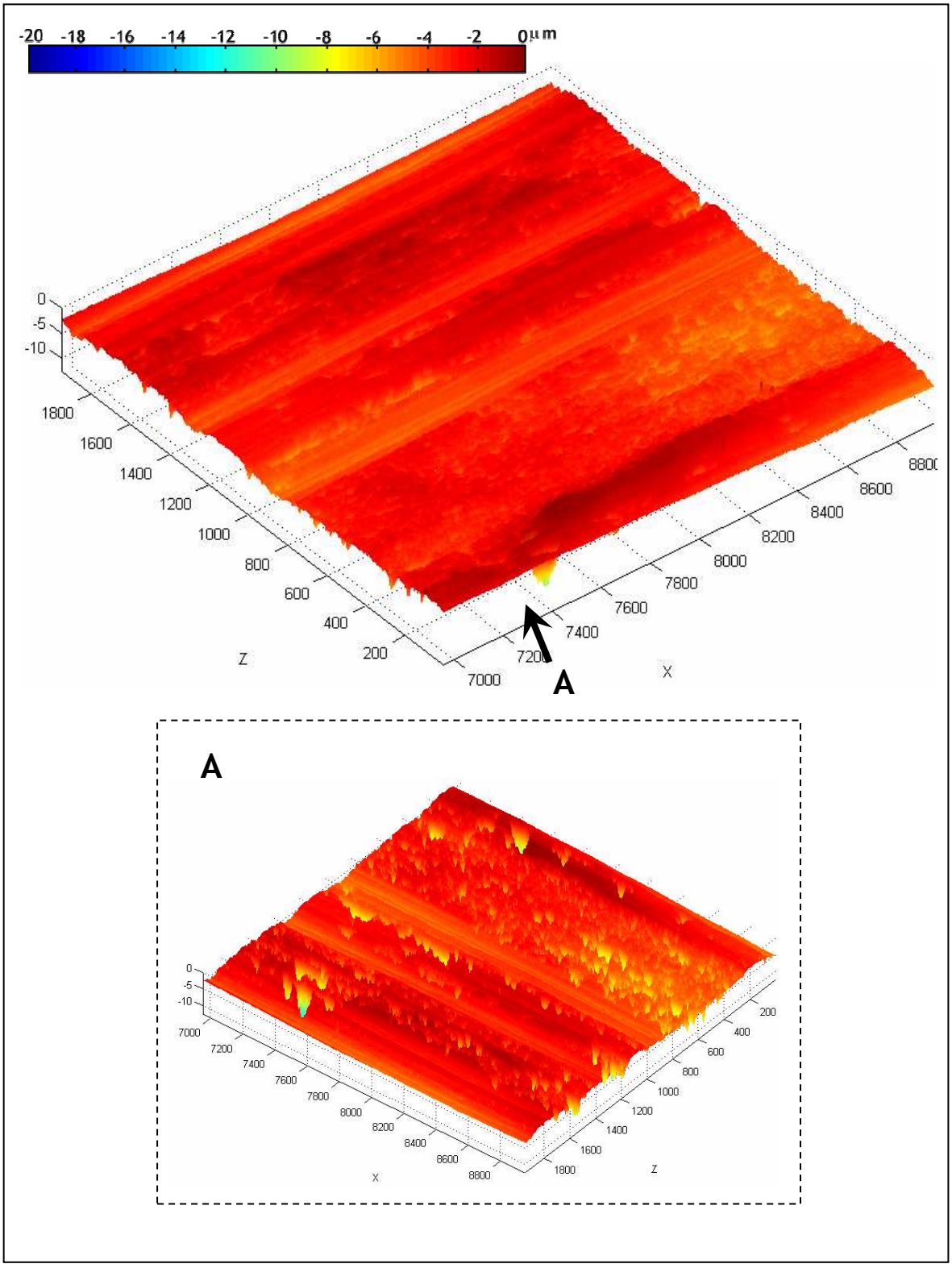
Surface topography measurements



Topography measurement (2X12 mm) made in the pinion of the carburized gear lubricated with ester E2 (dimensions in µm).



Part of the topography measurement (2X5 mm) made in the pinion of the carburized gear lubricated with ester E2 (dimensions in µm) and roughness profile presented in Table 4.16.



Topography measurement (2X12 mm) made in the pinion of the carburized gear lubricated with ester E2 (dimensions in µm).

FZG gear micropitting test of carburized gear lubricated by E3 gear oil (C-E3)

Test reference: GFKT-C14/8.3/90 **Oil reference: E3**

Gear type: C14 **Gear reference: 2C-1 Side: B**

Gear material: Carburized steel (DIN 20MnCr5)

Mass loss [mg]

Load stage	running in+k6	K8	K9
Pinion	11	7	13
Wheel	3	20	23
Total	14	27	36

Micropitted area [%]

	running in+k6	K8	K9
1st tooth	4	8	14
5^{th} tooth	5	11	16
Average	5	9	15

Ferrometry

Load stage	K3	K6	K8	K9
d	0.1	0.1	0.1	0.1
DL	17.9	21.2	13.3	20.6
DS	4.0	4.3	4.3	4.6
CPUC	219.0	255.0	176.0	252.0
ISUC	3.0E+04	4.3E+04	1.6E+04	4.0E+04

Surface roughness measurements

Surface roughness parameters [μm]

		Dir.		R_{max}	R_{z-D}	R_a	R_q	M_{r1}	R_{pk}	R_k	R_{vk}	M_{r2}	Vo
Wheel	Initial	Axial		1.60	1.04	0.18	0.25	11.0	0.29	0.56	0.38	85.51	29.0
		Radial		7.28	5.68	1.05	1.31	10.4	1.20	3.63	1.53	88.82	85.3
Pinion	Initial	Axial		1.48	1.02	0.18	0.24	9.7	0.24	0.59	0.40	86.17	29.8
		Radial		9.81	8.12	1.53	1.93	8.4	1.74	5.41	2.23	87.83	141.1
	After running-in	Axial	top	2.98	1.82	0.27	0.38	8.0	0.17	0.59	0.85	81.41	84.8
			bottom	1.45	0.86	0.12	0.18	11.8	0.16	0.34	0.41	85.23	30.1
		Radial	top	6.48	5.15	0.94	1.24	5.6	0.91	2.36	2.42	76.40	294.5
			bottom	7.64	5.86	1.08	1.40	8.3	1.45	3.10	2.14	80.50	205.4
	After K8	Axial	top	3.04	2.17	0.27	0.39	7.1	0.25	0.66	0.72	80.21	72.3
			bottom	2.01	1.68	0.22	0.32	7.4	0.16	0.49	0.84	81.42	75.0
		Radial	top	6.03	4.73	0.84	1.08	5.1	0.62	2.37	1.98	77.72	224.0
			bottom	6.74	5.00	0.89	1.16	8.1	0.95	2.54	1.77	78.08	189.3
	After K9	Axial	top	3.41	2.57	0.41	0.56	6.8	0.19	1.04	1.16	81.25	108.5
			bottom	4.19	2.93	0.33	0.50	9.3	0.25	0.75	1.10	83.06	95.1
		Radial	top	6.94	4.45	0.80	1.04	4.2	0.53	2.22	1.86	75.85	223.7
			bottom	8.13	5.18	0.83	1.12	9.3	0.88	2.48	1.86	81.27	165.9

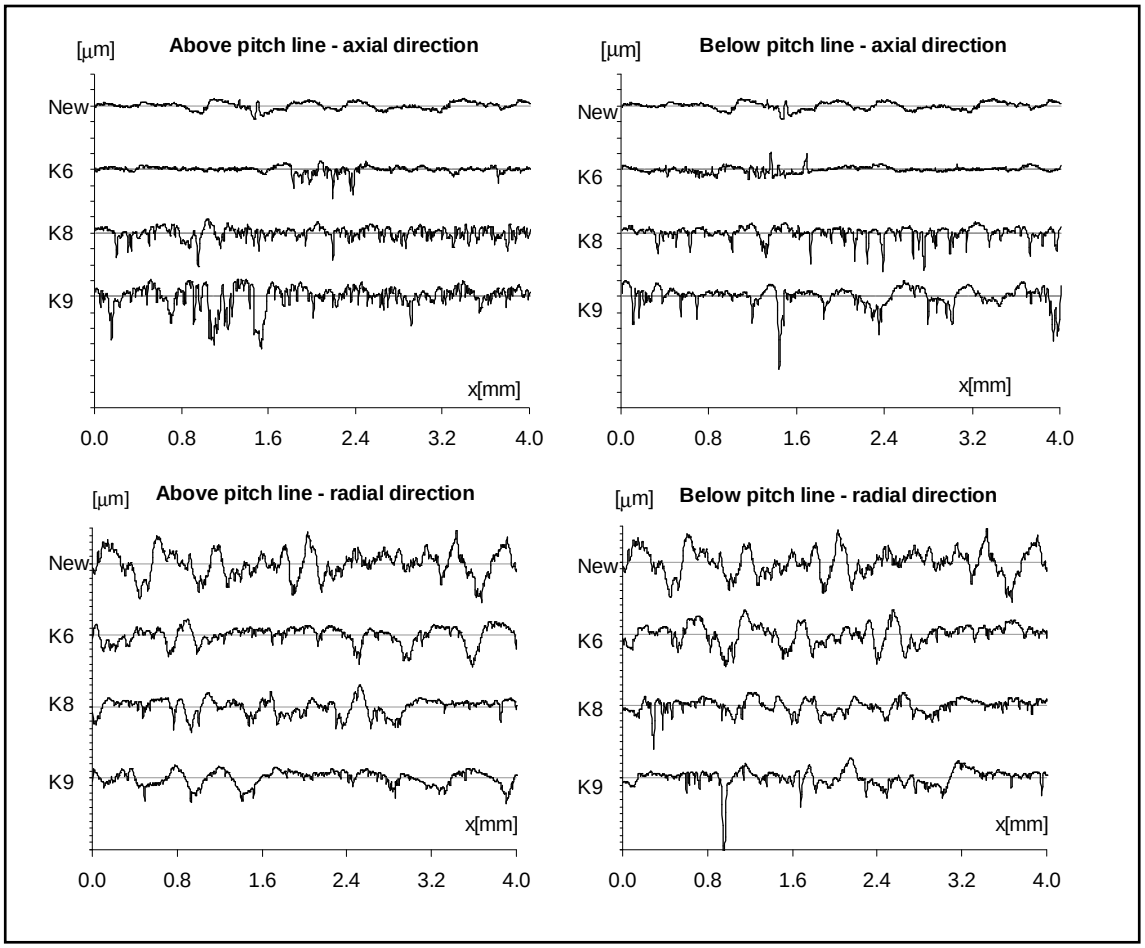
Axial direction pinion roughness parameters variation[%]

	R_{max}	R_{z-D}	R_a	R_q	R_{pk}	R_k	R_{vk}	V_o
$k6_{top}$-original	102	78	45	56	-29	0	111	185
$k6_{bottom}$- original	-2	-16	-32	-25	-34	-43	1	1
$k6_{bottom}$-$k6_{top}$	-51	-53	-54	-52	-7	-43	-52	-65
$k8_{top}$-$k6_{top}$	2	19	1	3	48	12	-15	-15
$k8_{bottom}$-$k6_{bottom}$	39	96	78	77	3	45	106	149
$k8_{bottom}$-$k8_{top}$	-34	-23	-19	-17	-35	-26	16	4
$k9_{top}$-$k8_{top}$	12	19	53	44	-25	57	61	50
$k9_{bottom}$-$k8_{bottom}$	109	75	49	55	53	55	31	27
$k9_{bottom}$-$k9_{top}$	23	14	-21	-11	33	-27	-5	-12

Radial direction pinion roughness parameters variation[%]								
	R_{max}	R_{z-D}	R_a	R_q	R_{pk}	R_k	R_{vk}	V_o
$k6_{top}$-original	-34	-37	-38	-36	-48	-56	9	109
$k6_{bottom}$- original	-22	-28	-30	-28	-17	-43	-4	46
$k6_{bottom}$-$k6_{top}$	18	14	14	13	60	31	-12	-30
$k8_{top}$-$k6_{top}$	-7	-8	-11	-12	-31	1	-18	-24
$k8_{bottom}$-$k6_{bottom}$	-12	-15	-17	-17	-35	-18	-17	-8
$k8_{bottom}$-$k8_{top}$	12	6	6	7	52	7	-10	-15
$k9_{top}$-$k8_{top}$	15	-6	-5	-3	-15	-6	-6	0
$k9_{bottom}$-$k8_{bottom}$	21	4	-7	-3	-7	-3	5	-12
$k9_{bottom}$-$k9_{top}$	17	16	4	7	66	12	0	-26

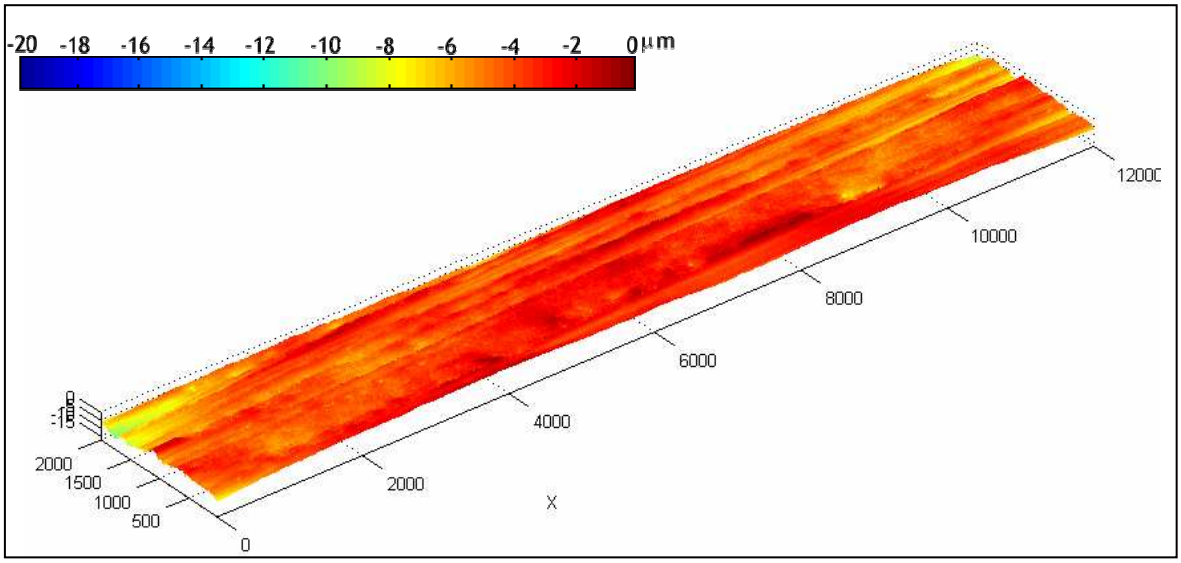
Legend:

top – above pitch line (view Figure 4.11)
bottom - below pitch line (view Figure 4.11)
original – new surface

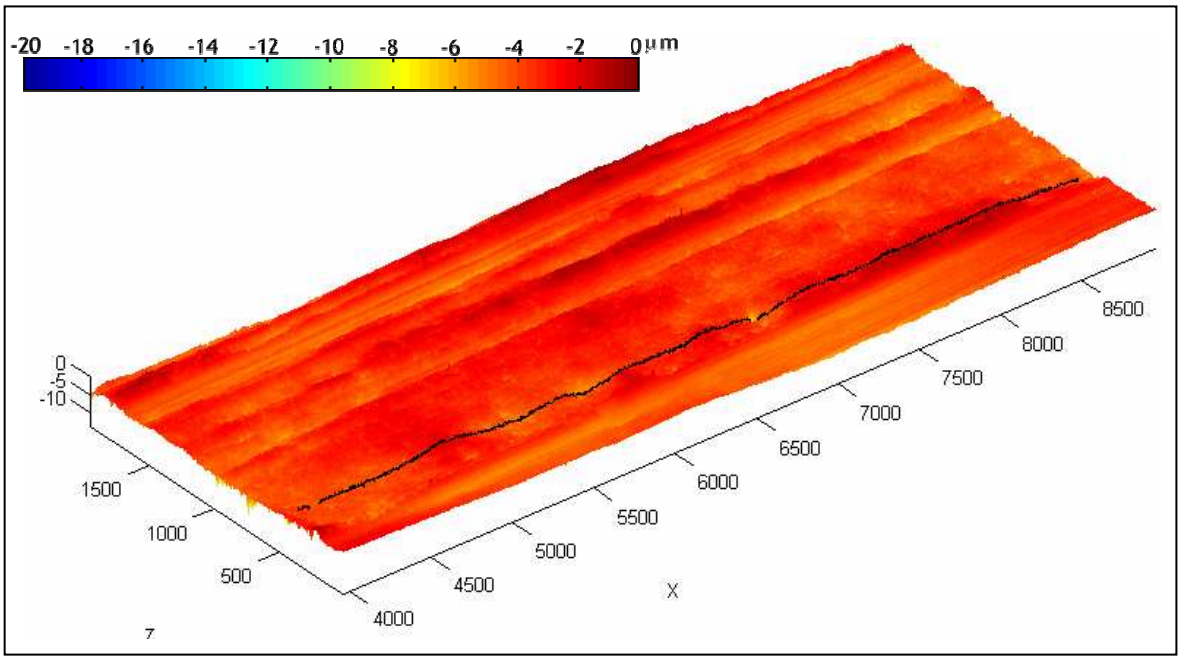


Roughness profiles measured during the gear micropitting tests.

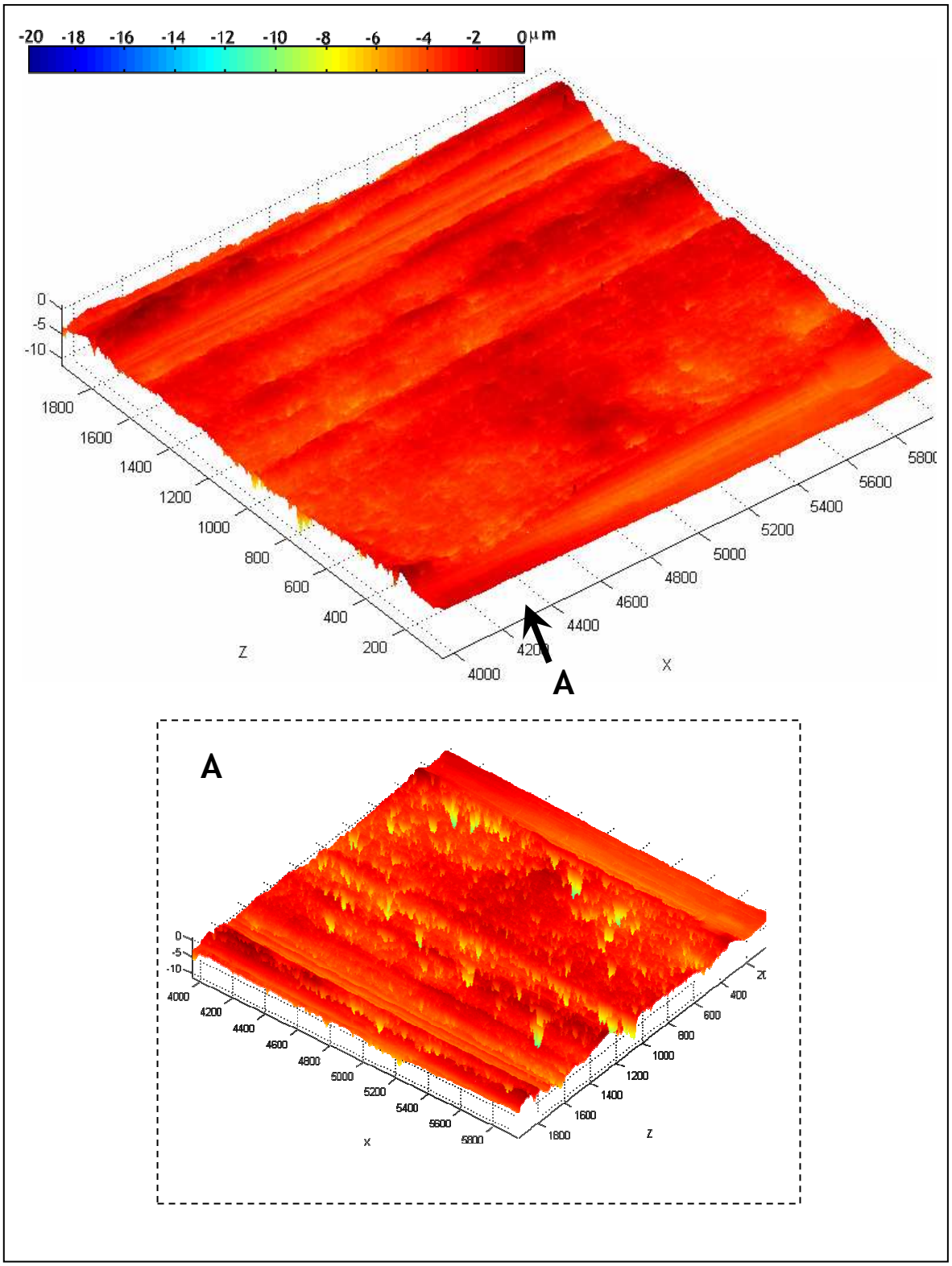
Surface topography measurements



Topography measurement (2X12 mm) made in the pinion of the carburized gear lubricated with ester E3 (dimensions in µm).



Part of the topography measurement (2X5 mm) made in the pinion of the carburized gear lubricated with ester E3 (dimensions in µm) and roughness profile presented in Table 4.16.



Part of the topography measurement (2X2 mm) made in the pinion of the carburized gear lubricated with ester E3 (dimensions in µm).

FZG gear micropitting test of nitrided gear lubricated by M1 gear oil (N-M1)

Test reference: GFKT-C14/8.3/90 **Oil reference: M1**

Gear type: C14 **Gear reference: 2NT-1 Side: A**

Gear material: High pressure nitrided steel (DIN 34 CrNiMo 6)

Mass loss [mg]

Load stage	running in+k6	K8	K9
Pinion	4	1	16
Wheel	1	9	11
Total	5	10	27

Micropitted area [%]

	running in+k6	K8	K9
1st tooth	0	0	10
5^{th} tooth	0	0	16
Average	0	0	13

Ferrometry

Load stage	K3	K6	K8	K9
d	0.1	0.1	0.1	0.1
DL	5.1	4.4	14.7	16.5
DS	2.6	1.6	3.3	5.5
CPUC	77.0	60.0	180.0	220.0
ISUC	1.9E+03	1.7E+03	2.1E+04	2.4E+04

Surface roughness measurements

Surface roughness parameters [µm]

		Dir.		R_{max}	R_{z-D}	R_a	R_q	M_{r1}	R_{pk}	R_k	R_{vk}	M_{r2}	Vo
Wheel	Initial	Axial		1.45	1.00	0.15	0.21	12.5	0.25	0.46	0.31	86.92	22.1
		Radial		8.10	6.81	1.12	1.42	8.4	1.16	3.59	1.99	87.93	119.3
Pinion	Initial	Axial		1.49	0.90	0.12	0.18	11.2	0.29	0.36	0.28	87.86	19.4
		Radial		7.39	6.34	1.11	1.38	6.7	1.05	3.90	1.44	88.73	81.8
	After running-in + K6	Axial	top	0.90	0.64	0.10	0.13	10.1	0.22	0.30	0.19	85.35	14.1
			bottom	1.42	1.02	0.15	0.21	6.7	0.08	0.43	0.47	83.20	38.1
		Radial	top	5.76	4.46	0.75	0.96	7.3	0.54	2.36	1.45	84.29	114.7
			bottom	6.83	4.95	0.92	1.17	6.5	1.22	2.58	1.87	78.12	206.2
	After K8	Axial	top	1.24	0.88	0.14	0.19	8.0	0.08	0.41	0.34	82.82	29.9
			bottom	2.74	1.38	0.15	0.27	5.5	0.09	0.33	0.49	77.87	53.2
		Radial	top	4.75	3.62	0.63	0.81	7.1	0.46	2.30	1.13	86.49	77.1
			bottom	4.74	3.80	0.69	0.85	4.7	0.33	2.05	1.30	80.11	132.7
	After K9	Axial	top	3.22	1.89	0.24	0.40	7.9	0.12	0.47	1.02	80.32	103.0
			bottom	7.71	3.50	0.40	0.83	15.1	0.35	0.40	2.24	82.98	190.0
		Radial	top	4.22	3.13	0.55	0.69	7.5	0.39	1.75	1.08	82.02	98.8
			bottom	8.83	5.29	0.92	1.25	7.2	1.02	2.87	2.37	84.95	180.8

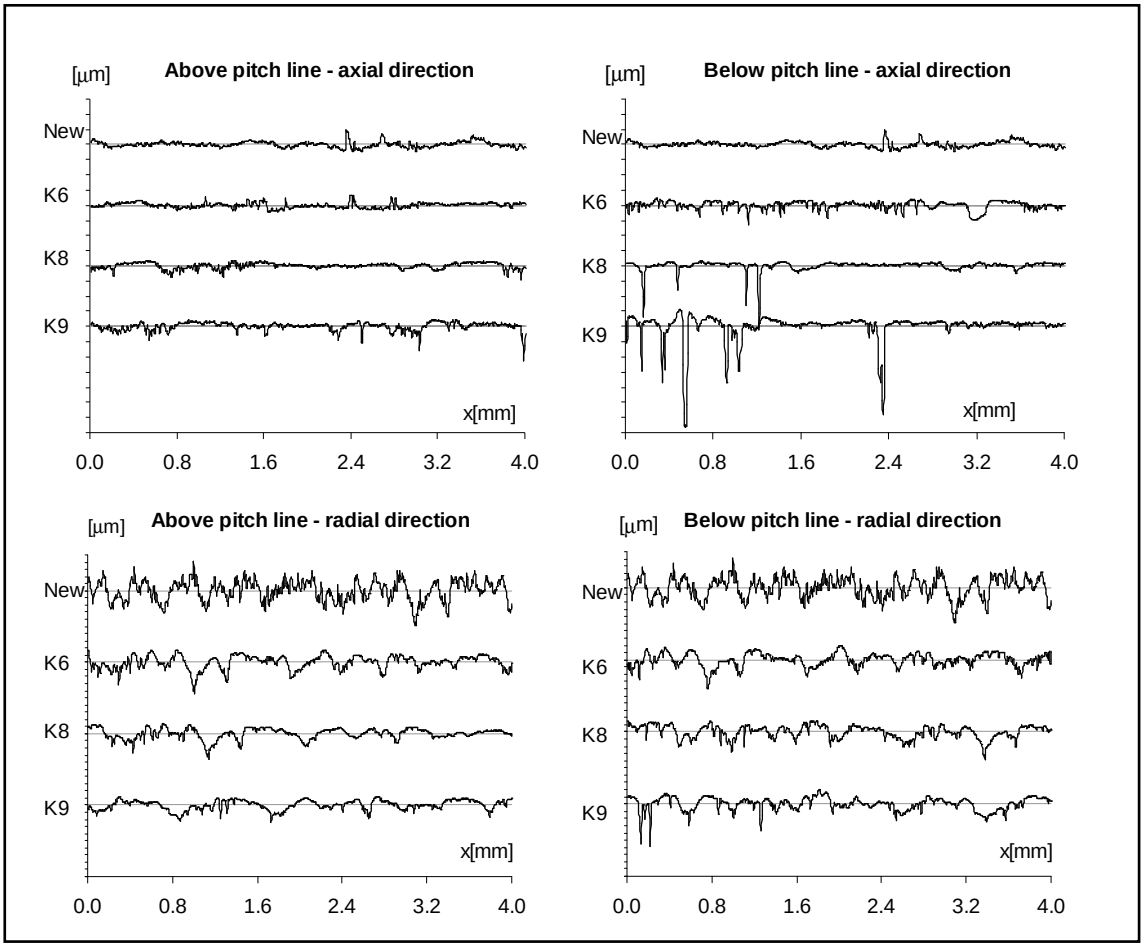
Axial direction pinion roughness parameters variation[%]

	R_{max}	R_{z-D}	R_a	R_q	R_{pk}	R_k	R_{vk}	V_o
$k6_{top}$-original	-39	-29	-23	-25	-24	-17	-32	-27
$k6_{bottom}$- original	-5	14	22	15	-71	18	70	97
$k6_{bottom}$-$k6_{top}$	57	60	60	53	-61	42	149	170
$k8_{top}$-$k6_{top}$	37	39	47	39	-63	38	80	112
$k8_{bottom}$-$k6_{bottom}$	93	35	-1	29	4	-22	5	40
$k8_{bottom}$-$k8_{top}$	121	56	7	42	9	-19	45	78
$k9_{top}$-$k8_{top}$	159	114	74	114	55	14	200	245
$k9_{bottom}$-$k8_{bottom}$	181	154	166	214	302	19	353	257
$k9_{bottom}$-$k9_{top}$	140	85	65	108	182	-16	119	84

Radial direction pinion roughness parameters variation[%]								
	R_{max}	R_{z-D}	R_a	R_q	R_{pk}	R_k	R_{vk}	V_o
$k6_{top}$-original	-22	-30	-33	-30	-49	-40	1	40
$k6_{bottom}$- original	-8	-22	-17	-15	16	-34	30	152
$k6_{bottom}$-$k6_{top}$	19	11	23	22	127	9	29	80
$k8_{top}$-$k6_{top}$	-17	-19	-16	-16	-14	-2	-22	-33
$k8_{bottom}$-$k6_{bottom}$	-31	-23	-25	-28	-73	-21	-30	-36
$k8_{bottom}$-$k8_{top}$	0	5	9	5	-28	-11	15	72
$k9_{top}$-$k8_{top}$	-11	-14	-13	-15	-16	-24	-4	28
$k9_{bottom}$-$k8_{bottom}$	86	39	33	48	206	40	82	36
$k9_{bottom}$-$k9_{top}$	109	69	68	82	161	64	119	83

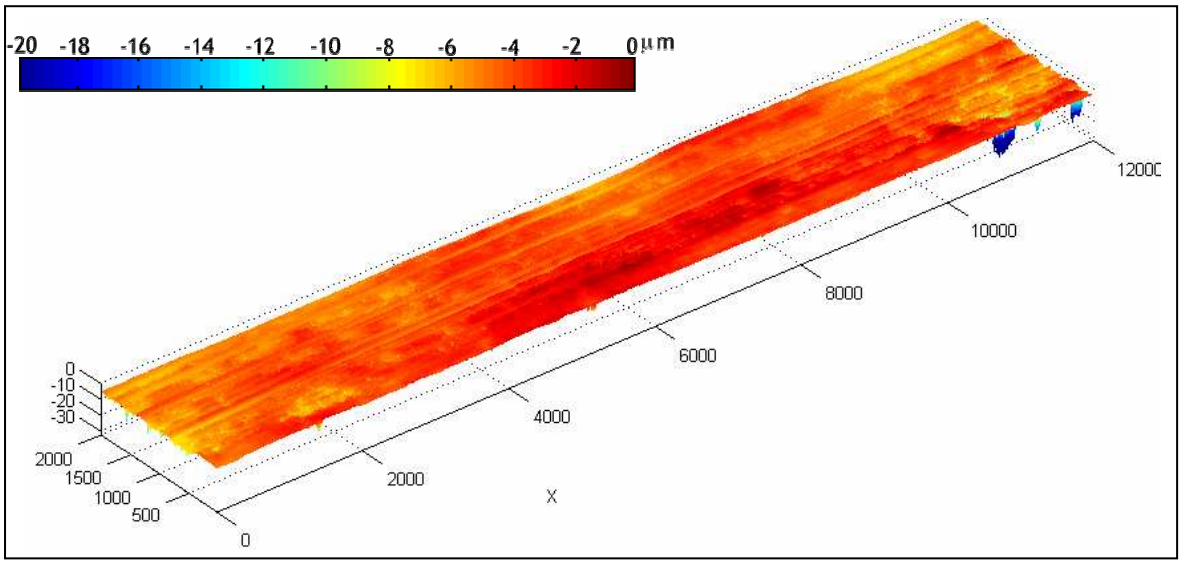
Legend:

top – above pitch line (view Figure 4.11)
bottom - below pitch line (view Figure 4.11)
original – new surface

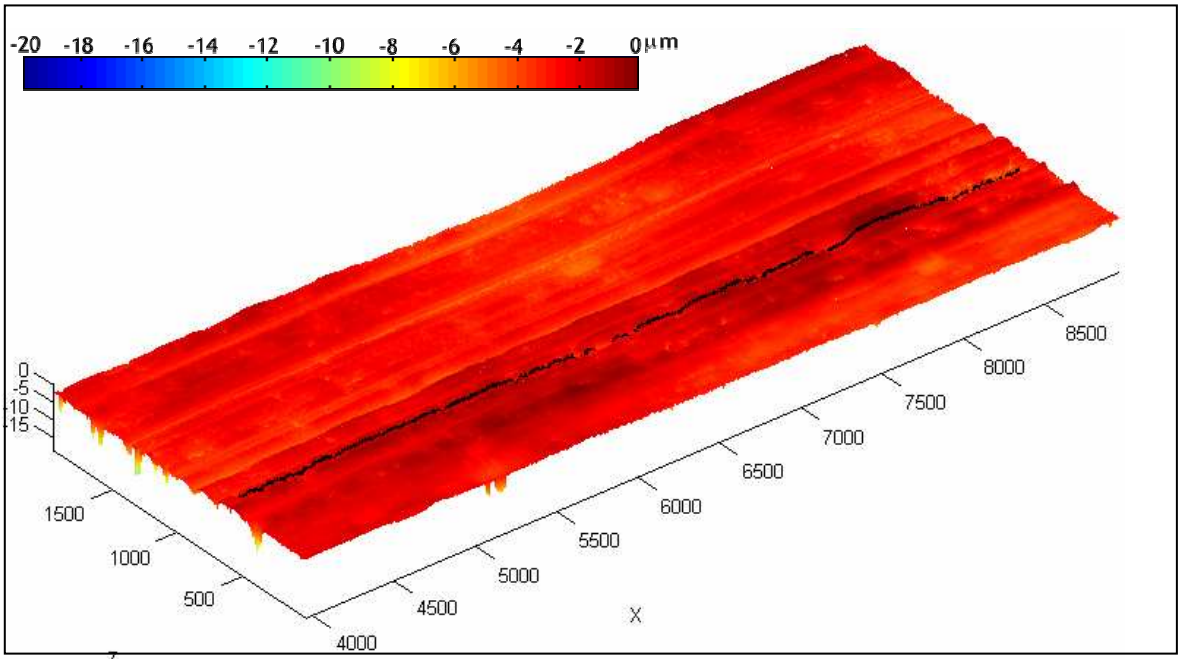


Roughness profiles measured during the gear micropitting tests.

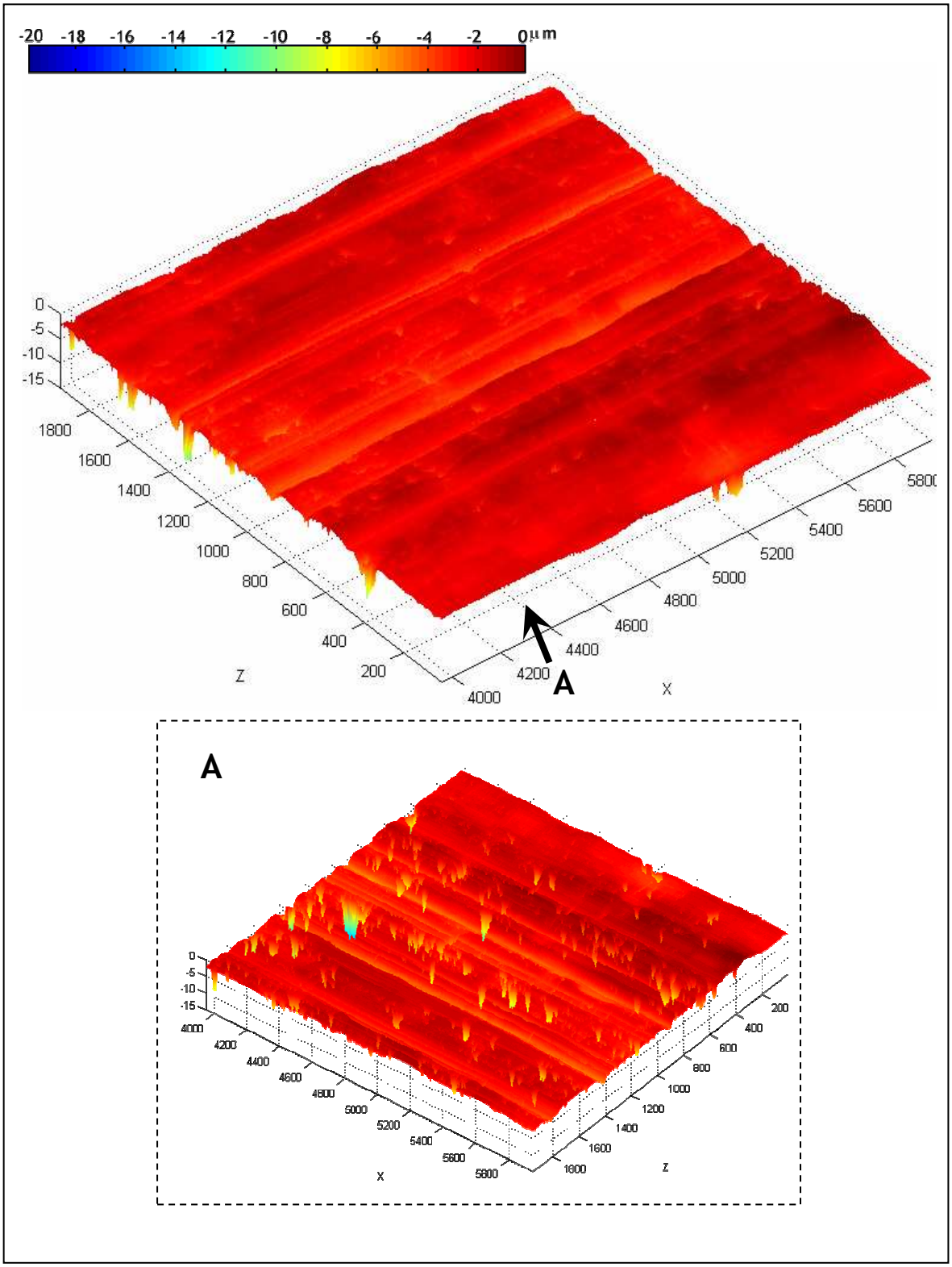
Surface topography measurements



Topography measurement (2X12 mm) made in the pinion of the nitrided gear lubricated with the mineral oil (dimensions in µm).

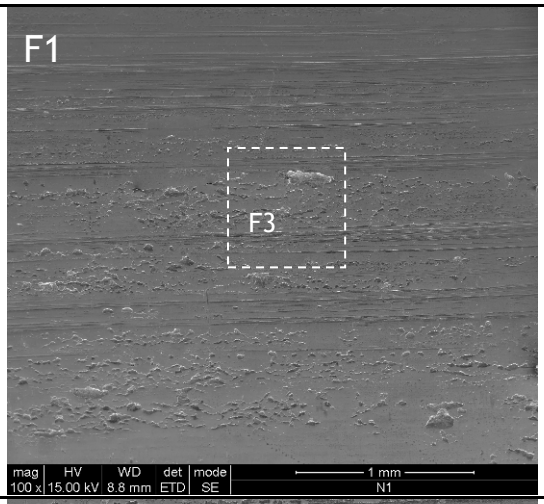
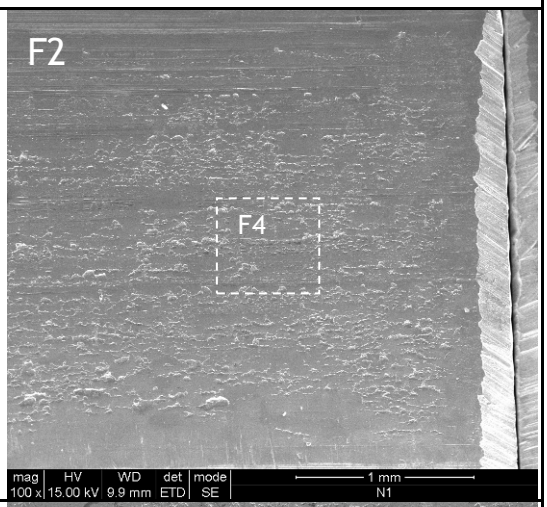
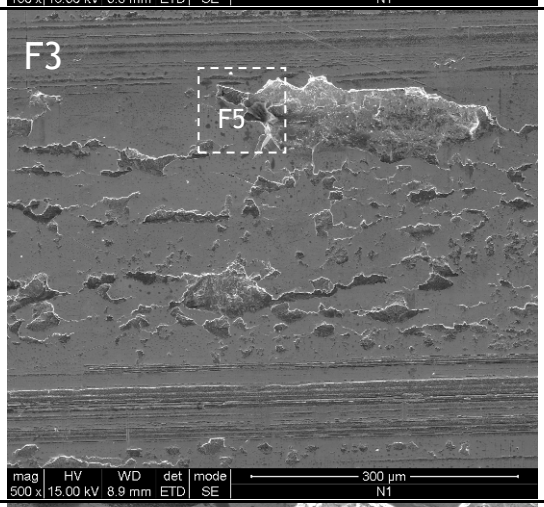
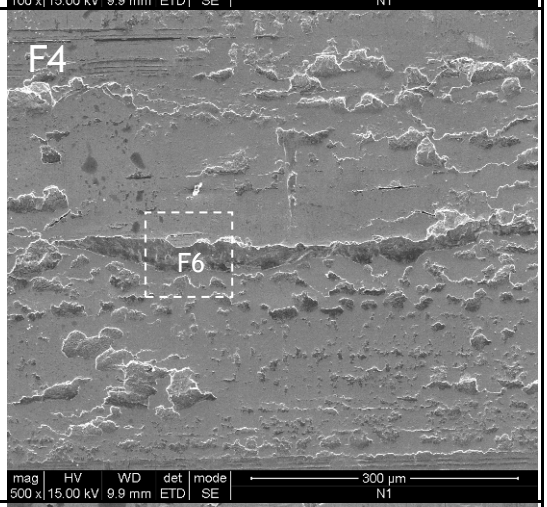
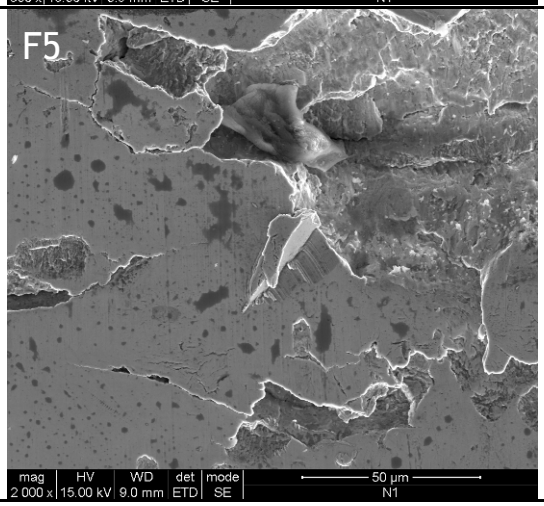
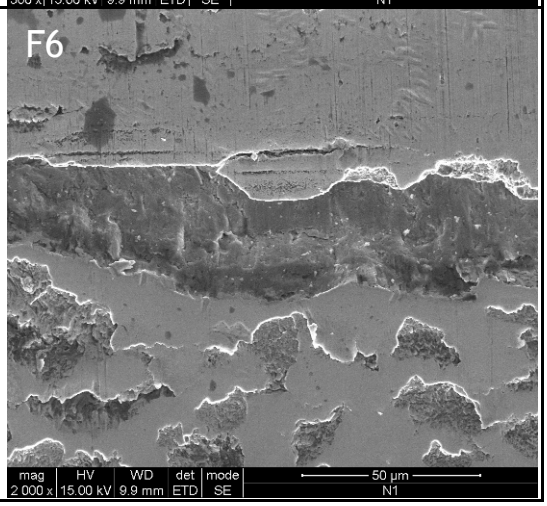


Part of the topography measurement (2X5 mm) made in the pinion of the nitrided gear lubricated with the mineral oil (dimensions in µm) and roughness profile presented in Table 4.16.



Part of the topography measurement (2X2 mm) made in the pinion of the nitrided gear lubricated with the mineral oil (dimensions in µm).

SEM micrographs taken in a pinion tooth flank taken below pith line

	Centre	Left side
100X		
500X		
2000X		

FZG gear micropitting test of nitrided gear lubricated by E1 gear oil (N-E1)

Test reference: GFKT-C14/8.3/90 **Oil reference: E1**

Gear type: C14 **Gear reference: 2NT-2 Side: A**

Gear material: High pressure nitrided steel (DIN 34 CrNiMo 6)

Mass loss [mg]

Load stage	running in+k6	K8	K9
Pinion	4	6	12
Wheel	5	8	29
Total	8	14	41

Micropitted area [%]

	running in+k6	K8	K9
1st tooth	0	0	5
5^{th} tooth	0	0	5
Average	0	0	5

Ferrometry

Load stage	K3	K6	K8	K9
d	0.1	0.1	0.1	0.1
DL	7.7	10	9.2	8.4
DS	2.7	3.6	4.2	3.7
CPUC	104.0	136.0	134.0	121.0
ISUC	5.2E+03	8.7E+03	6.7E+03	5.7E+03

Surface roughness measurements

Surface roughness parameters [µm]

		Dir.		R_{max}	R_{z-D}	R_a	R_q	M_{r1}	R_{pk}	R_k	R_{vk}	M_{r2}	Vo
Wheel	Initial	Axial		1.84	1.32	0.20	0.27	10.6	0.36	0.63	0.37	87.35	24.8
		Radial		7.38	6.50	1.06	1.32	8.2	1.03	3.53	1.39	89.13	75.5
Pinion	Initial	Axial		1.61	1.04	0.15	0.21	12.5	0.30	0.45	0.27	87.76	16.8
		Radial		7.74	6.80	1.19	1.46	6.6	1.03	4.05	1.53	86.33	106.2
	After running-in + K6	Axial	top	1.36	0.97	0.18	0.24	7.4	0.16	0.52	0.53	82.08	47.9
			bottom	0.65	0.44	0.06	0.08	9.1	0.06	0.17	0.13	85.85	9.6
		Radial	top	5.33	4.05	0.73	0.92	5.0	0.50	2.30	1.39	82.53	124.8
			bottom	5.89	4.57	0.84	1.04	5.5	0.63	2.43	1.61	79.21	168.3
	After K8	Axial	top	1.40	0.98	0.16	0.21	9.0	0.19	0.51	0.27	81.89	24.7
			bottom	1.09	0.80	0.15	0.19	10.0	0.11	0.43	0.37	84.28	29.8
		Radial	top	4.83	3.25	0.58	0.75	8.6	0.67	1.89	1.08	85.18	80.5
			bottom	4.36	3.61	0.71	0.88	5.9	0.50	2.16	1.42	79.87	146.8
	After K9	Axial	top	2.34	1.28	0.20	0.29	8.3	0.18	0.53	0.52	81.31	57.2
			bottom	3.92	3.10	0.35	0.56	8.0	0.16	0.63	1.45	84.25	135.4
		Radial	top	4.62	3.17	0.51	0.68	8.9	0.49	1.53	1.38	84.24	108.7
			bottom	6.57	4.22	0.70	0.91	7.5	0.46	2.21	1.64	83.41	136.9

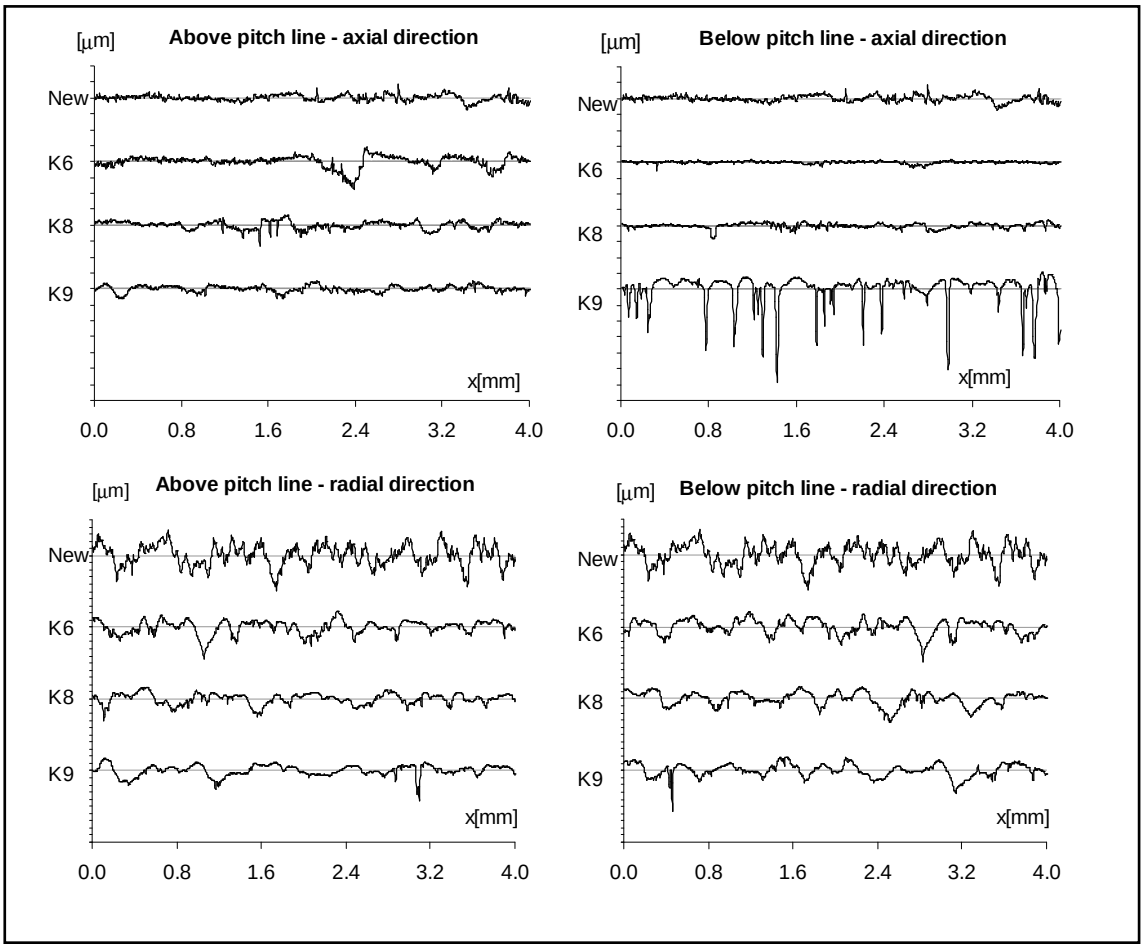
Axial direction pinion roughness parameters variation[%]

	R_{max}	R_{z-D}	R_a	R_q	R_{pk}	R_k	R_{vk}	V_o
$k6_{top}$-original	-15	-7	19	16	-45	15	94	185
$k6_{bottom}$- original	-59	-58	-62	-63	-81	-62	-52	-43
$k6_{bottom}$-$k6_{top}$	-52	-55	-68	-68	-65	-67	-75	-80
$k8_{top}$-$k6_{top}$	3	0	-8	-11	14	-1	-48	-48
$k8_{bottom}$-$k6_{bottom}$	67	81	157	151	98	149	184	211
$k8_{bottom}$-$k8_{top}$	-22	-18	-11	-9	-39	-17	36	20
$k9_{top}$-$k8_{top}$	67	31	22	35	-1	3	92	132
$k9_{bottom}$-$k8_{bottom}$	261	288	139	193	39	46	292	355
$k9_{bottom}$-$k9_{top}$	67	142	75	96	-14	19	177	136

Radial direction pinion roughness parameters variation[%]								
	R_{max}	R_{z-D}	R_a	R_q	R_{pk}	R_k	R_{vk}	V_o
$k6_{top}$-original	-31	-40	-39	-37	-51	-43	-9	18
$k6_{bottom}$- original	-24	-33	-29	-29	-39	-40	6	59
$k6_{bottom}$-$k6_{top}$	10	13	15	14	25	6	16	35
$k8_{top}$-$k6_{top}$	-9	-20	-20	-18	33	-18	-23	-36
$k8_{bottom}$-$k6_{bottom}$	-26	-21	-16	-16	-21	-11	-12	-13
$k8_{bottom}$-$k8_{top}$	-10	11	21	16	-26	14	32	82
$k9_{top}$-$k8_{top}$	-4	-2	-13	-10	-26	-19	28	35
$k9_{bottom}$-$k8_{bottom}$	51	17	-2	3	-7	2	15	-7
$k9_{bottom}$-$k9_{top}$	42	33	37	33	-6	44	19	26

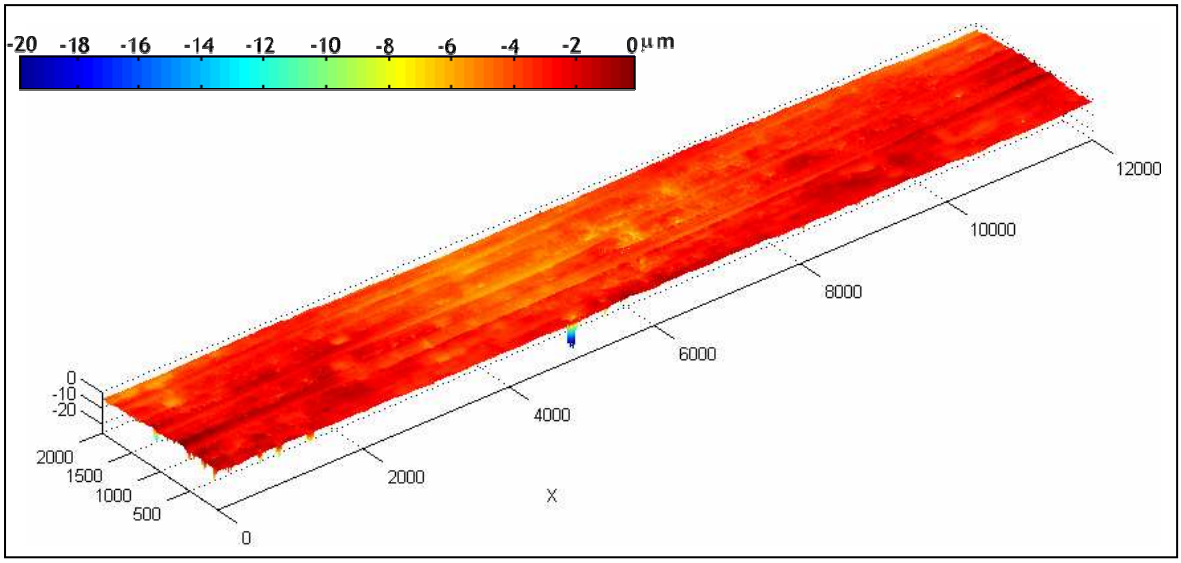
Legend:

top – above pitch line (view Figure 4.11)
bottom - below pitch line (view Figure 4.11)
original – new surface

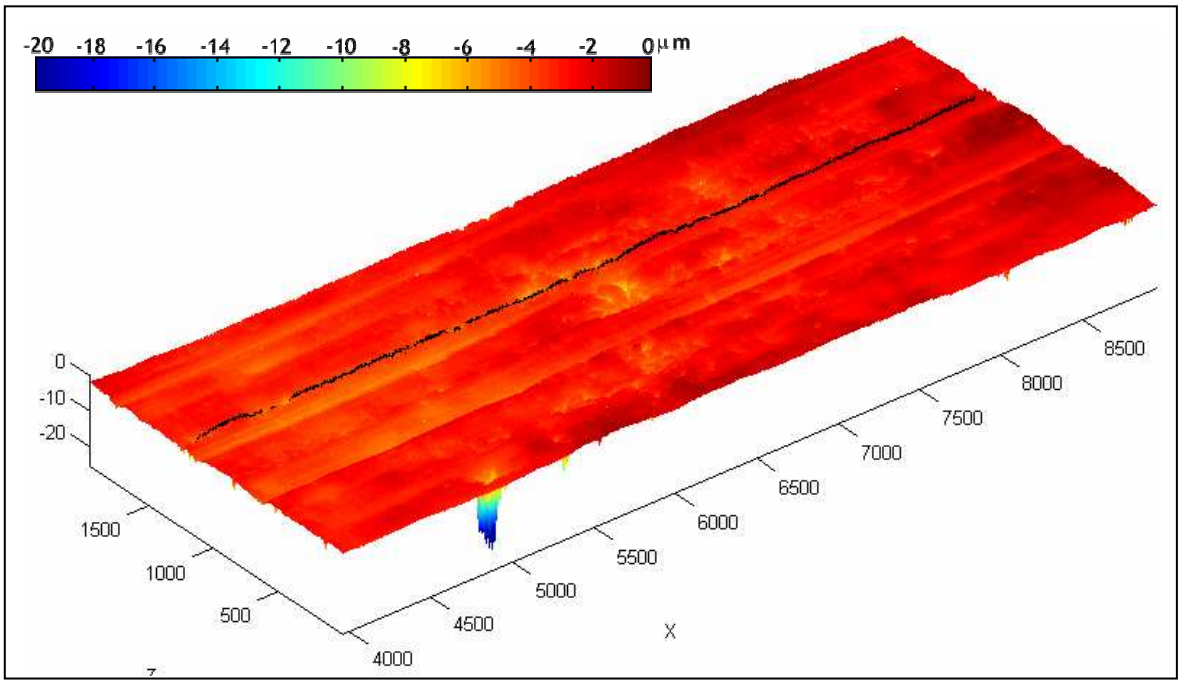


Roughness profiles measured during the gear micropitting tests.

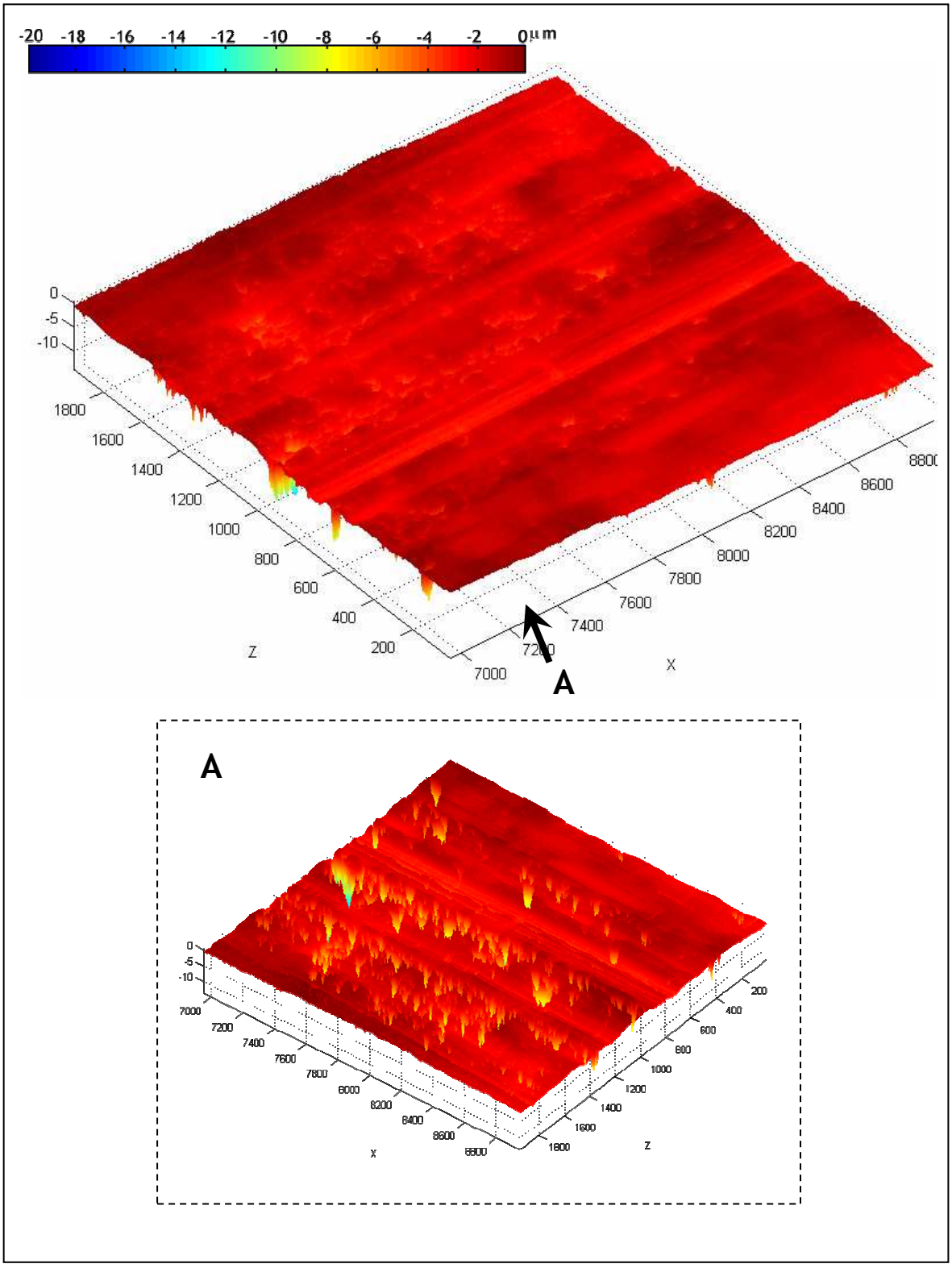
Surface topography measurements



Topography measurement (2X12 mm) made in the pinion of the nitrided gear lubricated with ester E1 (dimensions in µm).

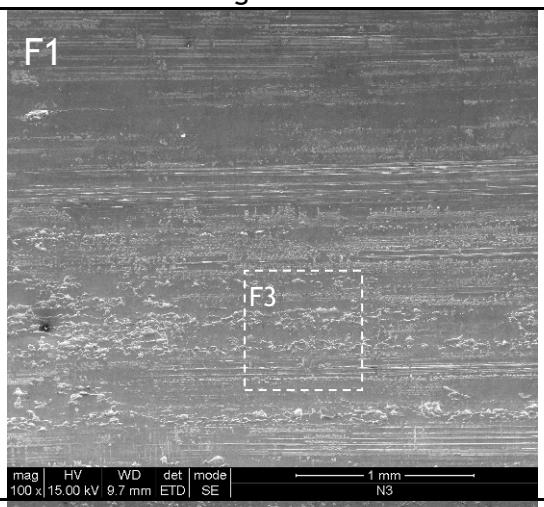
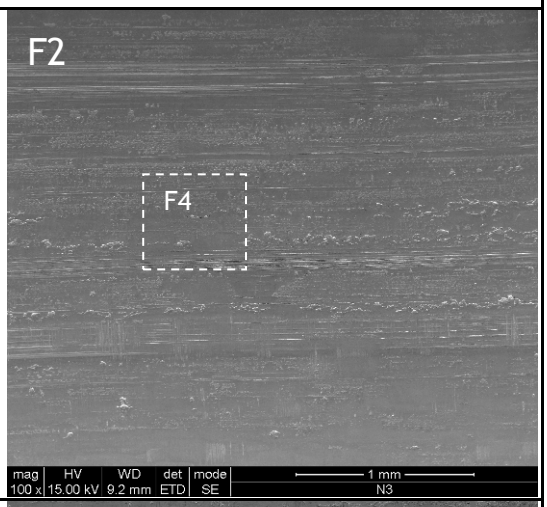
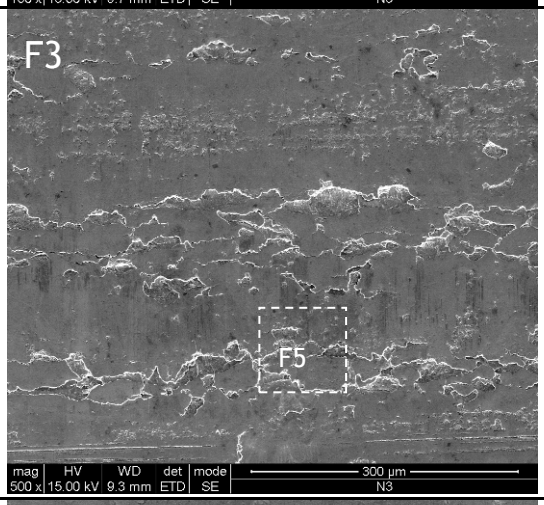
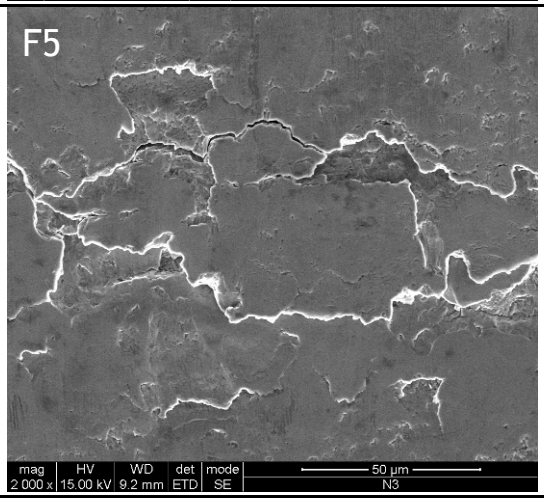
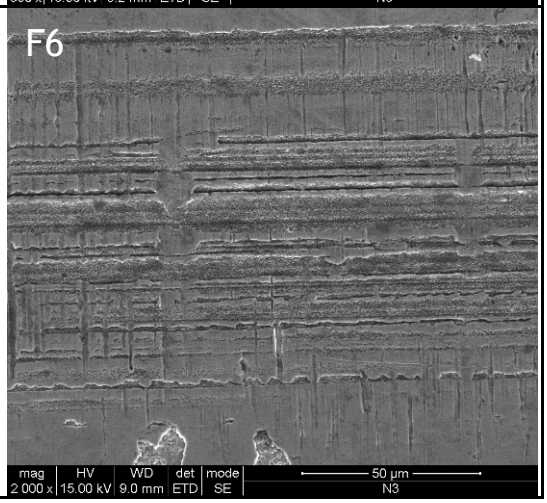


Part of the topography measurement (2X5 mm) made in the pinion of the nitrided gear lubricated with ester E1 (dimensions in µm) and roughness profile presented in Table 4.16.



Part of the topography measurement (2X2 mm) made in the pinion of the nitrided gear lubricated with ester E1 (dimensions in µm).

SEM micrographs taken in a pinion tooth flank below pith line

	Right side	Centre
100X		
500X		
2000X		

FZG gear micropitting test of nitrided gear lubricated by E2 gear oil (N-E2)

Test reference: GFKT-C14/8.3/90 **Oil reference: E2**

Gear type: C14 **Gear reference: 2NT-4 Side: A**

Gear material: High pressure nitrided steel (DIN 34 CrNiMo 6)

Mass loss [mg]

Load stage	running in+k6	K8	K9
Pinion	1	5	14
Wheel	6	7	11
Total	7	12	25

Micropitted area [%]

	running in+k6	K8	K9
1st tooth	0	0	0
5^{th} tooth	0	0	0
Average	0	0	0

Ferrometry

Load stage	K3	K6	K8	K9
d	0.1	0.1	0.1	0.1
DL	9.2	5.8	12.6	10.5
DS	2.2	2.1	2.9	3.7
CPUC	114.0	79.0	155.0	142.0
ISUC	8.0E+03	2.9E+03	1.5E+04	9.7E+03

Surface roughness measurements

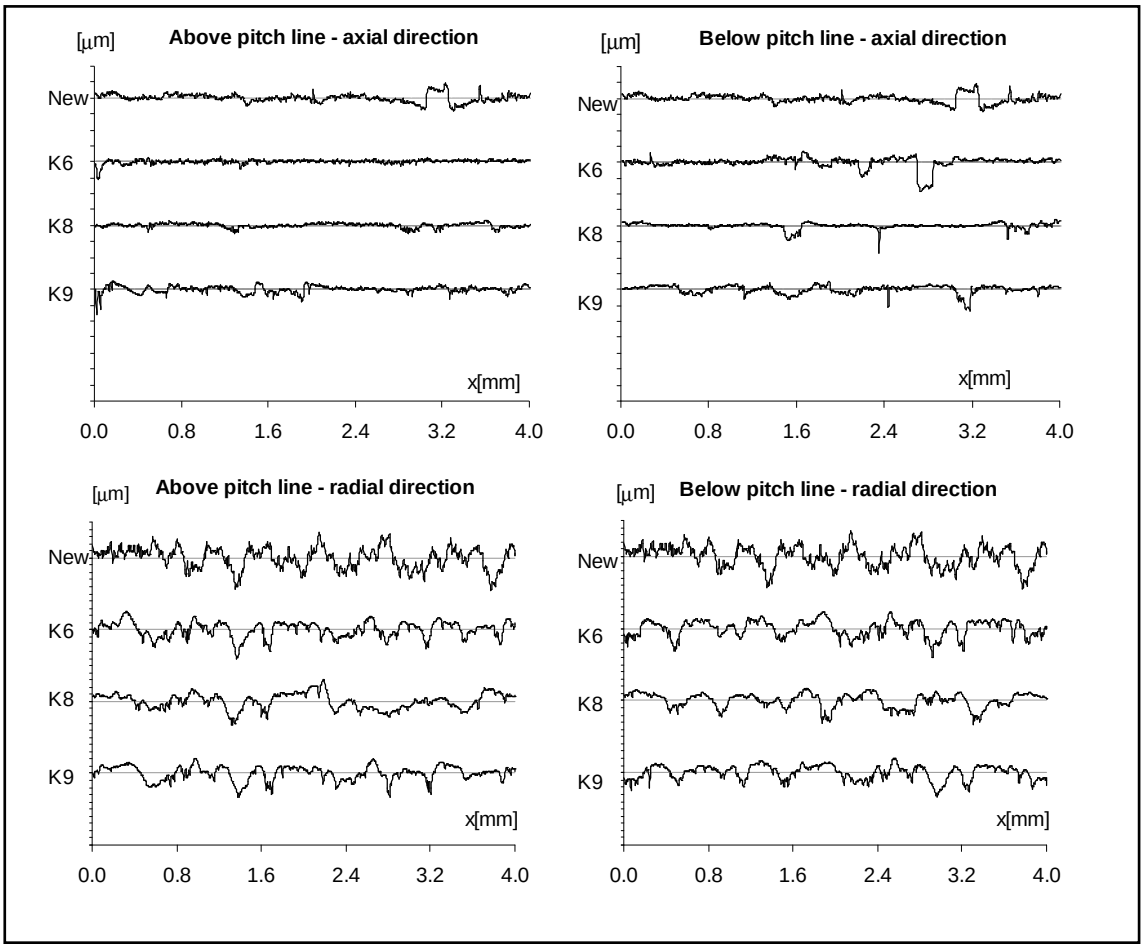
Surface roughness parameters [µm]												
		Dir.		**R_{max}**	**$R_{z\text{-}D}$**	**R_a**	**R_q**	**M_{r1}**	**R_{pk}**	**R_k**	**R_{vk}**	**M_{r2}**	**Vo**
Wheel	Initial	Axial		2.32	1.29	0.20	0.29	11.1	0.41	0.57	0.46	86.4	37.0
		Radial		6.98	5.94	0.96	1.20	9.9	1.07	3.14	1.19	89.4	63.5
Pinion	Initial	Axial		1.98	1.15	0.16	0.23	11.6	0.34	0.49	0.38	87.4	25.7
		Radial		7.32	6.27	1.15	1.40	6.6	1.21	3.85	1.38	86.3	95.4
	After running-in + K6	Axial	top	1.79	0.91	0.13	0.21	9.3	0.35	0.35	0.29	82.5	25.9
			bottom	1.32	0.74	0.12	0.19	8.9	0.14	0.29	0.47	86.2	37.3
		Radial	top	5.76	4.76	0.90	1.10	5.5	0.79	2.64	1.60	80.9	153.9
			bottom	5.47	4.46	0.92	1.11	5.2	0.62	2.55	1.77	77.3	201.3
	After K8	Axial	top	1.40	0.75	0.12	0.19	9.3	0.26	0.30	0.41	82.9	36.2
			bottom	1.61	0.76	0.09	0.15	13.8	0.11	0.21	0.45	87.3	29.1
		Radial	top	5.72	4.34	0.84	1.05	6.7	1.00	2.87	1.31	86.5	93.1
			bottom	4.73	3.91	0.80	0.98	5.5	0.58	2.08	1.69	74.2	217.1
	After K9	Axial	top	2.38	1.44	0.19	0.27	10.2	0.21	0.54	0.41	83.9	33.4
			bottom	1.21	0.82	0.14	0.20	7.2	0.13	0.35	0.49	79.7	50.0
		Radial	top	5.35	3.97	0.67	0.86	7.3	0.46	1.90	1.61	79.4	168.5
			bottom	5.61	4.05	0.79	0.97	5.5	0.67	2.26	1.62	78.9	179.0

Axial direction pinion roughness parameters variation[%]								
	R_{max}	$R_{z\text{-}D}$	R_a	R_q	R_{pk}	R_k	R_{vk}	V_o
$k6_{top}$-original	-9	-21	-23	-9	4	-29	-23	1
$k6_{bottom}$- original	-33	-36	-27	-20	-60	-42	22	45
$k6_{bottom}$-$k6_{top}$	-26	-19	-6	-12	-61	-19	59	44
$k8_{top}$-$k6_{top}$	-22	-18	-2	-13	-26	-14	39	40
$k8_{bottom}$-$k6_{bottom}$	22	4	-21	-17	-23	-26	-2	-22
$k8_{bottom}$-$k8_{top}$	15	2	-24	-17	-59	-30	12	-20
$k9_{top}$-$k8_{top}$	70	93	56	45	-17	79	0	-8
$k9_{bottom}$-$k8_{bottom}$	-25	7	53	30	21	65	8	72
$k9_{bottom}$-$k9_{top}$	-49	-43	-26	-26	-40	-35	21	50

Radial direction pinion roughness parameters variation[%]								
	R_{max}	R_{z-D}	R_a	R_q	R_{pk}	R_k	R_{vk}	V_o
$k6_{top}$-original	-21	-24	-22	-22	-35	-32	16	61
$k6_{bottom}$- original	-25	-29	-20	-21	-49	-34	28	111
$k6_{bottom}$-$k6_{top}$	-5	-6	3	1	-21	-3	11	31
$k8_{top}$-$k6_{top}$	-1	-9	-6	-5	27	9	-18	-40
$k8_{bottom}$-$k6_{bottom}$	-14	-12	-13	-12	-7	-18	-4	8
$k8_{bottom}$-$k8_{top}$	-17	-10	-5	-7	-42	-28	29	133
$k9_{top}$-$k8_{top}$	-6	-8	-20	-18	-54	-34	24	81
$k9_{bottom}$-$k8_{bottom}$	19	4	-1	0	15	9	-4	-18
$k9_{bottom}$-$k9_{top}$	5	2	18	13	46	19	1	6

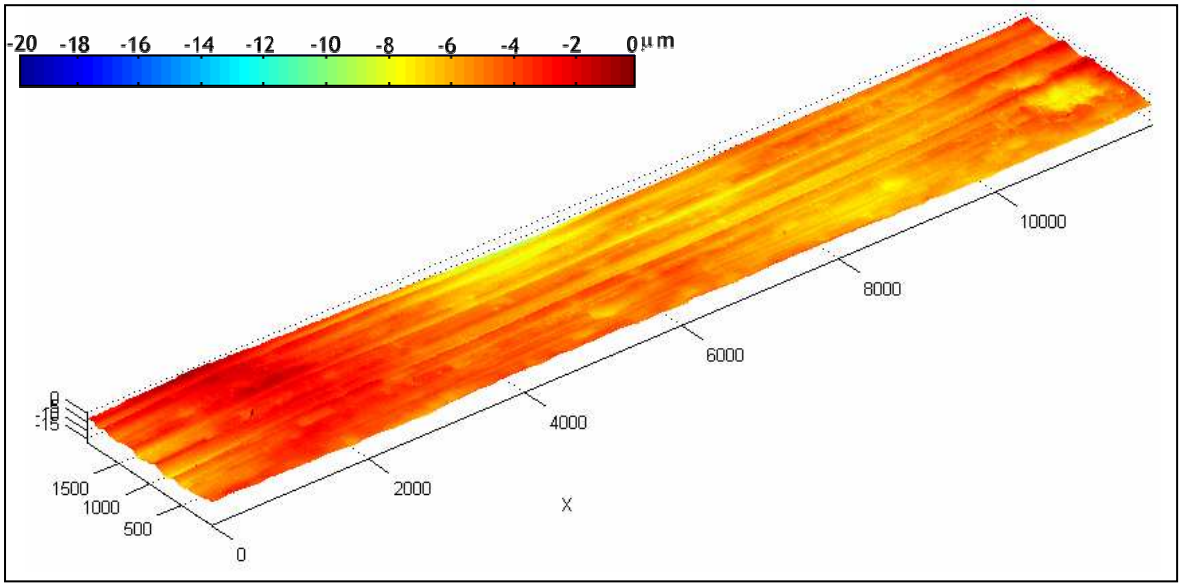
Legend:

top – above pitch line (view Figure 4.11)
bottom - below pitch line (view Figure 4.11)
original – new surface

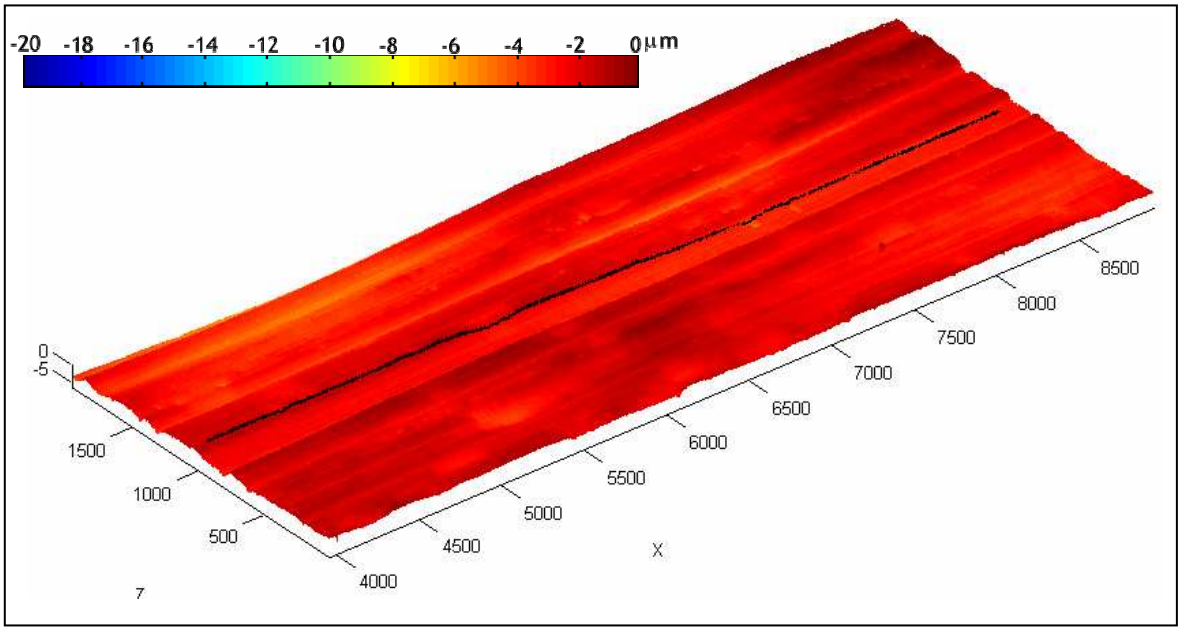


Roughness profiles measured during the gear micropitting tests.

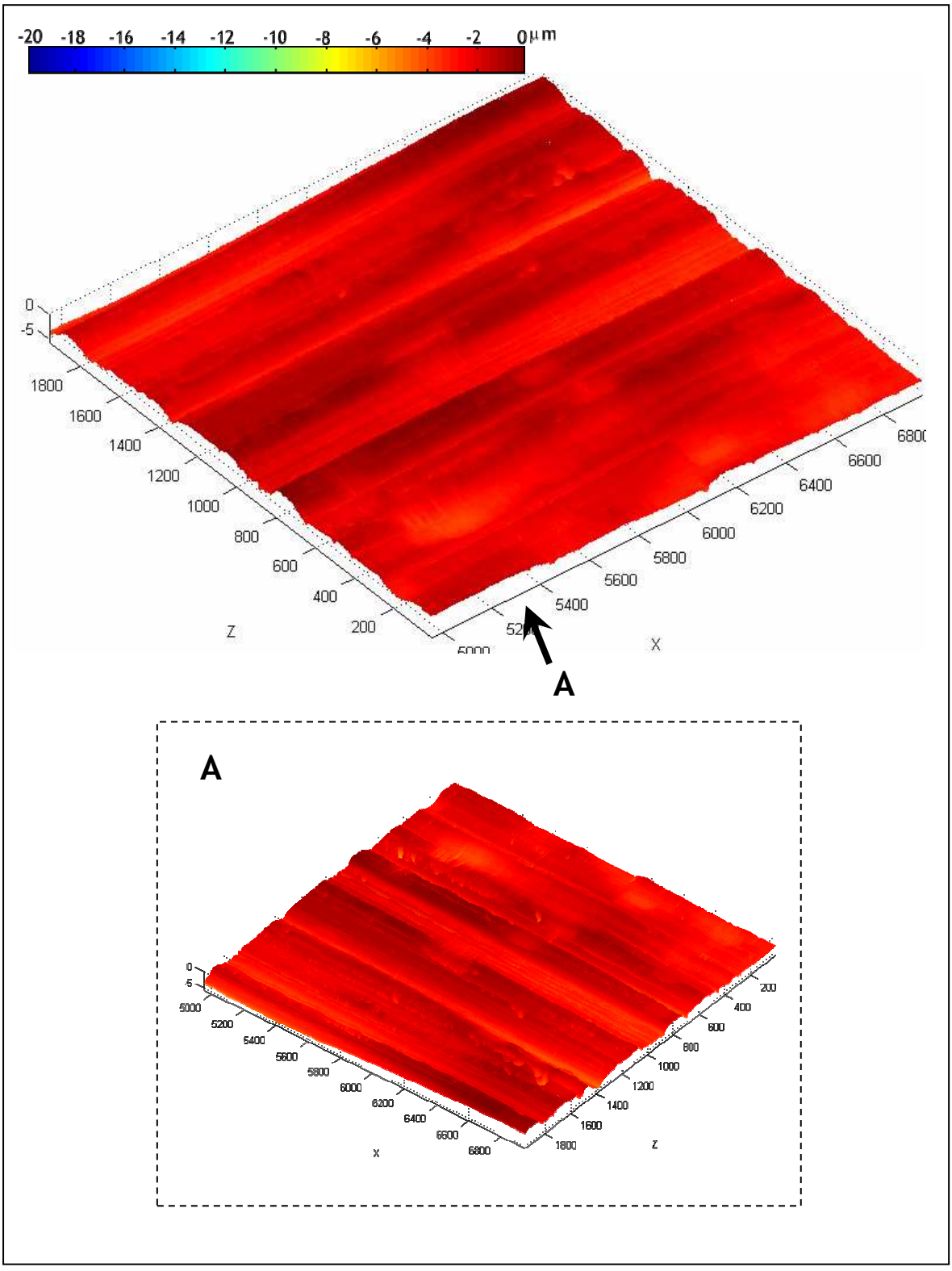
Surface topography measurements



Topography measurement (2X12 mm) made in the pinion of the nitrided gear lubricated with ester E2 (dimensions in µm).

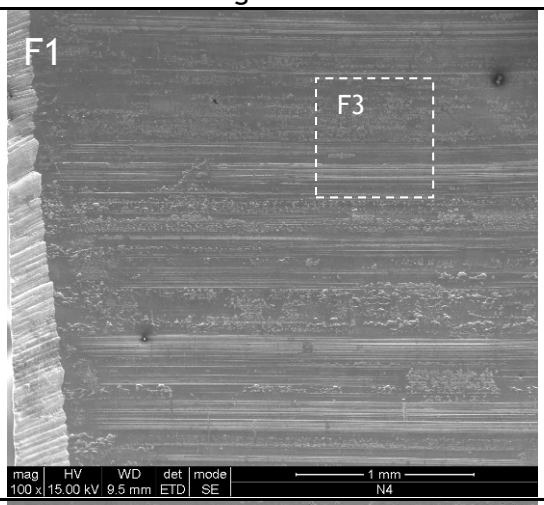
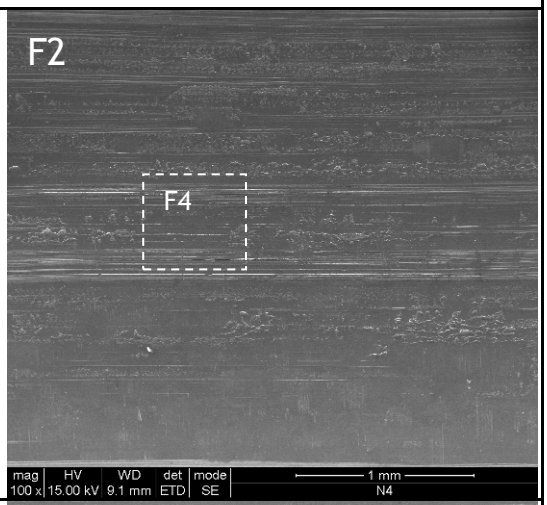
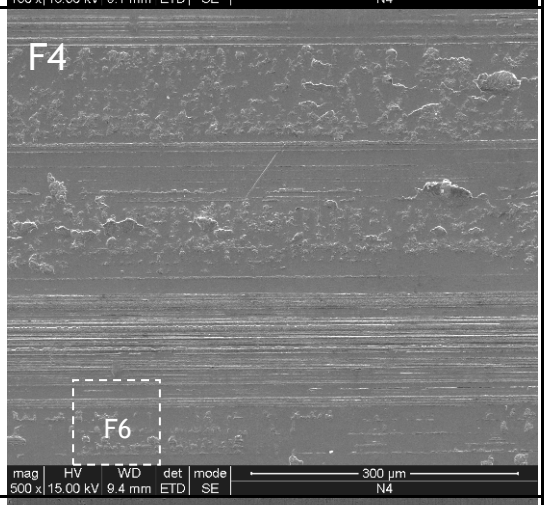
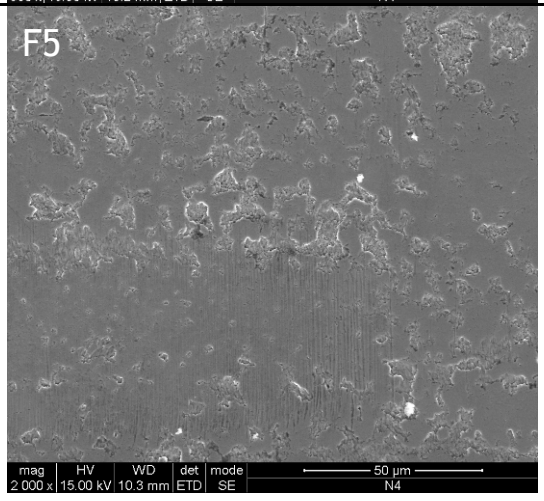
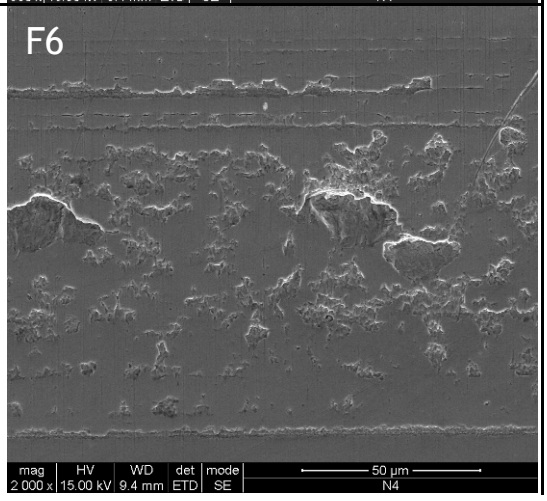


Part of the topography measurement (2X5 mm) made in the pinion of the nitrided gear lubricated with ester E2 (dimensions in µm) and roughness profile presented in Table 4.16.



Part of the topography measurement (2X2 mm) made in the pinion of the nitrided gear lubricated with ester E2 (dimensions in µm).

SEM micrographs taken in a pinion tooth flank below pith line

	Right side	Centre
100X		
500X		
2000X		

FZG gear micropitting test of coated gear lubricated by M1 gear oil (Mo-M1)

Test reference: GFKT-C14/8.3/90 **Oil reference: M1**

Gear type: C14 **Gear reference: C7 Side: A**

Gear material: Carburized steel (DIN 20MnCr5) + MoS_2/Ti coating

Mass loss [mg]

Load stage	running in+k6	K8	K9
Pinion	10	1	16
Wheel	6	5	9
Total	17	6	25

Micropitted area [%]

	running in+k6	K8	K9
1st tooth	2	6	19
5^{th} tooth	2	7	17
Average	2	6	18

Ferrometry

Load stage	K3	K6	K8	K9
d	0.1	0.1	0.1	0.1
DL	2.2	2.3	5.9	5
DS	1.2	1.5	2.1	2.4
CPUC	34.0	38.0	80.0	74.0
ISUC	3.4E+02	3.0E+02	3.0E+03	1.9E+03

Surface roughness measurements

Surface roughness parameters [µm]

		Dir.		R_{max}	R_{z-D}	R_a	R_q	M_{r1}	R_{pk}	R_k	R_{vk}	M_{r2}	Vo
Wheel	Initial	Axial		3.13	2.27	0.22	0.32	10.6	0.42	0.58	0.47	85.2	36.4
		Radial		8.46	5.98	1.11	1.42	7.7	1.07	3.53	2.18	85.1	162.6
Pinion	Initial	Axial		2.90	2.26	0.27	0.36	9.4	0.35	0.76	0.56	85.7	40.5
		Radial		7.97	6.35	1.23	1.54	8.9	1.27	4.43	1.77	88.6	106.3
	After running-in + K6	Axial	top	2.58	1.95	0.24	0.32	7.4	0.28	0.66	0.54	84.4	42.8
			bottom	1.95	1.44	0.17	0.23	8.0	0.16	0.45	0.44	84.2	33.7
		Radial	top	5.87	4.85	0.98	1.18	9.6	0.65	3.69	0.94	91.7	40.7
			bottom	6.20	4.78	0.93	1.14	5.0	0.63	3.43	1.48	85.8	105.0
	After K8	Axial	top	3.02	1.76	0.21	0.31	9.1	0.29	0.53	0.59	82.2	53.3
			bottom	5.74	3.27	0.48	0.75	9.0	0.22	0.66	1.79	77.3	224.1
		Radial	top	6.55	4.93	0.95	1.15	3.3	0.40	3.84	1.01	91.7	42.0
			bottom	7.57	5.35	0.93	1.18	7.9	0.87	3.12	1.48	83.7	123.6
	After K9	Axial	top	2.61	1.98	0.28	0.38	5.3	0.11	0.67	0.71	79.6	73.9
			bottom	9.74	6.28	0.92	1.46	13.5	0.81	0.90	4.50	76.4	546.1
		Radial	top	5.30	4.31	0.83	1.01	7.8	0.49	3.16	0.95	89.5	57.4
			bottom	7.93	5.85	0.92	1.17	5.9	0.69	3.09	1.53	83.7	124.9

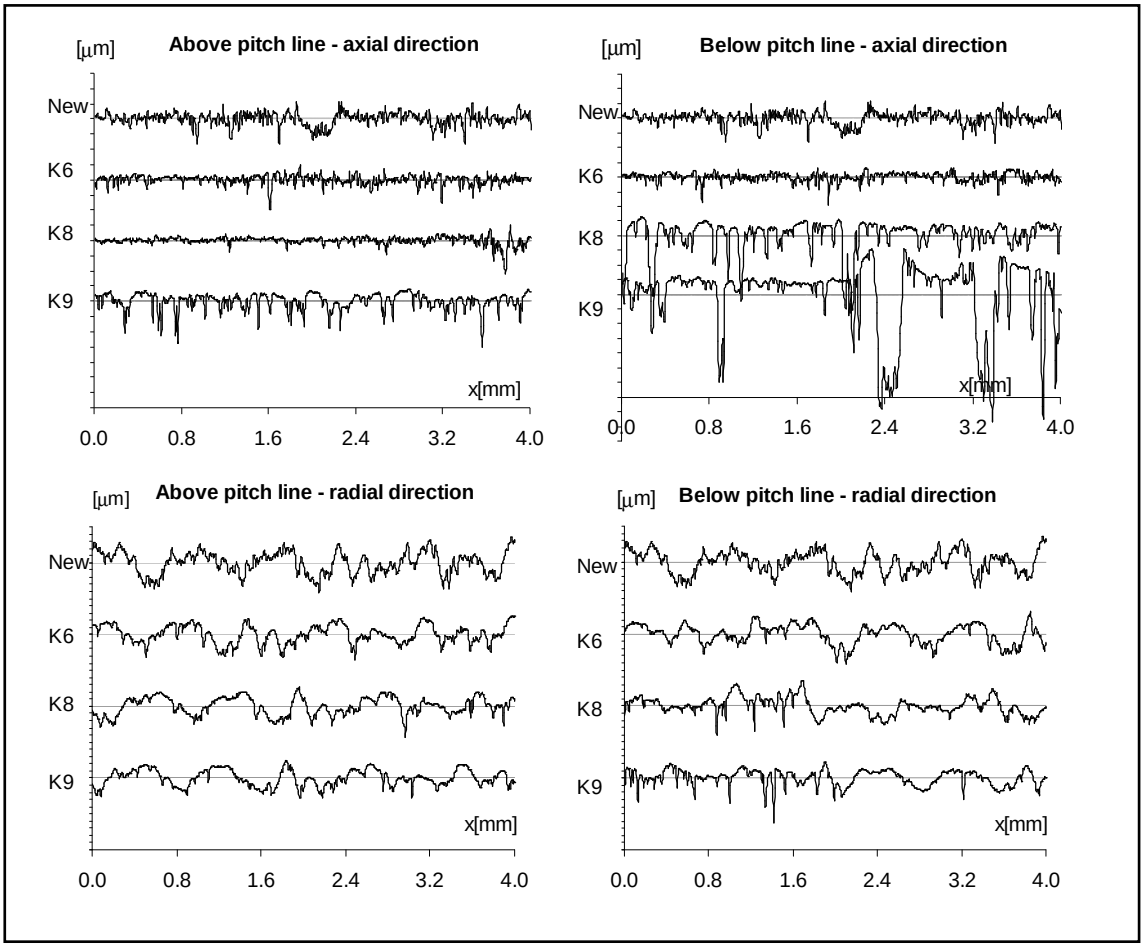
Axial direction pinion roughness parameters variation[%]

	R_{max}	R_{z-D}	R_a	R_q	R_{pk}	R_k	R_{vk}	V_o
$k6_{top}$-original	-11	-14	-12	-11	-19	-13	-3	6
$k6_{bottom}$- original	-33	-36	-39	-36	-53	-41	-22	-17
$k6_{bottom}$-$k6_{top}$	-24	-26	-30	-29	-42	-32	-20	-21
$k8_{top}$-$k6_{top}$	17	-10	-11	-4	2	-20	9	25
$k8_{bottom}$-$k6_{bottom}$	194	128	194	224	35	49	308	565
$k8_{bottom}$-$k8_{top}$	90	86	130	140	-23	26	200	320
$k9_{top}$-$k8_{top}$	-14	13	34	23	-61	27	20	38
$k9_{bottom}$-$k8_{bottom}$	70	92	91	95	271	36	152	144
$k9_{bottom}$-$k9_{top}$	273	217	228	281	625	35	532	639

Radial direction pinion roughness parameters variation[%]								
	R_{max}	R_{z-D}	R_a	R_q	R_{pk}	R_k	R_{vk}	V_o
$k6_{top}$-original	-26	-24	-21	-24	-49	-17	-47	-62
$k6_{bottom}$- original	-22	-25	-25	-26	-50	-22	-16	-1
$k6_{bottom}$-$k6_{top}$	6	-2	-5	-3	-2	-7	58	158
$k8_{top}$-$k6_{top}$	12	1	-3	-3	-38	4	7	3
$k8_{bottom}$-$k6_{bottom}$	22	12	0	3	37	-9	0	18
$k8_{bottom}$-$k8_{top}$	16	9	-2	3	118	-19	47	194
$k9_{top}$-$k8_{top}$	-19	-12	-13	-12	22	-18	-6	37
$k9_{bottom}$-$k8_{bottom}$	5	9	-1	0	-21	-1	3	1
$k9_{bottom}$-$k9_{top}$	50	36	11	16	41	-2	61	118

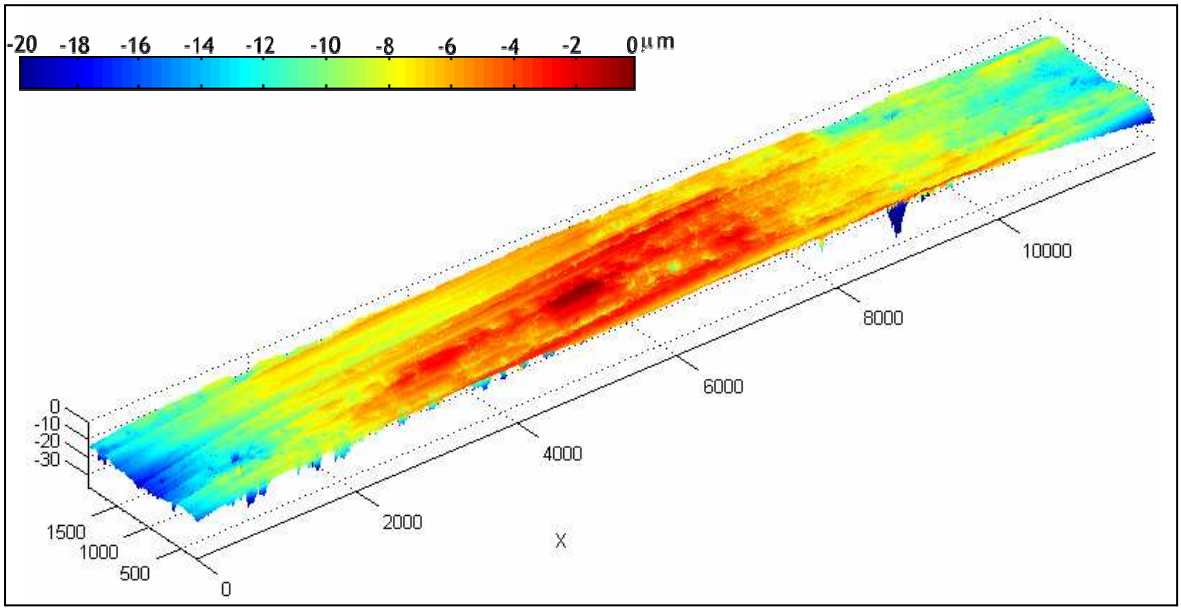
Legend:

top – above pitch line (view Figure 4.11)
bottom - below pitch line (view Figure 4.11)
original – new surface

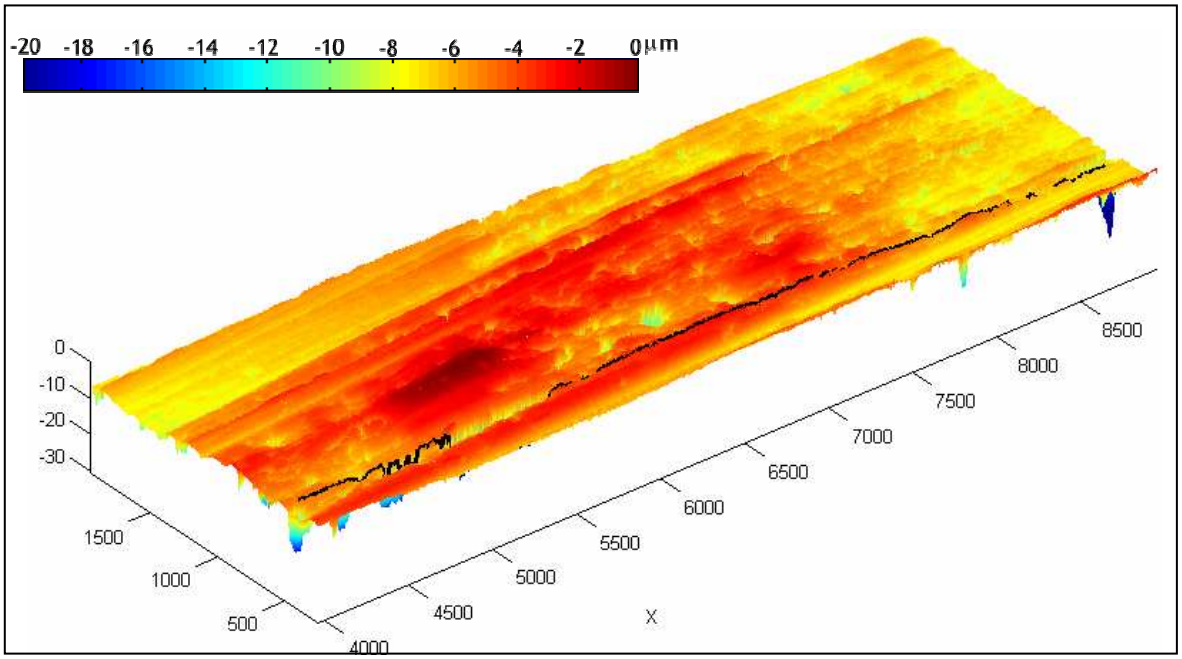


Roughness profiles measured during the gear micropitting tests.

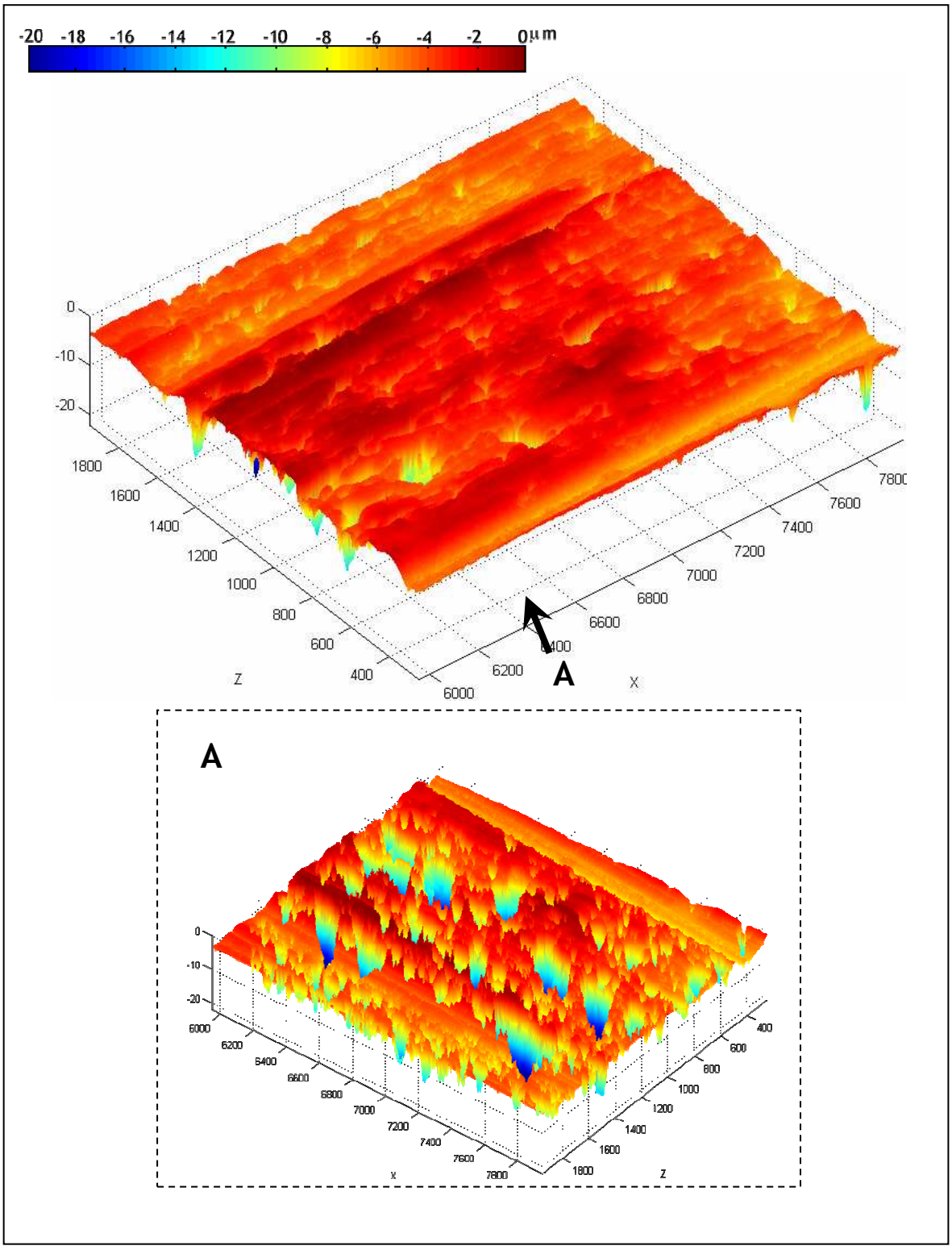
Surface topography measurements



Topography measurement (2X12 mm) made in the pinion of the coated gear lubricated with the mineral oil (dimensions in µm).



Part of the topography measurement (2X5 mm) made in the pinion of the coated gear lubricated with the mineral oil (dimensions in µm) and roughness profile presented in Table 4.16.



Part of the topography measurement (2X2 mm) made in the pinion of the coated gear lubricated with the mineral oil (dimensions in µm).

FZG gear micropitting test of coated gear lubricated by E1 gear oil (Mo-E1)

Test reference: GFKT-C14/8.3/90 **Oil reference: E1**

Gear type: C14 **Gear reference: C7 Side: B**

Gear material: Carburized steel (DIN 20MnCr5) + MoS_2/Ti coating

Mass loss [mg]

Load stage	running in+k6	K8	K9
Pinion	9	36	33
Wheel	11	14	24
Total	21	50	57

Micropitted area [%]

	running in+k6	K8	K9
1st tooth	7	18	24
5^{th} tooth	8	20	26
Average	8	19	25

Ferrometry

Load stage	K3	K6	K8	K9
d	0.1	0.1	0.1	0.1
DL	3.1	8.3	17.3	23.9
DS	1.3	2.4	4.9	7.5
CPUC	44.0	107.0	222.0	314.0
ISUC	7.9E+02	6.3E+03	2.8E+04	5.1E+04

Surface roughness measurements

Surface roughness parameters [µm]

		Dir.		R_{max}	R_{z-D}	R_a	R_q	M_{r1}	R_{pk}	R_k	R_{vk}	M_{r2}	Vo
Wheel	Initial	Axial		2.76	2.13	0.22	0.32	11.3	0.39	0.58	0.48	85.0	36.8
		Radial		8.49	6.69	1.24	1.55	9.7	1.18	4.25	1.88	89.0	104.4
Pinion	Initial	Axial		2.69	2.02	0.25	0.34	9.8	0.32	0.69	0.54	86.4	37.7
		Radial		7.63	6.31	1.15	1.45	10.6	1.38	3.92	1.42	89.0	79.7
	After running-in + K6	Axial	top	2.29	1.58	0.18	0.26	6.0	0.29	0.48	0.43	81.5	39.8
			bottom	5.22	4.04	0.63	0.88	6.5	0.25	1.30	2.03	79.2	211.6
		Radial	top	6.48	5.41	1.05	1.33	12.1	1.56	3.69	1.51	89.2	90.6
			bottom	7.14	5.77	1.01	1.28	10.4	1.18	3.37	1.63	87.6	101.6
	After K8	Axial	top	3.44	2.26	0.26	0.40	9.7	0.17	0.58	0.87	82.9	80.3
			bottom	7.34	4.47	0.54	0.89	6.4	0.18	0.98	2.22	80.9	211.6
		Radial	top	5.01	4.20	0.79	1.00	8.3	0.81	2.79	1.62	86.9	112.1
			bottom	6.14	4.80	0.79	1.01	10.4	0.81	2.64	1.31	87.1	86.9
	After K9	Axial	top	2.84	1.62	0.19	0.30	7.7	0.12	0.39	0.67	81.2	66.7
			bottom	5.98	3.67	0.49	0.72	7.3	0.34	1.12	1.60	81.9	144.9
		Radial	top	5.11	3.70	0.62	0.81	7.6	0.73	2.23	1.35	87.3	85.7
			bottom	7.05	4.91	0.78	1.04	10.5	1.10	2.55	1.45	88.0	89.0

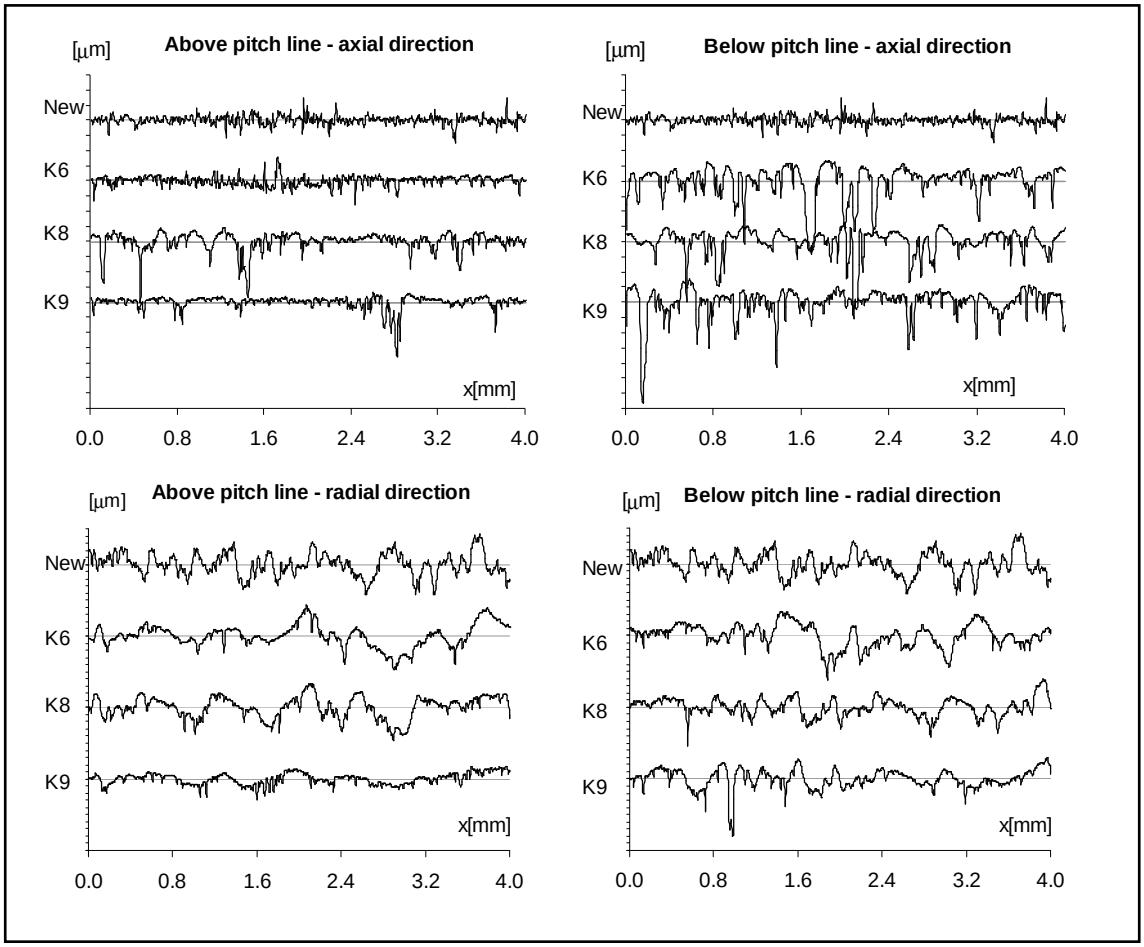
Axial direction pinion roughness parameters variation[%]

	R_{max}	R_{z-D}	R_a	R_q	R_{pk}	R_k	R_{vk}	V_o
$k6_{top}$-original	-15	-22	-27	-22	-10	-30	-19	6
$k6_{bottom}$- original	94	100	155	162	-24	88	278	461
$k6_{bottom}$-$k6_{top}$	128	157	247	237	-15	169	369	431
$k8_{top}$-$k6_{top}$	51	43	45	52	-42	21	100	102
$k8_{bottom}$-$k6_{bottom}$	40	11	-14	1	-28	-25	9	0
$k8_{bottom}$-$k8_{top}$	113	98	106	123	5	68	156	163
$k9_{top}$-$k8_{top}$	-17	-28	-29	-25	-29	-34	-22	-17
$k9_{bottom}$-$k8_{bottom}$	-19	-18	-10	-18	93	14	-28	-32
$k9_{bottom}$-$k9_{top}$	110	126	163	143	185	189	137	117

Radial direction pinion roughness parameters variation[%]								
	R_{max}	R_{z-D}	R_a	R_q	R_{pk}	R_k	R_{vk}	V_o
$k6_{top}$-original	-15	-14	-9	-8	13	-6	6	14
$k6_{bottom}$- original	-6	-9	-12	-11	-15	-14	15	27
$k6_{bottom}$-$k6_{top}$	10	7	-4	-3	-25	-9	8	12
$k8_{top}$-$k6_{top}$	-23	-22	-25	-25	-48	-24	8	24
$k8_{bottom}$-$k6_{bottom}$	-14	-17	-22	-21	-31	-22	-20	-14
$k8_{bottom}$-$k8_{top}$	23	14	0	2	0	-6	-19	-22
$k9_{top}$-$k8_{top}$	2	-12	-22	-19	-11	-20	-16	-24
$k9_{bottom}$-$k8_{bottom}$	15	2	-1	3	36	-3	11	2
$k9_{bottom}$-$k9_{top}$	38	33	27	29	52	15	7	4

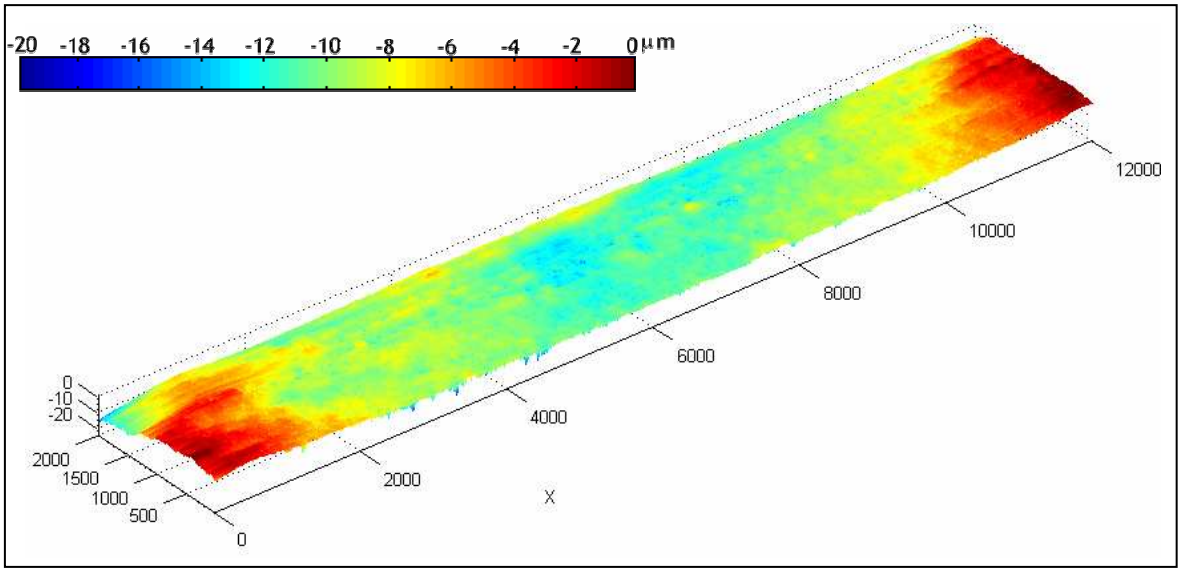
Legend:

top – above pitch line (view Figure 4.11)
bottom - below pitch line (view Figure 4.11)
original – new surface

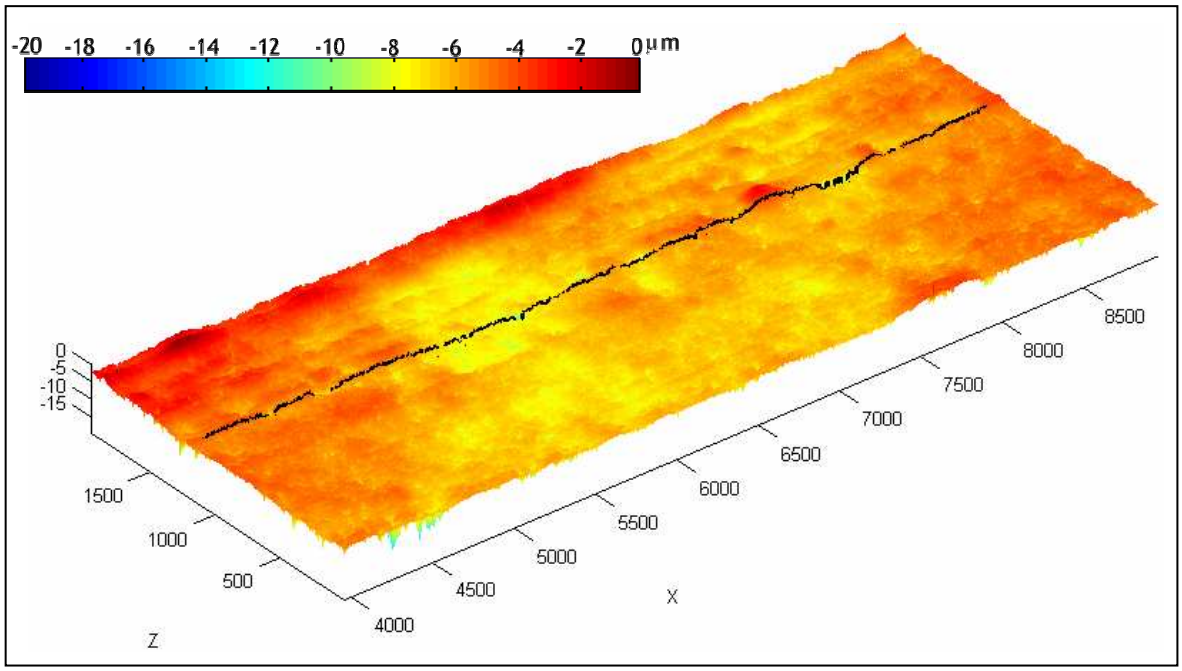


Roughness profiles measured during the gear micropitting tests.

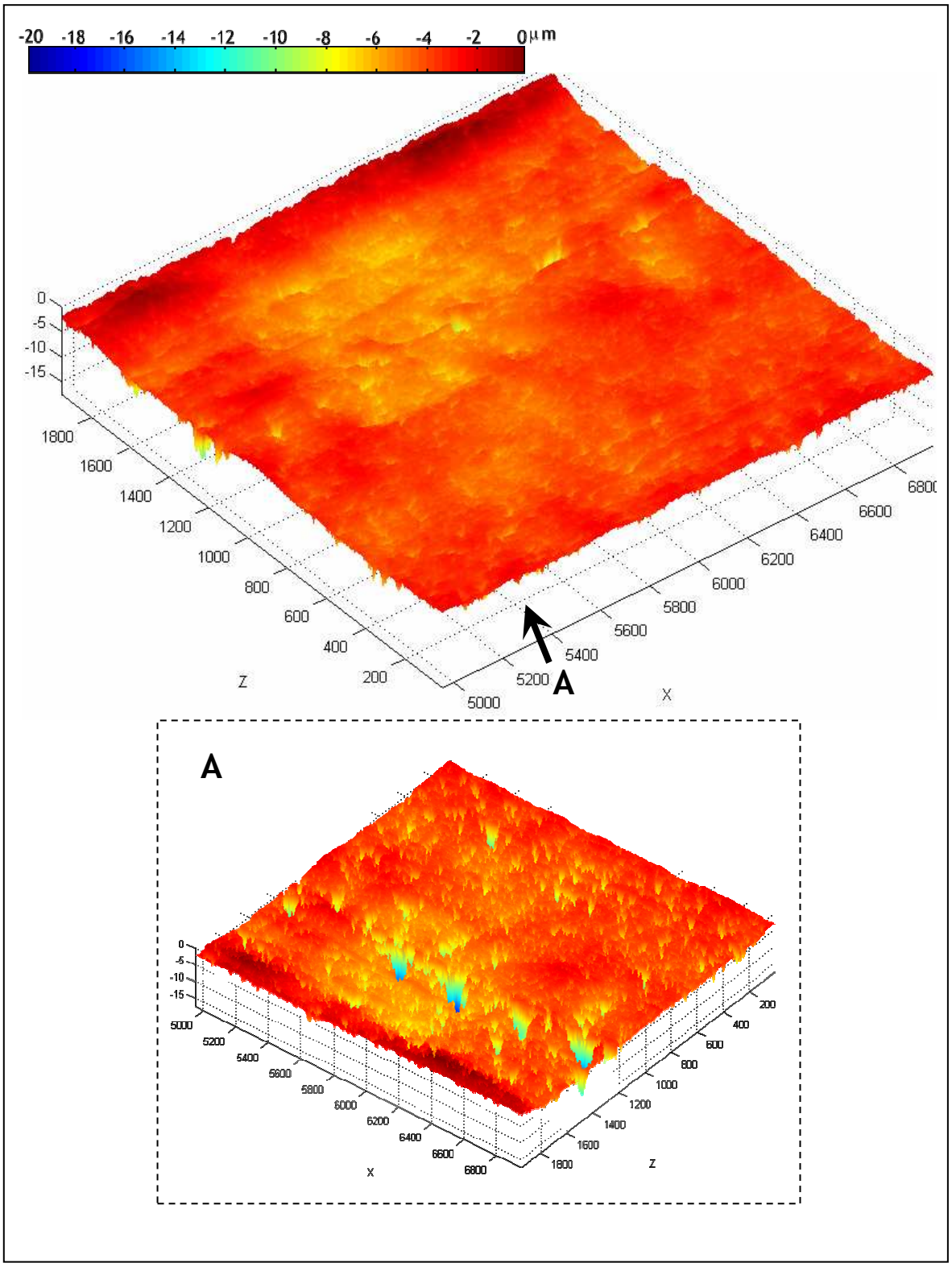
Surface topography measurements



Topography measurement (2X12 mm) made in the pinion of the coated gear lubricated with ester E1 (dimensions in µm).



Part of the topography measurement (2X5 mm) made in the pinion of the coated gear lubricated with ester E1 (dimensions in µm) and roughness profile presented in Table 4.16.



Part of the topography measurement (2X2 mm) made in the pinion of the coated gear lubricated with ester E1 (dimensions in µm).

FZG gear micropitting test of coated gear lubricated by E2 gear oil (Mo-E2)

Test reference: GFKT-C14/8.3/90 **Oil reference: E2**

Gear type: C14 **Gear reference: C6 Side: A**

Gear material: Carburized steel (DIN 20MnCr5) + MoS_2/Ti coating

Mass loss [mg]

Load stage	running in+k6	K8	K9
Pinion	9	13	24
Wheel	4	8	8
Total	13	21	32

Micropitted area [%]

	running in+k6	K8	K9
1st tooth	12	19	24
5^{th} tooth	11	19	24
Average	11	19	24

Ferrometry

Load stage	K3	K6	K8	K9
d	0.1	0.1	0.1	0.1
DL	2.1	3.1	5.4	11.4
DS	0.2	1.4	1.8	2.7
CPUC	23.0	45.0	72.0	141.0
ISUC	4.4E+02	7.7E+02	2.6E+03	1.2E+04

Surface roughness measurements

Surface roughness parameters [µm]

		Dir.		R_{max}	$R_{z\text{-}D}$	R_a	R_q	M_{r1}	R_{pk}	R_k	R_{vk}	M_{r2}	Vo
Wheel	Initial	Axial		3.35	2.47	0.31	0.42	8.3	0.37	0.87	0.67	85.8	47.6
		Radial		7.50	6.01	1.11	1.39	7.3	1.02	3.77	1.95	87.9	119.7
Pinion	Initial	Axial		3.08	2.11	0.23	0.33	10.2	0.30	0.60	0.61	85.5	45.1
		Radial		8.26	6.35	1.21	1.51	7.3	0.96	4.15	2.07	87.0	138.2
	After running-in	Axial	top	1.89	1.06	0.13	0.18	7.8	0.11	0.38	0.29	86.8	19.0
			bottom	5.20	3.63	0.46	0.69	8.6	0.21	0.66	1.73	76.8	204.5
		Radial	top	8.58	6.12	1.22	1.56	9.5	0.93	4.20	3.05	89.4	163.4
			bottom	8.36	5.36	0.99	1.23	6.7	1.12	3.50	1.38	85.4	100.4
	After K8	Axial	top	4.20	2.52	0.30	0.49	5.7	0.11	0.68	1.19	83.4	98.6
			bottom	6.11	4.02	0.60	0.85	7.3	0.30	1.06	1.89	76.1	228.4
		Radial	top	6.99	5.27	0.97	1.24	9.7	0.86	3.43	2.13	90.4	102.6
			bottom	8.02	5.16	0.91	1.15	7.5	0.94	3.10	1.47	86.0	102.3
	After K9	Axial	top	4.00	2.38	0.32	0.47	8.8	0.22	0.64	1.04	83.6	105.4
			bottom	4.56	3.70	0.39	0.60	8.5	0.25	0.84	1.41	82.1	125.4
		Radial	top	6.70	4.75	0.80	1.08	9.8	0.67	2.67	2.31	88.8	123.9
			bottom	8.65	5.92	0.83	1.13	8.2	0.81	2.40	1.82	82.2	148.3

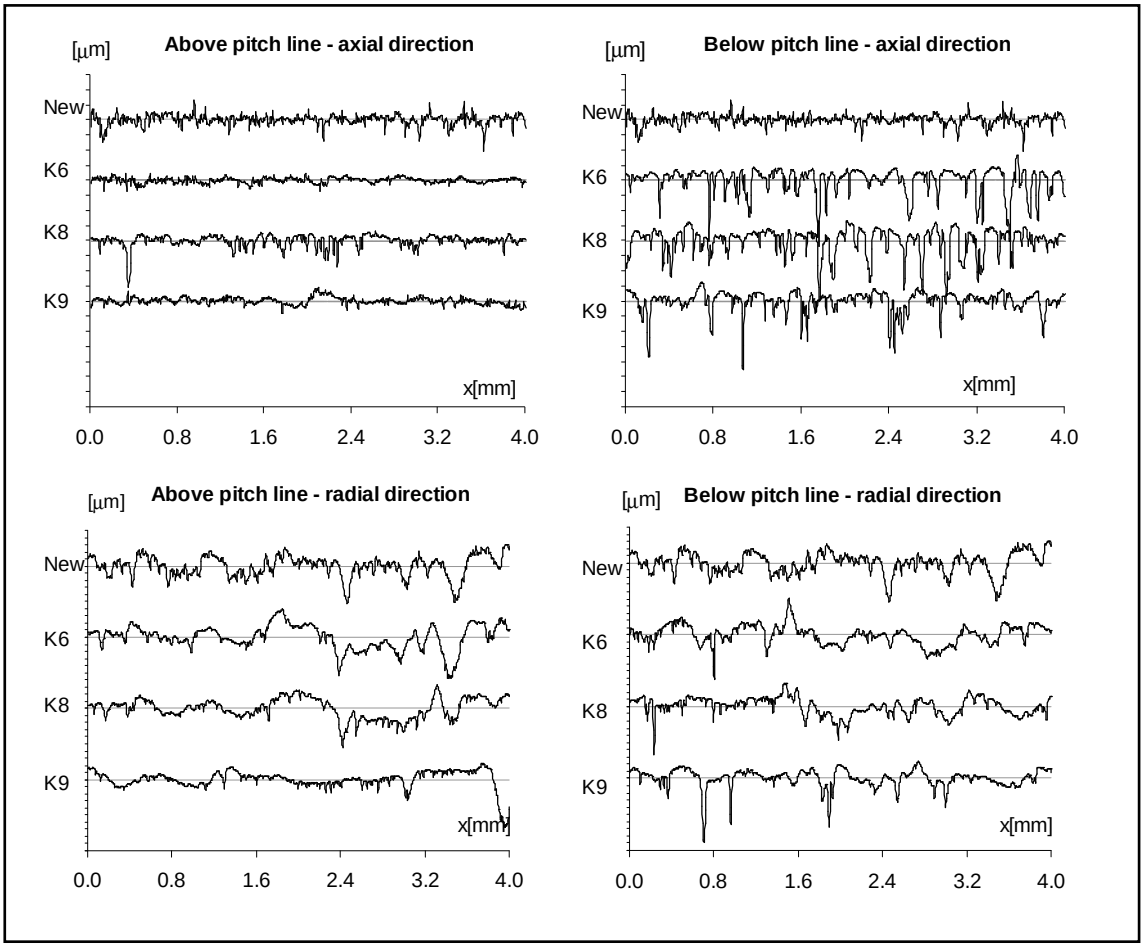
Axial direction pinion roughness parameters variation[%]

	R_{max}	$R_{z\text{-}D}$	R_a	R_q	R_{pk}	R_k	R_{vk}	V_o
$k6_{top}$-original	-39	-50	-45	-45	-65	-37	-53	-58
$k6_{bottom}$- original	69	72	97	107	-30	10	183	353
$k6_{bottom}$-$k6_{top}$	175	243	260	278	98	75	503	978
$k8_{top}$-$k6_{top}$	123	138	141	166	2	81	316	420
$k8_{bottom}$-$k6_{bottom}$	18	11	31	23	42	61	9	12
$k8_{bottom}$-$k8_{top}$	45	59	96	74	176	56	59	132
$k9_{top}$-$k8_{top}$	-5	-6	3	-3	108	-7	-13	7
$k9_{bottom}$-$k8_{bottom}$	-25	-8	-35	-29	-18	-21	-25	-45
$k9_{bottom}$-$k9_{top}$	14	55	24	26	9	32	36	19

Radial direction pinion roughness parameters variation[%]								
	R_{max}	R_{z-D}	R_a	R_q	R_{pk}	R_k	R_{vk}	V_o
$k6_{top}$-original	4	-4	1	3	-3	1	47	18
$k6_{bottom}$- original	1	-16	-18	-19	16	-16	-33	-27
$k6_{bottom}$-$k6_{top}$	-3	-12	-19	-21	20	-17	-55	-39
$k8_{top}$-$k6_{top}$	-19	-14	-21	-21	-8	-18	-30	-37
$k8_{bottom}$-$k6_{bottom}$	-4	-4	-8	-7	-16	-11	7	2
$k8_{bottom}$-$k8_{top}$	15	-2	-7	-7	10	-10	-31	0
$k9_{top}$-$k8_{top}$	-4	-10	-17	-13	-22	-22	9	21
$k9_{bottom}$-$k8_{bottom}$	8	15	-9	-2	-15	-23	24	45
$k9_{bottom}$-$k9_{top}$	29	25	3	5	20	-10	-21	20

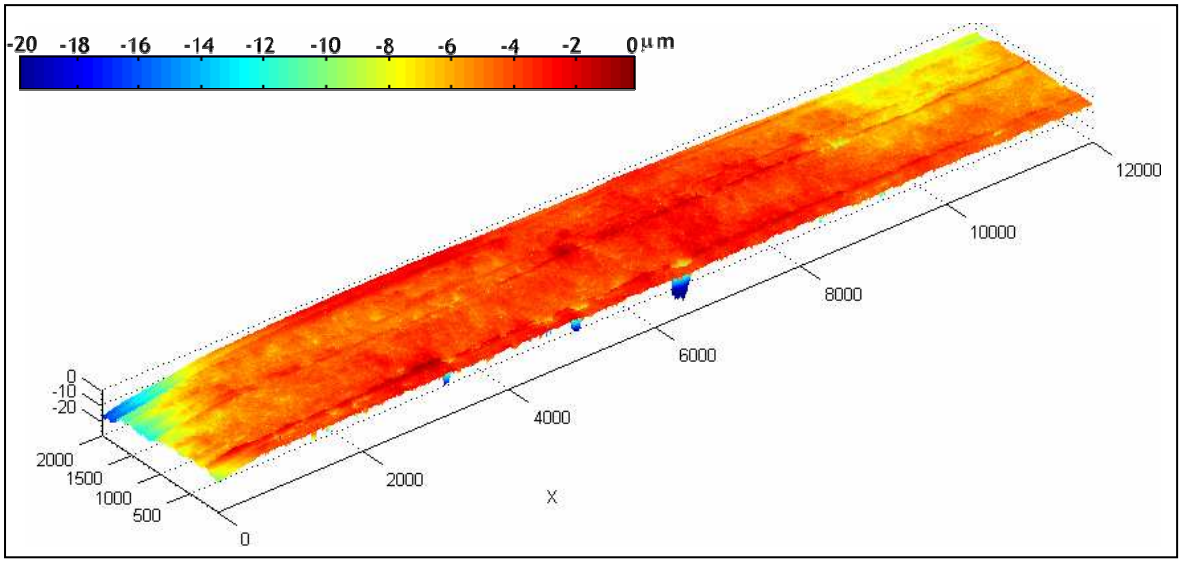
Legend:

top – above pitch line (view Figure 4.11)
bottom - below pitch line (view Figure 4.11)
original – new surface

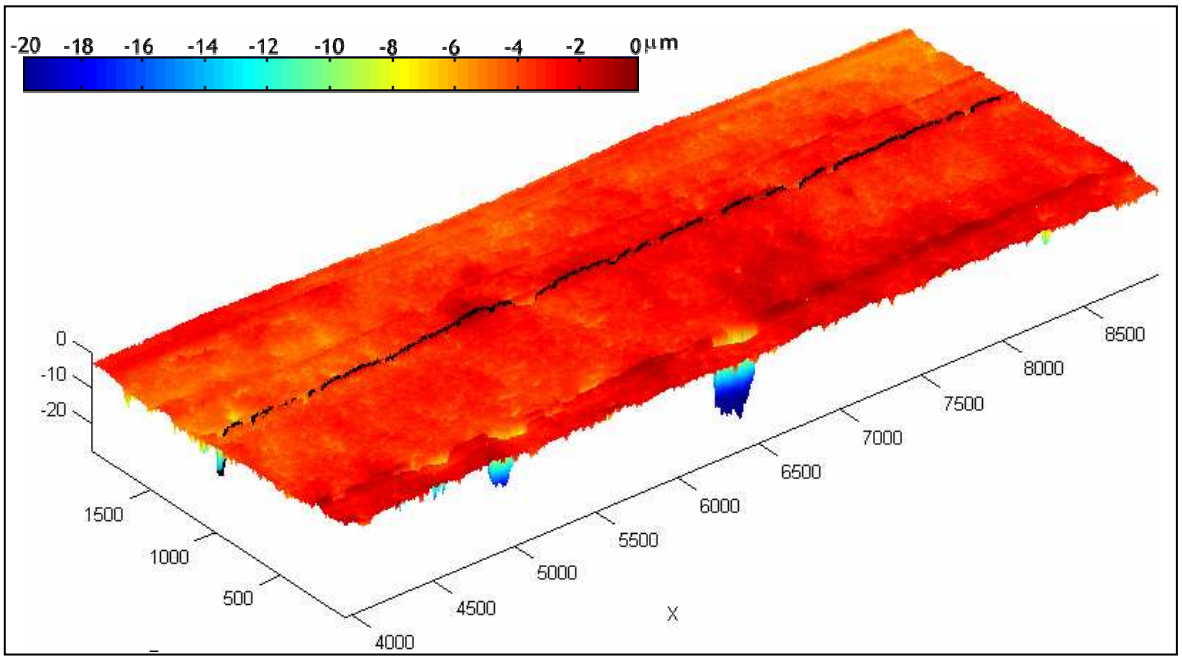


Roughness profiles measured during the gear micropitting tests.

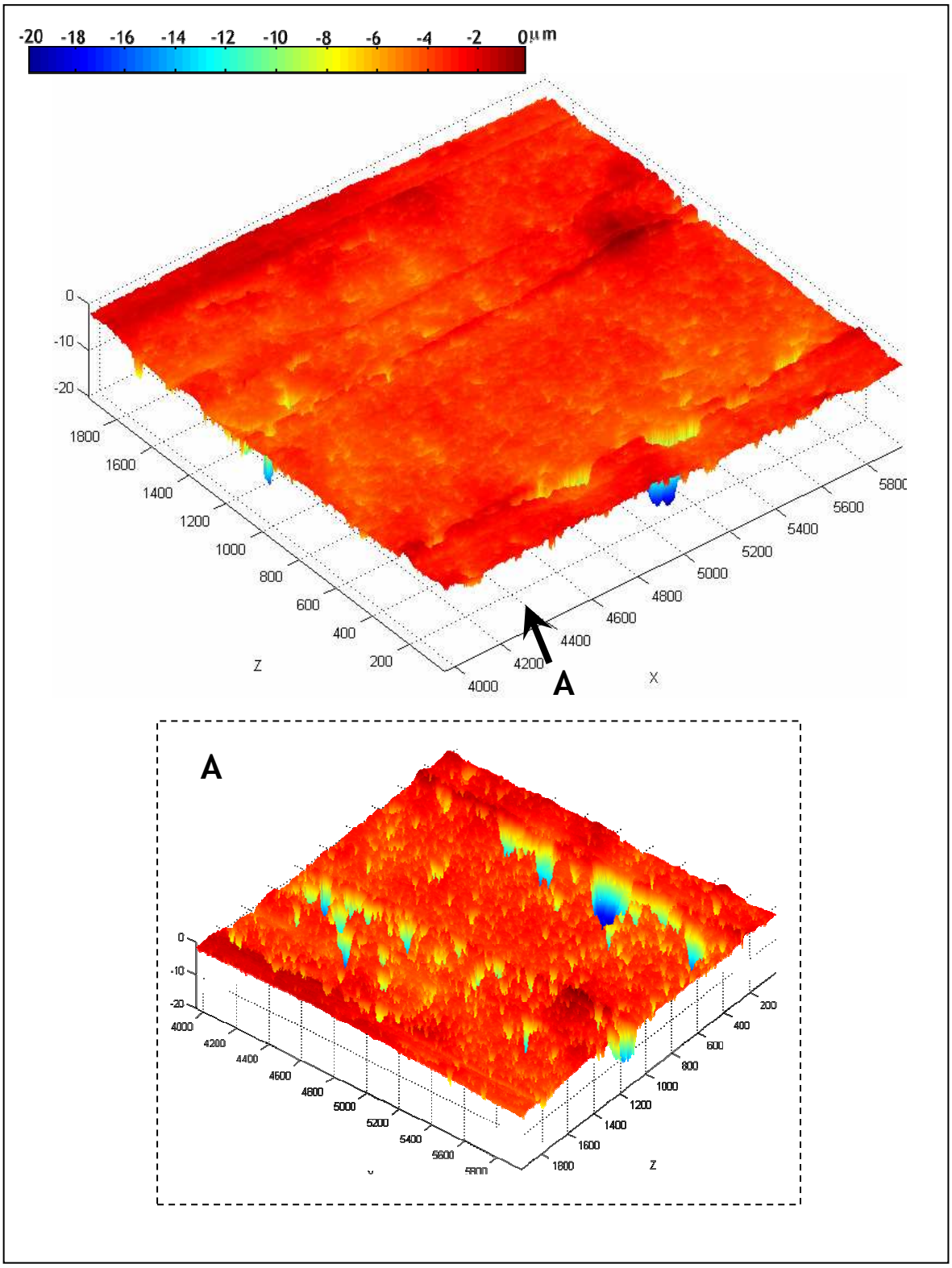
Surface topography measurements



Topography measurement (2X12 mm) made in the pinion of the coated gear lubricated with ester E2 (dimensions in µm).



Part of the topography measurement (2X5 mm) made in the pinion of the coated gear lubricated with ester E2 (dimensions in µm) and roughness profile presented in Table 4.16.



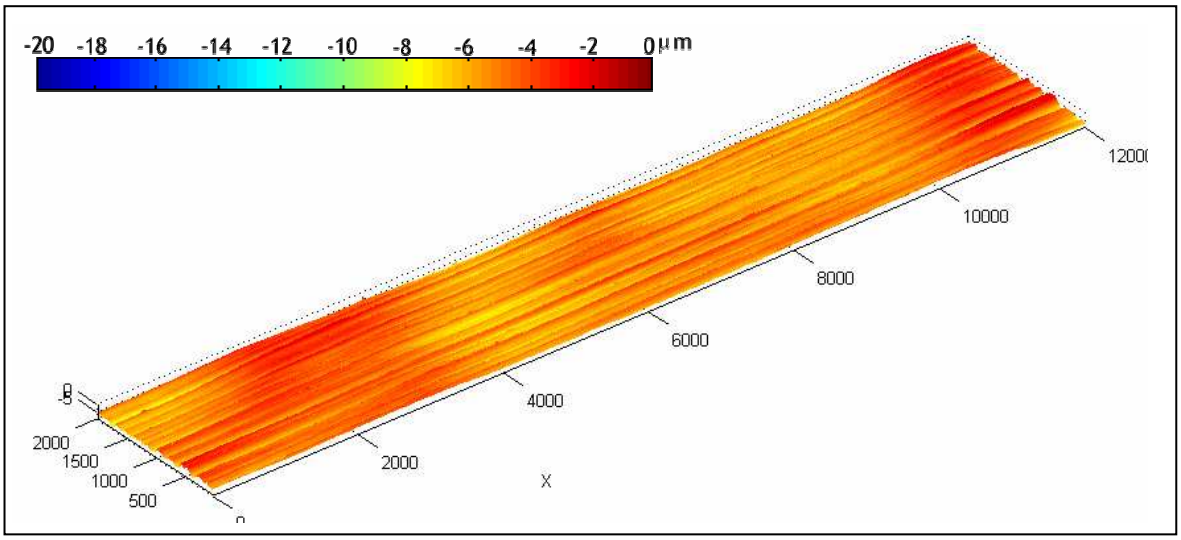
Part of the topography measurement (2X2 mm) made in the pinion of the coated gear lubricated with ester E2 (dimensions in µm).

Pinion tooth flank of a carburized gear after grinding and heat treatment

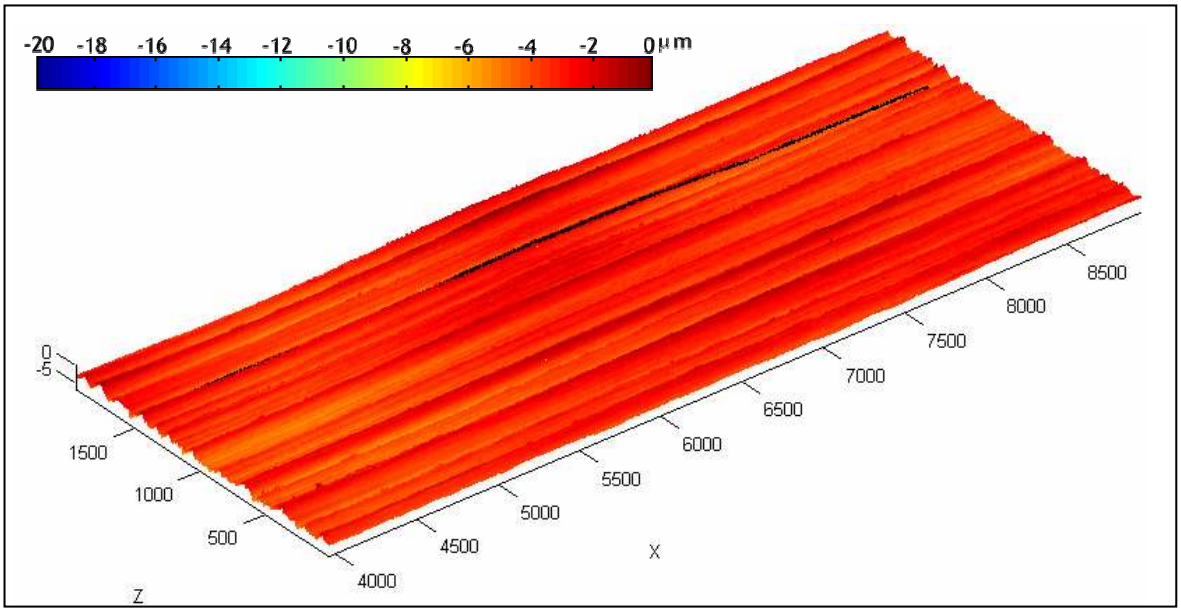
Gear type: C14 **Gear reference: 2C-6 Side: A**

Gear material: Carburized steel (DIN 20MnCr5)

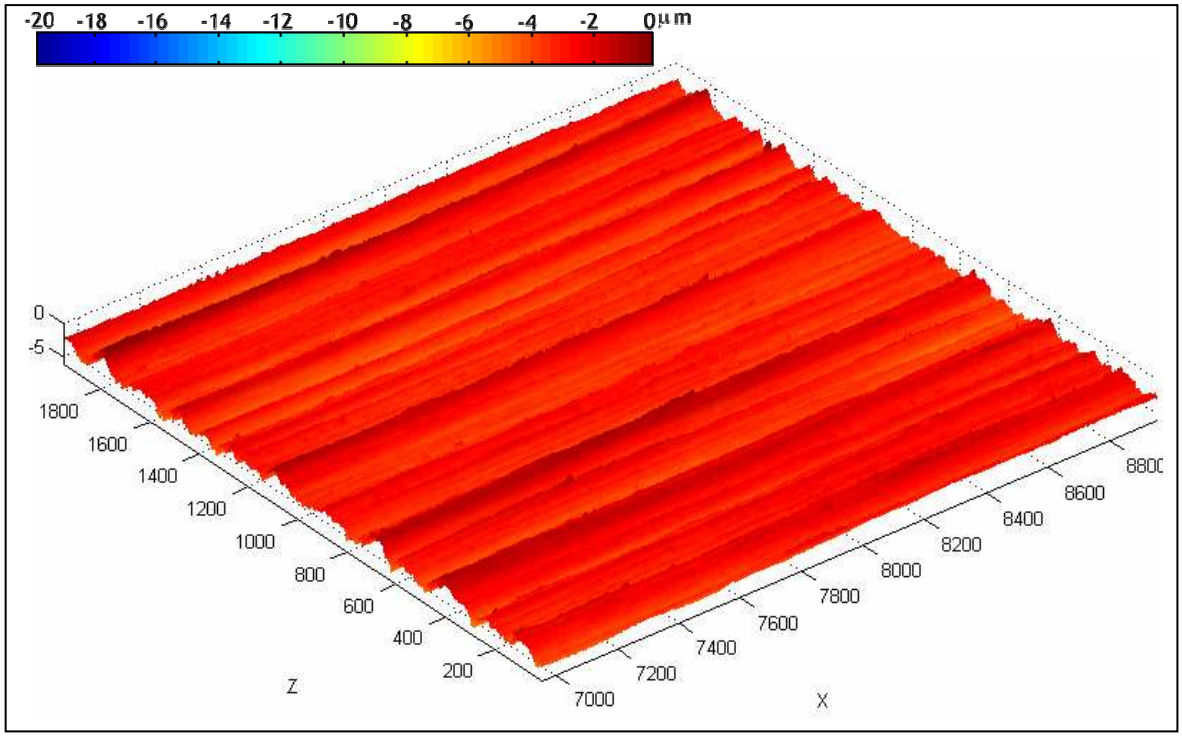
Surface topography measurements



Topography measurement (2X12 mm) made in the pinion of a new carburized gear (dimensions in µm).



Part of the topography measurement (2X5 mm) made in the pinion of a new carburized gear (dimensions in µm) and roughness profile presented in Table 4.16.



Part of the topography measurement (2X2 mm) made in the pinion of a new carburized gear (dimensions in µm).

Visual inspection



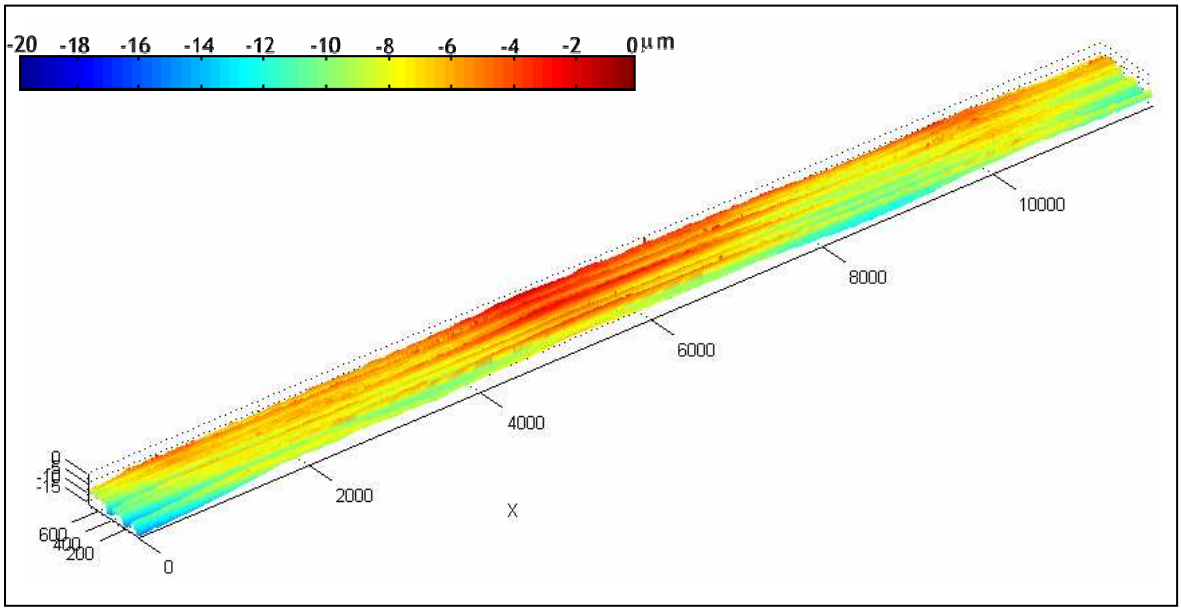
Picture of pinion tooth flank of a carburized gear after grinding and heat treatment.

Pinion tooth flank of a nitrided gear after grinding and heat treatment

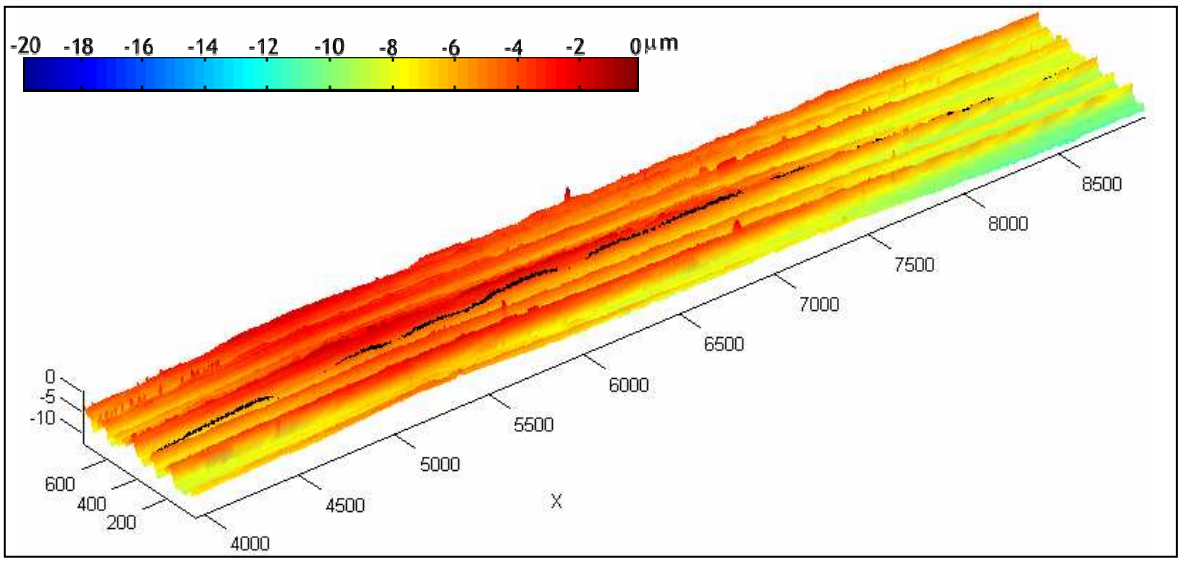
Gear type: C14 **Gear reference: NT-3 Side: B**

Gear material: High pressure nitrided steel (DIN 34 CrNiMo 6)

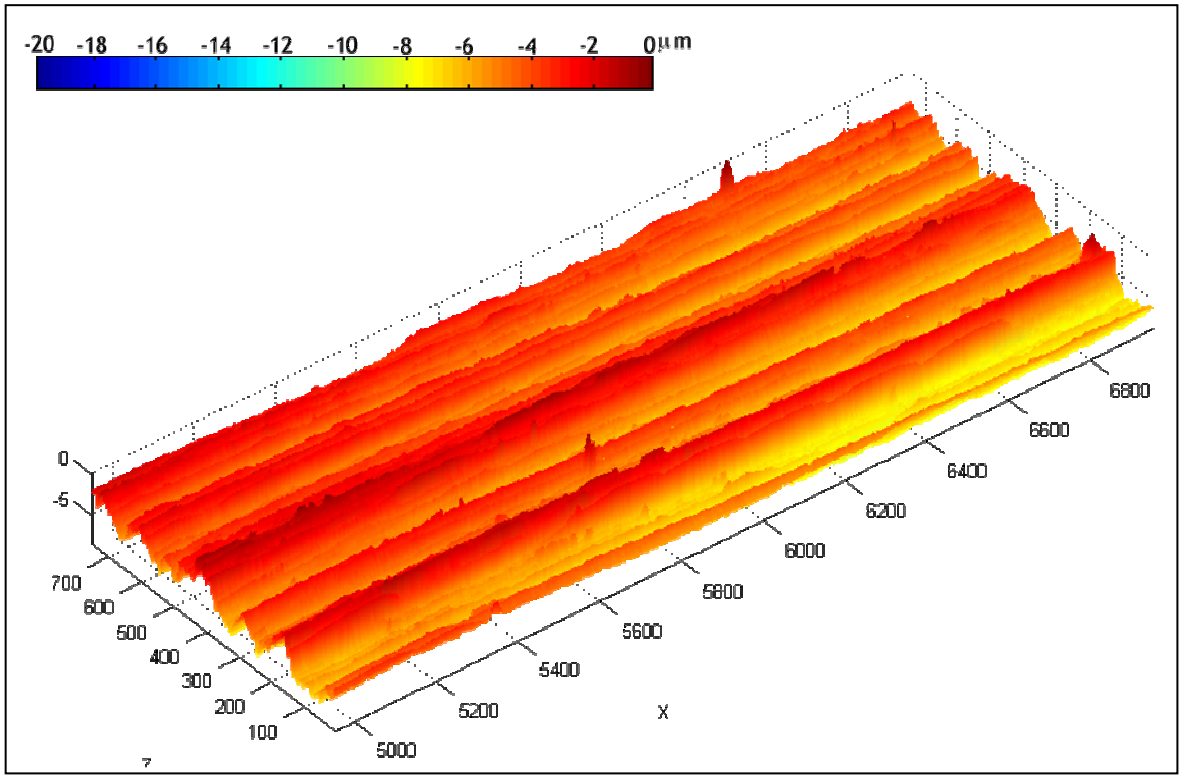
Topography measurements



Topography measurement (1,7 X 12,0 mm) made in the pinion of a new nitrided (dimensions in µm).



Part of the topography measurement (1,7 X 5,0 mm) made in the pinion of a new nitrided gear (dimensions in µm) and roughness profile presented in Table 4.16.



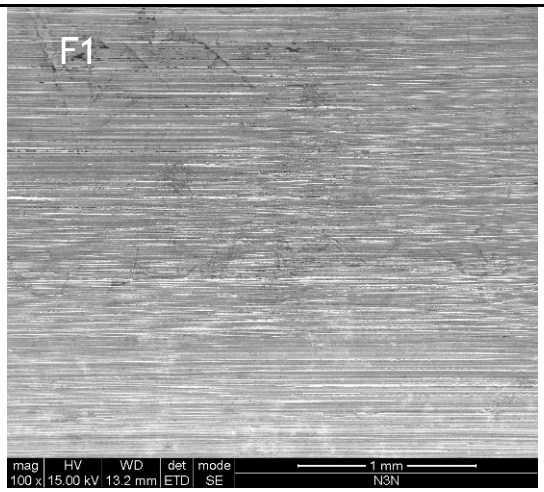
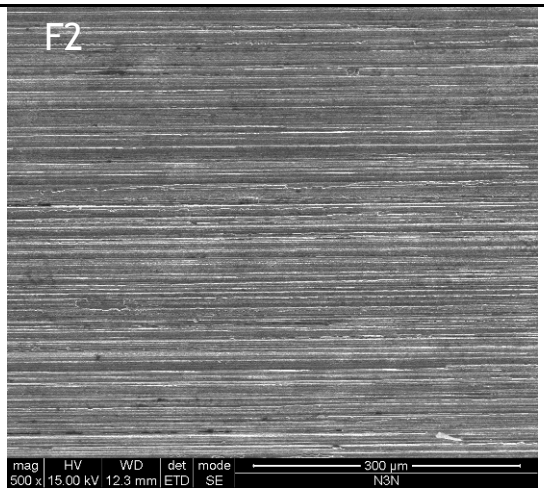
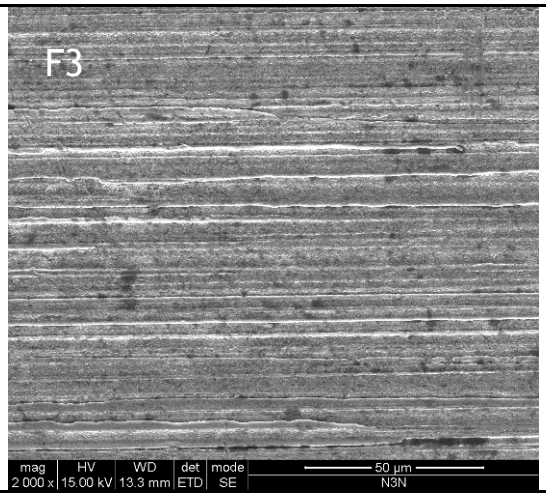
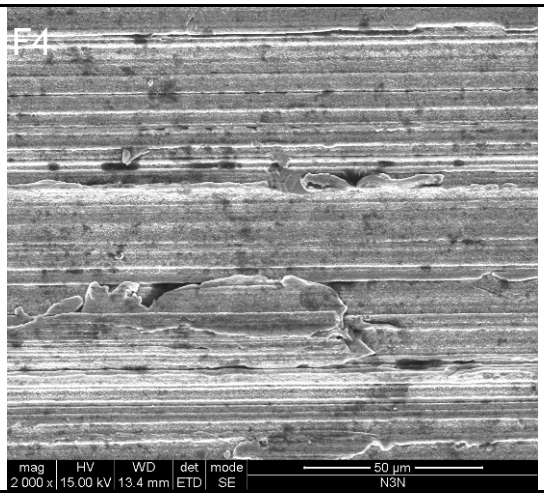
Part of the topography measurement (1,7 X 2,0 mm) made in the pinion of a new nitrided gear (dimensions in µm).

Visual inspection



Picture of pinion tooth flank of a high pressure nitrided gear after grinding and heat treatment.

SEM micrographs taken in a pinion tooth flank below pith line

100X		
500X		
2000X		

APPENDIX D – FZG GEAR POWER LOSS TESTS DATA SHEETS

FZG gear power loss test of carburized gear lubricated by M1 gear oil

Test reference: FZG efficiency test (C-M1) **Oil reference: M1**

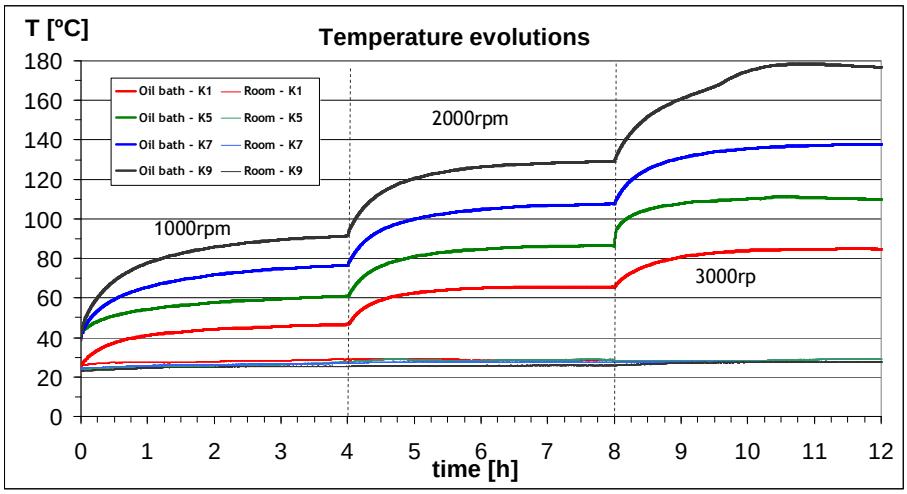
Gear type: C14 **Gear reference: 2C-5 Side: B**

Gear material: Carburized steel (DIN 20MnCr5)

N° of performed cycles and oil bath temperatures

FZG Load stage	Speed [rpm]	Pinion torque [N.m]	x10^5 n° of cycles	Final oil bath temperature [°C]	Final room temperature [°C]
k1	1000	3.30	2.40	46.7	29.0
	2000	3.30	4.80	65.6	27.5
	3000	3.30	7.20	84.8	27.4
k5	1000	70.00	2.40	60.8	27.7
	2000	70.00	4.80	86.7	28.8
	3000	70.00	8.44	110.1	29.2
k7	1000	132.50	2.40	76.5	26.9
	2000	132.50	4.80	107.7	26.4
	3000	132.50	7.20	137.8	27.7
k9	1000	215.60	2.40	91.5	25.4
	2000	215.60	4.80	129.0	25.8
	3000	215.60	7.20	176.7	27.6

Oil bath and room temperatures evolutions during the tests



Mass loss

Mass loss [mg]	
wheel	34.5
Pinion	20.2
total	54.7

Ferrometry

Load stage	nº of cycles	d	DL	DS	CPUC	ISUC
k1	1440000	0.1	19.6	3	226	3.8E+04
k5	3003840	0.1	27.9	3.9	318	7.6E+04
k7	4443840	0.1	26.5	4.5	310	6.8E+04
k9	5883840	0.1	29.4	7	364	8.2E+04

Surface roughness parameters

Surface roughness parameters (axial direction) [µm]											
			R_{max}	R_{Z-D}	R_a	R_q	M_{r1}	R_{pk}	R_k	R_{vk}	M_{r2}	Vo
Wheel	Initial	Above	1.58	1.20	0.21	0.28	8.8	0.29	0.68	0.45	86.0	30.4
		Below	1.17	0.84	0.16	0.20	8.8	0.13	0.50	0.28	84.1	22.9
Pinion	Initial	Above	1.83	1.15	0.18	0.25	10.4	0.26	0.53	0.42	84.1	34.1
		Below	1.60	0.91	0.16	0.22	11.8	0.22	0.45	0.51	86.5	34.2
	Final	Above	1.47	0.85	0.12	0.18	9.9	0.15	0.32	0.38	83.4	34.0
		Below	1.75	0.84	0.13	0.19	15.3	0.17	0.30	0.40	83.7	34.5
	Variation	Above	-20%	-27%	-30%	-28%	-5%	-44%	-39%	-8%	-1%	0%
		Below	9%	-8%	-19%	-14%	29%	-24%	-33%	-21%	-3%	1%

Surface roughness parameters (radial direction) [µm]											
			R_{max}	R_{Z-D}	R_a	R_q	M_{r1}	R_{pk}	R_k	R_{vk}	M_{r2}	Vo
Wheel	Initial	Above	7.43	6.14	1.20	1.48	10.4	1.23	4.31	1.55	89.9	82.5
		Below	7.03	5.66	0.94	1.18	9.9	0.99	3.14	1.43	89.0	80.0
Pinion	Initial	Above	9.16	7.16	1.30	1.60	8.4	1.27	4.61	1.85	91.1	82.1
		Below	9.02	6.65	1.37	1.65	8.4	1.25	5.10	1.50	92.5	58.0
	Final	Above	4.68	3.00	0.46	0.63	6.6	0.36	1.53	1.21	82.9	105.5
		Below	6.97	4.18	0.69	0.91	7.0	0.72	2.23	1.31	84.5	103.9
	Variation	Above	-49%	-58%	-65%	-61%	-22%	-72%	-67%	-35%	-9%	28%
		Below	-23%	-37%	-49%	-45%	-16%	-42%	-56%	-13%	-9%	79%

FZG gear power loss test of carburized gear lubricated by E1 gear oil

Test reference: FZG efficiency test (C-E1) **Oil reference: E1**

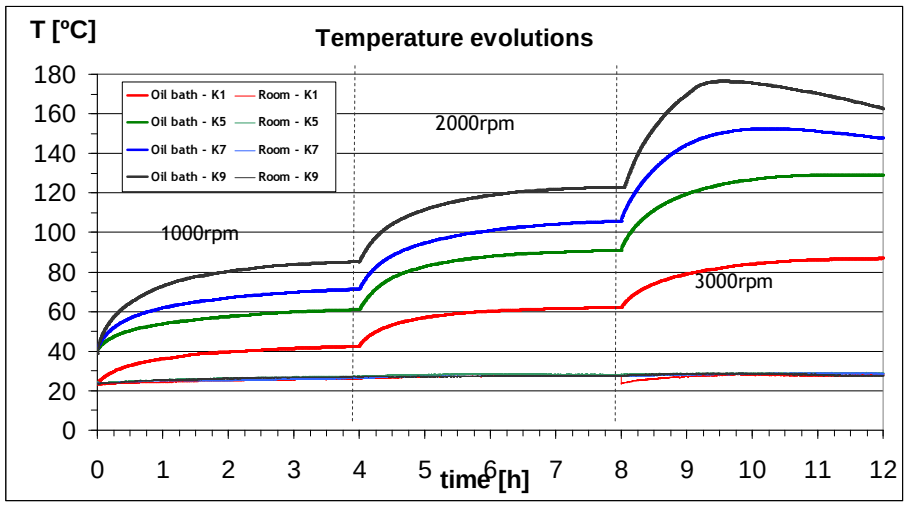
Gear type: C14 **Gear reference: 2C-2 Side: B**

Gear material: Carburized steel (DIN 20MnCr5)

N° of performed cycles and oil bath temperatures

FZG Load stage	Speed [rpm]	Pinion torque [N.m]	x10^5 n° of cycles	Final oil bath temperature [°C]	Final room temperature [°C]
k1	1000	3.30	2.40	46.7	29.0
	2000	3.30	4.80	65.6	27.5
	3000	3.30	14.40	84.8	27.4
k5	1000	70.00	2.40	60.8	27.7
	2000	70.00	4.80	86.7	28.8
	3000	70.00	7.20	110.1	29.2
k7	1000	132.50	2.40	76.5	26.9
	2000	132.50	4.80	107.7	26.4
	3000	132.50	7.20	137.8	27.7
k9	1000	215.60	2.40	91.5	25.4
	2000	215.60	4.80	129.0	25.8
	3000	215.60	7.20	176.7	27.6

Oil bath and room temperatures evolutions during the tests



Mass loss

Mass loss [mg]	
wheel	427.2
Pinion	98.2
total	525.3

Ferrometry

Load stage	nº of cycles	d	DL	DS	CPUC	ISUC
k1	2160000	0.1	6.6	2.7	93	3.6E+03
k5	3600000	0.1	21.4	3.5	249	4.5E+04
k7	5040000	0.1	25.2	3.4	286	6.2E+04
k9	6480000	0.01	73.3	14.5	8780	5.2E+07

Surface roughness parameters

Surface roughness parameters (axial direction) [µm]											
			R_{max}	R_{Z-D}	R_a	R_q	M_{r1}	R_{pk}	R_k	R_{vk}	M_{r2}	Vo
Wheel	Initial	Above	1.64	1.10	0.17	0.23	12.6	0.19	0.47	0.47	83.3	38.2
		Below	0.82	0.50	0.08	0.11	10.9	0.13	0.26	0.13	88.3	8.1
Pinion	Initial	Above	0.64	0.49	0.08	0.10	8.8	0.08	0.27	0.13	88.3	7.4
		Below	0.82	0.44	0.07	0.09	14.8	0.17	0.18	0.12	88.4	7.4
	Final	Above	4.67	3.76	0.54	0.73	7.5	0.40	1.45	1.39	84.2	110.0
		Below	2.11	1.47	0.28	0.36	16.4	0.50	0.81	0.46	89.7	23.6
	Variation	Above	628%	661%	573%	618%	-14%	392%	430%	1005%	-5%	1394%
		Below	156%	230%	313%	284%	11%	204%	342%	286%	1%	220%

Surface roughness parameters (radial direction) [µm]											
			R_{max}	R_{Z-D}	R_a	R_q	M_{r1}	R_{pk}	R_k	R_{vk}	M_{r2}	Vo
Wheel	Initial	Above	9.03	6.69	1.19	1.49	10.3	1.61	4.39	1.37	91.9	55.7
		Below	7.56	5.80	1.00	1.33	10.5	2.10	3.15	1.40	86.1	97.5
Pinion	Initial	Above	7.73	5.81	1.03	1.34	9.2	1.15	3.05	2.40	84.0	191.8
		Below	8.26	6.51	1.16	1.49	12.2	1.67	3.88	1.74	87.5	112.5
	Final	Above	5.30	3.41	0.60	0.79	9.6	0.74	1.89	1.22	80.4	120.8
		Below	11.82	5.62	0.76	1.14	10.8	0.97	2.31	1.77	83.8	143.7
	Variation	Above	-31%	-41%	-42%	-41%	4%	-36%	-38%	-49%	-4%	-37%
		Below	43%	-14%	-35%	-24%	-11%	-42%	-41%	2%	-4%	28%

FZG gear power loss test of carburized gear lubricated by E2 gear oil

Test reference: FZG efficiency test (C-E2) **Oil reference: E2**

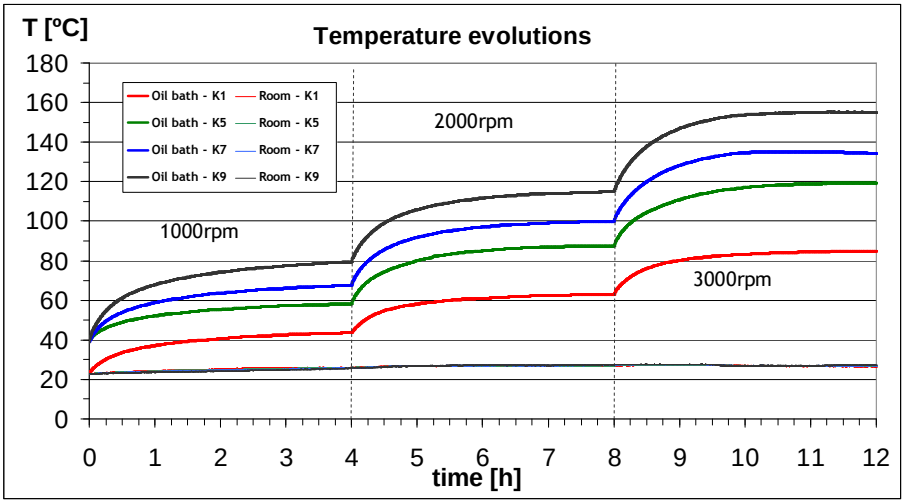
Gear type: C14 **Gear reference: 2C-2 Side: A**

Gear material: Carburized steel (DIN 20MnCr5)

N° of performed cycles and oil bath temperatures

FZG Load stage	Speed [rpm]	Pinion torque [N.m]	x10^5 n° of cycles	Final oil bath temperature [°C]	Final room temperature [°C]
k1	1000	3.30	2.40	46.7	29.0
	2000	3.30	4.80	65.6	27.5
	3000	3.30	7.20	84.8	27.4
k5	1000	70.00	2.40	60.8	27.7
	2000	70.00	4.80	86.7	28.8
	3000	70.00	7.20	110.1	29.2
k7	1000	132.50	2.40	76.5	26.9
	2000	132.50	4.80	107.7	26.4
	3000	132.50	7.20	137.8	27.7
k9	1000	215.60	2.40	91.5	25.4
	2000	215.60	4.80	129.0	25.8
	3000	215.60	3.94	176.7	27.6

Oil bath and room temperatures evolutions during the tests



Mass loss

Mass loss [mg]	
wheel	2.2
Pinion	4.8
total	7.0

Ferrometry

Load stage	nº of cycles	d	DL	DS	CPUC	ISUC
k1	1440000	0.1	12	2.2	142	1.4E+04
k5	2880000	0.1	15.4	3.5	189	2.2E+04
k7	4320000	0.1	16	3.5	195	2.4E+04
k9	5433700	0.1	13.1	3.6	167	1.6E+04

Surface roughness parameters

Surface roughness parameters (axial direction) [µm]											
			R_{max}	R_{Z-D}	R_a	R_q	M_{r1}	R_{pk}	R_k	R_{vk}	M_{r2}	Vo
Wheel	Initial	Above	0.74	0.50	0.07	0.10	13.2	0.14	0.22	0.12	89.6	6.6
		Below	0.59	0.39	0.06	0.08	11.3	0.09	0.23	0.10	90.7	4.5
Pinion	Initial	Above	0.98	0.69	0.12	0.15	10.3	0.14	0.36	0.19	86.0	13.4
		Below	1.11	0.68	0.12	0.15	10.9	0.14	0.37	0.32	88.3	22.5
	Final	Above	1.04	0.70	0.12	0.16	8.6	0.08	0.29	0.31	78.2	36.5
		Below	2.87	2.04	0.28	0.40	8.2	0.23	0.54	0.93	79.0	102.6
	Variation	Above	6%	0%	3%	5%	-17%	-38%	-20%	63%	-9%	173%
		Below	158%	199%	138%	162%	-25%	66%	46%	188%	-11%	357%

Surface roughness parameters (radial direction) [µm]											
			R_{max}	R_{Z-D}	R_a	R_q	M_{r1}	R_{pk}	R_k	R_{vk}	M_{r2}	Vo
Wheel	Initial	Above	6.27	5.32	1.02	1.25	5.4	1.10	3.33	1.29	85.9	91.3
		Below	9.38	7.32	1.33	1.66	11.6	2.14	4.49	1.91	89.5	100.0
Pinion	Initial	Above	5.60	4.44	0.76	0.94	7.3	0.54	2.75	1.20	90.3	57.2
		Below	7.71	5.99	1.27	1.58	9.7	1.58	4.78	2.09	86.6	146.3
	Final	Above	4.72	3.41	0.62	0.80	12.4	0.99	2.04	1.04	90.5	50.2
		Below	5.38	3.86	0.84	1.06	11.9	0.84	2.49	1.98	82.9	169.1
	Variation	Above	-16%	-23%	-18%	-15%	70%	84%	-26%	-13%	0%	-12%
		Below	-30%	-36%	-34%	-33%	22%	-47%	-48%	-5%	-4%	16%

FZG gear power loss test of carburized gear lubricated by E3 gear oil

Test reference: FZG efficiency test (C-E3) **Oil reference: E3**

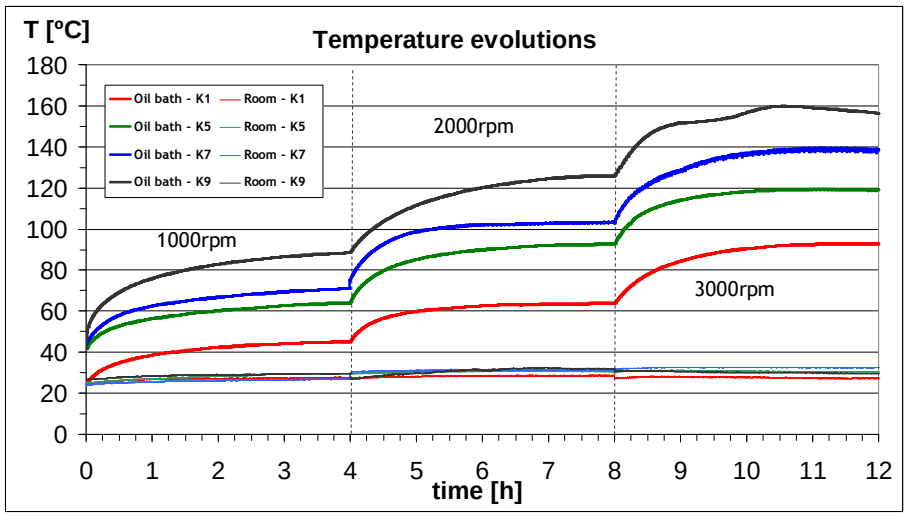
Gear type: C14 **Gear reference: 2C-4 Side: B**

Gear material: Carburized steel (DIN 20MnCr5)

N° of performed cycles and oil bath temperatures

FZG Load stage	Speed [rpm]	Pinion torque [N.m]	x10^5 n° of cycles	Final oil bath temperature [°C]	Final room temperature [°C]
k1	1000	3.30	2.40	46.7	29.0
	2000	3.30	4.80	65.6	27.5
	3000	3.30	14.40	84.8	27.4
k5	1000	70.00	2.40	60.8	27.7
	2000	70.00	4.80	86.7	28.8
	3000	70.00	7.20	110.1	29.2
k7	1000	132.50	4.80	76.5	26.9
	2000	132.50	4.80	107.7	26.4
	3000	132.50	7.20	137.8	27.7
k9	1000	215.60	2.40	91.5	25.4
	2000	215.60	9.60	129.0	25.8
	3000	215.60	14.40	176.7	27.6

Oil bath and room temperatures evolutions during the tests



Mass loss

Mass loss [mg]	
wheel	42.5
Pinion	29.5
total	72.0

Ferrometry

Load stage	nº of cycles	d	DL	DS	CPUC	ISUC
k1	2160000	0.1	17.2	4	212	2.8E+04
k5	3600000	0.1	20.3	4.1	244	4.0E+04
k7	5040000	0.1	40.5	6	465	1.6E+05
k9	6480000	0.1	56.1	8.9	650	3.1E+05

Surface roughness parameters

Surface roughness parameters (axial direction) [µm]											
			R_{max}	R_{Z-D}	R_a	R_q	M_{r1}	R_{pk}	R_k	R_{vk}	M_{r2}	Vo
Wheel	Initial	Above	2.16	1.51	0.25	0.33	9.8	0.38	0.84	0.50	89.9	26.4
		Below	0.85	0.60	0.11	0.14	12.5	0.15	0.35	0.15	87.1	9.6
Pinion	Initial	Above	1.07	0.67	0.12	0.16	12.1	0.24	0.31	0.22	83.7	20.4
		Below	1.15	0.75	0.12	0.16	10.5	0.20	0.36	0.29	86.8	21.4
	Final	Above	2.48	2.10	0.24	0.35	6.6	0.14	0.62	0.79	84.4	60.0
		Below	3.16	2.03	0.22	0.35	7.5	0.18	0.53	0.78	83.4	65.1
	Variation	Above	132%	215%	104%	115%	-45%	-40%	97%	263%	1%	194%
		Below	175%	169%	88%	117%	-29%	-7%	50%	171%	-4%	204%

Surface roughness parameters (radial direction) [µm]											
			R_{max}	R_{Z-D}	R_a	R_q	M_{r1}	R_{pk}	R_k	R_{vk}	M_{r2}	Vo
Wheel	Initial	Above	8.50	6.84	1.29	1.62	10.41	1.69	4.59	1.69	89.6	87.4
		Below	7.71	6.32	1.09	1.38	10.79	1.39	3.61	2.06	89.5	105.0
Pinion	Initial	Above	8.07	6.41	1.19	1.50	8.53	1.13	3.78	2.26	85.2	167.1
		Below	8.66	6.94	1.27	1.60	9.90	1.70	4.60	1.78	88.7	100.5
	Final	Above	5.00	3.24	0.47	0.64	8.72	0.48	1.55	1.23	85.3	91.8
		Below	5.35	3.64	0.57	0.75	7.47	0.66	1.80	1.27	82.7	111.9
	Variation	Above	-38%	-50%	-61%	-57%	2%	-58%	-59%	-46%	0%	-45%
		Below	-38%	-48%	-56%	-53%	-25%	-61%	-61%	-29%	-7%	11%

FZG gear power loss test of nitrided gear lubricated by M1 gear oil

Test reference: FZG efficiency test (N-M1) Oil reference: M1

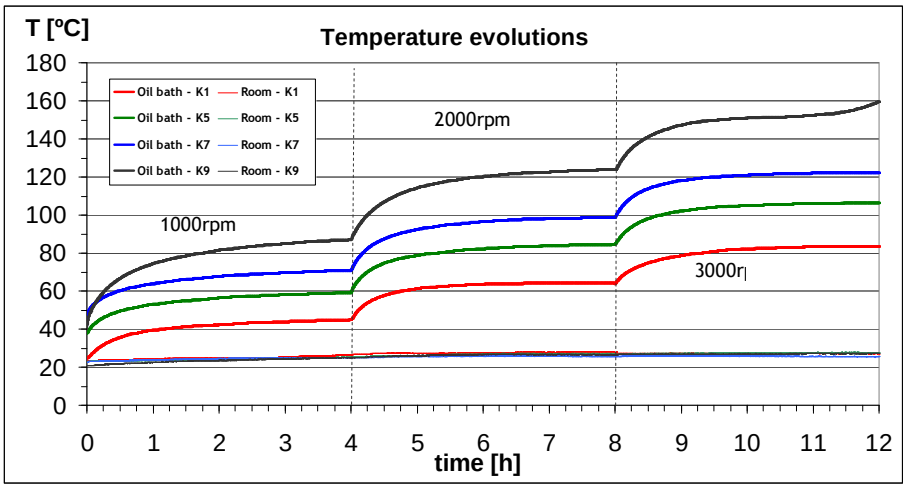
Gear type: C14 **Gear reference: NT-5 Side: A**

Gear material: High pressure nitrided steel (DIN 34 CrNiMo 6)

N° of performed cycles and oil bath temperatures

FZG Load stage	Speed [rpm]	Pinion torque [N.m]	x10^5 n° of cycles	Final oil bath temperature [°C]	Final room temperature [°C]
k1	1000	3.30	2.40	46.7	29.0
	2000	3.30	4.80	65.6	27.5
	3000	3.30	7.20	84.8	27.4
k5	1000	70.00	2.40	60.8	27.7
	2000	70.00	4.80	86.7	28.8
	3000	70.00	7.20	110.1	29.2
k7	1000	132.50	2.40	76.5	26.9
	2000	132.50	4.80	107.7	26.4
	3000	132.50	7.20	137.8	27.7
k9	1000	215.60	2.40	91.5	25.4
	2000	215.60	4.80	129.0	25.8
	3000	215.60	7.20	176.7	27.6

Oil bath and room temperatures evolutions during the tests



Mass loss

Mass loss [mg]	
wheel	45.3
Pinion	16.0
total	61.3

Ferrometry

Load stage	nº of cycles	d	DL	DS	CPUC	ISUC
k1	1440000	0.1	16.5	4.8	213	2.5E+04
k5	2880000	0.1	24.9	4.4	293	6.0E+04
k7	4320000	0.1	27.3	4	313	7.3E+04
k9	5760000	0.1	45.9	6.1	520	2.1E+05

Surface roughness parameters

Surface roughness parameters (axial direction) [µm]											
			R_{max}	R_{Z-D}	R_a	R_q	M_{r1}	R_{pk}	R_k	R_{vk}	M_{r2}	Vo
Wheel	Initial	Above	1.93	1.13	0.18	0.26	12.4	0.39	0.53	0.42	89.6	22.2
		Below	1.23	0.74	0.10	0.14	11.1	0.16	0.30	0.22	84.9	18.0
Pinion	Initial	Above	1.83	1.20	0.18	0.26	11.2	0.31	0.52	0.56	86.0	40.2
		Below	1.46	0.93	0.15	0.20	10.6	0.28	0.48	0.28	86.7	19.9
	Final	Above	2.81	1.16	0.15	0.28	10.0	0.09	0.34	0.65	88.0	41.6
		Below	10.63	3.96	0.61	1.24	16.3	0.49	0.53	3.99	82.0	359.6
	Variation	Above	53%	-3%	-21%	8%	-11%	-70%	-34%	16%	2%	3%
		Below	630%	327%	309%	515%	54%	76%	10%	1336%	-5%	1703%

Surface roughness parameters (radial direction) [µm]											
			R_{max}	R_{Z-D}	R_a	R_q	M_{r1}	R_{pk}	R_k	R_{vk}	M_{r2}	Vo
Wheel	Initial	Above	9.61	7.26	1.27	1.60	7.6	1.65	4.16	1.91	88.5	114.1
		Below	7.31	6.10	1.04	1.29	8.6	1.14	3.43	1.50	89.1	80.3
Pinion	Initial	Above	7.85	6.30	1.11	1.40	9.8	1.12	3.53	1.94	87.2	124.8
		Below	6.97	6.01	1.13	1.38	6.2	0.66	3.83	1.58	86.4	108.2
	Final	Above	4.06	2.83	0.48	0.64	8.1	0.35	1.44	1.21	80.5	118.9
		Below	5.80	3.33	0.58	0.74	5.6	0.29	1.76	1.17	79.5	119.3
	Variation	Above	-48%	-55%	-56%	-54%	-18%	-69%	-59%	-38%	-8%	-5%
		Below	-17%	-45%	-49%	-46%	-9%	-57%	-54%	-26%	-8%	10%

FZG gear power loss test of nitrided gear lubricated by E2 gear oil

Test reference: FZG efficiency test (N-E2) **Oil reference: E2**

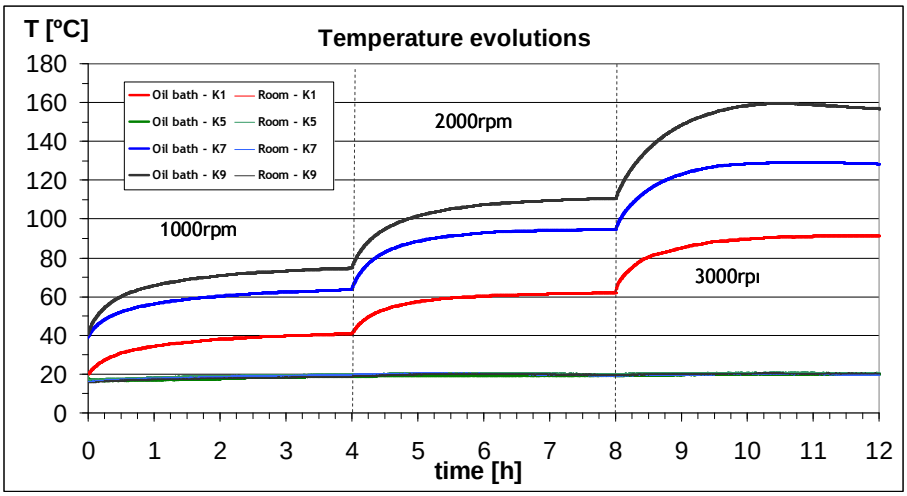
Gear type: C14 **Gear reference: NT-2 Side: A**

Gear material: High pressure nitrided steel (DIN 34 CrNiMo 6)

N° of performed cycles and oil bath temperatures

FZG Load stage	Speed [rpm]	Pinion torque [N.m]	x10^5 n° of cycles	Final oil bath temperature [°C]	Final room temperature [°C]
k1	1000	3.30	2.40	46.7	29.0
	2000	3.30	4.80	65.6	27.5
	3000	3.30	7.20	84.8	27.4
k5	1000	70.00	2.40	60.8	27.7
	2000	70.00	4.80	86.7	28.8
	3000	70.00	7.20	110.1	29.2
k7	1000	132.50	2.40	76.5	26.9
	2000	132.50	4.80	107.7	26.4
	3000	132.50	7.20	137.8	27.7
k9	1000	215.60	2.40	91.5	25.4
	2000	215.60	4.80	129.0	25.8
	3000	215.60	7.20	176.7	27.6

Oil bath and room temperatures evolutions during the tests



Mass loss

Mass loss [mg]	
wheel	20.0
Pinion	5.0
total	25.0

Ferrometry

Load stage	nº of cycles	d	DL	DS	CPUC	ISUC
k1	1440000	0.1	8.3	1.8	101	6.6E+03
k5	2880000	0.1	16.7	2.1	188	2.7E+04
k7	4320000	0.1	19.8	3.5	233	3.8E+04
k9	5760000	0.1	26.6	5.3	319	6.8E+04

Surface roughness parameters

Surface roughness parameters (axial direction) [µm]											
			R_{max}	R_{Z-D}	R_a	R_q	M_{r1}	R_{pk}	R_k	R_{vk}	M_{r2}	Vo
Wheel	Initial	Above	2.44	1.61	0.26	0.35	10.9	0.41	0.82	0.49	85.9	35.0
		Below	2.32	1.50	0.24	0.33	8.8	0.44	0.77	0.49	85.9	32.2
Pinion	Initial	Above	1.73	1.08	0.17	0.23	13.0	0.27	0.49	0.32	88.3	21.8
		Below	1.97	0.98	0.14	0.21	9.9	0.33	0.42	0.24	86.7	16.5
	Final	Above	1.04	0.56	0.08	0.12	5.8	0.06	0.24	0.21	85.3	15.5
		Below	0.63	0.34	0.04	0.07	9.1	0.04	0.12	0.16	84.8	12.3
	Variation	Above	-40%	-49%	-51%	-49%	-55%	-78%	-51%	-34%	-3%	-29%
		Below	-68%	-66%	-68%	-67%	-8%	-87%	-72%	-34%	-2%	-25%

Surface roughness parameters (radial direction) [µm]											
			R_{max}	R_{Z-D}	R_a	R_q	M_{r1}	R_{pk}	R_k	R_{vk}	M_{r2}	Vo
Wheel	Initial	Above	8.86	6.97	1.13	1.42	10.0	1.24	3.67	1.64	89.7	86.6
		Below	6.82	6.08	0.99	1.23	8.8	0.92	3.35	1.28	88.8	72.0
Pinion	Initial	Above	8.98	6.91	1.23	1.58	9.4	1.87	4.06	1.59	88.9	88.9
		Below	7.97	7.13	1.24	1.56	7.8	1.86	4.28	1.68	89.0	93.2
	Final	Above	0.43	0.33	0.08	0.10	6.8	0.06	0.14	0.12	82.6	10.7
		Below	0.55	0.39	0.10	0.12	8.5	0.06	0.22	0.13	83.6	10.6
	Variation	Above	-95%	-95%	-93%	-94%	-27%	-97%	-96%	-92%	-7%	-88%
		Below	-93%	-94%	-92%	-92%	8%	-97%	-95%	-92%	-6%	-89%